

ANALYSIS OF SHALLOW SHELLS
BY THE METHOD OF POINT MATCHING

Arthur W. Leissa
Adel S. Kadi

This document has been approved for public release and sale;
its distribution is unlimited.

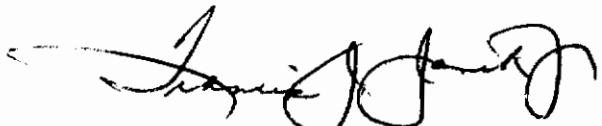
FOREWORD

This report was prepared by the Ohio State University Research Foundation, Columbus, Ohio, under USAF Contract No. F33615-67-C-1177. The report covers work conducted from December 1, 1966 to March 31, 1969.

The work was administered under direction of the Structures Division, Air Force Flight Dynamics Laboratory, Research and Technology Division, Wright-Patterson Air Force Base, Ohio; Mr. Robert M. Bader, acting as Project Engineer.

This manuscript was released by the authors in June 1969 for publication as a Technical Report.

This technical report has been reviewed and is approved.



FRANCIS J. JANIK, JR.
Chief, Solid Mechanics Branch
Structures Division

ABSTRACT

This report summarizes a study aimed at extending the applicability of the method of point matching to problems of statically loaded shallow shells, and deriving a set of shell equations for arbitrary curvature including the effects of orthotropy and thermal loading. The accuracy of the method is investigated by solving a problem for which an exact solution exists--the uniformly loaded, shallow spherical shell supported along a square boundary by means of shear diaphragms. Solutions to the governing system of differential equations are derived in polar coordinates in terms of Kelvin-Bessel functions and then expressed in a general form for boundaries having arbitrary normal and tangential directions. Further experiences with the method are demonstrated on problems of shallow spherical shells having regular polygonal and elliptical boundaries. For contrast, clamped and shear diaphragm edge conditions are studied. General solutions for circular cylindrical shallow shells, where the effects of rectangular orthotropy and thermal gradients are retained, are obtained by means of the auxiliary function approach.

Contrails

Contracts

TABLE OF CONTENTS

<u>Section</u>		<u>Page</u>
I	INTRODUCTION	1
II	EQUATIONS FOR ISOTROPIC SHALLOW SPHERICAL SHELLS AND GENERAL SOLUTIONS IN POLAR COORDINATES	5
	A. Complimentary Solution	5
	B. Basic Relations	8
	C. Boundary Conditions	9
	D. Equations for Arbitrary Shape	11
III	A STUDY OF THE ACCURACY OF THE POINT MATCHING METHOD	15
	A. Navier-Type Solution for a Spherical Shallow Shell	15
	B. Point Matching Solution	29
	1. Governing equation	29
	2. Complementary solution	29
	3. Particular solution	30
	4. Point matching method	32
	C. Comparison of Results	33
IV	SHALLOW SPHERICAL SHELLS HAVING REGULAR POLYGONAL PLANFORMS	45
	A. Point Matching Solutions	45
	B. Boundary Point Least Squares Solutions	66
	C. Discussion and Conclusions	76
V	SHALLOW SPHERICAL SHELLS HAVING ELLIPTICAL PLANFORMS	93
	A. Edges Clamped	94
	B. Edge Supported by a Shear Diaphragm	94
	C. Comparison between Clamped and Shear Diaphragm Supported Edges	94
VI	GENERAL EQUATIONS FOR SHALLOW SHELLS HAVING ARBITRARY CURVATURE	105
	A. Assumptions and Approximations	105
	B. The Mushtari-Donnell-Vlasov Approach	106
	C. Orthotropic Shallow Shells Subjected to Pressure and Thermal Loading	112
	1. Thermoelastic Isotropic Shallow Shells	126
	2. Elastic Isotropic Shallow Shell	126

Contrails

TABLE OF CONTENTS - continued

<u>Section</u>		<u>Page</u>
VII	SOLUTIONS OF THE ORTHOTROPIC THERMOELASTIC SHELL EQUATIONS FOR CIRCULAR CYLINDRICAL CURVATURE	127
	A. The Auxiliary Function Method	129
	B. Admissibility of the Technique	132
	C. A Special Case	141
	D. A Navier-Type of Solution	147
	E. A Voigt-Levy Type of Solution	151
	REFERENCES	153
	APPENDIX A	
	EXPLICIT EQUATIONS FOR SLOPES, BENDING MOMENTS, SHEARING FORCES, MEMBRANE FORCES AND TANGENTIAL DISPLACEMENTS FOR ISOTROPIC SHALLOW SPHERICAL SHELLS	157
	APPENDIX B	
	USEFUL KELVIN-BESSEL FUNCTION IDENTITIES	199
	APPENDIX C	
	A BIBLIOGRAPHY ON SHALLOW SHELLS	203

Contracts

LIST OF TABLES

<u>Table No.</u>		<u>Page</u>
1	Convergence of the Navier-Type Solution	20
2	Navier-Type Solution for Uniform Pressure Loading $R/a = 1.932$, $R/t = 50$, $E = 30 \times 10^6$ psi, $\nu = 0.3$, $a = b = 1$, Number of Terms = 64	23
3	Navier-Type Solution for Uniform Pressure Loading $R/a = 1.932$, $R/t = 50$, $E = 30 \times 10^6$ psi, $\nu = 0.3$, $a = b = 1$, Number of Terms = 625	26
4	Residuals Along the Boundary Shear Diaphragm (3, 4, 5 and 6 points matched), $R/t = 50$, $R/a = 1.932$	35
5	Ratio of Maximum Boundary Residuals to Maximum Values of Physical Parameters in the Shell Interior	39
6	Clamped Spherical Shell with Triangular Planform Obtained by Point Matching ($R/t = 50$, $R = 1.932$, $a = 1/\sqrt{2}$, $b = a \cos \pi/3$)	50
7	Clamped Spherical Shell with Square Planform Obtained by Point Matching ($R/t = 50$, $R = 1.932$, $a = 1/\sqrt{2}$, $b = a \cos \pi/4$)	51
8	Clamped Spherical Shell with Pentagonal Planform Obtained by Point Matching ($R/t = 50$, $R = 1.932$, $a = 1/\sqrt{2}$, $b = a \cos \pi/5$)	52
9	Clamped Spherical Shell with Hexagonal Planform Obtained by Point Matching ($R/t = 50$, $R = 1.932$, $a = 1/\sqrt{2}$, $b = a \cos \pi/6$)	53
10	Clamped Spherical Shell with Circular Planform Obtained by Point Matching ($R/t = 50$, $R = 1.932$, $a = 1/\sqrt{2}$)	54
11	Clamped Spherical Shell with Triangular Planform Obtained by Point Matching ($R/t = 200$, $R = 1.932$, $a = 1/\sqrt{2}$, $b = a \cos \pi/3$)	56
12	Clamped Spherical Shell with Square Planform Obtained by Point Matching ($R/t = 200$, $R = 1.932$, $a = 1/\sqrt{2}$, $b = a \cos \pi/4$)	57

Contracts

LIST OF TABLES - continued

<u>Table No.</u>		<u>Page</u>
13	Clamped Spherical Shell with Pentagonal Planform Obtained by Point Matching ($R/t = 200$, $R = 1.932$, $a = 1/\sqrt{2}$, $b = a \cos \pi/5$)	58
14	Clamped Spherical Shell with Hexagonal Planform Obtained by Point Matching ($R/t = 200$, $R = 1.932$, $a = 1/\sqrt{2}$, $b = a \cos \pi/6$)	59
15	Clamped Spherical Shell with Circular Planform Obtained by Point Matching ($R/t = 200$, $R = 1.932$, $a = 1/\sqrt{2}$)	60
16	Spherical Shell Supported at the Boundary by Shear Diaphragm. Triangular Planform Obtained by Point Matching ($R/t = 50$, $R = 1.932$, $a = 1/\sqrt{2}$, $b = a \cos \pi/3$)	61
17	Spherical Shell Supported at the Boundary by Shear Diaphragm. Square Planform Obtained by Point Matching ($R/t = 50$, $R = 1.932$, $a = 1/\sqrt{2}$, $b = a \cos \pi/4$)	62
18	Spherical Shell Supported at the Boundary by Shear Diaphragm. Pentagonal Planform Obtained by Point Matching. ($R/t = 50$, $R = 1.932$, $a = 1/\sqrt{2}$, $b = a \cos \pi/5$)	63
19	Spherical Shell Supported at the Boundary by Shear Diaphragm. Hexagonal Planform Obtained by Point Matching ($R/t = 50$, $R = 1.932$, $a = 1/\sqrt{2}$, $b = a \cos \pi/6$)	64
20	Spherical Shell Supported at the Boundary by Shear Diaphragm Circular Planform Obtained by Point Matching ($R/t = 50$, $R = 1.932$, $a = 1/\sqrt{2}$)	65
21	Clamped Spherical Shell with Triangular Planform Obtained by Least Squares Using Repeated Boundary Conditions ($R/t = 50$, $R = 1.932$, $a = 1/\sqrt{2}$, $b = a \cos \pi/3$)	68
22	Clamped Spherical Shell with Square Planform Obtained by Least Squares Using Repeated Boundary Conditions ($R/t = 50$, $R = 1.932$, $a = 1/\sqrt{2}$, $b = a \cos \pi/4$)	69
23	Clamped Spherical Shell with Pentagonal Planform Obtained by Least Squares Using Repeated Boundary Conditions ($R/t = 50$, $R = 1.932$, $a = 1/\sqrt{2}$, $b = a \cos \pi/5$)	70

Contracts

LIST OF TABLES - continued

<u>Table No.</u>		<u>Page</u>
24	Clamped Spherical Shell with Hexagonal Planform Obtained by Least Squares Using Repeated Boundary Conditions ($R/t = 50$, $R = 1.932$, $a = 1/\sqrt{2}$, $b = a \cos \pi/6$)	71
25	Spherical Shell Supported Along the Boundary by Shear Diaphragm Triangular Planform Obtained by Least Squares Using Repeated Boundary Conditions ($R/t = 50$, $R = 1.932$, $a = 1/\sqrt{2}$, $b = a \cos \pi/3$)	72
26	Spherical Shell Supported at the Boundary by Shear Diaphragm Square Planform Obtained by Least Squares Using Repeated Boundary Conditions ($R/t = 50$, $R = 1.932$, $a = 1/\sqrt{2}$, $b = a \cos \pi/4$)	73
27	Spherical Shell Supported at the Boundary by Shear Diaphragm Pentagonal Planform Obtained by Least Squares Using Repeated Boundary Conditions ($R/t = 50$, $R = 1.932$, $a = 1/\sqrt{2}$, $b = a \cos \pi/5$)	74
28	Spherical Shell Supported Along the Boundary by Shear Diaphragm Hexagonal Planform Obtained by Least Squares Using Repeated Boundary Conditions ($R/t = 50$, $R = 1.932$, $a = 1/\sqrt{2}$, $b = a \cos \pi/6$)	75
29	Clamped Spherical Shell with Triangular Planform Obtained by Least Squares Using Additional Points ($R/t = 50$, $R = 1.932$, $a = 1/\sqrt{2}$, $b = a \cos \pi/3$)	78
30	Clamped Spherical Shell with Square Planform Obtained by Least Squares Using Additional Points ($R/t = 50$, $R = 1.932$, $a = 1/\sqrt{2}$, $b = a \cos \pi/4$)	79
31	Clamped Spherical Shell with Pentagonal Planform Obtained by Least Squares Using Additional Points ($R/t = 90$, $R = 1.932$, $a = 1/\sqrt{2}$, $b = a \cos \pi/5$)	80
32	Clamped Spherical Shell with Hexagonal Planform Obtained by Least Squares Using Additional Points ($R/t = 50$, $R = 1.932$, $a = 1/\sqrt{2}$, $b = a \cos \pi/6$)	81
33	Spherical Shell Supported Along the Boundary Shear Diaphragm Triangular Planform Obtained by Least Squares Using Additional Points ($R/t = 50$, $R = 1.932$, $a = 1/\sqrt{2}$, $b = a \cos \pi/3$)	82

Contracts

LIST OF TABLES - continued

<u>Table No.</u>		<u>Page</u>
34	Spherical Shell Supported Along the Boundary by Shear Diaphragm Square Planform Obtained by Least Squares Using Additional Points ($R/t = 50$, $R = 1.932$, $a = 1/\sqrt{2}$, $b = a \cos \pi/4$)	83
35	Spherical Shell Supported Along the Boundary by Shear Diaphragm Pentagonal Planform Obtained by Least Squares Using Additional Points ($R/t = 50$, $R = 1.932$, $a = 1/\sqrt{2}$, $b = a \cos \pi/5$)	84
36	Spherical Shell Supported Along the Boundary by Shear Diaphragm Hexagonal Planform Obtained by Least Squares Using Additional Points ($R/t = 50$, $R = 1.932$, $a = 1/\sqrt{2}$, $b = a \cos \pi/6$)	85
37	Zeros of Bessel-Kelvin Functions of Order Zero	87
38	Comparison of Solutions by Three Methods	87
39	Values of Physical Parameters for Clamped Spherical Shells ($R/t = 50$, $R = 1.932$, $a = 1/\sqrt{2}$)	89
40	Values of Physical Parameters for a Spherical Shell Supported Along the Boundary by Shear Diaphragms; Triangular, Square and Circular Planforms	90
41	Uniformly Loaded Clamped Plates of Regular Polygonal Shape	90
42	Ratio of the Center Deflection of a Polygonal Plate to that of a Polygonal Shell Having the Same Uniform Normal Loading and Dimensions	91
43	Values of the Physical Parameters. Clamped Spherical Shell with Elliptical Planform ($R/t = 50$, $R = 5.8$ ", $(a/b) = 1.5$)	95
44	Residuals Along the Boundary. Clamped Spherical Shell with Elliptical Planform ($R/t = 50$, $R = 5.8$ ", $a/b = 1.5$)	97
45	Ratio of Maximum Residuals to Maximum Values of Physical Parameters Within the Shell. Clamped Spherical Shell with Elliptical Planform ($R/t = 50$, $R = 5.8$ ", $a/b = 1.5$)	98

Contrails

LIST OF TABLES - continued

<u>Table No.</u>		<u>Page</u>
46	Values of the Physical Parameters. Clamped Spherical Shell with Elliptical Planform ($R/t = 50$, $R = 5.8''$, $a/b = 1.0$)	98
47	Values of the Physical Parameters. Spherical Shell Supported at the Boundary by a Shear Diaphragm Elliptical Planform ($R/t = 50$, $R = 5.8''$, $a/b = 1.5$)	99
48	Residuals Along the Boundary. Spherical Shell Supported at the Boundary by a Shear Diaphragm Elliptical Planform ($R/t = 50$, $R = 5.8''$, $a/b = 1.5$)	101
49	Ratio of Maximum Residuals to Maximum Values of Physical Parameters within the Shell. Spherical Shell Supported at the Boundary by a Shear Diaphragm ($R/t = 50$, $R = 5.8''$, $a/b = 1.5$)	102
50	Values of the Physical Parameters Spherical Shell Supported at the Boundary by a Shear Diaphragm. Elliptical Planform ($R/t = 50$, $R = 5.8''$, $a/b = 1.0$)	102
51	Value of the Physical Parameters. Spherical Shallow Shell with Elliptical Planform ($R/t = 50$, $R = 5.8''$, $b = 1''$)	103

Contrails

LIST OF ILLUSTRATIONS

<u>Figure No.</u>		<u>Page</u>
1	Kelvin-Kirchhoff model for a shell	11
2	Normal and tangential coordinates on an arbitrary shape	12
3	Load variation along lines parallel to the x-axis	21
4	Load variation along lines parallel to the x-axis	22
5	Coordinates for shallow shell having square planform	33
6	Boundary points used with point matching method	34
7	Values of the deflection at interior points	40
8	Slope at interior points	41
9	Bending moment of interior points	42
10	Membrane force at interior points	43
11	Tangential displacement at interior points	44
12	Typical polygonal sector	47
13	Planform shape, points matched and coordinates	48
14	Residuals along the boundary, clamped spherical shell with triangular planform	55
15	Planform shape, points matched and coordinates	77
16	Bessel-Kelvin functions	86
17	Typical quadrant of an ellipse	93
18	Cylindrical shell	111
19	Shell element and its rectangular projection	113
20	Spherical shell	116
21	Sign convention for a shallow spherical shell	119

I. INTRODUCTION

The point matching method has long been known to be a useful technique for the solution of boundary value and eigenvalue problems. The method depends upon finding exact solutions to the governing differential equation(s) of the region, with boundary conditions being matched either exactly or in the least squares sense at a finite number of boundary points. The technique has been used extensively on various problems governed by second order and fourth order differential equations (cf., Refs. 1-11) and to a very limited extent on shell problems [12,13], which are represented by eighth order differential systems.

In spite of the relative complexity of systems of shell equations, some exact solutions are available, particularly in rectangular and polar coordinates. Correspondingly, these solutions can be forced to satisfy some sets of boundary conditions for rectangular and circular boundaries, respectively. However, for other sets of edge conditions (in particular, mixed boundary conditions) or for irregular (i.e., general) boundary shapes the prospects of satisfying the boundary conditions in the usual, classical, exact ways are indeed remote.

The point matching method would appear to be an excellent approach to handle arbitrary boundary shapes and edge conditions for shell problems. Indeed, as it was pointed out earlier, the technique has already achieved some earlier success in this use. Conway and Leissa [12] demonstrated the method for two problems involving shallow spherical shells: (1) one having a fully-fixed, square boundary and loaded by uniform pressure and (2) a rigid, elliptical insert which is loaded normal to a shell of unlimited extent. Clausen and Leissa [13] used the technique with multiple poles to study the effects of coupling between two closely located holes in a spherical shell upon the local stresses and deflections.

The present report summarizes a two-year study aimed at extending the applicability of the method of point matching to problems of deflection and stress analysis of statically loaded shallow shells. Chapters II, III, IV, and V deal with the application of the method to isotropic, shallow spherical shells having arbitrary transverse loading, boundary shape, and edge fixity conditions. In Chapter VI is derived a set of shallow shell equations for arbitrary curvature, including the effects of orthotropy and thermal loading. Solutions of these equations which could be used in future point matching applications are given in Chapter VII for circular cylindrical panels.

Reissner [14,15] formulated the theory for shallow spherical shells and presented solutions for the axisymmetric and antisymmetric loading components. These solutions were developed further in a paper by Niedenfuhr, Leissa, and Gaitens [16], wherein explicit expressions for useful quantities--displacements, bending moments, membrane forces, and

Contrails

transverse shearing forces--were listed for the same two Fourier components of loading, and structural applications were demonstrated.

In Chapter II a summary of the basic equations of shallow spherical shell theory in polar coordinates are first presented, and the primary solutions for the transverse deflection, w , and the Airy stress function, ϕ , are exhibited, as given previously in Refs. [14] and [16]. The equations in polar coordinates relating the in-plane displacements, bending moments, membrane forces, and transverse shearing forces to the functions w and ϕ are then listed. Next, the useful quantities defined in terms of arbitrarily oriented normal and tangential coordinates are related to those given previously in polar coordinates. Substitution of w and ϕ into these equations is then made to obtain explicit solutions for the useful quantities for all Fourier components of loading. These are given in Appendix A. The higher Fourier components will be necessary, in general, to handle all noncircular boundaries by the point matching method. The capability of the method in being able to accommodate irregular boundaries is, of course, its forte.

Approximate methods are only of value if an estimate of accuracy can be made. In the case of the point matching method an evaluation must be made of the residuals along the boundary and their effects within the region. In previous work using the point matching method on lower order differential systems these effects have been studied (cf., Refs. 17 and 18). For a thin shell the problem is more complicated for, as it will be shown in Chapter III, due to the rapid, oscillatory decay of some of the functions used, certain boundary residuals can be quite large without significantly affecting the stresses and deflections within the major portion of the shell.

The main objective of Chapter III is to provide some understanding of the accuracy of the point matching technique when used on shell problems. For this purpose a test problem is chosen which, not only has practical application, but has an exact solution for comparison purposes--the uniformly loaded, shallow spherical shell supported along a square boundary by shear diaphragms. The exact solution for this problem is a generalization of the Navier solution used for the bending of simply-supported rectangular plates. For the point matching method, suitable particular solutions corresponding to uniform pressure loading are added to the complementary solutions developed in Chapter II.

Using the experience gained in Chapter III the point matching method is applied in Chapters IV and V to yield extensive results for shallow spherical shells having regular polygonal and elliptical boundaries. The regular polygons considered are the triangle, square, pentagon, and hexagon. Clamped and shear diaphragm edge conditions are studied for contrast.

Chapter VI is a reasonably rigorous derivation of a set of equations governing the stresses and deflections of shallow shells of arbitrary

Contrails

curvature, material orthotropy, and subjected to thermal gradients. The Mushtari-Donnell-Vlasov formulation serves as a basis for the shallow shell theory derived. In Chapter VII solutions of the shallow shell equations are presented for the case of circular cylindrical curvature, where the effects of rectangular orthotropy and thermal gradients are retained. A general solution is obtained by means of the auxiliary function approach used by Vlasov [19], Ambartsumyan [20], and Goldenveizer [21]. Other solutions corresponding to certain special types of boundary conditions are also developed.

Contrails

II. EQUATIONS FOR ISOTROPIC SHALLOW SPHERICAL SHELLS AND SOLUTIONS IN POLAR COORDINATES

In this chapter the fundamental equations for the deflections of shallow spherical shells are presented in polar coordinates. Complementary solutions of a general form are derived for later use with the point matching method.

A. COMPLEMENTARY SOLUTION

The governing homogeneous differential equations of shallow spherical shells are [14]:

$$\nabla^4 w + \frac{1}{RD} \nabla^2 \phi = 0 \quad (2-1)$$

$$\nabla^4 \phi - \frac{Et}{R} \nabla^2 w = 0 \quad (2-2)$$

where w is the transverse deflection, ϕ is an Airy stress function, R is the spherical radius, D is the flexural rigidity $Et^3/12(1-\nu^2)$, E is Young's modulus, t is the shell thickness, and ν is Poisson's ratio.

Introducing the parameter λ as a multiplier to Eq. (2-2) and adding this to Eq. (2-1) yields

$$\nabla^4(w + \lambda\phi) - \frac{\lambda Et}{R} \nabla^2 \left(w - \frac{1}{\lambda Et D} \phi \right) = 0 \quad (2-3)$$

Setting

$$\lambda^2 = - \frac{1}{EtD}$$

and

$$l^2 = \frac{Rt}{\sqrt{12(1-\nu^2)}}$$

we get

$$\nabla^2 \left(\nabla^2 - \frac{1}{l^2} \right) (w + \lambda\phi) \quad (2-4)$$

Solutions of Eq. (2-4) are obtained in polar coordinates by assuming Fourier components:

Contrails

$$(w + \lambda\phi) = f_n(r) \cos n\theta + g_n(r) \sin n\theta \quad (2-5)$$

where $f_n(r)$ and $g_n(r)$ are solutions of

$$\frac{d^2 f_n}{dr^2} + \frac{1}{r} \frac{df_n}{dr} - \frac{n^2}{r^2} f_n = 0 \quad (2-6a)$$

$$\frac{d^2 g_n}{dr^2} + \frac{1}{r} \frac{dg_n}{dr} - \frac{n^2}{r^2} g_n = 0 \quad (2-6b)$$

$$\frac{d^2 f_n}{dr^2} + \frac{1}{r} \frac{df_n}{dr} - \left(\frac{n^2}{r^2} + \frac{i}{\ell^2} \right) f_n = 0 \quad (2-6c)$$

$$\frac{d^2 g_n}{dr^2} + \frac{1}{r} \frac{dg_n}{dr} - \left(\frac{n^2}{r^2} + \frac{i}{\ell^2} \right) g_n = 0 \quad (2-6d)$$

Solutions of Eqs. (2-6) are, respectively:

$$f_0(r) = A_0 + B_0 \ln r \quad n = 0 \quad (2-7a)$$

$$f_n(r) = A_n r^n + B_n r^{-n} \quad n \neq 0$$

$$g_n(r) = \bar{C}_n r^n + \bar{D}_n r^{-n} \quad n \neq 0 \quad (2-7b)$$

$$f_n(r) = C_n I_n\left(\frac{ri^{1/2}}{\ell}\right) + D_n K_n\left(\frac{ri^{1/2}}{\ell}\right) \quad (2-7c)$$

$$g_n(r) = \bar{C}_n I_n\left(\frac{ri^{1/2}}{\ell}\right) + \bar{D}_n K_n\left(\frac{ri^{1/2}}{\ell}\right) \quad (2-7d)$$

Recalling that

$$\begin{aligned} i^n I_n(\sqrt{i}x) &= \text{ber}_n x + i \text{bei}_n x \\ i^{-n} K_n(\sqrt{i}x) &= \text{ker}_n x + i \text{kei}_n x \end{aligned} \quad (2-8)$$

Contrails

Substituting Eqs. (2-7) into (2-5), and separating the real and imaginary parts of the resulting relation, we find the complementary solution of the form

$$\begin{aligned}
 w = & C_{01} + C_{02} \ln(x) + C_{03} \operatorname{ber} x + C_{04} \operatorname{bei} x \\
 & + C_{05} \operatorname{ker} x + C_{06} \operatorname{kei} x + \sum_{n=1}^{\infty} (C_{n1} x^n + C_{n2} x^{-n} \\
 & + C_{n3} \operatorname{ber}_n x + C_{n4} \operatorname{bei}_n x + C_{n5} \operatorname{ker}_n x + C_{n6} \operatorname{kei}_n x) \cos n\theta \\
 & + \sum_{n=1}^{\infty} (\bar{C}_{n1} x^n + \bar{C}_{n2} x^{-n} + \bar{C}_{n3} \operatorname{ber}_n x + \bar{C}_{n4} \operatorname{bei}_n x \\
 & + \bar{C}_{n5} \operatorname{ker}_n x + \bar{C}_{n6} \operatorname{kei}_n x) \sin n\theta \tag{2-9}
 \end{aligned}$$

$$\begin{aligned}
 |\lambda|\phi = & C_{03} \operatorname{bei} x - C_{04} \operatorname{ber} x + C_{05} \operatorname{kei} x - C_{06} \operatorname{ker} x \\
 & + C_{07} + C_{08} \ln(x) + C_{19} (x\theta \sin \theta - x \ln x \cos \theta) \\
 & + \bar{C}_{19} (x\theta \cos \theta + x \ln x \sin \theta) + \sum_{n=1}^{\infty} (C_{n3} \operatorname{bei}_n x \\
 & - C_{n4} \operatorname{ber}_n x + C_{n5} \operatorname{kei}_n x - C_{n6} \operatorname{ker}_n x + C_{n7} x^n \\
 & + C_{n8} x^{-n}) \cos n\theta + \sum_{n=1}^{\infty} (\bar{C}_{n3} \operatorname{bei}_n x - \bar{C}_{n4} \operatorname{ber}_n x \\
 & + \bar{C}_{n5} \operatorname{kei}_n x - \bar{C}_{n6} \operatorname{ker}_n x + \bar{C}_{n7} x^n + \bar{C}_{n8} x^{-n}) \sin n\theta \tag{2-10}
 \end{aligned}$$

where the nondimensional radius $x = r/\ell$ has been introduced.

C_{07} is immaterial as only derivatives of ϕ occur. To avoid multi-valued contribution to the displacement components u and v the following relations must hold (see Ref. 15):

$$\begin{aligned}
 C_{12} &= -C_{19} (1+\nu) \\
 \bar{C}_{12} &= C_{19} (1+\nu) \tag{2-11}
 \end{aligned}$$

Contrails

B. BASIC RELATIONS

Having the fundamental complementary solution given by Eqs. (2-9) and (2-10), it is desirable to have various useful quantities expressed in polar coordinates as listed below.

1. N - ϕ relations:

$$\left. \begin{aligned} N_r &= \frac{1}{r} \frac{\partial \phi}{\partial r} + \frac{1}{r^2} \frac{\partial^2 \phi}{\partial \theta^2} \\ N_\theta &= \frac{\partial^2 \phi}{\partial r^2} \\ N_{r\theta} &= - \frac{\partial}{\partial r} \left(\frac{1}{r} \frac{\partial \phi}{\partial \theta} \right) \end{aligned} \right\} \quad (2-12)$$

2. M - w relations:

$$\left. \begin{aligned} M_r &= -D \left[\frac{\partial^2 w}{\partial r^2} + \nu \left(\frac{1}{r} \frac{\partial w}{\partial r} + \frac{1}{r^2} \frac{\partial^2 w}{\partial \theta^2} \right) \right] \\ M_\theta &= -D \left[\frac{1}{r} \frac{\partial w}{\partial r} + \frac{1}{r^2} \frac{\partial^2 w}{\partial \theta^2} + \nu \frac{\partial^2 w}{\partial r^2} \right] \\ M_{r\theta} &= -D (1-\nu) \frac{\partial}{\partial r} \left(\frac{1}{r} \frac{\partial w}{\partial \theta} \right) \end{aligned} \right\} \quad (2-13)$$

3. Q - w relations:

$$\left. \begin{aligned} Q_r &= -D \frac{\partial}{\partial r} \nabla^2 w \\ Q_\theta &= -D \frac{1}{r} \frac{\partial}{\partial \theta} \nabla^2 w \end{aligned} \right\} \quad (2-14)$$

4. Kelvin - Kirchhoff relations:

$$\left. \begin{aligned} V_r &= Q_r + \frac{1}{r} \frac{\partial M_{r\theta}}{\partial r} \\ V_\theta &= Q_\theta + \frac{\partial M_{r\theta}}{\partial r} \end{aligned} \right\} \quad (2-15)$$

Contrails

5. Strain - displacement relations:

$$\left. \begin{aligned} \epsilon_r &= \frac{\partial u}{\partial r} + \frac{w}{R} \\ \epsilon_\theta &= \frac{1}{r} \frac{\partial v}{\partial \theta} + \frac{u}{r} + \frac{w}{R} \\ \epsilon_{r\theta} &= \frac{1}{r} \frac{\partial u}{\partial \theta} + \frac{\partial v}{\partial r} - \frac{v}{r} \end{aligned} \right\} \quad (2-16)$$

6. Strain - membrane force relations:

$$\left. \begin{aligned} \epsilon_r &= \frac{1}{Et} (N_r - \nu N_\theta) \\ \epsilon_\theta &= \frac{1}{Et} (N_\theta - \nu N_r) \\ \epsilon_{r\theta} &= \frac{2(1+\nu)}{Et} N_{r\theta} \end{aligned} \right\} \quad (2-17)$$

C. BOUNDARY CONDITIONS

Boundary conditions for arbitrary shapes are conveniently expressed in terms of the directions normal and tangent to the edge. In the general case, four independent boundary conditions are applied at each point along an edge. Two are associated with the in-plane directions, and involve the in-plane displacements and/or forces. The other two are associated with the transverse direction. Examples of the sets of boundary conditions which may be encountered follow.

1. Free edge

$$\left. \begin{aligned} N_n &= 0 \\ S_{nt} &= 0 \\ M_n &= 0 \\ V_n &= 0 \end{aligned} \right\} \quad (2-18)$$

2. Hinged edge with fixed support:

$$\left. \begin{aligned} u_n &= 0 \\ u_t &= 0 \\ w &= 0 \\ M_n &= 0 \end{aligned} \right\} \quad (2-19)$$

3. Clamped edge:

$$\left. \begin{aligned} u_n &= 0 \\ u_t &= 0 \\ w &= 0 \\ \frac{\partial w}{\partial n} &= 0 \end{aligned} \right\} \quad (2-20)$$

4. Hinged edge with support free to move in the normal direction (shear diaphragm):

$$\left. \begin{aligned} w &= 0 \\ u_t &= 0 \\ M_n &= 0 \\ N_n &= 0 \end{aligned} \right\} \quad (2-21)$$

In the foregoing equations, u_n and u_t are the normal and tangential components of displacement, respectively, w is the transverse displacement, $\partial w/\partial n$ is the change in slope in the normal direction, N_n is the normal component of membrane force, and M_n is the bending moment in the normal direction. The quantity V_n is the Kelvin-Kirchhoff transverse edge reaction, which is widely-known from classical plate theory. The quantity S_{nt} is the equivalent tangential edge reaction which arises from the Kelvin-Kirchhoff argument when the edge has transverse curvature. Although this quantity is widely described in texts on shell theory, it is frequently misused by workers in the field of shells.

Consider the infinitesimal edge length $2 dt$ as shown in Figure 1. The curvature of the shell in the plane tangent to the edge at this point is $1/R$. Using the usual positive conventions, the twisting moment $N_{nt}dt$ acting along the length dt can be replaced by two transverse forces of magnitude M_{nt} as shown. Similarly, the twisting moment on the second infinitesimal arc is replaced by two forces of magnitude $M_{nt} + (\partial M_{nt}/\partial t)dt$. Combining the transverse components it is seen that

$$Q_n + \frac{\partial M_{nt}}{\partial t} = 0 \quad (2-22)$$

which is the well-known Kelvin-Kirchhoff relation. Combining the tangential, in-plane components, the twisting moment effects from the two elements are additive, giving

$$N_{nt}dt + 2 M_{nt} \sin d\theta = 0$$

or

$$S_{nt} \equiv N_{nt} + \frac{M_{nt}}{R} = 0 \quad (2-23)$$

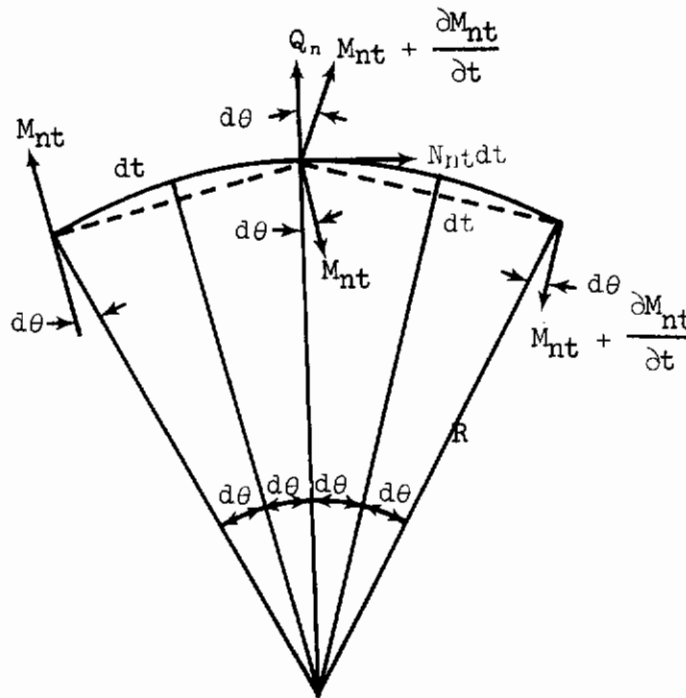


Figure 1. Kelvin-Kirchhoff model for a shell

D. EQUATIONS FOR ARBITRARY SHAPE

In applying the point matching method to boundaries of arbitrary shape, it is necessary to relate the normal and tangential directions

at the boundary to the polar coordinates r and θ . This relationship is shown in Fig. 2. In addition, as shown, the angle ϕ must be specified. This is defined as the angle by which the outer normal leads the radial direction (i.e., shown positive in Fig. 2).

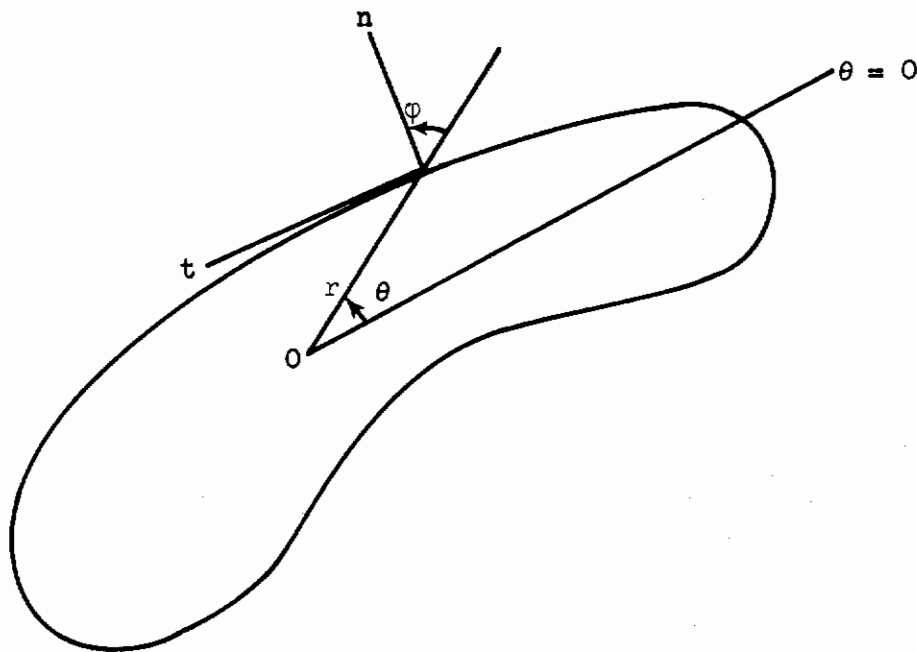


Figure 2. Normal and tangential coordinates on an arbitrary shape

The following equations relate useful quantities in the arbitrary directions n and t to the polar coordinates

1. Slope in the normal direction:

$$\frac{\partial w}{\partial n} = \frac{\partial w}{\partial r} \cos \phi + \frac{1}{r} \frac{\partial w}{\partial \theta} \sin \phi \quad (2-24)$$

2. Slope in the tangential direction:

Obtainable from Eq. (2-24) by replacing ϕ by $(\phi + \pi/2)$.

3. Moment in the normal direction:

$$M_n = \frac{1}{2} (M_r + M_\theta) + \frac{1}{2} (M_r - M_\theta) \cos 2\phi + M_{r\theta} \sin 2\phi \quad (2-25)$$

Contrails

4. Moment in the tangential direction:

Obtainable from Eq. (2-25) by replacing φ by $(\varphi + \pi/2)$.

5. Twisting moment:

$$M_{nt} = -\frac{1}{2} (M_r - M_\theta) \sin 2\varphi + M_{r\theta} \cos 2\varphi \quad (2-26)$$

6. Normal shear:

$$Q_n = Q_r \cos \varphi + Q_\theta \sin \varphi \quad (2-27)$$

7. Tangential shear:

Obtainable from Eq. (2-27) by replacing φ by $(\varphi + \pi/2)$.

8. Kelvin-Kirchoff shear:

$$V_n = Q_n + \left[-\frac{\partial M_{nt}}{\partial r} \sin \varphi + \frac{1}{r} \frac{\partial M_{nt}}{\partial \theta} \cos \varphi + \frac{\partial M_{nt}}{\partial \varphi} \left(-\frac{\partial \varphi}{\partial r} \sin \varphi + \frac{1}{r} \frac{\partial \varphi}{\partial \theta} \cos \varphi \right) \right]. \quad (2-28)$$

9. Normal membrane force:

$$N_n = \frac{N_r + N_\theta}{2} + \frac{(N_r - N_\theta)}{2} \cos 2\varphi + N_{r\theta} \sin 2\varphi \quad (2-29)$$

10. Tangential membrane force:

Obtainable from Eq. (2-29) by replacing φ by $(\varphi + \pi/2)$.

11. Shearing membrane force:

$$N_{nt} = -\frac{1}{2} (N_r - N_\theta) \sin 2\varphi + N_{r\theta} \cos 2\varphi + \frac{M_{nt}}{R} \quad (2-30)$$

12. Normal displacement:

$$u_n = u \cos \varphi + v \sin \varphi \quad (2-31)$$

13. Tangential displacement:

Obtainable from Eq. (2-31) by replacing φ by $(\varphi + \pi/2)$.

Contrails

To obtain explicit expressions for useful quantities in the normal and tangential directions in terms of r , θ , and φ , it is now necessary to substitute Eqs. (2-9) through (2-17) into Eqs. (2-24) through (2-31). The details of algebra will be omitted, and the final results are presented in Appendix A.

III. A STUDY OF THE ACCURACY OF THE POINT MATCHING METHOD

The primary purpose of this chapter is to evaluate the accuracy of the point matching method when applied to a representative shallow shell problem. A problem was chosen which has an exact solution in rectangular coordinates — the spherical shallow shell having a square planform, loaded by uniform pressure, and supported at its boundaries by shear diaphragms.

In the first part the exact solution of the problem is generated. It is a generalization of the well-known Navier solution of classical plate theory. A relatively simple computer program was written to implement this solution.

The point matching method is then applied to the same problem. Particular solutions are obtained for the uniform pressure loading. These are added to the complementary solutions presented in the previous chapter and together they supply the complete solution in polar coordinates. The problem is solved using various numbers of boundary points. Residuals along the boundary are tabulated for the point matching solutions. Further, deflections, bending moments, and membrane forces obtained from the solutions within the interior of the shell are compared with the exact values.

A. NAVIER-TYPE SOLUTION FOR A SPHERICAL SHALLOW SHELL

Consider a shallow, spherical shell whose planform dimensions are $a \times b$, having a spherical radius R . In this case the general equations for a shallow, isotropic shell (cf., Ref. 16, Eqs. 10 and 11) the governing system of differential equations reduces to

$$\left. \begin{aligned} \nabla^4 \phi - \frac{Et}{R} \nabla^2 w &= - (1-\nu) \nabla^2 \Omega \\ \nabla^4 w + \frac{1}{RD} \nabla^2 \phi &= \frac{q}{D} - \frac{2\Omega}{RD} \end{aligned} \right\} \quad (3-1)$$

where the notation used is the same as that of Chapter I. Furthermore, q is the transverse pressure loading and Ω is a suitable potential function which, when differentiated with respect to each of the shell coordinates, gives the components of tangential loading.

A Navier-type solution assumes that all edges are supported by "shear diaphragms," i.e., the following boundary conditions

$$w = M_n = N_n = u_t = 0 \quad (3-2)$$

Contrails

where M_n and N_n are the normal bending moment and membrane force, respectively, and u_t is the displacement tangent to both the middle surface of the shell and the boundary curve. The boundary conditions are satisfied exactly by choosing

$$\left. \begin{aligned} w &= \sum_m \sum_n A_{mn} \sin \alpha x \sin \beta y \\ \Phi &= \sum_m \sum_n B_{mn} \sin \alpha x \sin \beta y \end{aligned} \right\} \quad (3-3)$$

provided that the loading functions are also represented by compatible double sine series; i.e.,

$$\left. \begin{aligned} q &= \sum_m \sum_n a_{mn} \sin \alpha x \sin \beta y \\ \Omega &= \sum_m \sum_n b_{mn} \sin \alpha x \sin \beta y \end{aligned} \right\} \quad (3-4)$$

where

$$\left. \begin{aligned} \alpha &= \frac{m\pi}{a} & (m = 1, 2, \dots) \\ \beta &= \frac{n\pi}{b} & (n = 1, 2, \dots) \end{aligned} \right\} \quad (3-5)$$

Substituting Eqs. (3-3) and (3-4) into Eqs. (3-1) gives

$$\begin{aligned} &\sum_m \sum_n \left[\left(\frac{Et}{R} \right) (\alpha^2 + \beta^2) A_{mn} + (\alpha^2 + \beta^2)^2 B_{mn} \right] \sin \alpha x \sin \beta y \\ &= (1-\nu) \sum_m \sum_n (\alpha^2 + \beta^2) b_{mn} \sin \alpha x \sin \beta y \end{aligned}$$

Contrails

$$\begin{aligned} & \sum_m \sum_n (\alpha^2 + \beta^2)^2 A_{mn} - \frac{1}{RD} (\alpha^2 + \beta^2) B_{mn} \sin \alpha x \sin \beta y \\ & = \sum_m \sum_n \left(\frac{1}{D} a_{mn} - \frac{2}{RD} b_{mn} \right) \sin \alpha x \sin \beta y \end{aligned}$$

which have a solution

$$A_{mn} = \frac{\frac{1}{D} \left[a_{mn} - \frac{1}{R} (1 + \nu) b_{mn} \right]}{\left[\frac{Et}{R^2 D} + (\alpha^2 + \beta^2)^2 \right]} \quad (3-6)$$

$$B_{mn} = \frac{b_{mn} \left[(1-\nu)(\alpha^2 + \beta^2)^2 + \frac{2Et}{R^2 D} \right] - \frac{Et}{RD} a_{mn}}{(\alpha^2 + \beta^2) \left[\frac{Et}{R^2 D} + (\alpha^2 + \beta^2)^2 \right]}$$

Solution functions for slopes, bending and twisting moments, transverse shears, membrane forces, and displacements are:

$$\frac{\partial w}{\partial x} = \sum_m \sum_n \alpha A_{mn} \cos \alpha x \sin \beta y \quad (3-7a)$$

$$\frac{\partial w}{\partial y} = \sum_m \sum_n \beta B_{mn} \sin \alpha x \cos \beta y \quad (3-7b)$$

$$M_x = D \sum_m \sum_n (\alpha^2 + \nu \beta^2) A_{mn} \sin \alpha x \sin \beta y \quad (3-7c)$$

$$M_y = D \sum_m \sum_n (\nu \alpha^2 + \beta^2) A_{mn} \sin \alpha x \sin \beta y \quad (3-7d)$$

Contrails

$$M_{xy} = -D(1-\nu) \sum_m \sum_n \alpha \beta A_{mn} \cos \alpha x \cos \beta y \quad (3-7e)$$

$$Q_x = D \sum_m \sum_n \alpha (\alpha^2 + \beta^2) A_{mn} \cos \alpha x \sin \beta y \quad (3-7f)$$

$$Q_y = D \sum_m \sum_n \beta (\alpha^2 + \beta^2) A_{mn} \sin \alpha x \cos \beta y \quad (3-7g)$$

$$N_x = \sum_m \sum_n (b_{mn} - \beta^2 B_{mn}) \sin \alpha x \sin \beta y \quad (3-7h)$$

$$N_y = \sum_m \sum_n (b_{mn} - \alpha^2 B_{mn}) \sin \alpha x \sin \beta y \quad (3-7i)$$

$$N_{xy} = -\sum_m \sum_n \alpha \beta B_{mn} \cos \alpha x \cos \beta y \quad (3-7j)$$

$$u_x = -\sum_m \sum_n \frac{1}{\alpha} \left[\frac{1}{Et} \left((1-\nu) b_{mn} - (\beta^2 - \nu \alpha^2) B_{mn} \right) - \frac{A_{mn}}{R} \right] \cos \alpha x \sin \beta y \quad (3-7k)$$

$$u_y = -\sum_m \sum_n \frac{1}{\beta} \left[\frac{1}{Et} \left((1-\nu) b_{mn} - (\alpha^2 - \nu \beta^2) B_{mn} \right) - \frac{A_{mn}}{R} \right] \sin \alpha x \cos \beta y \quad (3-7l)$$

For the particular case of loading consisting solely of uniform normal pressure, the Fourier load coefficients become

$$\left. \begin{aligned} a_{mn} &= \frac{4}{ab} \int_0^a \int_0^b q_0 \sin \alpha x \sin \beta y \\ &= \frac{16q_0}{\pi^2 mn} \quad \left(\begin{array}{l} m = 1, 3, \dots \\ n = 1, 3, \dots \end{array} \right) \\ b_{mn} &= 0 \end{aligned} \right\} \quad (3-8)$$

Contrails

and in this case Eqs. (3-6) become

$$A_{mn} = \frac{16q_0a^4}{D\pi^2mn \left[12 \left(\frac{a}{R} \right)^4 \left(\frac{R}{t} \right)^2 (1-\nu^2) + \pi^4 \left(m^2 + \left(\frac{na}{b} \right)^2 \right)^2 \right]} \quad (3-9a)$$

$$B_{mn} = - \frac{16q_0R}{\pi^2mn (\alpha^2 + \beta^2) \left[1 + \frac{\pi^4}{12(1-\nu^2)} \left(\frac{R}{a} \right)^4 \left(\frac{t}{R} \right)^2 \left(m^2 + \left(\frac{na}{b} \right)^2 \right)^2 \right]} \quad (3-9b)$$

A study was conducted to determine the number of terms to be used for the production of acceptable results. The following values were assigned for the constants

$$a/b = 1$$

$$R/t = 50$$

$$R/a = 1.932$$

$$\nu = 0.3$$

Table 1 shows the number of terms and the corresponding deflection evaluated at the center and the transverse shear evaluated at the mid-point ($x = 1.0, y = 0.5$). The transverse shear, which requires third derivatives of w , clearly will have a slower rate of convergence.

From the results shown in Table 1 and a comparison of the execution times, it was decided that 25 terms in each direction is sufficient, making the total number of terms retained $(25)^2 = 625$. The approximation to the loading was also investigated; using 625 terms in the series, it was found, as shown in Figs. 3 and 4, that the series only had difficulty in approximating the uniform pressure in the vicinity of the boundaries. Obviously, exactly at the boundaries the series for q sums identically to zero. The loading requires fourth derivatives of the solution functions and, hence, shows the greatest deviation.

Tables 2 and 3 give the deflections, slopes, moments, shears, membrane forces, and displacements at various points throughout the shell using 64 and 625 terms in the series, respectively. This information not only indicates the rapidity of convergence of the Navier-type solution, but also is available for comparison with the approximate results obtained by point matching in the next section.

Contrails

Table 1. Convergence of the Navier-Type Solution

No. of Terms	$\frac{w}{q_0} \mid \begin{array}{l} x = 0.5 \\ y = 0.5 \end{array}$	$\frac{Q_x}{q_0} \mid \begin{array}{l} x = 1.0 \\ y = 0.5 \end{array}$
1	$0.43545389 \times 10^{-5}$	$- 0.42795316 \times 10^{-1}$
25	$0.38486531 \times 10^{-5}$	$- 0.97275573 \times 10^{-1}$
64	$0.38478501 \times 10^{-5}$	$- 1.03458060 \times 10^{-1}$
169	$0.38479280 \times 10^{-5}$	$- 1.08853860 \times 10^{-1}$
625	$0.38479084 \times 10^{-5}$	$- 1.12482890 \times 10^{-1}$
1444	$0.38478848 \times 10^{-5}$	$- 1.13810580 \times 10^{-1}$

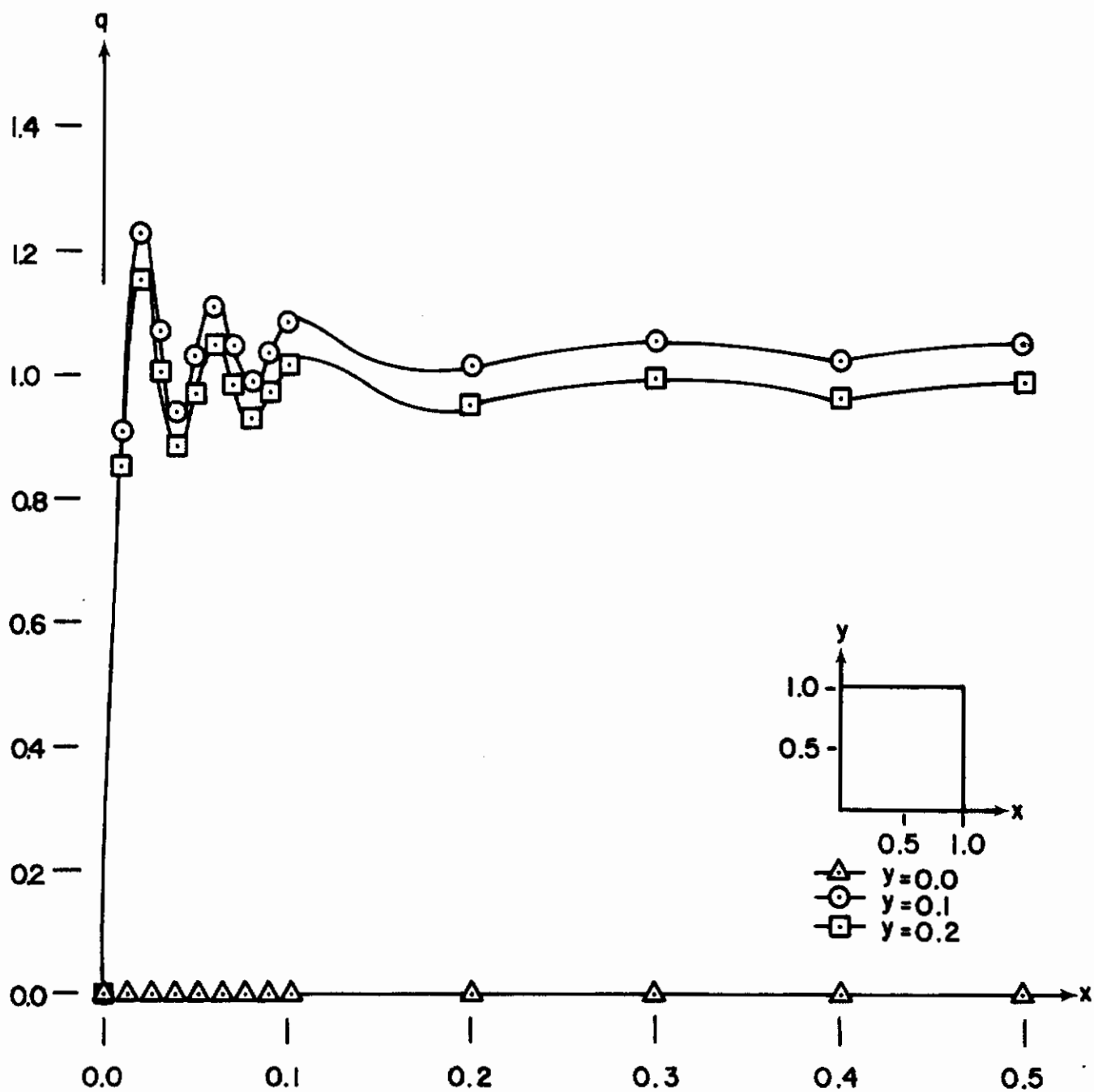


Figure 3. Load variation along lines parallel to the x-axis.

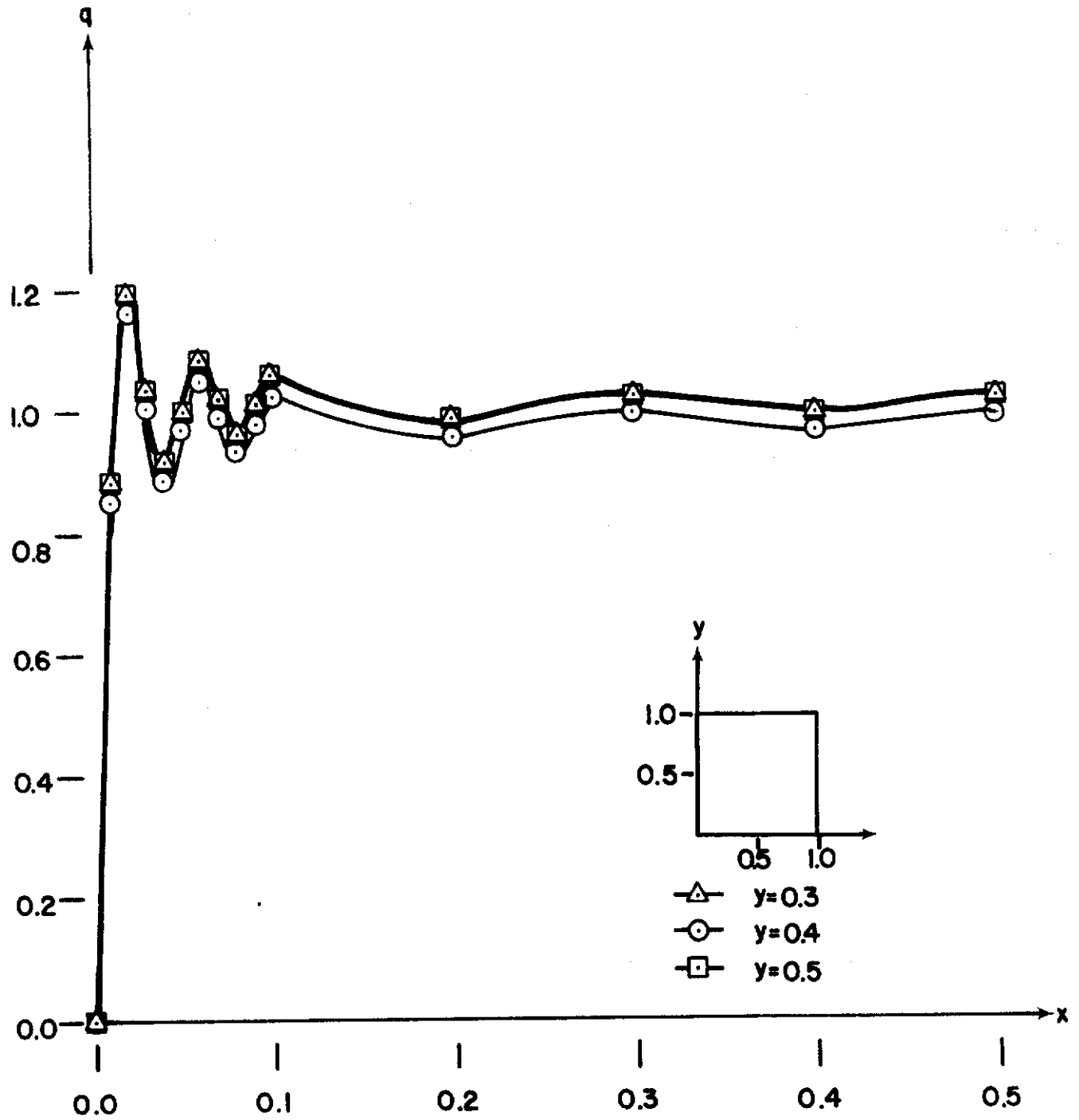


Figure 4. Load variation along lines parallel to the x-axis.

Contrails

Table A. Navier-Type Solution for Uniform Pressure Loading $R/a = 1.932$,
 $R/t = 50$, $E = 30 \times 10^8$ psi, $\nu = 0.3$, $a = b = 1$
Number of Terms = 64

X= 0.5000 Y= 0.5000	W= 0.38478501E-05 DWDX=-0.13041679E-12 DWDY=-0.13041679E-12 MX= 0.44538945E-02 MY= 0.44538945E-02 MXY=-0.78610743E-18	QX=-0.19223935E-08 QY=-0.19223934E-08 NX= 0.11542757E 01 NY= 0.11542757E 01 NXY= 0.26504187E-16	U=-0.10300316E-14 V=-0.10300316E-14 PHI=-0.12903575E-00
X= 0.6000 Y= 0.5000	W= 0.37361565E-05 DWDX=-0.22981250E-05 DWDY=-0.12784766E-12 MX= 0.50118640E-02 MY= 0.45107777E-02 MXY=-0.60956205E-11	QX= 0.80371936E-02 QY=-0.19205952E-08 NX= 0.11010940E 01 NY= 0.11404449E 01 NXY= 0.57331012E-09	U=-0.12897775E-06 V=-0.99866266E-15 PHI=-0.12327480E-00
X= 0.6000 Y= 0.6000	W= 0.36283672E-05 DWDX=-0.22185553E-05 DWDY=-0.22185552E-05 MX= 0.50508108E-02 MY= 0.50508108E-02 MXY=-0.18012210E-03	QX= 0.74831089E-02 QY= 0.74831088E-02 NX= 0.10884349E 01 NY= 0.10884349E 01 NXY= 0.10523273E-00	U=-0.12305577E-06 V=-0.12305577E-06 PHI=-0.11777879E-00
X= 0.7000 Y= 0.5000	W= 0.33655563E-05 DWDX=-0.52753238E-05 DWDY=-0.11856699E-12 MX= 0.63928835E-02 MY= 0.45717604E-02 MXY=-0.15578952E-10	QX= 0.10746192E-01 QY=-0.18940995E-08 NX= 0.94412875E 00 NY= 0.10750657E 01 NXY= 0.12980685E-08	U=-0.25394616E-06 V=-0.89570087E-15 PHI=-0.10615052E-00
X= 0.7000 Y= 0.6000	W= 0.32702825E-05 DWDX=-0.51016269E-05 DWDY=-0.19629878E-05 MX= 0.63894525E-02 MY= 0.50541433E-02 MXY=-0.39419181E-03	QX= 0.97670715E-02 QY= 0.59560393E-02 NX= 0.93453532E 00 NY= 0.10274988E 01 NXY= 0.20529043E-00	U=-0.24240056E-06 V=-0.10556208E-06 PHI=-0.10143691E-00
X= 0.7000 Y= 0.7000	W= 0.29526388E-05 DWDX=-0.45371791E-05 DWDY=-0.45371791E-05 MX= 0.62567844E-02 MY= 0.62567844E-02 MXY=-0.87757199E-03	QX= 0.71691055E-02 QY= 0.71691046E-02 NX= 0.88573054E 00 NY= 0.88573054E 00 NXY= 0.40189137E-00	U=-0.20821289E-06 V=-0.20821289E-06 PHI=-0.87409064E-01
X= 0.8000 Y= 0.5000	W= 0.26477524E-05 DWDX=-0.92324314E-05 DWDY=-0.97879541E-13 MX= 0.75900620E-02 MY= 0.42933699E-02 MXY=-0.31664059E-10	QX=-0.16844181E-03 QY=-0.17710666E-08 NX= 0.69282541E 00 NY= 0.89571662E 00 NXY= 0.22344198E-08	U=-0.36587747E-06 V=-0.69931683E-15 PHI=-0.78370326E-01
X= 0.8000 Y= 0.6000	W= 0.25751530E-05 DWDX=-0.89520703E-05 DWDY=-0.14982857E-05 MX= 0.75502381E-02 MY= 0.46637573E-02 MXY=-0.63856087E-03	QX=-0.13610643E-02 QY= 0.38213376E-02 NX= 0.68703108E 00 NY= 0.85795423E 00 NXY= 0.29168044E-00	U=-0.34948723E-06 V=-0.77512109E-07 PHI=-0.74910295E-01

Contrails

Table 2 (Cont'd)

X= 0.8000 Y= 0.7000	W= 0.23318271E-05 DWDX=-0.80250659E-05 DWDY=-0.34893607E-05 MX= 0.73079337E-02 MY= 0.56155304E-02 MXY=-0.14562886E-02	QX=-0.42541102E-02 QY= 0.39132683E-02 NX= 0.65474574E 00 NY= 0.74425409E 00 NXY= 0.57385169E 00	U=-0.30079144E-06 V=-0.15315961E-06 PHI=-0.64600812E-01
X= 0.8000 Y= 0.8000	W= 0.18512241E-05 DWDX=-0.62530776E-05 DWDY=-0.62530776E-05 MX= 0.64694702E-02 MY= 0.64694700E-02 MXY=-0.25088192E-02	QX=-0.66994822E-02 QY=-0.66994830E-02 NX= 0.55532881E 00 NY= 0.55532882E 00 NXY= 0.82548441E 00	U=-0.22188409E-06 V=-0.22188409E-06 PHI=-0.47799507E-01
X= 0.9000 Y= 0.5000	W= 0.15050569E-05 DWDX=-0.13546921E-04 DWDY=-0.59247110E-13 MX= 0.65618465E-02 MY= 0.30633624E-02 MXY=-0.54423467E-10	QX=-0.36894398E-01 QY=-0.13907572E-08 NX= 0.36722885E-00 NY= 0.53574296E 00 NXY= 0.31998990E-08	U=-0.44802705E-06 V=-0.39290655E-15 PHI=-0.41786474E-01
X= 0.9000 Y= 0.6000	W= 0.14653825E-05 DWDX=-0.13174562E-04 DWDY=-0.82075447E-06 MX= 0.65235182E-02 MY= 0.32759986E-02 MXY=-0.85116442E-03	QX=-0.38117140E-01 QY= 0.15209614E-02 NX= 0.36474476E-00 NY= 0.51442403E 00 NXY= 0.35198696E-00	U=-0.42826341E-06 V=-0.41108276E-07 PHI=-0.39951971E-01
X= 0.9000 Y= 0.7000	W= 0.13317246E-05 DWDX=-0.11925807E-04 DWDY=-0.19248686E-05 MX= 0.63219856E-02 MY= 0.38188720E-02 MXY=-0.19860957E-02	QX=-0.40659945E-01 QY= 0.11921909E-02 NX= 0.34936808E-00 NY= 0.44961163E-00 NXY= 0.69572318E 00	U=-0.36936320E-06 V=-0.81358078E-07 PHI=-0.34480081E-01
X= 0.9000 Y= 0.8000	W= 0.10647960E-05 DWDX=-0.94569685E-05 DWDY=-0.34976881E-05 MX= 0.56599788E-02 MY= 0.43348913E-02 MXY=-0.35654522E-02	QX=-0.40499630E-01 QY=-0.54971462E-02 NX= 0.29912873E-00 NY= 0.33970486E-00 NXY= 0.10083515E 01	U=-0.27333590E-06 V=-0.11818073E-06 PHI=-0.25543400E-01
X= 0.9000 Y= 0.9000	W= 0.61949925E-06 DWDX=-0.54186674E-05 DWDY=-0.54186674E-05 MX= 0.39053223E-02 MY= 0.39053223E-02 MXY=-0.53810747E-02	QX=-0.29187502E-01 QY=-0.29187505E-01 NX= 0.18583696E-00 NY= 0.18583696E-00 NXY= 0.12426039E 01	U=-0.14607707E-06 V=-0.14607707E-06 PHI=-0.13668797E-01
X= 1.0000 Y= 0.5000	W= 0.62561984E-12 DWDX=-0.15895015E-04 DWDY=-0.26232143E-19 MX= 0.38966114E-08 MY= 0.16026986E-08 MXY=-0.73094366E-10	QX=-0.10345806E-00 QY=-0.95417048E-15 NX= 0.14297178E-06 NY= 0.23237426E-06 NXY= 0.36667678E-08	U=-0.47923015E-06 V=-0.16153129E-21 PHI=-0.16363647E-07
X= 1.0000 Y= 0.6000	W= 0.60967749E-12 DWDX=-0.15485826E-04	QX=-0.10494275E-00 QY= 0.53549732E-10	U=-0.45824489E-06 V=-0.16014428E-13

Contrails

Table 2 (Concluded)

	DWDY=-0.33114605E-12	NX= 0.14224349E-06	PHI=-0.15649197E-07
	MX= 0.38773694E-03	NY= 0.22353730E-06	
	MY= 0.16938348E-08	NXY= 0.37387365E-00	
	MXY=-0.94229245E-03		
X= 1.0000	W= 0.55572691E-12	QX=-0.10777537E-00	U=-0.39562279E-06
Y= 0.7000	DWDX=-0.14104036E-04	QY=-0.14057183E-09	V=-0.31746039E-13
	DWDY=-0.78034297E-12	NX= 0.13693887E-06	PHI=-0.13515830E-07
	MX= 0.37764155E-09	NY= 0.19647428E-06	
	MY= 0.19266986E-08	NXY= 0.74042526E 00	
	MXY=-0.22138847E-02		
X= 1.0000	W= 0.44700166E-12	QX=-0.10619010E-00	U=-0.29325483E-06
Y= 0.8000	DWDX=-0.11329952E-04	QY=-0.25383757E-08	V=-0.46234777E-13
	DWDY=-0.14322107E-11	NX= 0.11827709E-06	PHI=-0.10024174E-07
	MX= 0.34435526E-08	NY= 0.14990538E-06	
	MY= 0.21515774E-08	NXY= 0.10767769E 01	
	MXY=-0.40455281E-02		
X= 1.0000	W= 0.26286833E-12	QX=-0.85946724E-01	U=-0.15704199E-06
Y= 0.9000	DWDX=-0.66532575E-05	QY=-0.13247278E-07	V=-0.57328466E-13
	DWDY=-0.22604874E-11	NX= 0.74498713E-07	PHI=-0.53710541E-09
	MX= 0.25224582E-08	NY= 0.83211414E-07	
	MY= 0.19829201E-08	NXY= 0.13330962E 01	
	MXY=-0.63564648E-02		
X= 1.0000	W= 0.11294884E-18	QX=-0.54385938E-07	U=-0.61752853E-13
Y= 1.0000	DWDX=-0.28557048E-11	QY=-0.54385938E-07	V=-0.61752853E-13
	DWDY=-0.28557048E-11	NX= 0.33882317E-13	PHI=-0.21131477E-14
	MX= 0.14186006E-14	NY= 0.33882318E-13	
	MY= 0.14186006E-14	NXY= 0.14349075E 01	
	MXY=-0.80124234E-02		

Contrails

Table 3. Navier-Type solution for Uniform Pressure Loading $R/a = 1.932$,
 $R/t = 50$, $E = 30 \times 10^8$ psi, $\nu = 0.3$, $a = b = 1$
Number of Terms = 625

X= 0.5000 Y= 0.5000	W= 0.32479024E-05 DWDX=-0.12927729E-12 DWDY=-0.12927729E-12 MX= 0.44743642E-02 MY= 0.44743642E-02 MXY=-0.74099937E-12	UX=-0.15925931E-03 UY=-0.15925929E-02 NX= 0.11542930E 01 NY= 0.11542930E 01 NXY= 0.22447696E-16	U=-0.10299179E-14 V=-0.10299179E-14 PHI=-0.12903525E-00
X= 0.6000 Y= 0.5000	W= 0.37362009E-05 DWDX=-0.22962922E-05 DWDY=-0.12729860E-12 MX= 0.50218763E-02 MY= 0.45281960E-02 MXY=-0.60030328E-11	UX= 0.27933791E-02 UY=-0.15848158E-08 NX= 0.1101121E 01 NY= 0.11404500E 01 NXY= 0.57313077E-09	U=-0.12897679E-06 V=-0.99254732E-15 PHI=-0.12327458E-00
X= 0.6000 Y= 0.6000	W= 0.36283897E-05 DWDX=-0.22167110E-05 DWDY=-0.22167110E-05 MX= 0.50577001E-02 MY= 0.50577001E-02 MXY=-0.18001679E-03	UX= 0.82491202E-02 UY= 0.82491192E-02 NX= 0.10884401E 01 NY= 0.10884401E 01 NXY= 0.10523238E-00	U=-0.12305483E-06 V=-0.12305483E-06 PHI=-0.1177860E-00
X= 0.7000 Y= 0.5000	W= 0.33655559E-05 DWDX=-0.52736766E-05 DWDY=-0.11799808E-12 MX= 0.63848143E-02 MY= 0.45839360E-02 MXY=-0.15504784E-10	UX= 0.11361124E-01 UY=-0.15443185E-08 NX= 0.94414916E 00 NY= 0.10750437E 01 NXY= 0.12979566E-08	U=-0.25394472E-06 V=-0.89558218E-15 PHI=-0.10615026E-00
X= 0.7000 Y= 0.6000	W= 0.32702603E-05 DWDX=-0.50999699E-05 DWDY=-0.19611194E-05 MX= 0.63780886E-02 MY= 0.50556139E-02 MXY=-0.39410477E-03	UX= 0.10389632E-01 UY= 0.67420094E-02 NX= 0.93454249E 00 NY= 0.10274770E 01 NXY= 0.20528982E-00	U=-0.24239919E-06 V=-0.10556137E-06 PHI=-0.10143668E-00
X= 0.7000 Y= 0.7000	W= 0.29525708E-05 DWDX=-0.45355022E-05 DWDY=-0.45355022E-05 MX= 0.62396792E-02 MY= 0.62396792E-02 MXY=-0.27749754E-03	UX= 0.78071206E-02 UY= 0.78071184E-02 NX= 0.88571043E 00 NY= 0.88571043E 00 NXY= 0.40189028E-00	U=-0.20821195E-06 V=-0.20821195E-06 PHI=-0.87408796E-01
X= 0.8000 Y= 0.5000	W= 0.26477264E-05 DWDX=-0.92333522E-05 DWDY=-0.97300575E-13 MX= 0.75710898E-02 MY= 0.43023558E-02 MXY=-0.31722903E-10	UX=-0.73249305E-03 UY=-0.14161032E-08 NX= 0.69284587E 00 NY= 0.89568104E 00 NXY= 0.22344691E-08	U=-0.36587662E-06 V=-0.69919809E-15 PHI=-0.78370089E-01
X= 0.8000 Y= 0.6000	W= 0.25751043E-05 DWDX=-0.89529976E-05 DWDY=-0.14964095E-05 MX= 0.75279172E-02 MY= 0.46669846E-02 MXY=-0.63863663E-03	UX=-0.19338506E-02 UY= 0.46160163E-02 NX= 0.68703829E 00 NY= 0.85791856E 00 NXY= 0.29167941E-00	U=-0.34948640E-06 V=-0.77511380E-07 PHI=-0.74910090E-01
X= 0.8000 Y= 0.7000	W= 0.23317323E-05 DWDX=-0.20270135E-05	UX=-0.48444270E-02 UY= 0.45581158E-02	U=-0.30079058E-06 V=-0.15315868E-06

Contrails

Table 3 (Cont'd)

	DWDY=-0.34876824E-05	NX= 0.65472551E 00	PHI=-0.64600563E-01
	MX= 0.72797223E-02	NY= 0.74421819E 00	
	MY= 0.55950049E-02	NXY= 0.57384960E 00	
	MXY=-0.14563469E-02		
X= 0.8000	W= 0.19511071E-05	QX=-0.72974095E-02	U=-0.22188377E-06
Y= 0.8000	DWDX=-0.62540495E-05	QY=-0.72974140E-02	V=-0.22188377E-06
	DWDY=-0.62540495E-05	NX= 0.55529291E 00	PHI=-0.47799376E-01
	MX= 0.64377920E-02	NY= 0.55529297E 00	
	MY= 0.64377914E-02	NXY= 0.82548244E 00	
	MXY=-0.25087483E-02		
X= 0.9000	W= 0.15050595E-05	QX=-0.39178356E-01	U=-0.44802706E-06
Y= 0.5000	DWDX=-0.13551607E-04	QY=-0.10491474E-08	V=-0.39279389E-15
	DWDY=-0.58689459E-13	NX= 0.36724931E-00	PHI=-0.41786345E-01
	MX= 0.65624081E-02	NY= 0.53572326E 00	
	MY= 0.30777773E-02	NXY= 0.32000600E-08	
	MXY=-0.54637600E-10		
X= 0.9000	W= 0.14653635E-05	QX=-0.40429399E-01	U=-0.42826348E-06
Y= 0.6000	DWDX=-0.13179265E-04	QY= 0.22894565E-02	V=-0.41107707E-07
	DWDY=-0.81893658E-06	NX= 0.36475249E-00	PHI=-0.39951854E-01
	MX= 0.65208384E-02	NY= 0.51440419E 00	
	MY= 0.32799299E-02	NXY= 0.35198556E-00	
	MXY=-0.85129534E-03		
X= 0.9000	W= 0.13316610E-05	QX=-0.43030044E-01	U=-0.36936320E-06
Y= 0.7000	DWDX=-0.11930542E-04	QY= 0.18159800E-02	V=-0.81357403E-07
	DWDY=-0.19232436E-05	NX= 0.34934970E-00	PHI=-0.34479939E-01
	MX= 0.63136931E-02	NY= 0.44959211E-00	
	MY= 0.38046929E-02	NXY= 0.69572071E 00	
	MXY=-0.19861635E-02		
X= 0.9000	W= 0.10647065E-05	QX=-0.42893407E-01	U=-0.27333590E-06
Y= 0.8000	DWDX=-0.94617152E-05	QY=-0.60741531E-02	V=-0.11818063E-06
	DWDY=-0.34986479E-05	NX= 0.29909518E-00	PHI=-0.25543318E-01
	MX= 0.56482729E-02	NY= 0.33968489E-00	
	MY= 0.43098377E-02	NXY= 0.10083474E 01	
	MXY=-0.35652263E-02		
X= 0.9000	W= 0.61943819E-06	QX=-0.31506182E-01	U=-0.14607751E-06
Y= 0.9000	DWDX=-0.54233207E-05	QY=-0.31506192E-01	V=-0.14607751E-06
	DWDY=-0.54233207E-05	NX= 0.18581878E-00	PHI=-0.13668749E-01
	MX= 0.38998261E-02	NY= 0.18581878E-00	
	MY= 0.38998261E-02	NXY= 0.12426012E 01	
	MXY=-0.53807371E-02		
X= 1.0000	W= 0.62607561E-12	QX=-0.11243289E-00	U=-0.47923005E-06
Y= 0.5000	DWDX=-0.15905852E-04	QY=-0.56039826E-15	V=-0.16146122E-21
	DWDY=-0.25834229E-19	NX= 0.14298717E-06	PHI=-0.16363652E-07
	MX= 0.42686226E-08	NY= 0.23263245E-06	
	MY= 0.17270877E-08	NXY= 0.36651794E-08	
	MXY=-0.71967630E-10		
X= 1.0000	W= 0.61011454E-12	QX=-0.11364172E-00	U=-0.45824580E-06
Y= 0.6000	DWDX=-0.15496200E-04	QY= 0.83110748E-09	V=-0.16014045E-13
	DWDY=-0.32961290E-12	NX= 0.14224924E-06	PHI=-0.15649211E-07
	MX= 0.42438433E-08	NY= 0.22379440E-06	

Contrails

Table 3 (Concluded)

MY= 0.18068056E-08 NXY= 0.37396531E-00
MXY=-0.93801108E-03

X= 1.0000 W= 0.55612635E-12 QX=-0.11607017E-00 U=-0.39562340E-06
Y= 0.7000 DWDX=-0.14113485E-04 QY= 0.47374141E-09 V=-0.31745619E-13
DWDY=-0.77900640E-12 NX= 0.13692545E-06 PHI=-0.13515858E-07
MX= 0.41362059E-08 NY= 0.19672748E-06
MY= 0.20256497E-08 NXY= 0.74041636E 00
MXY=-0.22101512E-02

X= 1.0000 W= 0.44737985E-12 QX=-0.11413287E-00 U=-0.29325499E-06
Y= 0.8000 DWDX=-0.11338844E-04 QY=-0.31399309E-08 V=-0.46234779E-13
DWDY=-0.14331050E-11 NX= 0.11825279E-06 PHI=-0.10024188E-07
MX= 0.37971626E-08 NY= 0.15015638E-06
MY= 0.22382715E-08 NXY= 0.10767751E 01
MXY=-0.40480227E-02

X= 1.0000 W= 0.26326835E-12 QX=-0.94544816E-01 U=-0.15704298E-06
Y= 0.9000 DWDX=-0.66627169E-05 QY=-0.15722420E-07 V=-0.57329048E-13
DWDY=-0.22648345E-11 NX= 0.74490459E-07 PHI=-0.53710939E-08
MX= 0.28853406E-08 NY= 0.83459752E-07
MY= 0.20945771E-08 NXY= 0.13331102E 01
MXY=-0.63685905E-02

X= 1.0000 W= 0.11393553E-18 QX=-0.84500299E-07 U=-0.61755604E-13
Y= 1.0000 DWDX=-0.28796535E-11 QY=-0.84500302E-07 V=-0.61755604E-13
DWDY=-0.28796536E-11 NX= 0.34178321E-13 PHI=-0.21132486E-14
MX= 0.22315691E-14 NY= 0.34178324E-13
MY= 0.22315686E-14 NXY= 0.14349679E 01
MXY=-0.80768553E-02

B. POINT MATCHING SOLUTION

1. Governing Equation

The solution of the governing differential equations (Eq. 3-1) for a shallow, spherical, isotropic shell can be written as

$$\left. \begin{aligned} w &= w_p + w_c \\ \Phi &= \Phi_p + \Phi_c \end{aligned} \right\} \quad (3-10)$$

where w_p and Φ_p are the particular solutions and w_c and Φ_c are the complementary solutions.

2. Complementary Solution

For a simply connected region containing the coordinate origin the complementary solution in polar coordinates, Eqs. (2-9) and (2-10) reduce to

$$\begin{aligned} w_c &= C_{01} + C_{03} \text{ber } x + C_{04} \text{bei } x + \sum_{n=1}^{\infty} (C_{n1} x^n \\ &\quad + C_{n3} \text{ber}_n x + C_{n4} \text{bei}_n x) \cos n\theta + \\ &\quad \sum_{n=1}^{\infty} (\bar{C}_{n1} x^n + \bar{C}_{n3} \text{ber}_n x + \bar{C}_{n4} \text{bei}_n x) \sin n\theta \end{aligned} \quad (3-11)$$

$$\begin{aligned} |\Lambda| \Phi_c &= C_{03} \text{bei } x - C_{04} \text{ber } x + C_{19} (x\theta \sin \theta - x \ln x \cos \theta) \\ &\quad + \bar{C}_{19} (x\theta \cos \theta + x \ln x \sin \theta) + \sum_{n=1}^{\infty} (C_{n3} \text{bei } x \\ &\quad - C_{n4} \text{ber } x + C_{n7} x^n) \cos n\theta + \sum_{n=1}^{\infty} (\bar{C}_{n3} \text{bei}_n x \\ &\quad - \bar{C}_{n4} \text{ber } x + \bar{C}_{n7} x^n) \sin n\theta \end{aligned} \quad (3-12)$$

Contrails

where now, it is recalled, x is a nondimensional radius.

If the applied load and boundary conditions have symmetry properties with respect to two or more axes, then one can take advantage of this by selecting a solution which reflects the symmetry properties and satisfies the boundary conditions only along as much of the boundary as needed. Hence, Eqs. (3-11) and (3-12) reduce to

$$w_c = C_{01} + C_{03}ber\ x + C_{04}bei\ x + \sum_{n=m, 2m}^{\infty} (C_{n1}x^n + C_{n3}ber_n\ x + C_{n4}bei_n\ x) \cos\ n\theta \quad (3-13)$$

$$|\Lambda|\phi_c = C_{03}bei\ x + C_{04}ber\ x + \sum_{n=m, 2m}^{\infty} (C_{n3}bei_n\ x - C_{n4}ber\ x + C_{n7}x^n) \cos\ n\theta \quad (3-14)$$

where m = number of symmetry axes. For numerical computation, the upper limit of this series is chosen as N . The number of unknown coefficients retained will be

$$L = 3 + \frac{4N}{m} \quad (3-15)$$

3. Particular Solution

Consider the particular solution of

$$\nabla^4 \phi_p - \frac{Et}{R} \nabla^2 w_p = -(1-\nu) \nabla^2 \Omega \quad (3-16a)$$

$$\nabla^4 w_p + \frac{1}{RD} \nabla^2 \phi_p = \frac{q}{D} - \frac{2\Omega}{RD} \quad (3-16b)$$

From Eq. (3-16b)

$$\nabla^4 \phi = R \nabla^2 q - 2 \nabla^2 \Omega - RD \nabla^6 w_p$$

Substituting into Eq. (3-16a) gives

Contrails

$$\nabla^6 w_p + \frac{Et}{R^2 D} \nabla^2 w_p = - \frac{(1+\nu)}{RD} \nabla^2 \Omega + \frac{1}{D} \nabla^2 q \quad (3-17a)$$

Similarly substituting for $\nabla^4 w_p$ from Eq. (3-16a) into Eq. (3-16b) we get

$$\nabla^8 \phi_p + \frac{Et}{R^2 D} \nabla^2 \phi_p = \frac{Et}{RD} q - \frac{2Et\Omega}{R^2 D} - (1-\nu) \nabla^4 \Omega \quad (3-17b)$$

The tangential components of the loading are obtained from the potential function Ω by

$$\left. \begin{aligned} p_r &= - \frac{\partial \Omega}{\partial r} \\ p_\theta &= - \frac{1}{r} \frac{\partial \Omega}{\partial \theta} \end{aligned} \right\} \quad (3-18)$$

For the case of uniform pressure normal to the surface we have

$$\left. \begin{aligned} q &= q_0 \\ p_r &= p_\theta = 0 \end{aligned} \right\} \quad (3-19)$$

Therefore, $\Omega = 0$.

Equations (3-17) become

$$\nabla^6 w_p + \frac{Et}{R^2 D} \nabla^2 w_p = 0$$

$$\nabla^8 \phi_p + \frac{Et}{R^2 D} \nabla^2 \phi_p = \frac{Et}{RD} q_0$$

yielding the particular solutions

$$\left. \begin{aligned} w_p &= 0 \\ \phi_p &= \frac{q_0 R}{4} r^2 \end{aligned} \right\} \quad (3-20)$$

Substituting the values of w_p and ϕ_p into Eqs. (2-12), (2-13), (2-16), (2-17), (2-24), (2-25), (2-26), (2-29), (2-30) and (2-31), we find

$$\left. \begin{aligned}
 w_p &= \frac{\partial w_p}{\partial n} = \frac{\partial w_p}{\partial t} = 0 \\
 (M_n)_p &= (M_t)_p = (M_{nt})_p = 0 \\
 (N_{nt})_p &= 0 \\
 (N_n)_p &= (N_t)_p = \frac{q_0 R}{2} \\
 (u_n)_p &= \frac{(1-\nu) q_0 R \cos \phi}{2 E t} r \\
 (u_t)_p &= - \frac{(1-\nu) q_0 R \sin \phi}{2 E t} r
 \end{aligned} \right\}$$

(Quantities in the tangential direction are obtained from the above equations by replacing ϕ by $(\phi + \pi/2)$).

4. Point Matching Method

The unknown constants C_{01} , C_{03} , C_{04} , C_{n1} , C_{n3} , C_{n4} , and C_{n7} in Eqs. (3-12) and (3-14) can be determined by satisfying the boundary conditions at discrete points, where the number of boundary condition equations obtained from these discrete points is equal to the number of unknown constants. In the case of shallow shells we can apply four independent boundary conditions along an edge (cf., Eqs. (2-18), (2-19), (2-20), and (2-21)). A computer program was written which is capable of setting up the boundary condition equations and solving them for shallow, spherical, isotropic shells having arbitrary boundary shapes. For the sake of determining the accuracy of the point matching method, the case of a uniformly loaded, square shallow shell was taken, the shell having the same dimensions and properties as given previously in this chapter. The shear diaphragm boundary conditions were approximated at discrete points by the point matching method.

The shell has four axes of symmetry (Fig. 5) and the load has symmetric properties with respect to any axes (polar symmetry). The unknown constants were determined by satisfying the boundary conditions along 1/8 of the entire boundary. The number of boundary condition equations is

$$k = 3 + 4 (I-1)$$

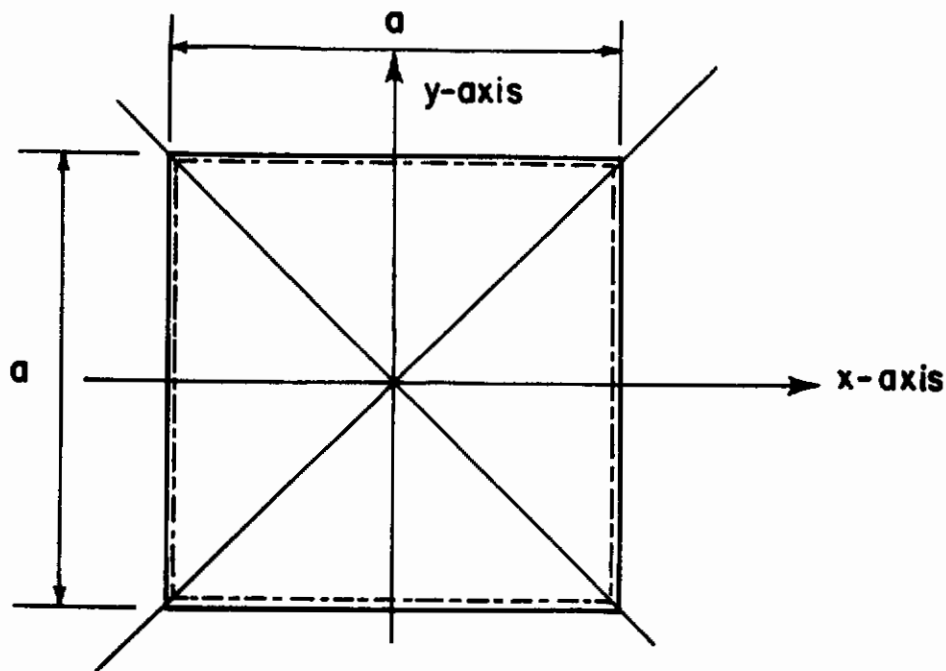


Figure 5. Coordinates for shallow shell having square planform

where k = number of boundary equations, and I = number of points chosen along the boundary segment. The cases where 3, 4, 5, and 6 points (Fig. 6) on the segment were considered.

Table 4-a, 4-b, 4-c, 4-d shows the residuals obtained for the various solutions. The maximum value of the residual for each case is compared with the maximum value of the parameter under consideration within the shell in Table 5. These ratios provide a meaningful interpretation of the scale of the maximum boundary residuals. Finally, numerical results for the various point matching solutions for the different physical parameters evaluated within the shell are compared with these given by the Navier (exact) solution in Figs. 7 through 11. The values given at each point correspond, from top to bottom, to the point matching results using 3, 4, 5, and 6 points, sequentially. The exact results are given in parentheses.

C. COMPARISON OF RESULTS

The residuals along the boundary were low (Tables 4) which implies that a good solution was expected.

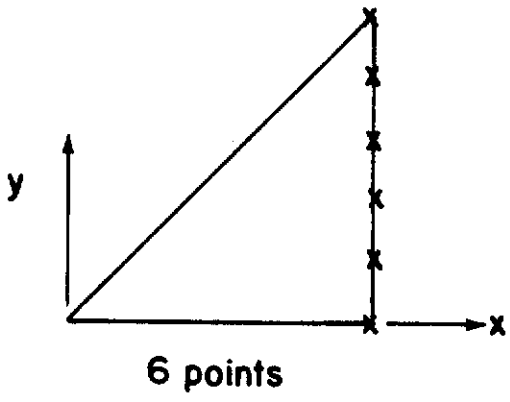
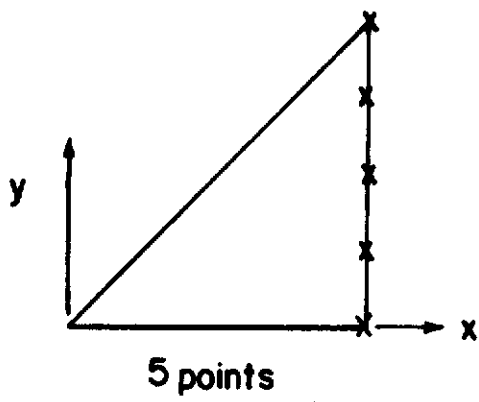
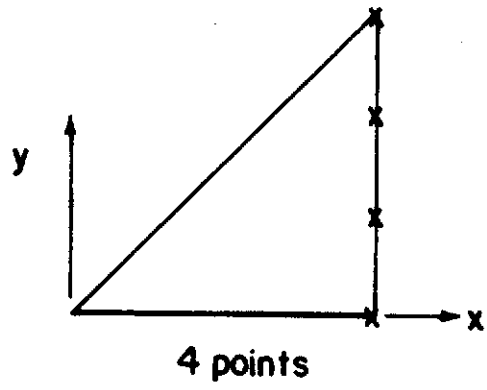
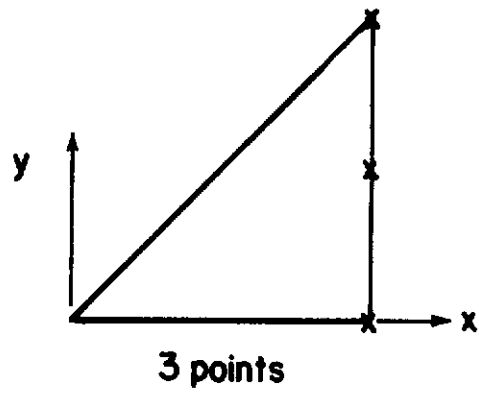


Figure 6. Boundary points used with point matching method

Contrails

Table 4-a. Residuals Along the Boundary, Shear Diaphragm
(3 Points Matched), R/t = 50, R/a = 1.932

Y	w	Mn	v	Nn
0.000*	-0.37403 x 10 ⁻¹²	0.46609 x 10 ⁻⁸	0.00	-0.21830 x 10 ⁻⁵
0.025	-0.35745 x 10 ⁻⁹	0.91708 x 10 ⁻⁸	-0.21051 x 10 ⁻⁹	-0.20095 x 10 ⁻⁹
0.050	-0.13672 x 10 ⁻⁸	0.35090 x 10 ⁻⁵	-0.39881 x 10 ⁻⁹	-0.76190 x 10 ⁻⁹
0.075	-0.28528 x 10 ⁻⁸	0.73489 x 10 ⁻⁵	-0.54514 x 10 ⁻⁹	-0.15831 x 10 ⁻²
0.100	-0.45385 x 10 ⁻⁸	0.11764 x 10 ⁻⁴	-0.63435 x 10 ⁻⁹	-0.25073 x 10 ⁻²
0.125	-0.60798 x 10 ⁻⁸	0.15890 x 10 ⁻⁴	-0.65770 x 10 ⁻⁹	-0.33403 x 10 ⁻²
0.150	-0.71008 x 10 ⁻⁸	0.18757 x 10 ⁻⁴	-0.61396 x 10 ⁻⁹	-0.38746 x 10 ⁻²
0.175	-0.72402 x 10 ⁻⁸	0.19377 x 10 ⁻⁴	-0.50970 x 10 ⁻⁹	-0.39174 x 10 ⁻²
0.200	-0.61997 x 10 ⁻⁸	0.16859 x 10 ⁻⁴	-0.35883 x 10 ⁻⁹	-0.33204 x 10 ⁻²
0.225	-0.37945 x 10 ⁻⁸	0.10516 x 10 ⁻⁴	-0.18109 x 10 ⁻⁹	-0.20080 x 10 ⁻²
0.250*	0.12013 x 10 ⁻¹¹	-0.16114 x 10 ⁻⁷	0.19849 x 10 ⁻¹²	-0.23320 x 10 ⁻⁵
0.275	0.50172 x 10 ⁻⁸	-0.14668 x 10 ⁻⁴	0.16123 x 10 ⁻⁹	0.25595 x 10 ⁻²
0.300	0.10865 x 10 ⁻⁷	-0.32829 x 10 ⁻⁴	0.28104 x 10 ⁻⁹	0.54203 x 10 ⁻²
0.325	0.16937 x 10 ⁻⁷	-0.53261 x 10 ⁻⁴	0.34510 x 10 ⁻⁹	0.82125 x 10 ⁻²
0.350	0.22433 x 10 ⁻⁷	-0.74025 x 10 ⁻⁴	0.34834 x 10 ⁻⁹	0.10490 x 10 ⁻¹
0.375	0.26422 x 10 ⁻⁷	-0.92429 x 10 ⁻⁴	0.20728 x 10 ⁻⁹	0.11786 x 10 ⁻¹
0.400	0.27948 x 10 ⁻⁷	-0.10500 x 10 ⁻³	0.20998 x 10 ⁻⁹	0.11698 x 10 ⁻¹
0.425	0.26188 x 10 ⁻⁷	-0.10747 x 10 ⁻³	0.11355 x 10 ⁻⁹	0.10017 x 10 ⁻¹
0.450	0.20669 x 10 ⁻⁷	-0.94799 x 10 ⁻⁴	0.37403 x 10 ⁻¹⁰	0.68901 x 10 ⁻²
0.475	0.11555 x 10 ⁻⁷	-0.61164 x 10 ⁻⁴	0.17482 x 10 ⁻¹¹	0.30348 x 10 ⁻³
0.500*	0.37090 x 10 ⁻¹¹	-0.67796 x 10 ⁻⁸	-0.62753 x 10 ⁻¹²	0.24661 x 10 ⁻⁵

*Points on the boundary matched.

Contrails

Table 4-b. Residuals Along the Boundary, Shear Diaphragm
(4 Points Matched), R/t = 50, R/a = 1.932

y	w	Mn	v	Nn
0.00*	0.24426 x 10 ⁻¹¹	0.11616 x 10 ⁻⁷	0.0	0.25332 x 10 ⁻⁸
0.025	-0.36628 x 10 ⁻⁹	-0.72022 x 10 ⁻⁶	0.37883 x 10 ⁻⁹	-0.38356 x 10 ⁻⁸
0.050	-0.13466 x 10 ⁻⁸	-0.27650 x 10 ⁻⁵	0.70204 x 10 ⁻⁹	-0.13941 x 10 ⁻²
0.075	-0.25807 x 10 ⁻⁸	-0.56308 x 10 ⁻⁵	0.91506 x 10 ⁻⁹	-0.26367 x 10 ⁻²
0.100	-0.35324 x 10 ⁻⁸	-0.83494 x 10 ⁻⁵	0.96618 x 10 ⁻⁹	-0.35435 x 10 ⁻²
0.125	-0.35730 x 10 ⁻⁸	-0.93069 x 10 ⁻⁵	0.80956 x 10 ⁻⁹	-0.34963 x 10 ⁻²
0.150*	-0.20861 x 10 ⁻⁸	-0.60704 x 10 ⁻⁵	0.40992 x 10 ⁻⁹	-0.19762 x 10 ⁻²
0.175	0.14188 x 10 ⁻⁸	0.47111 x 10 ⁻⁵	-0.25129 x 10 ⁻⁹	0.12829 x 10 ⁻²
0.200	0.71989 x 10 ⁻⁸	0.27256 x 10 ⁻⁴	-0.11687 x 10 ⁻⁸	0.61597 x 10 ⁻²
0.225	0.15190 x 10 ⁻⁷	0.66363 x 10 ⁻⁴	-0.23056 x 10 ⁻⁸	0.12058 x 10 ⁻¹
0.250	0.24957 x 10 ⁻⁷	0.12683 x 10 ⁻³	-0.35884 x 10 ⁻⁸	0.17894 x 10 ⁻¹
0.275	0.35684 x 10 ⁻⁷	0.21247 x 10 ⁻³	-0.49037 x 10 ⁻⁸	0.22175 x 10 ⁻¹
0.300	0.46230 x 10 ⁻⁷	0.32478 x 10 ⁻³	-0.61018 x 10 ⁻⁸	0.23203 x 10 ⁻¹
0.325	0.55235 x 10 ⁻⁷	0.46115 x 10 ⁻³	-0.70064 x 10 ⁻⁸	0.19394 x 10 ⁻¹
0.350*	0.61285 x 10 ⁻⁷	0.61275 x 10 ⁻³	-0.74367 x 10 ⁻⁸	0.97341 x 10 ⁻²
0.375	0.63111 x 10 ⁻⁷	0.76218 x 10 ⁻³	-0.72381 x 10 ⁻⁸	-0.56520 x 10 ⁻²
0.400	0.59817 x 10 ⁻⁷	0.88104 x 10 ⁻³	-0.63289 x 10 ⁻⁸	-0.24845 x 10 ⁻¹
0.425	0.51085 x 10 ⁻⁷	0.92784 x 10 ⁻³	-0.47573 x 10 ⁻⁸	-0.43428 x 10 ⁻¹
0.450	0.37322 x 10 ⁻⁷	0.84637 x 10 ⁻³	-0.27707 x 10 ⁻⁸	-0.53788 x 10 ⁻¹
0.475	0.19695 x 10 ⁻⁷	0.56539 x 10 ⁻³	-0.89267 x 10 ⁻⁹	-0.44519 x 10 ⁻¹
0.500*	-0.16929 x 10 ⁻¹¹	-0.27792 x 10 ⁻⁷	-0.20522 x 10 ⁻¹¹	0.26022 x 10 ⁻⁶

* Points on the boundary matched.

Contrails

Table 4-c. Residuals Along the Boundary, Shear Diagram
(5 Points Matched), R/t = 50, R/a = 1.932

y	w	Mn	v	Nn
0.000*	-0.59021 x 10 ⁻¹¹	0.85943 x 10 ⁻⁸	0.0	0.14976 x 10 ⁻⁵
0.025	-0.16852 x 10 ⁻¹⁰	0.21831 x 10 ⁻⁸	-0.33812 x 10 ⁻¹¹	-0.53719 x 10 ⁻⁵
0.050	-0.41607 x 10 ⁻¹⁰	0.70221 x 10 ⁻⁸	-0.54489 x 10 ⁻¹¹	-0.21122 x 10 ⁻⁴
0.075	-0.60514 x 10 ⁻¹⁰	0.10816 x 10 ⁻⁵	-0.55872 x 10 ⁻¹¹	-0.33490 x 10 ⁻⁴
0.100	-0.50980 x 10 ⁻¹⁰	0.92525 x 10 ⁻⁸	-0.35224 x 10 ⁻¹¹	-0.28864 x 10 ⁻⁴
0.125*	-0.63921 x 10 ⁻¹²	-0.31978 x 10 ⁻⁷	-0.21280 x 10 ⁻¹²	-0.37253 x 10 ⁻⁷
0.150	0.82922 x 10 ⁻¹⁰	-0.16836 x 10 ⁻⁵	0.30948 x 10 ⁻¹¹	0.47944 x 10 ⁻⁴
0.175	0.16880 x 10 ⁻⁹	-0.34592 x 10 ⁻⁵	0.50910 x 10 ⁻¹¹	0.96574 x 10 ⁻⁴
0.200	0.20977 x 10 ⁻⁹	-0.44063 x 10 ⁻⁵	0.49694 x 10 ⁻¹¹	0.11880 x 10 ⁻³
0.225	0.15916 x 10 ⁻⁹	-0.34821 x 10 ⁻⁵	0.28667 x 10 ⁻¹¹	0.89958 x 10 ⁻⁴
0.250*	-0.53000 x 10 ⁻¹¹	-0.19448 x 10 ⁻⁷	-0.22428 x 10 ⁻¹²	0.14901 x 10 ⁻⁵
0.275	-0.25869 x 10 ⁻⁹	0.57242 x 10 ⁻⁵	-0.27672 x 10 ⁻¹¹	-0.12758 x 10 ⁻³
0.300	-0.51689 x 10 ⁻⁹	0.12117 x 10 ⁻⁴	-0.35103 x 10 ⁻¹¹	-0.24860 x 10 ⁻³
0.325	-0.64692 x 10 ⁻⁹	0.16027 x 10 ⁻⁴	-0.22048 x 10 ⁻¹¹	-0.29558 x 10 ⁻³
0.350	-0.50629 x 10 ⁻⁹	0.13284 x 10 ⁻⁴	-0.54246 x 10 ⁻¹¹	-0.21371 x 10 ⁻³
0.375*	-0.11775 x 10 ⁻¹⁰	-0.25972 x 10 ⁻⁷	0.76039 x 10 ⁻¹²	0.69290 x 10 ⁻⁶
0.400	0.77816 x 10 ⁻⁹	-0.25298 x 10 ⁻⁴	-0.15964 x 10 ⁻¹¹	0.26707 x 10 ⁻³
0.425	0.15988 x 10 ⁻⁸	-0.58237 x 10 ⁻⁴	-0.65635 x 10 ⁻¹¹	0.42116 x 10 ⁻³
0.450	0.19921 x 10 ⁻⁸	-0.85134 x 10 ⁻⁴	-0.10107 x 10 ⁻¹⁰	0.29610 x 10 ⁻³
0.475	0.14733 x 10 ⁻⁸	-0.79438 x 10 ⁻⁴	-0.69453 x 10 ⁻¹¹	-0.64053 x 10 ⁻⁴
0.500*	-0.63118 x 10 ⁻¹¹	-0.18039 x 10 ⁻⁷	-0.72345 x 10 ⁻¹²	0.91642 x 10 ⁻⁶

*Points on the boundary matched.

Contrails

Table 4-d. Residuals Along the Boundary, Shear Diaphragm
(6 Points Matched), R/t = 50, R/a = 1.932

y	w	Mn	v	Nn
0.000*	-0.16343 x 10 ⁻¹³	0.29838 x 10 ⁻⁸	0.0	-0.38669 x 10 ⁻⁵
0.025	0.23017 x 10 ⁻¹¹	-0.85006 x 10 ⁻⁷	0.40713 x 10 ⁻¹²	-0.23022 x 10 ⁻⁵
0.050	0.67970 x 10 ⁻¹¹	-0.24954 x 10 ⁻⁸	0.56945 x 10 ⁻¹²	0.56624 x 10 ⁻⁶
0.075	0.68862 x 10 ⁻¹¹	-0.26976 x 10 ⁻⁸	0.39028 x 10 ⁻¹²	0.51409 x 10 ⁻⁶
0.100*	-0.16516 x 10 ⁻¹¹	0.29357 x 10 ⁻⁷	0.41886 x 10 ⁻¹³	-0.52750 x 10 ⁻⁵
0.125	-0.16729 x 10 ⁻¹⁰	0.59331 x 10 ⁻⁸	-0.17195 x 10 ⁻¹²	-0.15192 x 10 ⁻⁴
0.150	-0.28338 x 10 ⁻¹⁰	0.10786 x 10 ⁻⁵	0.27001 x 10 ⁻¹³	-0.22538 x 10 ⁻⁴
0.175	-0.23217 x 10 ⁻¹⁰	0.98430 x 10 ⁻⁸	0.66788 x 10 ⁻¹²	-0.18626 x 10 ⁻⁴
0.200*	0.62130 x 10 ⁻¹¹	-0.30880 x 10 ⁻⁷	0.14247 x 10 ⁻¹¹	0.60350 x 10 ⁻⁶
0.225	0.52053 x 10 ⁻¹⁰	-0.17752 x 10 ⁻⁵	0.18417 x 10 ⁻¹¹	0.29273 x 10 ⁻⁴
0.250	0.87968 x 10 ⁻¹⁰	-0.33128 x 10 ⁻⁵	0.15236 x 10 ⁻¹¹	0.50485 x 10 ⁻⁴
0.275	0.78015 x 10 ⁻¹⁰	-0.31622 x 10 ⁻⁵	0.58652 x 10 ⁻¹²	0.43601 x 10 ⁻⁴
0.300*	-0.16470 x 10 ⁻¹¹	-0.45375 x 10 ⁻⁷	-0.41410 x 10 ⁻¹²	-0.18999 x 10 ⁻⁵
0.325	-0.13551 x 10 ⁻⁹	0.58990 x 10 ⁻⁵	-0.66477 x 10 ⁻¹²	-0.71906 x 10 ⁻⁴
0.350	-0.25191 x 10 ⁻⁹	0.11909 x 10 ⁻⁴	0.18023 x 10 ⁻¹²	-0.12401 x 10 ⁻³
0.375	-0.23792 x 10 ⁻⁹	0.12262 x 10 ⁻⁴	0.14816 x 10 ⁻¹¹	-0.10656 x 10 ⁻³
0.400*	-0.29024 x 10 ⁻¹²	-0.11316 x 10 ⁻⁷	0.16703 x 10 ⁻¹¹	-0.14230 x 10 ⁻⁵
0.425	0.43259 x 10 ⁻⁹	-0.28175 x 10 ⁻⁴	-0.37109 x 10 ⁻¹²	0.12857 x 10 ⁻³
0.450	0.82101 x 10 ⁻⁹	-0.63860 x 10 ⁻⁴	-0.34533 x 10 ⁻¹¹	0.14268 x 10 ⁻³
0.475	0.75229 x 10 ⁻⁹	-0.75373 x 10 ⁻⁴	-0.35560 x 10 ⁻¹¹	-0.37177 x 10 ⁻⁴
0.500*	0.33329 x 10 ⁻¹¹	-0.14762 x 10 ⁻⁷	-0.55293 x 10 ⁻¹²	0.19669 x 10 ⁻⁵

*Points on the boundary matched.

Table 5 . Ratio of Maximum Boundary Residuals to Maximum Values of Physical Parameters in the Shell Interior

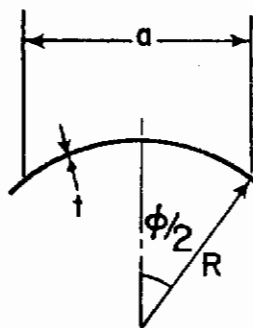
No. of Points Matched	$\left(\frac{\text{Res. } w}{w}\right)_{\text{max.}}$	$\left(\frac{\text{Res. } M_n}{M_n}\right)_{\text{max.}}$	$\left(\frac{\text{Res. } v}{v}\right)_{\text{max.}}$	$\left(\frac{\text{Res. } N_n}{N_n}\right)_{\text{max.}}$
3	0.73 %	1.42 %	0.16 %	1.07 %
4	1.64 %	12.25 %	3.35 %	4.88 %
5	0.05 %	1.12 %	0.01 %	0.04 %
6	0.02 %	1.00 %	0.002 %	0.01 %

As the number of points matched on the boundary was increased, the solution converged rapidly, and five points were enough to obtain an accurate solution as compared to that given by the Navier-type solution.

Throughout the shell, except along the boundary, the point matching solution gave very good results when compared with the 625-term Navier-type solution (Figs. 7 through 11). Here it must be remembered (see Figs. 3 and 4) that the Navier solution itself loses accuracy near the boundary.

Contrails

$w \times 10^5$



SHEAR DIAPHRAGM

$R/t=50$

$R/a=1.932$

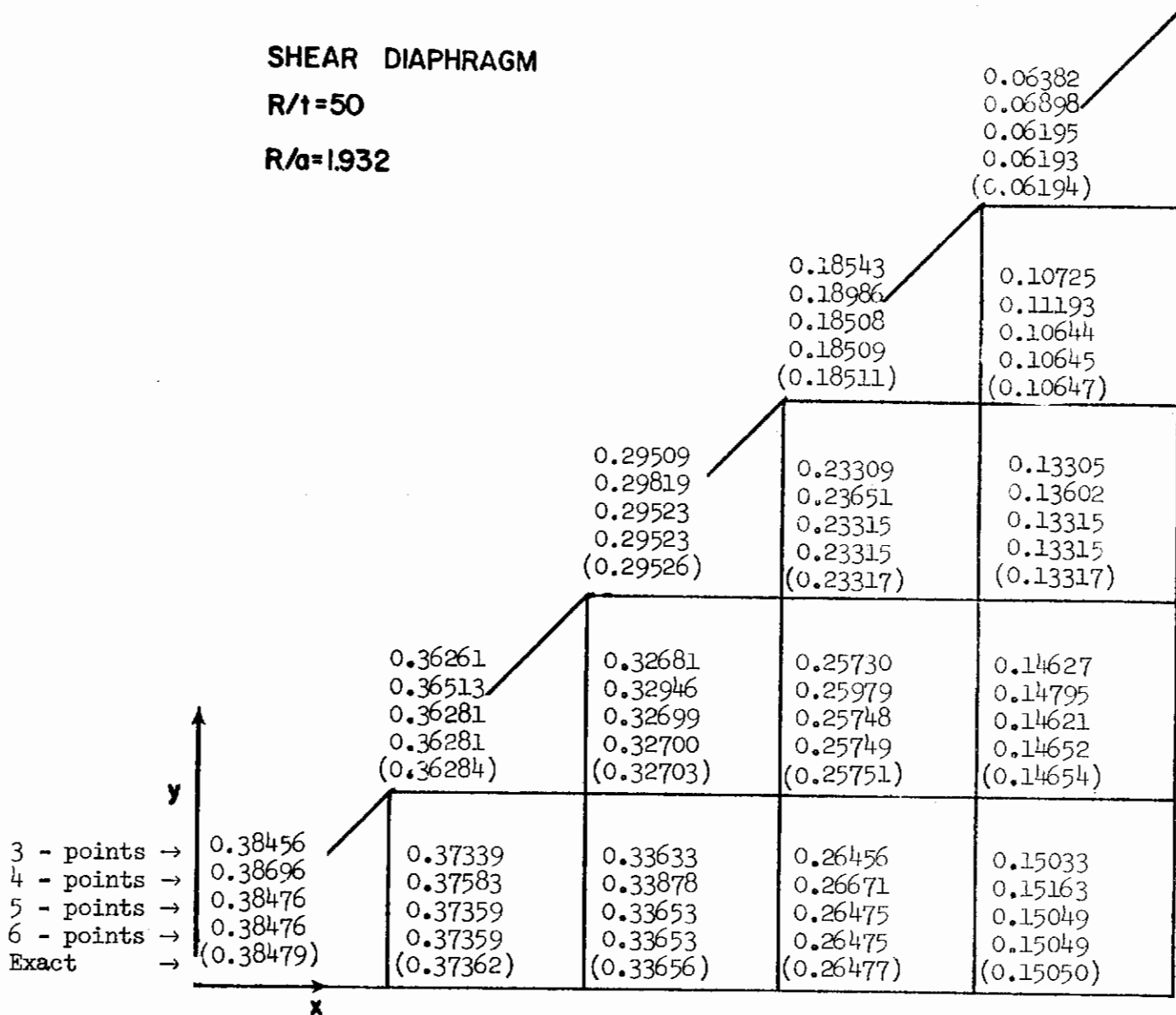


Figure 7. Values of the deflection at interior points

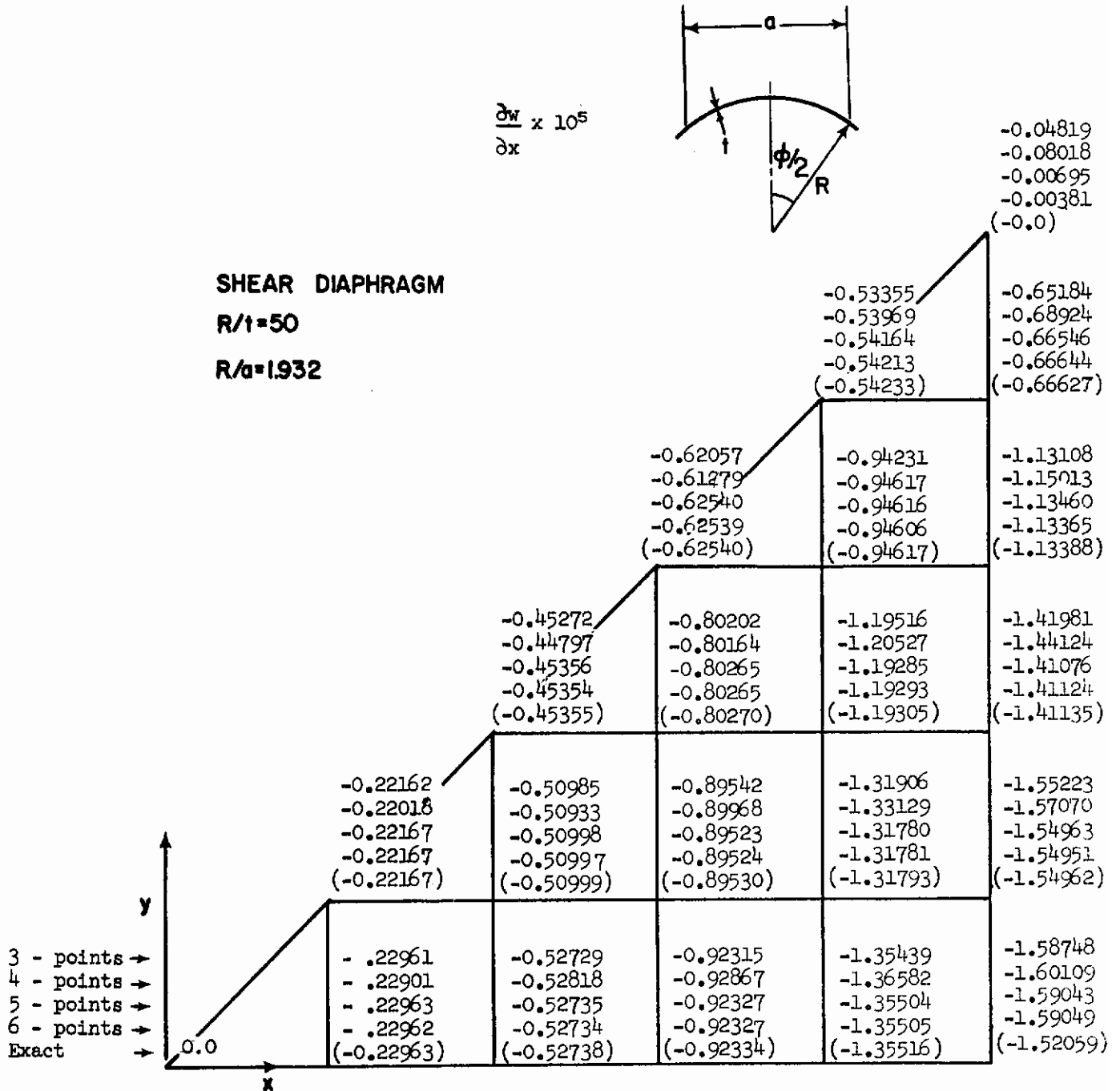
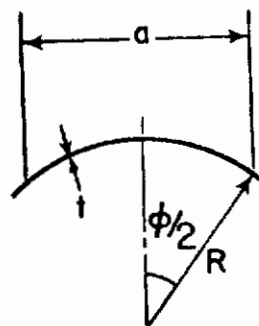


Figure 8. Slope at interior points.

Contrails

$M_x \times 10^2$



SHEAR DIAPHRAGM

$R/t=50$

$R/a=1.932$

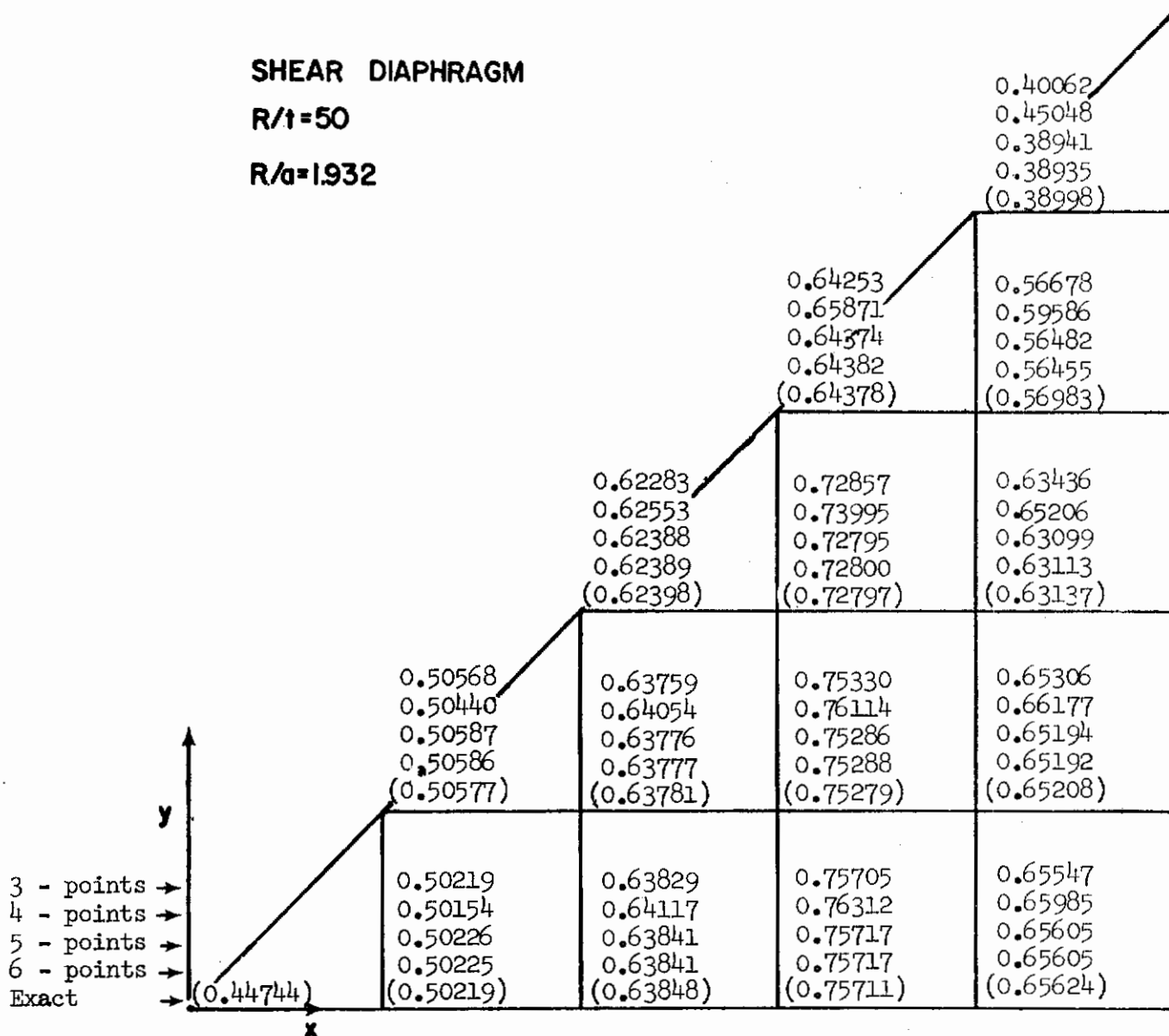
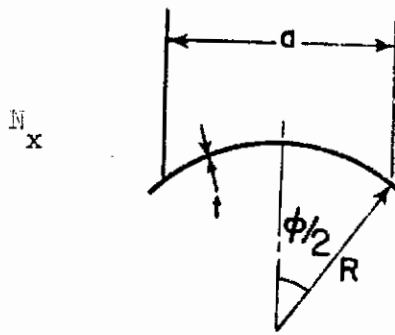


Figure 9. Bending moment of interior points



SHEAR DIAPHRAGM
 $R/t=50$
 $R/a=1.932$

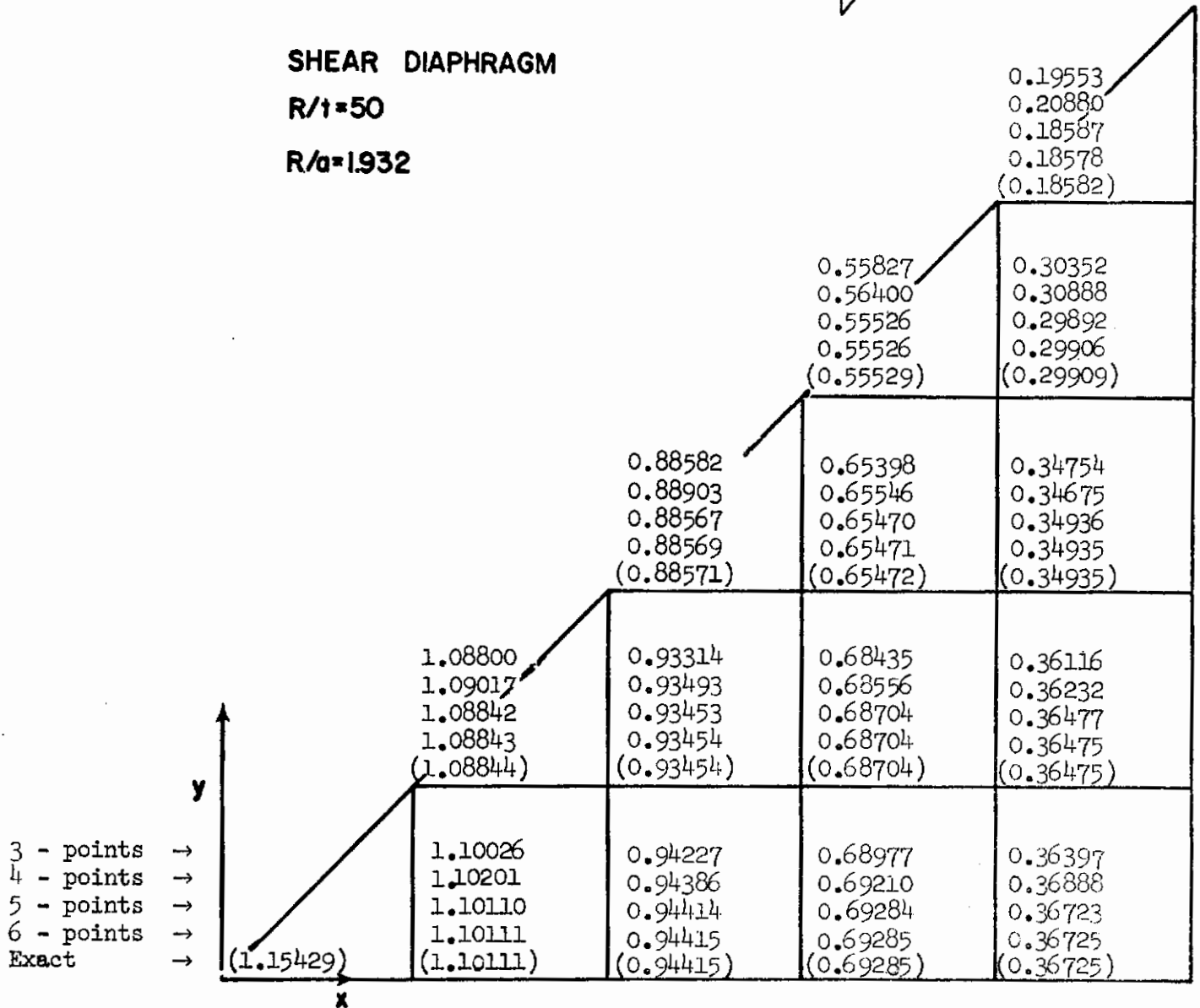


Figure 10. Membrane force at interior points

IV. SHALLOW SPHERICAL SHELLS HAVING REGULAR POLYGONAL PLANFORMS

In this chapter the method of point matching is applied to the problem of the uniformly loaded, shallow, spherical shell having regular polygonal planform. Two drastically different types of boundaries are considered; i.e., clamped edges and edges supported by shear diaphragms. Extensive numerical results are presented for these types of boundary conditions for polygons having 3, 4, 5, and 6 sides and for two R/t (spherical radius/thickness) ratios. These problems generally have no previous solutions in the published literature.

The point matching method is then extended to utilize more boundary condition equations than unknown deflection modes. This technique, called the "boundary point least squares" method, is found to improve the accuracy of the results, giving accurate results for the problems solved earlier by point matching. This modified technique is demonstrated in two different ways.

An attempt to summarize and compare the great number of results presented in this report is made in the last part.

A. POINT MATCHING SOLUTIONS

For a simply connected region containing the coordinate axes, the applied load and the boundary conditions have symmetry properties with respect to two or more axes, the complementary solution in polar coordinates, Eqs. (3-11) and (3-12), are reduced to

$$w_c = C_{01} + C_{03} \operatorname{ber} x + C_{04} \operatorname{bei} x + \sum_{n=m, 2m}^{\infty} (C_{n1} x^n + C_{n3} \operatorname{ber}_n x + C_{n4} \operatorname{bei}_n x) \cos n\theta \quad (4-1)$$

and

$$|\lambda| \phi_c = C_{03} \operatorname{bei} x - C_{04} \operatorname{ber} x + \sum_{n=m, 2m}^{\infty} (C_{n3} \operatorname{bei}_n x - C_{n4} \operatorname{ber}_n x + C_{n7} x^n) \cos n\theta, \quad (4-2)$$

where m is the number of symmetry axes.

Suitable particular solutions for a uniform pressure normal to the surface have already been given in Eqs. (3-20) and (3-21) and will be used here.

Contrails

Two types of conditions will be applied uniformly around each boundary: (1) the clamped edge, described by Eqs. (2-20), and (2) the shear diaphragm support, described by Eqs. (2-21).

The unknown constants in Eqs. (4-1) and (4-2) can be determined by satisfying the boundary conditions at discrete points, where the number of equations obtained from discrete points is equal to the number of unknown constants. If the boundary of the shell has a length "c" and if the applied load and the boundary conditions have symmetry properties along a repeated segment whose length L is

$$L = c/2m \quad . \quad (4-3)$$

(In the limiting case of a spherical shell loaded by uniform pressure with circular boundary, the boundary conditions will be satisfied at one point because of the infinite number of symmetry axes.)

The number of unknowns depends on the number of points at which the boundary conditions are to be satisfied. If "I" is the number of such points, then the number of unknown constants will be

$$n = (4I-1) \quad . \quad (4-4)$$

The upper limit "N" of the series in Eqs. (4-1) and (4-2) depends on both the number of symmetry axes "m" and the number of points "I" at which the boundary conditions are satisfied and "N" will be

$$N = m(I-1) \quad . \quad (4-5)$$

The shallow shell having a spherical radius R and a regular, polygonal planform, is loaded by a uniform pressure of intensity q_0 normal to the surface. If S is the interior of the planform which is inscribed within a circle of radius "a," then the polar coordinates "r" and " θ " and the angle " φ " by which the outer normal leads the radial direction are

$$\left. \begin{aligned} r &= \left[a^2 \cos^2\left(\frac{\pi}{m}\right) + y^2 \right]^{1/2} \\ \theta &= \arctan \left[\frac{y}{a \cos\left(\frac{\pi}{m}\right)} \right] \\ \varphi &= -\theta \end{aligned} \right\} \quad (4-6)$$

the origin of the coordinates being the center of the region S (Fig. 12). The problem was solved for polygons having 3, 4, 5, 6, and ∞ sides. Five points matched on the length L of the boundary as shown in Fig. 13. The following values were assigned for the constants

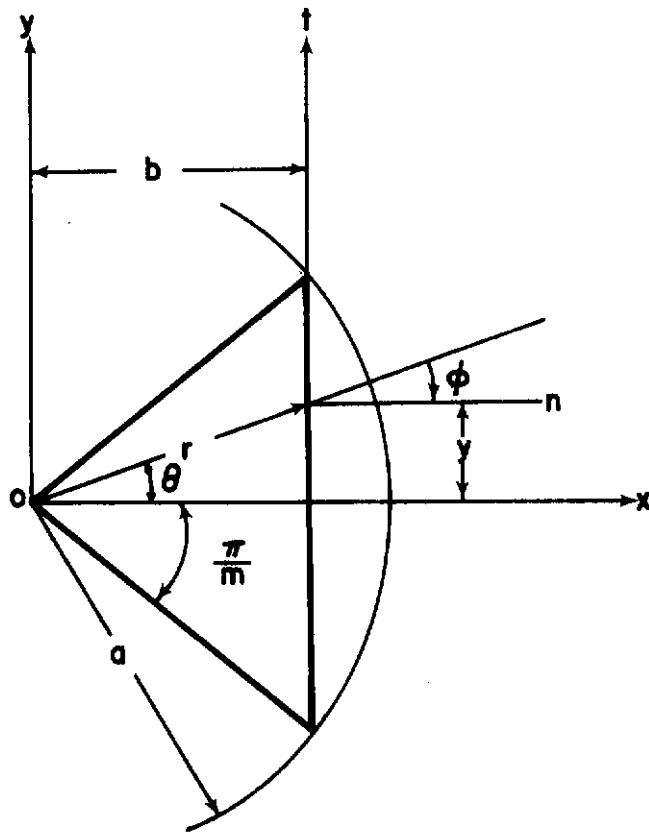


Figure 12. Typical polygonal sector

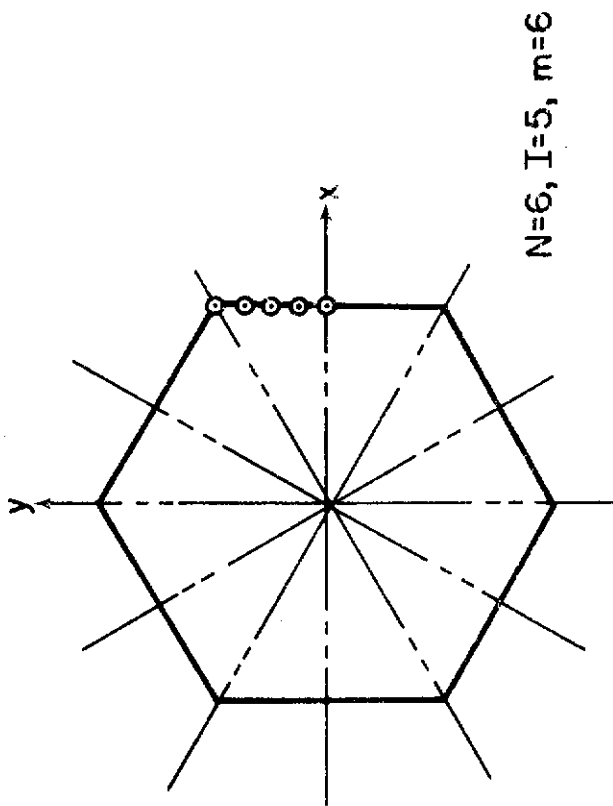
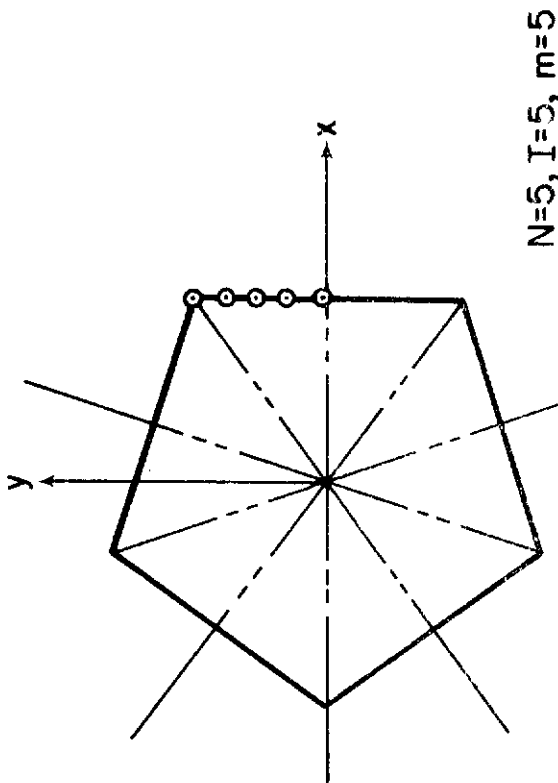
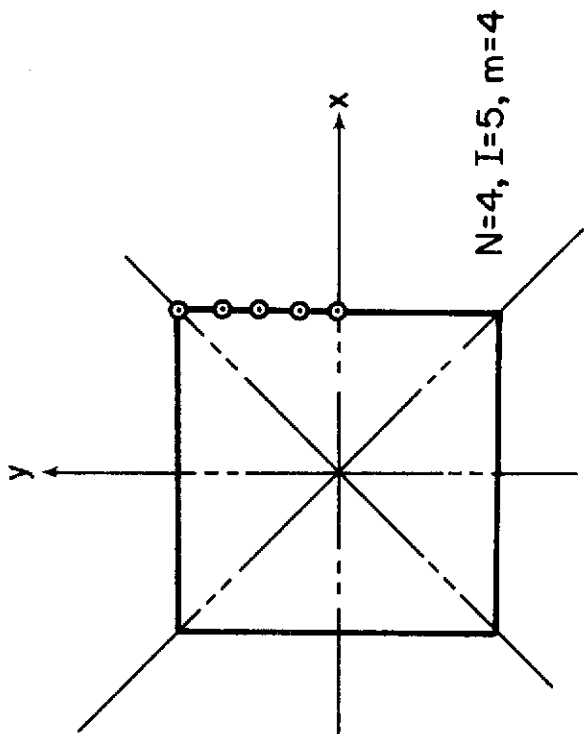
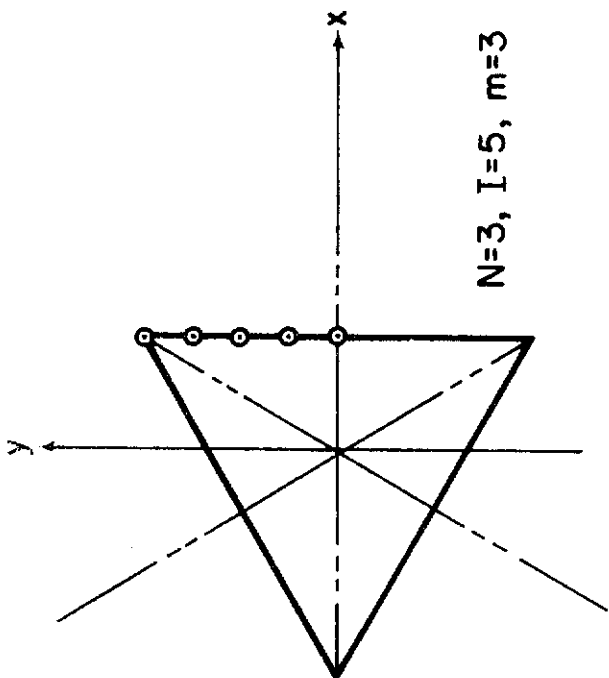


Figure 13. Planform shape, points matched and coordinates

Contrails

$$E = 30 \times 10^8$$

$$R = 1.932$$

$$q_0 = 1$$

$$a = 1/\sqrt{2}$$

$$\nu = 0.3$$

To test the efficacy of the point matching method, solutions were obtained for clamped and shear diaphragm types of boundaries. These give widely different physical and mathematical behavior.

1. Edges Clamped - Two Cases

To judge the effect of varying R/t ratio, two cases were used, the first being a relatively thick shell according to thin shell theory.

Case I - R/t 50 (t = 0.03864)

Tables 6 through 10 give results for N = 3, 4, 5, 6, and ∞ , respectively. Each table consists of three parts. The first part summarizes useful physical quantities along the symmetry axis $\theta = 0$. The second part gives the values of the residuals along the boundary. By themselves, the residuals are useless information. Therefore, in the last part of each table, the ratios are given of the maximum value of the residual for each case to the maximum value of the physical parameter found within the shell. The computer program, as written, has difficulty in evaluating some of the functions at the origin.

Figure 14 shows the oscillating character of the residuals for a typical clamped boundary.

Case II - R/t = 200 (t = 0.00966)

Results are summarized by Tables 11 through 15 in the same manner as in Case I.

2. Edges Supported by Shear Diaphragms

Results are given in Tables 16 through 20 for R/t = 50. Corresponding results for R/t = 200 are available in Ref. 22 and have not been repeated here.

Table 6. Clamped Spherical Shell with Triangular Planform Obtained by Point Matching
($R/t = 50$, $R = 1.932$, $a = 1/\sqrt{2}$, $b = a \cos \pi/3$)

a. Values of the Physical Parameters along $\theta=0$

x/b	0.0	0.2	0.4	0.6	0.8	1.0
w	$.12228 \times 10^{-5}$	$.11478 \times 10^{-5}$	$.91900 \times 10^{-6}$	$.56670 \times 10^{-6}$	$.19215 \times 10^{-6}$	$.15919 \times 10^{-11}$
$\frac{\partial w}{\partial n}$.0	$-.21569 \times 10^{-5}$	$-.42500 \times 10^{-5}$	$-.54838 \times 10^{-5}$	$-.46360 \times 10^{-5}$	$-.13657 \times 10^{-10}$
M_n		$.60325 \times 10^{-2}$	$.47962 \times 10^{-2}$	$.13426 \times 10^{-2}$	$-.53115 \times 10^{-2}$	$-.16177 \times 10^{-1}$
u_n	.0	$-.18567 \times 10^{-7}$	$-.31882 \times 10^{-7}$	$-.34278 \times 10^{-7}$	$-.22464 \times 10^{-7}$	$.11702 \times 10^{-11}$
N_n		.58168	.54953	.50824	.46524	.42669

b. Residuals along the Boundary

y	w	$\frac{\partial w}{\partial n}$	u_n	u_t
.0000*	$.15973 \times 10^{-11}$	$-.12925 \times 10^{-10}$	$.11746 \times 10^{-11}$	$.00000 \times 10^{-89}$
.0765	$.81091 \times 10^{-10}$	$.12162 \times 10^{-8}$	$-.12009 \times 10^{-9}$	$-.43059 \times 10^{-9}$
.1531*	$.29338 \times 10^{-11}$	$-.87990 \times 10^{-11}$	$.28229 \times 10^{-11}$	$.61708 \times 10^{-12}$
.2296	$-.30557 \times 10^{-9}$	$-.51747 \times 10^{-8}$	$.56234 \times 10^{-9}$	$.60410 \times 10^{-9}$
.3062*	$-.59270 \times 10^{-11}$	$-.16761 \times 10^{-10}$	$.11724 \times 10^{-11}$	$-.57975 \times 10^{-12}$
.3827	$.81991 \times 10^{-9}$	$.17316 \times 10^{-7}$	$-.22920 \times 10^{-8}$	$-.11847 \times 10^{-8}$
.4593*	$.55087 \times 10^{-11}$	$-.17379 \times 10^{-10}$	$.10518 \times 10^{-12}$	$-.24293 \times 10^{-11}$
.5358	$-.17604 \times 10^{-8}$	$-.74954 \times 10^{-7}$	$.14591 \times 10^{-7}$	$.29954 \times 10^{-8}$
.6124*	$.10683 \times 10^{-10}$	$.41223 \times 10^{-10}$	$-.56495 \times 10^{-12}$	$-.11049 \times 10^{-11}$

*Points matched on the boundary

c. Ratios of Maximum Residuals to Maximum Values of Physical Parameter within the Shell

	w	$\frac{\partial w}{\partial n}$	u_n	u_t
Maximum residual along the boundary	$.17604 \times 10^{-8}$	$.74954 \times 10^{-7}$	$.14591 \times 10^{-7}$	$.29954 \times 10^{-8}$
Maximum value of the parameter within the shell	$.12228 \times 10^{-5}$	$.54838 \times 10^{-5}$	$.34278 \times 10^{-7}$	$.34278 \times 10^{-7}$
Percentage of maximum residual to maximum value	0.144%	1.367%	42.566%	8.731%

Table 7. Clamped Spherical Shell with Square Planform Obtained by Point Matching
($R/t = 50$, $R = 1.932$, $a = 1/\sqrt{2}$, $b = a \cos \pi/4$)

a. Values of the Physical Parameters along $\theta=0$

x/b	0.0	0.2	0.4	0.6	0.8	1.0
w	$.18161 \times 10^{-5}$	$.17146 \times 10^{-5}$	$.14066 \times 10^{-5}$	$.90700 \times 10^{-6}$	$.32631 \times 10^{-6}$	$.48696 \times 10^{-11}$
$\frac{\partial w}{\partial n}$.0	$-.20400 \times 10^{-5}$	$-.41074 \times 10^{-5}$	$-.57230 \times 10^{-5}$	$-.53588 \times 10^{-5}$	$.14323 \times 10^{-11}$
M_n		$.41782 \times 10^{-2}$	$.38489 \times 10^{-2}$	$.19838 \times 10^{-2}$	$-.34010 \times 10^{-2}$	$-.14682 \times 10^{-1}$
u_n	.0	$-.36698 \times 10^{-7}$	$-.63566 \times 10^{-7}$	$-.70107 \times 10^{-7}$	$-.47988 \times 10^{-7}$	$.40777 \times 10^{-12}$
N_n		.90453	.85414	.78264	.70690	.68088

b. Residuals along the Boundary

y	w	$\frac{\partial w}{\partial n}$	u_n	u_t
.0000*	$-.48805 \times 10^{-11}$	$.20697 \times 10^{-11}$	$.41922 \times 10^{-12}$	$.00000 \times 10^{-09}$
.0625	$.40851 \times 10^{-9}$	$.61411 \times 10^{-8}$	$-.14434 \times 10^{-8}$	$-.24450 \times 10^{-8}$
.1250*	$-.12959 \times 10^{-11}$	$.65755 \times 10^{-11}$	$-.83278 \times 10^{-13}$	$.52404 \times 10^{-15}$
.1875	$-.15157 \times 10^{-8}$	$-.23463 \times 10^{-7}$	$.62103 \times 10^{-8}$	$.26352 \times 10^{-8}$
.2500*	$.67968 \times 10^{-12}$	$-.51469 \times 10^{-11}$	$.26942 \times 10^{-12}$	$.34359 \times 10^{-12}$
.3125	$.36491 \times 10^{-8}$	$.62504 \times 10^{-7}$	$-.22065 \times 10^{-7}$	$-.14888 \times 10^{-8}$
.3750*	$-.10543 \times 10^{-11}$	$.84290 \times 10^{-10}$	$.13811 \times 10^{-12}$	$.56488 \times 10^{-12}$
.4375	$-.63952 \times 10^{-8}$	$-.15272 \times 10^{-6}$	$.10900 \times 10^{-6}$	$-.21870 \times 10^{-7}$
.5000*	$-.10899 \times 10^{-10}$	$.33243 \times 10^{-9}$	$-.41817 \times 10^{-11}$	$-.43270 \times 10^{-11}$

*Points matched on the boundary

c. Ratios of Maximum Residuals to Maximum Values of Physical Parameter within the Shell

	w	$\frac{\partial w}{\partial n}$	u_n	u_t
Maximum residual along the boundary	$.63952 \times 10^{-8}$	$.15272 \times 10^{-6}$	$.10900 \times 10^{-6}$	$.21870 \times 10^{-7}$
Maximum value of the parameter within the shell	$.18161 \times 10^{-5}$	$.57230 \times 10^{-5}$	$.70107 \times 10^{-7}$	$.70107 \times 10^{-7}$
Percentage of maximum residual to maximum value	0.352%	26.685%	155.476%	31.195%

Table 8. Clamped Spherical Shell with Pentagonal Planform Obtained by Point Matching
 ($R/t = 50$, $R = 1.932$, $a = 1/\sqrt{2}$, $b = a \cos \pi/5$)

a. Values of the Physical Parameters along $\theta=0$

x/b	0.0	0.2	0.4	0.6	0.8	1.0
w	$.13616 \times 10^{-5}$	$.18605 \times 10^{-5}$	$.15503 \times 10^{-5}$	$.10281 \times 10^{-5}$	$.38438 \times 10^{-5}$	$-.42698 \times 10^{-11}$
$\frac{\partial w}{\partial n}$.0	$-.17782 \times 10^{-5}$	$-.36611 \times 10^{-5}$	$-.53640 \times 10^{-5}$	$-.53781 \times 10^{-5}$	$.54661 \times 10^{-13}$
N_n		$.32493 \times 10^{-2}$	$.32866 \times 10^{-2}$	$.21848 \times 10^{-2}$	$-.24143 \times 10^{-2}$	$-.13735 \times 10^{-1}$
u_n	.0	$-.45475 \times 10^{-7}$	$-.78995 \times 10^{-7}$	$-.87576 \times 10^{-7}$	$-.59735 \times 10^{-7}$	$.12666 \times 10^{-11}$
N_n		.98006	.93658	.87122	.79690	.70814

b. Residuals along the Boundary

y	w	$\frac{\partial w}{\partial n}$	u_n	u_t
.0*	$-.42729 \times 10^{-11}$	$.68621 \times 10^{-12}$	$.12602 \times 10^{-11}$.0
.05195	$-.87246 \times 10^{-10}$	$-.16539 \times 10^{-8}$	$.50640 \times 10^{-9}$	$.32292 \times 10^{-9}$
.10390*	$-.41499 \times 10^{-11}$	$-.85079 \times 10^{-11}$	$.12948 \times 10^{-11}$	$.25830 \times 10^{-12}$
.15586	$.29532 \times 10^{-9}$	$.63519 \times 10^{-8}$	$-.20665 \times 10^{-9}$	$-.10931 \times 10^{-9}$
.20781*	$-.32161 \times 10^{-11}$	$-.80868 \times 10^{-11}$	$.11237 \times 10^{-11}$	$-.29581 \times 10^{-12}$
.25977	$-.69812 \times 10^{-9}$	$-.18008 \times 10^{-7}$	$.65895 \times 10^{-9}$	$-.12081 \times 10^{-9}$
.31172*	$-.31064 \times 10^{-11}$	$-.79302 \times 10^{-11}$	$.11630 \times 10^{-11}$	$.14087 \times 10^{-11}$
.36367	$.11807 \times 10^{-9}$	$.63282 \times 10^{-7}$	$-.26680 \times 10^{-7}$	$.11352 \times 10^{-7}$
.41563*	$-.12031 \times 10^{-10}$	$-.28506 \times 10^{-10}$	$.14975 \times 10^{-11}$	$.99926 \times 10^{-12}$

*Points matched on the boundary

c. Ratios of Maximum Residuals to Maximum Values of Physical Parameter within the Shell

	w	$\frac{\partial w}{\partial n}$	u_n	u_t
Maximum residual along the boundary	$.11807 \times 10^{-9}$	$.63282 \times 10^{-7}$	$.26680 \times 10^{-7}$	$.11352 \times 10^{-7}$
Maximum value of the parameter within the shell	$.13616 \times 10^{-5}$	$.53781 \times 10^{-5}$	$.87576 \times 10^{-7}$	$.87576 \times 10^{-7}$
Percentage of maximum residual to maximum value	0.060%	1.177%	30.464%	12.962%

Table 9. Clamped Spherical Shell with Hexagonal Planform Obtained by Point Matching
 ($R/t = 50$, $R = 1.932$, $a = 1/\sqrt{2}$, $b = a \cos \pi/6$)

a. Values of the Physical Parameters along $\theta=0$

x/b	0.0	0.2	0.4	0.6	0.8	1.0
w	$.19939 \times 10^{-5}$	$.18971 \times 10^{-5}$	$.15951 \times 10^{-5}$	$.10743 \times 10^{-5}$	$.41102 \times 10^{-6}$	$.41308 \times 10^{-11}$
$\frac{\partial w}{\partial n}$.0	$-.15982 \times 10^{-5}$	$-.33627 \times 10^{-5}$	$-.50681 \times 10^{-5}$	$-.52826 \times 10^{-5}$	$-.22990 \times 10^{-10}$
M_n		$.27769 \times 10^{-2}$	$.29784 \times 10^{-2}$	$.22264 \times 10^{-2}$	$-.18709 \times 10^{-2}$	$-.13176 \times 10^{-1}$
u_n	.0	$-.49045 \times 10^{-7}$	$-.85699 \times 10^{-7}$	$-.95840 \times 10^{-7}$	$-.65930 \times 10^{-7}$	$-.22338 \times 10^{-11}$
N_n		1.00470	.96280	.89957	.82749	.72304

b. Residuals along the Boundary

y	w	$\partial w / \partial n$	u_n	u_t
.0000*	$.41407 \times 10^{-11}$	$-.22429 \times 10^{-10}$	$-.22224 \times 10^{-11}$.0
.04419	$-.13906 \times 10^{-8}$	$-.26604 \times 10^{-8}$	$.15713 \times 10^{-8}$	$-.76701 \times 10^{-9}$
.08839*	$.38586 \times 10^{-11}$	$-.24961 \times 10^{-12}$	$-.19459 \times 10^{-11}$	$-.50153 \times 10^{-12}$
.13258	$.50310 \times 10^{-9}$	$.93930 \times 10^{-8}$	$-.61820 \times 10^{-8}$	$.21401 \times 10^{-8}$
.17678*	$.24327 \times 10^{-11}$	$-.50288 \times 10^{-10}$	$-.20742 \times 10^{-11}$	$-.94892 \times 10^{-13}$
.22097	$-.10848 \times 10^{-8}$	$-.22139 \times 10^{-7}$	$.17974 \times 10^{-7}$	$-.82427 \times 10^{-8}$
.26517*	$.25384 \times 10^{-11}$	$.88710 \times 10^{-10}$	$-.22955 \times 10^{-11}$	$-.62808 \times 10^{-12}$
.30936	$.16709 \times 10^{-8}$	$.49586 \times 10^{-7}$	$-.61483 \times 10^{-7}$	$.42108 \times 10^{-7}$
.35356*	$.23409 \times 10^{-10}$	$-.39436 \times 10^{-9}$	$-.28208 \times 10^{-11}$	$-.17554 \times 10^{-11}$

*Points matched on the boundary

c. Ratios of Maximum Residuals to Maximum Values of Physical Parameter within the Shell

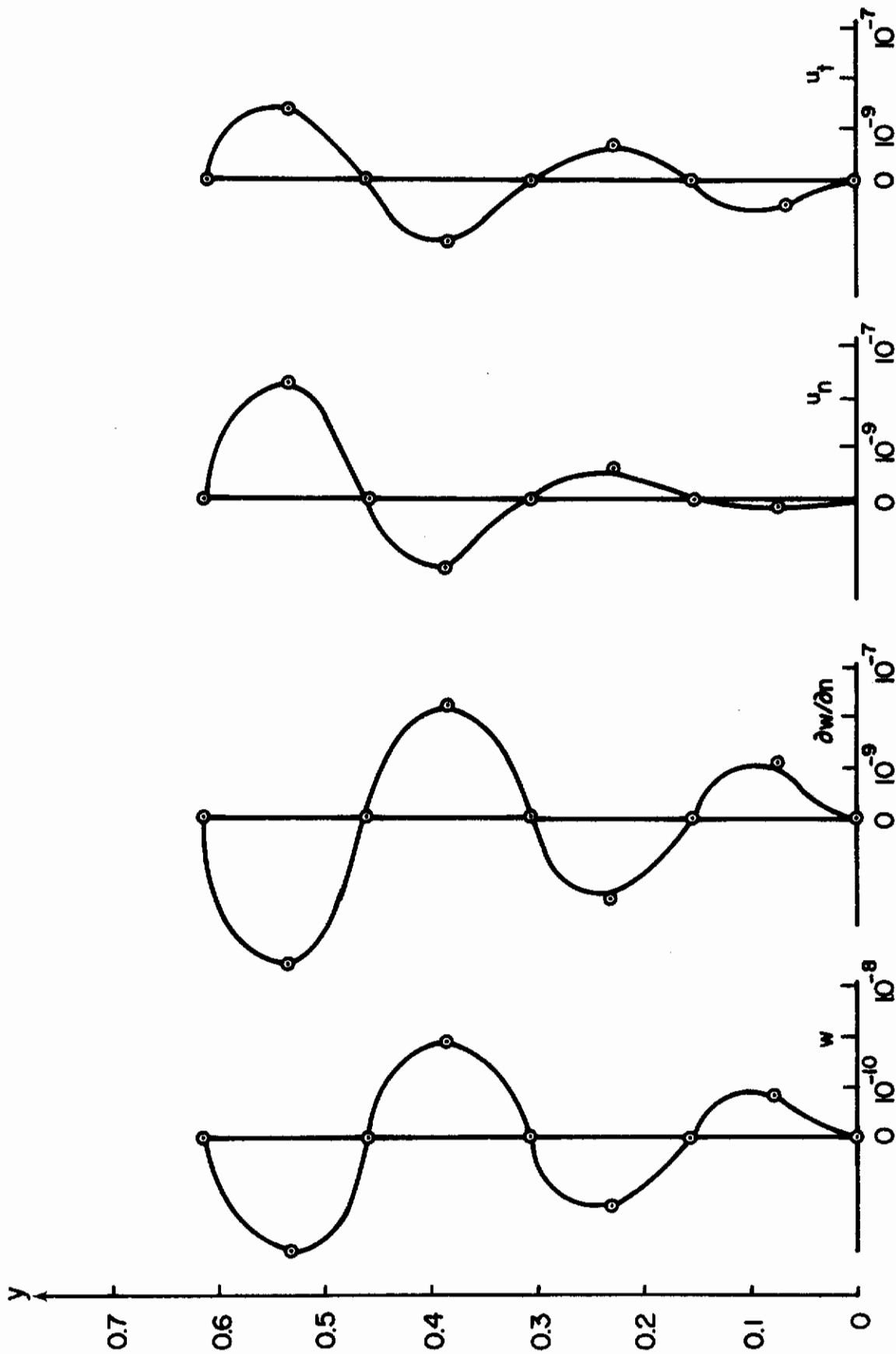
	w	$\partial w / \partial n$	u_n	u_t
Maximum residual along the boundary	$.16709 \times 10^{-8}$	$.49586 \times 10^{-7}$	$.61483 \times 10^{-7}$	$.42108 \times 10^{-7}$
Maximum value of the parameter within the shell	$.19939 \times 10^{-5}$	$.52826 \times 10^{-5}$	$.95840 \times 10^{-7}$	$.95840 \times 10^{-7}$
Percentage of maximum residual to maximum value	0.084%	0.938%	64.151%	43.936%

Table 10. Clamped Spherical Shell with Circular Planform Obtained by Point Matching
($R/t = 50$, $R = 1.932$, $a = 1/\sqrt{2}$)

Values of the Physical Parameters along $\theta=0$

x/a	0.0	0.2	0.4	0.6	0.8	1.0
w	$.19509 \times 10^{-5}$	$.18725 \times 10^{-5}$	$.16064 \times 10^{-5}$	$.11010 \times 10^{-5}$	$.42237 \times 10^{-6}$	$.35314 \times 10^{-11}$
$\frac{\partial w}{\partial n}$.0	$-.11494 \times 10^{-5}$	$-.26904 \times 10^{-5}$	$-.44084 \times 10^{-5}$	$-.47208 \times 10^{-5}$	$.10589 \times 10^{-10}$
M_n		$.18524 \times 10^{-2}$	$.24150 \times 10^{-2}$	$.21017 \times 10^{-2}$	$-.11911 \times 10^{-2}$	$-.10027 \times 10^{-1}$
u_n	.0	$-.51941 \times 10^{-7}$	$-.91802 \times 10^{-7}$	$-.10378 \times 10^{-6}$	$-.71944 \times 10^{-7}$	$-.15924 \times 10^{-11}$
N_n		1.03079	.99270	.92140	.81669	.70329

Contours



($R/1=50$, $R=1,932$, $\alpha=1/\sqrt{2}$)

Figure 14. Residuals Along the Boundary, Clamped Spherical Shell with Triangular Planform

Table 11. Clamped Spherical Shell with Triangular Planform Obtained by Point Matching
($R/t = 200$, $R = 1.932$, $a = 1/\sqrt{2}$, $b = a \cos \pi/3$)

a. Values of the Physical Parameters along $\theta=0$

x/b	0.0	0.2	0.4	0.6	0.8	1.0
w	$.17132 \times 10^{-4}$	$.16635 \times 10^{-4}$	$.14134 \times 10^{-4}$	$.85796 \times 10^{-5}$	$.21193 \times 10^{-5}$	$-.12718 \times 10^{-9}$
$\frac{\partial w}{\partial n}$.0	$-.17227 \times 10^{-4}$	$-.57577 \times 10^{-4}$	$-.95115 \times 10^{-4}$	$-.72110 \times 10^{-4}$	$-.15196 \times 10^{-8}$
M_n		$.84068 \times 10^{-3}$	$.11783 \times 10^{-2}$	$.28049 \times 10^{-3}$	$-.20416 \times 10^{-2}$	$.39017 \times 10^{-2}$
u_n	.0	$.37185 \times 10^{-6}$	$-.53885 \times 10^{-6}$	$-.36630 \times 10^{-6}$	$-.15856 \times 10^{-6}$	$-.16969 \times 10^{-10}$
N_n		1.49894	2.01789	2.67512	2.79152	2.70252

b. Residuals along the Boundary

y	w	$\frac{\partial w}{\partial n}$	u_n	u_t
.0000*	$-.12659 \times 10^{-9}$	$-.15150 \times 10^{-8}$	$-.17067 \times 10^{-10}$.0
.07655	$-.78782 \times 10^{-5}$	$-.12365 \times 10^{-3}$	$.66343 \times 10^{-6}$	$.24098 \times 10^{-5}$
.15309*	$.26409 \times 10^{-9}$	$.54793 \times 10^{-8}$	$.63962 \times 10^{-11}$	$-.20112 \times 10^{-10}$
.22964	$.31549 \times 10^{-4}$	$.52864 \times 10^{-3}$	$-.32132 \times 10^{-5}$	$-.39212 \times 10^{-5}$
.30619*	$-.83583 \times 10^{-9}$	$-.17837 \times 10^{-7}$	$-.19746 \times 10^{-10}$	$-.20111 \times 10^{-10}$
.38273	$-.89726 \times 10^{-4}$	$-.18006 \times 10^{-2}$	$.14351 \times 10^{-4}$	$.96115 \times 10^{-5}$
.45927*	$.15784 \times 10^{-6}$	$-.85974 \times 10^{-7}$	$-.23711 \times 10^{-9}$	$.13283 \times 10^{-9}$
.53583	$.20156 \times 10^{-3}$	$.74546 \times 10^{-2}$	$-.99503 \times 10^{-4}$	$-.30100 \times 10^{-4}$
.61237*	$-.27940 \times 10^{-7}$	$-.44923 \times 10^{-6}$	$-.68952 \times 10^{-9}$	$-.40573 \times 10^{-9}$

*Points matched on the boundary

c. Ratios of Maximum Residuals to Maximum Values of Physical Parameter within the Shell

	w	$\frac{\partial w}{\partial n}$	u_n	u_t
Maximum residual along the boundary	$.20156 \times 10^{-3}$	$.74546 \times 10^{-2}$	$.99503 \times 10^{-4}$	$.30100 \times 10^{-4}$
Maximum value of the parameter within the shell	$.17132 \times 10^{-4}$	$.95115 \times 10^{-4}$	$.53885 \times 10^{-6}$	$.53885 \times 10^{-6}$
Percentage of maximum residual to maximum value	1176%	7837%	18465%	5586%

Table 12. Clamped Spherical Shell with Square Planform Obtained by Point Matching
($R/t = 200$, $R = 1.932$, $a = 1/\sqrt{2}$, $b = a \cos \pi/4$)

a. Values of the Physical Parameters along $\theta=0$

x/b	0.0	0.2	0.4	0.6	0.8	1.0
w	$.60717 \times 10^{-5}$	$.61444 \times 10^{-5}$	$.61413 \times 10^{-5}$	$.52848 \times 10^{-5}$	$.26242 \times 10^{-5}$	$-.92472 \times 10^{-11}$
$\frac{\partial w}{\partial n}$.0	$.11205 \times 10^{-5}$	$-.24883 \times 10^{-5}$	$-.16659 \times 10^{-4}$	$-.34733 \times 10^{-4}$	$-.13918 \times 10^{-9}$
M_n		$-.71580 \times 10^{-4}$	$.18532 \times 10^{-3}$	$.47517 \times 10^{-3}$	$.17939 \times 10^{-3}$	$-.24783 \times 10^{-2}$
u_n	.0	$-.79406 \times 10^{-7}$	$-.16820 \times 10^{-6}$	$-.24310 \times 10^{-6}$	$-.21581 \times 10^{-6}$	$.31374 \times 10^{-11}$
N_n		.97787	.96346	.94062	.91145	.87621

b. Residuals along the Boundary

y	w	$\frac{\partial w}{\partial n}$	u_n	u_t
.0000*	$-.92609 \times 10^{-11}$	$-.13175 \times 10^{-9}$	$.31406 \times 10^{-11}$.0
.0625	$-.85950 \times 10^{-10}$	$-.17647 \times 10^{-7}$	$-.25186 \times 10^{-9}$	$-.43919 \times 10^{-9}$
.1250*	$-.10981 \times 10^{-10}$	$-.64222 \times 10^{-10}$	$.38164 \times 10^{-11}$	$.21881 \times 10^{-10}$
.1875	$.69935 \times 10^{-9}$	$.88229 \times 10^{-7}$	$.10837 \times 10^{-8}$	$.41858 \times 10^{-9}$
.2500*	$-.19239 \times 10^{-10}$	$.14182 \times 10^{-10}$	$.39625 \times 10^{-11}$	$.59988 \times 10^{-12}$
.3125	$-.43366 \times 10^{-8}$	$-.40629 \times 10^{-6}$	$-.36592 \times 10^{-8}$	$.12407 \times 10^{-9}$
.3750*	$-.23856 \times 10^{-11}$	$.36108 \times 10^{-9}$	$.38209 \times 10^{-11}$	$.48317 \times 10^{-12}$
.4375	$.18005 \times 10^{-7}$	$.27214 \times 10^{-5}$	$.16136 \times 10^{-7}$	$-.67564 \times 10^{-8}$
.5000*	$.96605 \times 10^{-10}$	$.80631 \times 10^{-9}$	$.30402 \times 10^{-11}$	$.29993 \times 10^{-11}$

*Points matched on the boundary

c. Ratios of Maximum Residuals to Maximum Values
of Physical Parameter within the Shell

	w	$\frac{\partial w}{\partial n}$	u_n	u_t
Maximum residual along the boundary	$.18005 \times 10^{-7}$	$.27214 \times 10^{-5}$	$.16136 \times 10^{-7}$	$.67564 \times 10^{-8}$
Maximum value of the parameter within the shell	$.61444 \times 10^{-5}$	$.34733 \times 10^{-4}$	$.24310 \times 10^{-6}$	$.24310 \times 10^{-6}$
Percentage of maximum residual to maximum value	0.293%	7.83%	6.63%	2.78%

Table 13. Clamped Spherical Shell with Pentagonal Planform Obtained by Point Matching
 ($R/t = 200$, $R = 1.932$, $a = 1/\sqrt{2}$, $b = a \cos \pi/5$)

a. Values of the Physical Parameters along $\theta=0$

x/b	0.0	0.2	0.4	0.6	0.8	1.0
w	$.57815 \times 10^{-5}$	$.58781 \times 10^{-5}$	$.60465 \times 10^{-5}$	$.55826 \times 10^{-5}$	$.30600 \times 10^{-5}$	$-.77343 \times 10^{-11}$
$\frac{\partial w}{\partial n}$.0	$.15739 \times 10^{-5}$	$.43728 \times 10^{-6}$	$-.11017 \times 10^{-4}$	$-.32670 \times 10^{-4}$	$-.47889 \times 10^{-10}$
M_n		$-.33708 \times 10^{-4}$	$.89148 \times 10^{-4}$	$.40114 \times 10^{-3}$	$.31150 \times 10^{-3}$	$-.24121 \times 10^{-2}$
u_n	.0	$-.76691 \times 10^{-7}$	$-.16442 \times 10^{-6}$	$-.25070 \times 10^{-6}$	$-.24024 \times 10^{-6}$	$-.15702 \times 10^{-11}$
N_n		.97119	.97180	.96288	.94016	.88218

b. Residuals along the Boundary

y	w	$\frac{\partial w}{\partial n}$	u_n	u_t
.0*	$-.77112 \times 10^{-11}$	$-.40656 \times 10^{-10}$	$-.15102 \times 10^{-11}$.0
.0519	$-.76806 \times 10^{-8}$	$-.13445 \times 10^{-6}$	$.30109 \times 10^{-6}$	$.15402 \times 10^{-8}$
.1039*	$.75317 \times 10^{-11}$	$-.10022 \times 10^{-10}$	$-.37476 \times 10^{-12}$	$-.10380 \times 10^{-11}$
.1559	$.27583 \times 10^{-7}$	$.50056 \times 10^{-6}$	$-.12377 \times 10^{-7}$	$-.35830 \times 10^{-3}$
.2078*	$.89706 \times 10^{-11}$	$.57674 \times 10^{-10}$	$-.11042 \times 10^{-11}$	$.92705 \times 10^{-12}$
.2598	$-.63336 \times 10^{-7}$	$-.12778 \times 10^{-5}$	$.39671 \times 10^{-7}$	$-.72016 \times 10^{-8}$
.3117*	$-.23732 \times 10^{-11}$	$-.77983 \times 10^{-9}$	$-.25813 \times 10^{-11}$	$-.69038 \times 10^{-14}$
.3636	$.10406 \times 10^{-6}$	$.32527 \times 10^{-5}$	$-.16146 \times 10^{-6}$	$.67599 \times 10^{-7}$
.4156*	$.91859 \times 10^{-10}$	$.21905 \times 10^{-8}$	$.17334 \times 10^{-11}$	$.71431 \times 10^{-12}$

*Points matched on the boundary

c. Ratios of Maximum Residuals to Maximum Values of Physical Parameter within the Shell

	w	$\frac{\partial w}{\partial n}$	u_n	u_t
Maximum residual along the boundary	$.10406 \times 10^{-6}$	$.32527 \times 10^{-5}$	$.16146 \times 10^{-6}$	$.67599 \times 10^{-7}$
Maximum value of the parameter within the shell	$.60465 \times 10^{-5}$	$.32670 \times 10^{-4}$	$.25070 \times 10^{-6}$	$.25070 \times 10^{-3}$
Percentage of maximum residual to maximum value	1.72%	9.95%	64.40%	26.96%

Fig. 14. Clamped Spherical Shell with Hexagonal Planform Obtained by Point Matching
($R/t = 200$, $R = 1.932$, $a = 1/\sqrt{2}$, $b = a \cos \pi/6$)

a. Values of the Physical Parameters along $\theta=0$

x/b	0.0	0.2	0.4	0.6	0.8	1.0
w	$.56675 \times 10^{-5}$	$.57582 \times 10^{-5}$	$.59713 \times 10^{-5}$	$.57028 \times 10^{-5}$	$.33037 \times 10^{-5}$	$.47109 \times 10^{-11}$
$\frac{\partial w}{\partial n}$.0	$.14641 \times 10^{-5}$	$.13367 \times 10^{-5}$	$-.82845 \times 10^{-5}$	$-.31343 \times 10^{-4}$	$-.12575 \times 10^{-9}$
M_n		$-.35754 \times 10^{-4}$	$.49820 \times 10^{-4}$	$.35532 \times 10^{-3}$	$.37342 \times 10^{-3}$	$-.24042 \times 10^{-2}$
u_n	.0	$-.75724 \times 10^{-7}$	$-.16240 \times 10^{-6}$	$-.25305 \times 10^{-6}$	$-.25293 \times 10^{-6}$	$-.13893 \times 10^{-11}$
N_n		.96805	.97407	.97324	.95407	.88947

b. Residuals along the Boundary

y	w	$\frac{\partial w}{\partial n}$	u_n	u_t
.0000*	$.47251 \times 10^{-11}$	$-.11847 \times 10^{-9}$	$-.14002 \times 10^{-11}$.0
.0442	$-.60930 \times 10^{-8}$	$-.10373 \times 10^{-6}$	$.46307 \times 10^{-8}$	$-.21668 \times 10^{-8}$
.0884*	$.50164 \times 10^{-11}$	$-.42168 \times 10^{-10}$	$-.13602 \times 10^{-11}$	$-.23782 \times 10^{-14}$
.1326	$.21160 \times 10^{-7}$	$.36035 \times 10^{-6}$	$-.18228 \times 10^{-7}$	$.60049 \times 10^{-8}$
.1768*	$.97913 \times 10^{-11}$	$.22692 \times 10^{-10}$	$-.19589 \times 10^{-11}$	$-.70997 \times 10^{-12}$
.2210	$-.45190 \times 10^{-7}$	$-.77440 \times 10^{-6}$	$.53199 \times 10^{-7}$	$-.23257 \times 10^{-7}$
.2652*	$.47748 \times 10^{-11}$	$.47501 \times 10^{-9}$	$-.34294 \times 10^{-12}$	$.10333 \times 10^{-11}$
.3093	$.66251 \times 10^{-7}$	$.12000 \times 10^{-5}$	$-.18290 \times 10^{-6}$	$.12045 \times 10^{-6}$
.3535*	$-.69122 \times 10^{-10}$	$.79874 \times 10^{-9}$	$-.30268 \times 10^{-11}$	$-.21189 \times 10^{-11}$

*Points matched on the boundary

c. Ratios of Maximum Residuals to Maximum Values
of Physical Parameter within the Shell

	w	$\frac{\partial w}{\partial n}$	u_n	u_t
Maximum residual along the boundary	$.66251 \times 10^{-7}$	$.12000 \times 10^{-5}$	$.18290 \times 10^{-6}$	$.12045 \times 10^{-6}$
Maximum value of the parameter within the shell	$.59713 \times 10^{-5}$	$.31343 \times 10^{-4}$	$.25305 \times 10^{-6}$	$.25305 \times 10^{-6}$
Percentage of maximum residual to maximum value	1.39%	3.83%	72.28%	47.60%

Table 15. Clamped Spherical Shell with Circular Planform Obtained by Point Matching
 (R/t = 200, R = 1.932, a = 1/√2)

a. Values of the Physical Parameters along $\theta=0$

x/a	0.0	0.2	0.4	0.6	0.8	1.0
w	$.54521 \times 10^{-5}$	$.55070 \times 10^{-5}$	$.57234 \times 10^{-5}$	$.57397 \times 10^{-5}$	$.36603 \times 10^{-5}$	$-.11697 \times 10^{-10}$
$\frac{\partial w}{\partial n}$.0	$.89145 \times 10^{-6}$	$.19394 \times 10^{-5}$	$-.40989 \times 10^{-5}$	$-.27302 \times 10^{-4}$	$-.98330 \times 10^{-10}$
M_n		$-.27200 \times 10^{-4}$	$.18577 \times 10^{-6}$	$.26278 \times 10^{-8}$	$.45619 \times 10^{-9}$	$-.22253 \times 10^{-2}$
u_n	.0	$-.71687 \times 10^{-7}$	$-.15305 \times 10^{-6}$	$-.24712 \times 10^{-6}$	$-.26545 \times 10^{-6}$	$.23275 \times 10^{-11}$
N_n		.96402	.97165	.98086	.95562	.85102

Table 16. Spherical Shell Supported at the Boundary by Shear Diaphragm.
 Triangular Planform Obtained by Point Matching
 ($R/t = 50$, $R = 1.932$, $a = 1/\sqrt{2}$, $b = a \cos \pi/3$)

a. Values of the Physical Parameters along $\theta=0$

x/b	0.0	0.2	0.4	0.6	0.8	1.0
w	$.30354 \times 10^{-5}$	$.29241 \times 10^{-5}$	$.25664 \times 10^{-5}$	$.19328 \times 10^{-5}$	$.10577 \times 10^{-5}$	$-.11337 \times 10^{-12}$
$\frac{\partial w}{\partial n}$.0	$-.32384 \times 10^{-5}$	$-.69373 \times 10^{-5}$	$-.10761 \times 10^{-4}$	$-.14011 \times 10^{-4}$	$-.15472 \times 10^{-4}$
M_n		$.94380 \times 10^{-2}$	$.97975 \times 10^{-2}$	$.90611 \times 10^{-2}$	$.62413 \times 10^{-2}$	$.13223 \times 10^{-7}$
u_n	.0	$-.76022 \times 10^{-7}$	$-.15352 \times 10^{-6}$	$-.22188 \times 10^{-6}$	$-.26967 \times 10^{-6}$	$-.28702 \times 10^{-6}$
N_n		.76597	.59627	.40786	.20702	$-.23916 \times 10^{-5}$

b. Residuals along the Boundary

y	w	M_n	u_t	N_n
.0000*	$-.25381 \times 10^{-12}$	$.12376 \times 10^{-7}$	$.00000 \times 10^{-39}$	$-.24140 \times 10^{-5}$
.0765	$.94195 \times 10^{-12}$	$.48486 \times 10^{-8}$	$.14135 \times 10^{-11}$	$-.21756 \times 10^{-5}$
.1531*	$.42942 \times 10^{-12}$	$-.70529 \times 10^{-9}$	$.22513 \times 10^{-11}$	$-.23693 \times 10^{-5}$
.2296	$-.67536 \times 10^{-11}$	$.91259 \times 10^{-8}$	$.23975 \times 10^{-11}$	$-.31590 \times 10^{-5}$
.3062*	$-.15881 \times 10^{-10}$	$-.11645 \times 10^{-7}$	$.21843 \times 10^{-11}$	$-.25257 \times 10^{-5}$
.3827	$-.17412 \times 10^{-10}$	$-.86784 \times 10^{-7}$	$.20033 \times 10^{-11}$	$-.14379 \times 10^{-5}$
.4593*	$-.15996 \times 10^{-10}$	$-.13238 \times 10^{-7}$	$.23776 \times 10^{-11}$	$-.83745 \times 10^{-5}$
.5358	$-.26169 \times 10^{-10}$	$.45932 \times 10^{-6}$	$.37939 \times 10^{-11}$	$-.20787 \times 10^{-4}$
.6124*	$-.41424 \times 10^{-11}$	$-.22676 \times 10^{-6}$	$.48992 \times 10^{-11}$	$-.35837 \times 10^{-5}$

*Points matched on the boundary

c. Ratios of Maximum Residuals to Maximum Values
 of Physical Parameter within the Shell

	w	M_n	u_t	N_n
Maximum residual along the boundary	$.26169 \times 10^{-10}$	$.45932 \times 10^{-6}$	$.48992 \times 10^{-11}$	$.20787 \times 10^{-4}$
Maximum value of the parameter within the shell	$.30354 \times 10^{-5}$	$.97975 \times 10^{-2}$	$.28702 \times 10^{-6}$.96600
Percentage of maximum residual to maximum value	0.0009%	0.0047%	0.0017%	.0021%

Contrails

Table 17. Spherical Shell Supported at the Boundary by Shear Diaphragm.
 Square Planform Obtained by Point Matching
 ($R/t = 50$, $R = 1.932$, $a = 1/\sqrt{2}$, $b = a \cos \pi/4$)

a. Values of the Physical Parameters along $\theta=0$

x/b	0.0	0.2	0.4	0.6	0.8	1.0
w	$.38476 \times 10^{-5}$	$.37359 \times 10^{-5}$	$.33653 \times 10^{-5}$	$.26475 \times 10^{-5}$	$.15049 \times 10^{-5}$	$-.59814 \times 10^{-11}$
$\frac{\partial w}{\partial n}$.0	$-.22963 \times 10^{-5}$	$-.52735 \times 10^{-5}$	$-.92327 \times 10^{-5}$	$-.13550 \times 10^{-4}$	$-.15904 \times 10^{-4}$
M_n		$.50226 \times 10^{-2}$	$.63841 \times 10^{-2}$	$.75717 \times 10^{-2}$	$.65605 \times 10^{-2}$	$.14409 \times 10^{-7}$
u_n	.0	$-.12896 \times 10^{-8}$	$-.25392 \times 10^{-8}$	$-.36583 \times 10^{-8}$	$-.44797 \times 10^{-8}$	$-.47917 \times 10^{-8}$
N_n		1.1011	.94414	$.69284 \times 10^{-6}$.36723	$.14454 \times 10^{-5}$

b. Residuals along the Boundary

y	w	M_n	u_t	N_n
.0000*	$-.60898 \times 10^{-11}$	$.13615 \times 10^{-7}$	$.00000 \times 10^{-39}$	$.14156 \times 10^{-5}$
.0625	$-.53363 \times 10^{-10}$	$.93780 \times 10^{-6}$	$-.57855 \times 10^{-11}$	$-.28796 \times 10^{-4}$
.1250*	$-.71024 \times 10^{-12}$	$-.30630 \times 10^{-7}$	$-.18244 \times 10^{-12}$	$-.36507 \times 10^{-6}$
.1875	$.19824 \times 10^{-9}$	$-.41055 \times 10^{-5}$	$.53471 \times 10^{-11}$	$.11259 \times 10^{-6}$
.2500*	$-.50723 \times 10^{-11}$	$-.25369 \times 10^{-7}$	$-.19464 \times 10^{-12}$	$.15721 \times 10^{-5}$
.3125	$-.60709 \times 10^{-9}$	$.14620 \times 10^{-4}$	$-.30495 \times 10^{-11}$	$-.28538 \times 10^{-3}$
.3750*	$-.11742 \times 10^{-10}$	$-.34839 \times 10^{-7}$	$.82423 \times 10^{-12}$	$.18626 \times 10^{-6}$
.4375	$.18815 \times 10^{-8}$	$-.73771 \times 10^{-4}$	$-.87698 \times 10^{-11}$	$.39805 \times 10^{-3}$
.5000*	$-.73039 \times 10^{-11}$	$-.20239 \times 10^{-7}$	$-.56112 \times 10^{-12}$	$.52154 \times 10^{-6}$

*Points matched on the boundary

c. Ratios of Maximum Residuals to Maximum Values
 of Physical Parameter within the Shell

	w	M_n	u_t	N_n
Maximum residual along the boundary	$.18815 \times 10^{-8}$	$.73771 \times 10^{-4}$	$.87698 \times 10^{-11}$	$.39805 \times 10^{-3}$
Maximum value of the parameter within the shell	$.38476 \times 10^{-5}$	$.75717 \times 10^{-2}$	$.47917 \times 10^{-7}$	1.01100
Percentage of maximum residual to maximum value	0.0489%	0.9743%	0.0183%	0.0394%

Table 18. Spherical Shell Supported at the Boundary by Shear Diaphragm.
 Pentagonal Planform Obtained by Point Matching
 ($R/t = 50$, $R = 1.932$, $a = 1/\sqrt{2}$, $b = a \cos \pi/5$)

a. Values of the Physical Parameters along $\theta=0$

x/b	0.0	0.2	0.4	0.6	0.8	1.0
w	$.39822 \times 10^{-5}$	$.33900 \times 10^{-5}$	$.35662 \times 10^{-5}$	$.28794 \times 10^{-5}$	$.16817 \times 10^{-5}$	$.40258 \times 10^{-11}$
$\frac{\partial w}{\partial n}$.0	$-.16804 \times 10^{-5}$	$-.41803 \times 10^{-6}$	$-.80677 \times 10^{-5}$	$-.12884 \times 10^{-4}$	$-.15754 \times 10^{-4}$
M_n		$.33914 \times 10^{-2}$	$.50847 \times 10^{-2}$	$.69904 \times 10^{-2}$	$.67940 \times 10^{-2}$	$-.16089 \times 10^{-7}$
u_n	.0	$-.15282 \times 10^{-6}$	$-.29735 \times 10^{-6}$	$-.42400 \times 10^{-6}$	$-.51637 \times 10^{-6}$	$-.55153 \times 10^{-6}$
N_n		1.15832	1.06050	.84092	.47810	$-.41947 \times 10^{-5}$

b. Residuals along the Boundary

y	w	M_n	u_t	N_n
.0000*	$.38925 \times 10^{-11}$	$-.16799 \times 10^{-7}$	$.00000 \times 10^{-39}$	$-.42096 \times 10^{-5}$
.0519	$-.55790 \times 10^{-9}$	$.23013 \times 10^{-6}$	$-.95182 \times 10^{-9}$	$.25972 \times 10^{-1}$
.1040*	$.18530 \times 10^{-12}$	$.37388 \times 10^{-9}$	$-.39241 \times 10^{-13}$	$-.14827 \times 10^{-5}$
.1559	$.21702 \times 10^{-8}$	$-.78015 \times 10^{-5}$	$.23287 \times 10^{-6}$	$-.10918$
.2078*	$.94769 \times 10^{-12}$	$.58026 \times 10^{-7}$	$-.16672 \times 10^{-11}$	$-.41798 \times 10^{-5}$
.2597	$-.61586 \times 10^{-8}$	$.13735 \times 10^{-4}$	$-.89042 \times 10^{-8}$.36932
.3117*	$.32685 \times 10^{-11}$	$.12483 \times 10^{-8}$	$.18302 \times 10^{-12}$	$.13024 \times 10^{-4}$
.3637	$.20828 \times 10^{-7}$	$.27191 \times 10^{-4}$	$.50829 \times 10^{-7}$	$-.16792 \times 10^{+1}$
.4156*	$-.23086 \times 10^{-10}$	$-.15019 \times 10^{-6}$	$-.15018 \times 10^{-11}$	$-.11221 \times 10^{-4}$

*Points matched on the boundary

c. Ratios of Maximum Residuals to Maximum Values
 of Physical Parameter within the Shell

	w	M_n	u_t	N_n
Maximum residual along the boundary	$.20828 \times 10^{-7}$	$.27191 \times 10^{-4}$	$.50829 \times 10^{-7}$	1.67918
Maximum value of the parameter within the shell	$.39822 \times 10^{-5}$	$.69902 \times 10^{-2}$	$.55153 \times 10^{-6}$	1.15832
Percentage of maximum residual to maximum value	0.523%	0.389%	9.216%	144.96%

Table 19. Spherical Shell Supported at the Boundary by Shear Diaphragm.
Hexagonal Planform Obtained by Point Matching
($R/t = 50$, $R = 1.932$, $a = 1/\sqrt{2}$, $b = a \cos \pi/6$)

a. Values of the Physical Parameters along $\theta=0$

x/b	0.0	0.2	0.4	0.6	0.8	1.0
w	$.71257 \times 10^{-5}$	$.70034 \times 10^{-5}$	$.65277 \times 10^{-5}$	$.53841 \times 10^{-5}$	$.31946 \times 10^{-5}$	$-.55630 \times 10^{-10}$
$\frac{\partial w}{\partial n}$.0	$-.21444 \times 10^{-5}$	$-.60653 \times 10^{-5}$	$-.13188 \times 10^{-4}$	$-.22626 \times 10^{-4}$	$-.27996 \times 10^{-4}$
M_n		$.43584 \times 10^{-2}$	$.79168 \times 10^{-2}$	1.2200×10^{-2}	1.20297×10^{-2}	$.34089 \times 10^{-5}$
u_n	.0	$-.34890 \times 10^{-6}$	$-.67775 \times 10^{-6}$	$-.94603 \times 10^{-6}$	-1.09836×10^{-6}	$-.11317 \times 10^{-5}$
N_n		1.34094	1.31870	1.30496	1.08531	$-.34720 \times 10^{-4}$

b. Residuals along the Boundary

y	w	M_n	u_t	N_n
.0000*	$-.55929 \times 10^{-10}$	$.34098 \times 10^{-5}$	$.00000 \times 10^{-38}$	$-.34414 \times 10^{-4}$
.0442	$-.41105 \times 10^{-8}$	$-.16754 \times 10^{-3}$	$-.50824 \times 10^{-7}$	$.10899 \times 10^1$
.0884*	$.14051 \times 10^{-10}$	$-.45790 \times 10^{-5}$	$-.13120 \times 10^{-11}$	$.17993 \times 10^{-4}$
.1326	$.14605 \times 10^{-7}$	$.69149 \times 10^{-3}$	$.10237 \times 10^{-6}$	$-.43884 \times 10^1$
.1768*	$-.11818 \times 10^{-9}$	$.75166 \times 10^{-5}$	$-.22372 \times 10^{-11}$	$.13614 \times 10^{-3}$
.2210	$-.35099 \times 10^{-7}$	$-.22017 \times 10^{-2}$	$-.32127 \times 10^{-2}$	$.13514 \times 10^2$
.2652*	$.14887 \times 10^{-9}$	$-.22502 \times 10^{-4}$	$.31058 \times 10^{-11}$	$.11861 \times 10^{-4}$
.3093	$.89569 \times 10^{-7}$	$.83108 \times 10^{-2}$	$.14860 \times 10^{-5}$	$-.51844 \times 10^2$
.3536*	$-.14699 \times 10^{-9}$	$.12071 \times 10^{-3}$	$-.69139 \times 10^{-11}$	$-.23516 \times 10^{-3}$

*Points matched on the boundary

c. Ratios of Maximum Residuals to Maximum Values
of Physical Parameter within the Shell

	w	M_n	u_t	N_n
Maximum residual along the boundary	$.89569 \times 10^{-7}$	$.83108 \times 10^{-2}$	$.14860 \times 10^{-5}$	51.8499
Maximum value of the parameter within the shell	$.71257 \times 10^{-5}$	1.22000×10^{-2}	$.11317 \times 10^{-5}$	1.34094
Percentage of maximum residual to maximum value	1.257%	68.12%	131.30%	3866.24%

Table 20. Spherical Shell Supported at the Boundary by Shear Diaphragm Circular Planform
 Obtained by Point Matching
 ($R/t = 50$, $R = 1.932$, $a = 1/\sqrt{2}$)

a. Values of the Physical Parameters along $\theta=0$

x/b	0.0	0.2	0.4	0.6	0.8	1.0
w	$.13865 \times 10^{-4}$	$.13774 \times 10^{-4}$	$.13181 \times 10^{-4}$	$.11207 \times 10^{-4}$	$.68142 \times 10^{-5}$	$.11472 \times 10^{-10}$
$\frac{\partial w}{\partial n}$.0	$-.16704 \times 10^{-5}$	$-.77859 \times 10^{-4}$	$-.21489 \times 10^{-4}$	$-.40921 \times 10^{-4}$	$-.51823 \times 10^{-4}$
M_n		$.41400 \times 10^{-2}$	$.12089 \times 10^{-1}$	$.22137 \times 10^{-1}$	$.24793 \times 10^{-1}$	$-.38683 \times 10^{-7}$
u_n	.0	$-.87348 \times 10^{-6}$	$-.17250 \times 10^{-5}$	$-.24842 \times 10^{-5}$	$-.30016 \times 10^{-5}$	$-.30821 \times 10^{-5}$
N_n		1.62080	1.55172	1.33455	.84472	$.10430 \times 10^{-5}$

B. BOUNDARY POINT LEAST SQUARES SOLUTIONS

For an exact solution the differential equations and the boundary conditions should be satisfied exactly at all points of the region under consideration. By using the point matching technique, the differential equations were satisfied within the region while the boundary conditions were satisfied at discrete points along the boundary. The residuals were calculated at numerous points along the boundary since in most cases the magnitude of the residuals (in the absence of an exact solution) may be used for evaluating the solution. It was found that the residuals are zero at the points matched, and that they oscillate between these points with increasing amplitude as the polar coordinate "r" increases, as was shown in Fig. 14. This behavior is typical with the point matching method, as discovered on other boundary value problems previously (e.g., St. Venant torsion, plate bending).

It is desirable in some cases to minimize the integral of the square of the error (residuals in this case) to obtain convergence in the mean in the limit. The technique consists of retaining "N" unknown coefficients in the solution of the differential equations, then writing the boundary equations at "K" points, or using some of the equations more than once at a point. In this way "M" equations will be generated in "N" unknowns such that $M > N$.

In order to solve "M" equations with "N" unknowns, let the equations be designated by

$$\sum_{j=1}^N a_{ij}X_j = b_i, \quad i = 1, 2, \dots, M. \quad (4-7)$$

Let a possible solution vector be " \bar{X}_j " which does not satisfy Eq. (4-7) exactly, but leads to some residual error " ϵ_i " such that

$$\sum_{j=1}^N (a_{ij}\bar{X}_j - b_i) = \epsilon_i, \quad i = 1, 2, \dots, M. \quad (4-8)$$

The sum of the squares of the residuals " ϵ_i " is given by

$$E = \sum_{i=1}^M \epsilon_i \epsilon_i = \sum_{i=1}^M \sum_{j=1}^N (a_{ij}\bar{X}_j - b_i) \sum_{j=1}^N (a_{ij}\bar{X}_j - b_i). \quad (4-9)$$

Contrails

The condition that the X's be chosen to minimize the integral of the square of the error is

$$\partial E / \partial \bar{X}_n = 0 \quad (n = 1, \dots, N) \quad (4-10)$$

or

$$\sum_{i=1}^M a_{in} \sum_{j=1}^N (a_{ij} \bar{X}_j - b_i) = 0 \quad .$$
$$\sum_{i=1}^M a_{in} \sum_{j=1}^N a_{ij} \bar{X}_j = \sum_{i=1}^M a_{in} b_i \quad n = 1, 2, \dots, N \quad (4-11)$$

or, in matrix notation,

$$[a]^T [a] [X] = [a]^T [b] \quad , \quad (4-12)$$

where $[a]^T$ is the transpose of the matrix $[a]$.

Hence the "M" equations in "N" unknowns are reduced to "N" equations in "N" unknowns in an operation which assures optimal satisfaction of the boundary conditions in a least squares sense in any given problem.

The example problems solved in the previous section by means of point matching was also analyzed by the least squares method. Two cases were considered.

Case I - At each point where the boundary conditions are to be matched as shown in Fig. 13, the equations associated with the transverse displacement, rotation, and/or moments were written once, while the equations associated with the in-plane displacements and/or membrane forces were written twice. The latter boundary conditions were repeated because they were seen to have the largest percent residuals in the point matching results seen in Tables 6-20. Because the boundary conditions were satisfied at five discrete points on each typical boundary segment, there resulted 28 equations in 19 unknowns. These reduced to 19 equations in 19 unknowns by means of Eq. (4-12).

Tables 21-24 summarize the results for the case of a clamped spherical shell with n-sided polygonal planform ($R/t = 50$, $R = 1.932$, $a = 1/\sqrt{2}$).

Tables 25-28 summarize the results for the case of a spherical shallow shell supported at the boundary by shear diaphragms ($R/t = 50$, $R = 1.932$, $a = 1/\sqrt{2}$).

Contrails

Table 21. Clamped Spherical Shell with Triangular Planform Obtained by Least Squares Using Repeated Boundary Conditions
($R/t = 50$, $R = 1.932$, $a = 1/\sqrt{2}$, $b = a \cos \pi/3$)

a. Values of the Physical Parameters along $\theta=0$

x/b	0.0	0.2	0.4	0.6	0.8	1.0
w	$.12216 \times 10^{-5}$	$.111467 \times 10^{-5}$	$.91809 \times 10^{-6}$	$.56641 \times 10^{-6}$	$.19287 \times 10^{-6}$	$.14507 \times 10^{-6}$
$\frac{\partial w}{\partial n}$.0	$-.21549 \times 10^{-5}$	$-.42440 \times 10^{-5}$	$-.54722 \times 10^{-5}$	$-.46200 \times 10^{-5}$	$-.36606 \times 10^{-5}$
M_n		$.60270 \times 10^{-2}$	$.47890 \times 10^{-2}$	$.13384 \times 10^{-2}$	$-.52905 \times 10^{-2}$	$-.16030 \times 10^{-1}$
u_n	.0	$-.18534 \times 10^{-7}$	$-.31846 \times 10^{-7}$	$-.34244 \times 10^{-7}$	$-.22513 \times 10^{-7}$	$.19429 \times 10^{-11}$
N_n		.58168	.54896	.50749	.46486	.42952

b. Residuals along the Boundary

y	w	$\frac{\partial w}{\partial n}$	u_n	u_t
.0000*	$.14507 \times 10^{-6}$	$-.36599 \times 10^{-6}$	$.19473 \times 10^{-11}$.0
.0765	$.39188 \times 10^{-10}$	$-.42535 \times 10^{-9}$	$-.21759 \times 10^{-9}$	$-.77507 \times 10^{-9}$
.1531*	$-.23510 \times 10^{-8}$	$.56405 \times 10^{-8}$	$-.22681 \times 10^{-11}$	$.14564 \times 10^{-11}$
.2296	$-.21644 \times 10^{-8}$	$.71317 \times 10^{-8}$	$.99582 \times 10^{-9}$	$.10849 \times 10^{-8}$
.3062*	$.12572 \times 10^{-8}$	$-.25166 \times 10^{-8}$	$.13145 \times 10^{-11}$	$.44698 \times 10^{-12}$
.3827	$.32147 \times 10^{-8}$	$-.20461 \times 10^{-7}$	$-.40616 \times 10^{-8}$	$-.20892 \times 10^{-8}$
.4593*	$-.48939 \times 10^{-9}$	$.59196 \times 10^{-9}$	$.25084 \times 10^{-12}$	$-.88383 \times 10^{-12}$
.5358	$-.34611 \times 10^{-8}$	$.14228 \times 10^{-6}$	$.25693 \times 10^{-7}$	$.51652 \times 10^{-6}$
.6124*	$.15767 \times 10^{-9}$	$-.43379 \times 10^{-9}$	$.81647 \times 10^{-13}$	$-.56823 \times 10^{-13}$

*w and $\frac{\partial w}{\partial n}$ were forced once while u_t and u_n were forced twice.

c. Ratios of Maximum Residuals to Maximum Values of Physical Parameter within the Shell

	w	$\frac{\partial w}{\partial n}$	u_n	u_t
Maximum residual along the boundary	$.34611 \times 10^{-8}$	$.14228 \times 10^{-6}$	$.25693 \times 10^{-7}$	$.51652 \times 10^{-6}$
Maximum value of the parameter within the shell	$.12216 \times 10^{-5}$	$.53722 \times 10^{-5}$	$.34244 \times 10^{-7}$	$.34244 \times 10^{-7}$
Percentage of maximum residual to maximum value	0.283%	2.60%	75.03%	15.08%

Table 22. Clamped Spherical Shell with Square Planform Obtained by Least Squares Using Repeated Boundary Conditions
($R/t = 50$, $R = 1.932$, $a = 1/\sqrt{2}$, $b = a \cos \pi/4$)

a. Values of the Physical Parameters along $\theta=0$

x/b	0.0	0.2	0.4	0.6	0.8	1.0
w	$.18420 \times 10^{-5}$	$.17397 \times 10^{-5}$	$.14273 \times 10^{-5}$	$.92009 \times 10^{-6}$	$.33076 \times 10^{-6}$	$.26345 \times 10^{-6}$
$\frac{\partial w}{\partial n}$.0	$-.20685 \times 10^{-6}$	$-.41683 \times 10^{-6}$	$-.53103 \times 10^{-6}$	$-.54346 \times 10^{-6}$	$-.57397 \times 10^{-6}$
M_n		$.42375 \times 10^{-2}$	$.39065 \times 10^{-2}$	$.20068 \times 10^{-2}$	$-.34703 \times 10^{-2}$	$-.14782 \times 10^{-1}$
u_n	.0	$-.37999 \times 10^{-7}$	$-.65605 \times 10^{-7}$	$-.71864 \times 10^{-7}$	$-.48370 \times 10^{-7}$	$-.13224 \times 10^{-12}$
N_n		.90585	.86036	.79557	.72506	.66067

b. Residuals along the Boundary

y	w	$\frac{\partial w}{\partial n}$	u_n	u_t
.0000*	$.26347 \times 10^{-9}$	$-.57324 \times 10^{-9}$	$-.13856 \times 10^{-12}$.0
.0625	$.49002 \times 10^{-10}$	$.41157 \times 10^{-9}$	$-.17208 \times 10^{-9}$	$-.26159 \times 10^{-9}$
.1250*	$-.41454 \times 10^{-9}$	$.88043 \times 10^{-9}$	$-.34973 \times 10^{-12}$	$-.24994 \times 10^{-12}$
.1875	$-.52257 \times 10^{-9}$	$-.64087 \times 10^{-9}$	$.73791 \times 10^{-9}$	$.26666 \times 10^{-9}$
.2500*	$.21380 \times 10^{-9}$	$-.34522 \times 10^{-9}$	$-.38072 \times 10^{-12}$	$.13221 \times 10^{-12}$
.3125	$.89558 \times 10^{-9}$	$.10786 \times 10^{-8}$	$-.26147 \times 10^{-9}$	$-.55896 \times 10^{-10}$
.3750*	$-.76185 \times 10^{-10}$	$.84869 \times 10^{-10}$	$-.39524 \times 10^{-13}$	$.43698 \times 10^{-12}$
.4375	$-.12238 \times 10^{-6}$	$.15886 \times 10^{-7}$	$.12821 \times 10^{-7}$	$-.31733 \times 10^{-6}$
.5000*	$.14431 \times 10^{-10}$	$-.32146 \times 10^{-10}$	$-.71432 \times 10^{-12}$	$-.73875 \times 10^{-12}$

*w and $\frac{\partial w}{\partial n}$ were forced once while u_t and u_n were forced twice.

c. Ratios of Maximum Residuals to Maximum Values of Physical Parameter within the Shell

	w	$\frac{\partial w}{\partial n}$	u_n	u_t
Maximum residual along the boundary	$.12238 \times 10^{-6}$	$.15886 \times 10^{-7}$	$.12821 \times 10^{-7}$	$.31733 \times 10^{-6}$
Maximum value of the parameter within the shell	$.18420 \times 10^{-5}$	$.58103 \times 10^{-5}$	$.71864 \times 10^{-7}$	$.71864 \times 10^{-7}$
Percentage of maximum residual to maximum value	0.0664%	0.273%	17.84%	4.42%

Contrails

Table 23. Clamped Spherical Shell with Pentagonal Planform Obtained by Least Squares Using Repeated Boundary Conditions
($R/t = 50$, $R = 1.932$, $a = 1/\sqrt{2}$, $b = a \cos \pi/5$)

a. Values of the Physical Parameters along $\theta=0$

x/b	0.0	0.2	0.4	0.6	0.8	1.0
w	$.19524 \times 10^{-5}$	$.18518 \times 10^{-5}$	$.15430 \times 10^{-5}$	$.10233 \times 10^{-5}$	$.38269 \times 10^{-6}$	$.12862 \times 10^{-6}$
$\frac{\partial w}{\partial n}$.0	$-.17704 \times 10^{-5}$	$-.36442 \times 10^{-5}$	$-.53379 \times 10^{-5}$	$-.53523 \times 10^{-5}$	$-.23382 \times 10^{-6}$
M_n		$.32349 \times 10^{-2}$	$.32709 \times 10^{-2}$	$.21752 \times 10^{-2}$	$-.23983 \times 10^{-2}$	$-.13665 \times 10^{-1}$
u_n	.0	$-.44960 \times 10^{-7}$	$-.78105 \times 10^{-7}$	$-.86682 \times 10^{-7}$	$-.59361 \times 10^{-7}$	$.72299 \times 10^{-12}$
N_n		.97976	.93516	.86724	.79015	.71389

b. Residuals along the Boundary

y	w	$\frac{\partial w}{\partial n}$	u_n	u_t
.0000*	$.12862 \times 10^{-6}$	$-.23320 \times 10^{-6}$	$.73445 \times 10^{-12}$.0
.0519	$-.57306 \times 10^{-10}$	$-.12758 \times 10^{-6}$	$-.36522 \times 10^{-10}$	$.69766 \times 10^{-10}$
.1039*	$-.23054 \times 10^{-6}$	$.37884 \times 10^{-6}$	$.17921 \times 10^{-12}$	$.39419 \times 10^{-12}$
.1558	$-.15713 \times 10^{-11}$	$.56202 \times 10^{-6}$	$.14822 \times 10^{-6}$	$-.13223 \times 10^{-6}$
.2078*	$.15355 \times 10^{-6}$	$-.26568 \times 10^{-6}$	$.71515 \times 10^{-12}$	$-.10206 \times 10^{-11}$
.2598	$-.17174 \times 10^{-6}$	$-.18116 \times 10^{-7}$	$-.44171 \times 10^{-6}$	$.40982 \times 10^{-6}$
.3117*	$-.66051 \times 10^{-10}$	$-.63870 \times 10^{-10}$	$.46312 \times 10^{-12}$	$.39263 \times 10^{-12}$
.3637	$.66143 \times 10^{-6}$	$.77030 \times 10^{-7}$	$.15217 \times 10^{-6}$	$-.20512 \times 10^{-6}$
.4156*	$.21336 \times 10^{-10}$	$.16824 \times 10^{-10}$	$-.81536 \times 10^{-12}$	$-.58170 \times 10^{-12}$

*w and $\partial w/\partial n$ were forced once while u_t and u_n were forced twice

c. Ratios of Maximum Residuals to Maximum Values of Physical Parameter within the Shell

	w	$\frac{\partial w}{\partial n}$	u_n	u_t
Maximum residual along the boundary	$.66143 \times 10^{-6}$	$.77030 \times 10^{-7}$	$.15217 \times 10^{-6}$	$.20512 \times 10^{-6}$
Maximum value of the parameter within the shell	$.19524 \times 10^{-5}$	$.53523 \times 10^{-5}$	$.86682 \times 10^{-7}$	$.86682 \times 10^{-7}$
Percentage of maximum residual to maximum value	0.034%	1.439%	1.755%	2.366%

Contrails

Table 24. Clamped Spherical Shell with Hexagonal Planform Obtained by Least Squares Using Repeated Boundary Conditions
($R/t = 50$, $R = 1.932$, $a = 1/\sqrt{2}$, $b = a \cos \pi/6$)

a. Values of the Physical Parameters along $\theta=0$

x/b	0.0	0.2	0.4	0.6	0.8	1.0
w	$.19756 \times 10^{-5}$	$.18797 \times 10^{-5}$	$.15803 \times 10^{-5}$	$.10644 \times 10^{-5}$	$.40739 \times 10^{-6}$	$.12767 \times 10^{-9}$
$\frac{\partial w}{\partial n}$.0	$-.15844 \times 10^{-5}$	$-.33326 \times 10^{-5}$	$-.50199 \times 10^{-5}$	$-.52326 \times 10^{-5}$	$-.22680 \times 10^{-9}$
M_u		$.27527 \times 10^{-22}$	$.29506 \times 10^{-2}$	$.22058 \times 10^{-2}$	$-.18444 \times 10^{-2}$	$-.13054 \times 10^{-1}$
u_n	.0	$-.47944 \times 10^{-77}$	$-.83694 \times 10^{-7}$	$-.93627 \times 10^{-7}$	$-.64790 \times 10^{-7}$	$-.37218 \times 10^{-12}$
\bar{u}_n		1.00418	.96105	.89272	.81309	.73016

b. Residuals along the Boundary

y	w	$\frac{\partial w}{\partial n}$	u_n	u_t
.0000*	$.12767 \times 10^{-9}$	$-.22619 \times 10^{-9}$	$-.36428 \times 10^{-12}$.0
.0442	$-.12123 \times 10^{-9}$	$-.23706 \times 10^{-9}$	$.16505 \times 10^{-9}$	$.33645 \times 10^{-10}$
.0884*	$-.25554 \times 10^{-9}$	$.38977 \times 10^{-9}$	$.32974 \times 10^{-13}$	$.31027 \times 10^{-12}$
.1326	$.17142 \times 10^{-9}$	$.94335 \times 10^{-9}$	$-.65353 \times 10^{-9}$	$.60238 \times 10^{-10}$
.1768*	$.18324 \times 10^{-9}$	$-.31250 \times 10^{-9}$	$.27766 \times 10^{-12}$	$.11557 \times 10^{-11}$
.2209	$-.52408 \times 10^{-9}$	$-.25722 \times 10^{-7}$	$.19354 \times 10^{-9}$	$-.51421 \times 10^{-9}$
.2652*	$-.75807 \times 10^{-10}$	$.70480 \times 10^{-10}$	$.16295 \times 10^{-12}$	$.76458 \times 10^{-12}$
.3093	$.11737 \times 10^{-9}$	$.76212 \times 10^{-7}$	$-.69038 \times 10^{-9}$	$.32755 \times 10^{-9}$
.3535*	$.15741 \times 10^{-10}$	$-.38363 \times 10^{-10}$	$.10018 \times 10^{-10}$	$.55385 \times 10^{-12}$

*w and $\frac{\partial w}{\partial n}$ were forced once while u_t and u_n were forced twice.

c. Ratios of Maximum Residuals to Maximum Values of Physical Parameter within the Shell

	w	$\frac{\partial w}{\partial n}$	u_n	u_t
Maximum residual along the boundary	$.11737 \times 10^{-9}$	$.76212 \times 10^{-7}$	$.69038 \times 10^{-9}$	$.32755 \times 10^{-9}$
Maximum value of the parameter within the shell	$.19756 \times 10^{-5}$	$.52326 \times 10^{-5}$	$.93627 \times 10^{-7}$	$.93627 \times 10^{-7}$
Percentage of maximum residual to maximum value	0.059%	1.456%	7.374%	3.498%

Contrails

Table 25. Spherical Shell Supported Along the Boundary by Shear Diaphragm Triangular Planform
 Obtained by Least Squares Using Repeated Boundary Conditions
 ($R/t = 50$, $R = 1.932$, $a = 1/\sqrt{2}$, $b = a \cos \pi/3$)

a. Values of the Physical Parameters along $\theta=0$

x/b	0.0	0.2	0.4	0.6	0.8	1.0
w	$.15858 \times 10^{-5}$	$.15298 \times 10^{-5}$	$.13480 \times 10^{-5}$	$.10249 \times 10^{-5}$	$.55890 \times 10^{-6}$	$-.21028 \times 10^{-7}$
$\frac{\partial w}{\partial n}$.0	$-.16345 \times 10^{-5}$	$-.35451 \times 10^{-5}$	$-.56018 \times 10^{-5}$	$-.75183 \times 10^{-5}$	$-.86575 \times 10^{-5}$
M_n		$.47795 \times 10^{-2}$	$.50883 \times 10^{-2}$	$.49450 \times 10^{-2}$	$.38009 \times 10^{-2}$	$-.75443 \times 10^{-4}$
u_n	.0	$-.20885 \times 10^{-7}$	$-.45544 \times 10^{-7}$	$-.70962 \times 10^{-7}$	$-.94663 \times 10^{-7}$	$-.10346 \times 10^{-8}$
N_n		.83863	.69706	.47765	.17153	$-.11069 \times 10^{-2}$

b. Residuals along the Boundary

y	w	M_n	u_t	N_n
.0*	$-.21028 \times 10^{-7}$	$-.75444 \times 10^{-4}$.0	$-.11069 \times 10^{-2}$
.0765	$.13358 \times 10^{-7}$	$-.19234 \times 10^{-3}$	$-.31621 \times 10^{-7}$.36050
.1531*	$.34441 \times 10^{-7}$	$.12505 \times 10^{-3}$	$-.13029 \times 10^{-7}$.96756
.2296	$-.27954 \times 10^{-7}$	$.10090 \times 10^{-2}$	$-.74829 \times 10^{-7}$	1.01584
.3062*	$-.18539 \times 10^{-7}$	$-.68810 \times 10^{-4}$	$.17875 \times 10^{-6}$.48252
.3827	$.16464 \times 10^{-6}$	$-.39791 \times 10^{-2}$	$.17559 \times 10^{-6}$.13775
.4593*	$.60680 \times 10^{-8}$	$.24775 \times 10^{-4}$	$-.52679 \times 10^{-10}$	$-.21733 \times 10^{-3}$
.5358	$-.96840 \times 10^{-6}$	$.25942 \times 10^{-1}$	$-.15979 \times 10^{-6}$	-1.20479
.6123*	$-.82582 \times 10^{-6}$	$-.65084 \times 10^{-5}$	$.18640 \times 10^{-9}$	$-.10839 \times 10^{-2}$

*w and M_n were forced once while u_t and N_n were forced twice.

c. Ratios of Maximum Residuals to Maximum Values
 of Physical Parameter within the Shell

	w	M_n	u_t	N_n
Maximum residual along the boundary	$.96840 \times 10^{-6}$	$.25942 \times 10^{-1}$	$.17875 \times 10^{-5}$	1.20479
Maximum value of the parameter within the shell	$.15858 \times 10^{-5}$	$.50883 \times 10^{-2}$	$.10346 \times 10^{-6}$.83863
Percentage of maximum residual to maximum value	61.07%	50.98%	172.77%	143.66%

Table 26. Spherical Shell Supported at the Boundary by Shear Diaphragm Square Planform
 Obtained by Least Squares Using Repeated Boundary Conditions
 ($R/t = 50$, $R = 1.932$, $a = 1/\sqrt{2}$, $b = a \cos \pi/4$)

a. Values of the Physical Parameters along $\theta=0$

x/b	0.0	0.2	0.4	0.6	0.8	1.0
w	.38476 10^{-5}	.37359 $\times 10^{-5}$.33653 $\times 10^{-5}$.26475 $\times 10^{-5}$.15049 $\times 10^{-5}$	-.59814 $\times 10^{-11}$
$\frac{\partial w}{\partial n}$.0	-.22963 $\times 10^{-5}$	-.52735 $\times 10^{-5}$	-.92327 $\times 10^{-5}$	-.13550 $\times 10^{-4}$	-.15904 $\times 10^{-4}$
M_n		.50226 $\times 10^{-2}$.63841 $\times 10^{-2}$.75717 $\times 10^{-2}$.65605 $\times 10^{-2}$.14409 $\times 10^{-7}$
u_n	.0	-.12896 $\times 10^{-6}$	-.25392 $\times 10^{-6}$	-.36583 $\times 10^{-6}$	-.44797 $\times 10^{-6}$	-.47917 $\times 10^{-6}$
N_n		1.1011	.94414	.69284	.36723	.14454 $\times 10^{-5}$

b. Residuals along the Boundary

y	w	M_n	u_t	N_n
.0*	-.49418 $\times 10^{-10}$	-.55708 $\times 10^{-7}$.0	-.34571 $\times 10^{-5}$
.0625	-.38415 $\times 10^{-10}$.85851 $\times 10^{-8}$	-.47841 $\times 10^{-11}$	-.31717 $\times 10^{-4}$
.125*	.98619 $\times 10^{-10}$.80022 $\times 10^{-7}$.31405 $\times 10^{-12}$	-.62436 $\times 10^{-5}$
.1875	.26856 $\times 10^{-9}$	-.36678 $\times 10^{-5}$.49874 $\times 10^{-11}$.97796 $\times 10^{-4}$
.250*	-.50184 $\times 10^{-10}$	-.79051 $\times 10^{-7}$	-.64968 $\times 10^{-13}$	-.31814 $\times 10^{-5}$
.3125	-.68091 $\times 10^{-9}$.13261 $\times 10^{-4}$	-.21648 $\times 10^{-11}$	-.26420 $\times 10^{-3}$
.375*	.17054 $\times 10^{-10}$	-.21226 $\times 10^{-7}$.10356 $\times 10^{-11}$	-.13709 $\times 10^{-5}$
.4375	.19578 $\times 10^{-9}$	-.67472 $\times 10^{-4}$	-.90505 $\times 10^{-11}$.33992 $\times 10^{-3}$
.5000*	-.22161 $\times 10^{-12}$	-.12213 $\times 10^{-6}$	-.90574 $\times 10^{-12}$.11846 $\times 10^{-5}$

*w and M_n were forced once while u_t and N_n were forced twice.

c. Ratios of Maximum Residuals to Maximum Values
 of Physical Parameter within the Shell

	w	M_n	u_t	N_n
Maximum residual along the boundary	.19578 $\times 10^{-9}$.67472 $\times 10^{-4}$.90505 $\times 10^{-11}$.33992 $\times 10^{-3}$
Maximum value of the parameter within the shell	.38476 $\times 10^{-5}$.75717 $\times 10^{-2}$.47917 $\times 10^{-7}$	1.01100
Percentage of maximum residual to maximum value	0.051%	0.890%	0.019%	0.034%

Table 27. Spherical Shell Supported at the Boundary by Shear Diaphragm Pentagonal Planform
 Obtained by Least Squares Using Repeated Boundary Conditions
 ($R/t = 50$, $R = 1.932$, $a = 1/\sqrt{2}$, $b = a \cos \pi/5$)

a. Values of the Physical Parameters along $\theta=0$

x/b	0.0	0.2	0.4	0.6	0.8	1.0
w	$.39822 \times 10^{-5}$	$.38900 \times 10^{-5}$	$.35662 \times 10^{-5}$	$.28794 \times 10^{-5}$	$.16817 \times 10^{-5}$	$.40258 \times 10^{-11}$
$\frac{\partial w}{\partial n}$.0	$-.16804 \times 10^{-5}$	$-.41803 \times 10^{-5}$	$-.80677 \times 10^{-5}$	$-.12884 \times 10^{-4}$	$-.15754 \times 10^{-4}$
M_n		$.33914 \times 10^{-2}$	$.50847 \times 10^{-2}$	$.69904 \times 10^{-2}$	$.67940 \times 10^{-2}$	$-.16089 \times 10^{-7}$
u_n	.0	$-.15282 \times 10^{-6}$	$-.29735 \times 10^{-6}$	$-.42400 \times 10^{-6}$	$-.51637 \times 10^{-6}$	$-.55153 \times 10^{-6}$
N_n		1.15832	1.0605	.84092	.47810	$-.41947 \times 10^{-5}$

b. Residuals along the Boundary

y	w	M_n	u_t	N_n
.000*	$-.16238 \times 10^{-10}$	$-.64294 \times 10^{-7}$.0	$-.25332 \times 10^{-5}$
.0519	$-.56910 \times 10^{-8}$	$.22762 \times 10^{-5}$	$-.95047 \times 10^{-8}$	$.25969 \times 10^{-1}$
.1039*	$.60933 \times 10^{-11}$	$.29611 \times 10^{-7}$	$.16305 \times 10^{-11}$	$-.11049 \times 10^{-4}$
.1559	$.21835 \times 10^{-8}$	$-.77434 \times 10^{-5}$	$.23295 \times 10^{-8}$	-.10920
.2078*	$.57998 \times 10^{-11}$	$.50149 \times 10^{-7}$	$-.20455 \times 10^{-11}$	$-.72494 \times 10^{-5}$
.2598	$-.61665 \times 10^{-8}$	$.13641 \times 10^{-4}$	$-.89046 \times 10^{-8}$.36933
.3117*	$-.77369 \times 10^{-11}$	$.17846 \times 10^{-6}$	$.15206 \times 10^{-11}$	$.56550 \times 10^{-5}$
.3637	$.20825 \times 10^{-7}$	$.27570 \times 10^{-4}$	$.50833 \times 10^{-7}$	1.67921
.4156*	$-.10800 \times 10^{-10}$	$-.68514 \times 10^{-6}$	$.33697 \times 10^{-11}$	$.11369 \times 10^{-4}$

*w and M_n were forced once while u_t and N_n were forced twice.

c. Ratios of Maximum Residuals to Maximum Values
 of Physical Parameter within the Shell

	w	M_n	u_t	N_n
Maximum residual along the boundary	$.20825 \times 10^{-7}$	$.27570 \times 10^{-4}$	$.50833 \times 10^{-7}$	1.67921
Maximum value of the parameter within the shell	$.39822 \times 10^{-5}$	$.69904 \times 10^{-2}$	$.55153 \times 10^{-6}$	1.15832
Percentage of maximum residual to maximum value	0.523%	0.394%	9.217%	144.969%

Table 28. Spherical Shell Supported Along the Boundary by Shear Diaphragm Hexagonal Platform
 Obtained by Least Squares Using Repeated Boundary Conditions
 ($R/t = 50$, $R = 1.932$, $a = 1/\sqrt{2}$, $b = a \cos \pi/6$)

a. Values of the Physical Parameters along $\theta=0$

x/b	0.0	0.2	0.4	0.6	0.8	1.0
w	$.74052 \times 10^{-5}$	$.72806 \times 10^{-5}$	$.67932 \times 10^{-5}$	$.56126 \times 10^{-5}$	$.33377 \times 10^{-5}$	$.22834 \times 10^{-7}$
$\frac{\partial w}{\partial n}$.0	$-.21880 \times 10^{-5}$	$-.62351 \times 10^{-5}$	$-.13657 \times 10^{-4}$	$-.23580 \times 10^{-4}$	$-.29913 \times 10^{-4}$
M_n		$.44640 \times 10^{-2}$	$.81913 \times 10^{-2}$	1.27111×10^{-2}	1.26664×10^{-2}	$.98221 \times 10^{-5}$
u_n	.0	$-.36539 \times 10^{-6}$	$-.71005 \times 10^{-6}$	$-.99138 \times 10^{-6}$	$-.11509 \times 10^{-5}$	-1.18583×10^{-6}
N_n		1.35706	1.33807	1.33612	1.12255	$-.46487 \times 10^{-2}$

b. Residuals along the Boundary

y	w	M_n	u_t	N_n
.0000*	$-.22835 \times 10^{-7}$	$.98221 \times 10^{-5}$.0	$-.46482 \times 10^{-2}$
.0442	$.38924 \times 10^{-6}$	$-.23344 \times 10^{-3}$	$-.55817 \times 10^{-7}$	1.17124
.0884*	$.49123 \times 10^{-7}$	$.64832 \times 10^{-4}$	$-.98686 \times 10^{-6}$	$-.62943 \times 10^{-2}$
.1326	$.42787 \times 10^{-7}$	$.11311 \times 10^{-2}$	$.11067 \times 10^{-6}$	-4.74366
.1768*	$-.26835 \times 10^{-7}$	$.26209 \times 10^{-4}$	$.13009 \times 10^{-6}$	$-.78536 \times 10^{-2}$
.2210	$-.56258 \times 10^{-7}$	$-.32414 \times 10^{-2}$	$-.34649 \times 10^{-6}$	14.57286
.2652*	$.46793 \times 10^{-7}$	$.46060 \times 10^{-4}$	$-.31689 \times 10^{-6}$	$.11267 \times 10^{-1}$
.3093	$.15403 \times 10^{-6}$	$.11471 \times 10^{-1}$	$-.15989 \times 10^{-5}$	-55.9279
.3535*	$.63732 \times 10^{-6}$	$.91584 \times 10^{-4}$	$.28395 \times 10^{-6}$	$-.95251 \times 10^{-2}$

* w and M_n were forced once while u_t and N_n were forced twice.

c. Ratios of Maximum Residuals to Maximum Values
 of Physical Parameter within the Shell

	w	M_n	u_t	N_n
Maximum residual along the boundary	$.15403 \times 10^{-6}$	$.11471 \times 10^{-1}$	$.15989 \times 10^{-5}$	55.9279
Maximum value of the parameter within the shell	$.74052 \times 10^{-5}$	$.12711 \times 10^{-1}$	$.11858 \times 10^{-5}$	1.35706
Percentage of maximum residual to maximum value	20.800%	90.245%	134.837%	4121.255%

Case II - In this case 7 points were chosen on the boundary as shown in Fig. 15. Points 1, 2, 3, 5, and 7 are equally spaced along the edge and points 4 and 6 are located midway between points 3, 5, and 7. At points 1, 2, 3, 5, and 7, all the equations for the boundary conditions were written, while at points 4 and 6 only the equations associated with the in-plane displacements and/or forces were written, giving 23 equations in 19 unknowns which were solved in the least squares sense.

Tables 29-32 are the results for the case of a clamped spherical shell with n-sided polygonal planform ($R/t = 50$, $R = 1.932$, $a = 1/\sqrt{2}$).

Tables 33-36 summarize the results for the case of a spherical shallow shell with n-sided polygonal planform supported at the boundary by shear diaphragms ($R/t = 50$, $R = 1.932$, $a = 1/\sqrt{2}$).

C. DISCUSSION AND CONCLUSIONS

As the number of points on the boundary to be matched increases, the size of the coefficient matrix increases and the solution usually improves; however, there is a turning point where the computing round-off error caused by matrix inversion increases at a faster rate than the improvement caused by increasing the size of the coefficient matrix.

In the case of the shallow shells, in contrast with plate-bending problems solved using the point matching technique, the boundary shape affects the accuracy of the solution more. The complementary solution for a simply connected plate with symmetric properties with respect to the ($\theta = 0$) axes is

$$w_c = \sum_{n=0,m}^N (A_n r^n + C_n r^{n+2}) \cos n\theta ,$$

where r^n and r^{n+2} are continuous functions increasing continuously as r increases. In the case of shallow shells, the Bessel-Kelvin functions used and their derivatives are also continuous functions; but as the argument increases, these functions oscillate (Fig. 16) with rapidly increasing amplitudes, having zeros as shown by Table 37 for the Bessel-Kelvin functions of zeroth order (Ref. 23); consequently, these functions are increasingly difficult to control along a boundary as r increases. However, it is also seen from the various results that edge residuals of a fairly large magnitude can be tolerated as an acceptable solution, particularly if the shell is thin.

In the case of the clamped shallow shell with regular n-sided polygonal planform the residuals along the boundary were reduced successfully by use of the boundary point least squares technique. For example, results obtained for a spherical shallow shell with a square planform are summarized in Table 38.

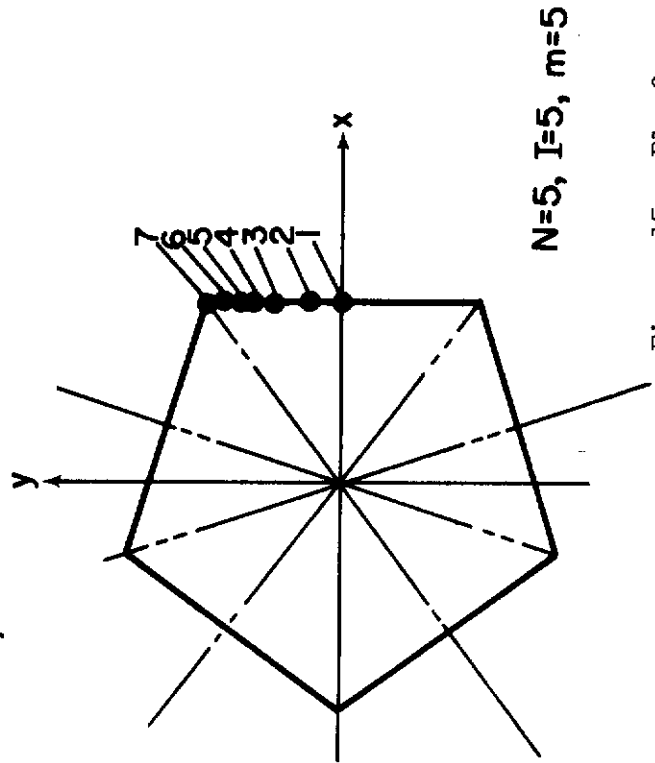
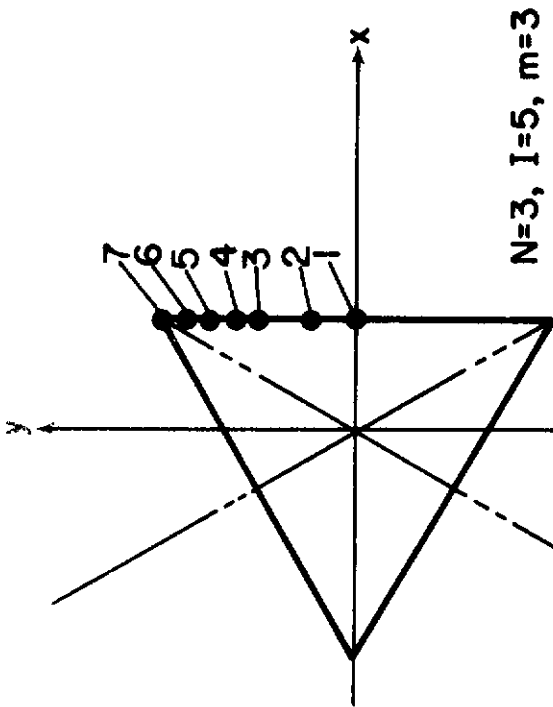
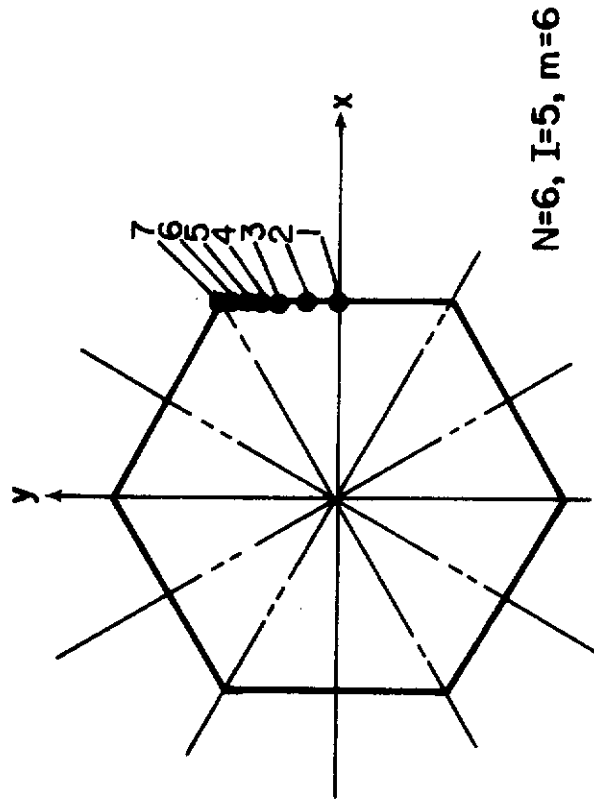
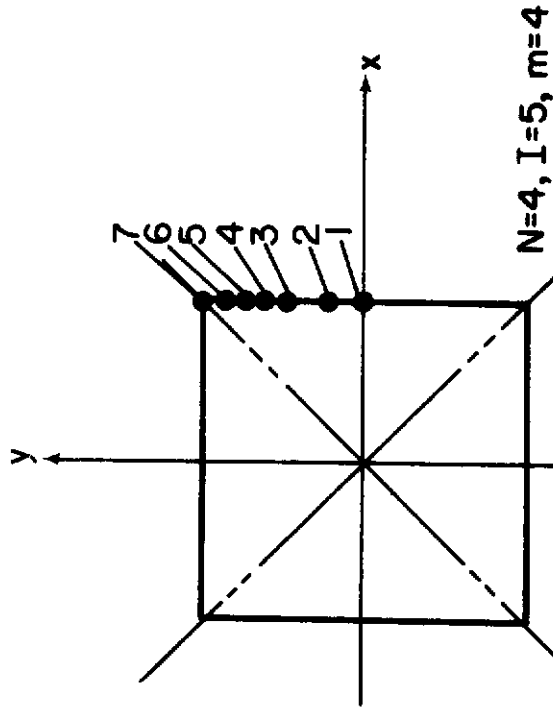


Figure 15. Planform shape, points matched and coordinates

Contrails

Table 29. Clamped Spherical Shell with Triangular Planform Obtained by Least Squares Using Additional Points
 $(R/t = 50, R = 1.932, a = 1/\sqrt{2}, b = a \cos \pi/3)$

a. Values of the Physical Parameters along $\theta=0$

x/b	0.0	0.2	0.4	0.6	0.8	1.0
w	$.12242 \times 10^{-5}$	$.11491 \times 10^{-5}$	$.92004 \times 10^{-5}$	$.56736 \times 10^{-6}$	$.19246 \times 10^{-6}$	$.19804 \times 10^{-6}$
$\frac{\partial w}{\partial n}$.0	$-.21592 \times 10^{-5}$	$-.42547 \times 10^{-5}$	$-.54894 \times 10^{-5}$	$-.46395 \times 10^{-5}$	$-.25271 \times 10^{-6}$
M_n		$.60392 \times 10^{-2}$	$.48011 \times 10^{-2}$	$.13427 \times 10^{-2}$	$-.53172 \times 10^{-2}$	$-.16171 \times 10^{-1}$
u_n	.0	$-.18612 \times 10^{-7}$	$-.31924 \times 10^{-7}$	$-.34236 \times 10^{-7}$	$-.22372 \times 10^{-7}$	$.69096 \times 10^{-11}$
u_t		.58182	.55020	.50945	.46647	.42374

b. Residuals along the Boundary

y	w	$\frac{\partial w}{\partial n}$	u_n	u_t
.000*	$.19804 \times 10^{-6}$	$-.25189 \times 10^{-9}$	$.69140 \times 10^{-11}$	$.0000 \times 10^{-39}$
.0383	$.14251 \times 10^{-6}$	$-.30826 \times 10^{-9}$	$.49721 \times 10^{-11}$	$.78835 \times 10^{-11}$
.7655	$.33786 \times 10^{-12}$	$-.37892 \times 10^{-9}$	$.31759 \times 10^{-13}$	$.13120 \times 10^{-10}$
.1148	$-.16527 \times 10^{-9}$	$-.24572 \times 10^{-9}$	$-.56523 \times 10^{-11}$	$.13731 \times 10^{-10}$
.1531*	$-.27906 \times 10^{-9}$	$.25485 \times 10^{-9}$	$-.93966 \times 10^{-11}$	$.90663 \times 10^{-11}$
.1914	$-.28675 \times 10^{-9}$	$.10353 \times 10^{-8}$	$-.92886 \times 10^{-11}$	$.23883 \times 10^{-12}$
.2296	$-.18112 \times 10^{-9}$	$.16646 \times 10^{-8}$	$-.51622 \times 10^{-11}$	$-.98008 \times 10^{-11}$
.2679	$-.89824 \times 10^{-11}$	$.14707 \times 10^{-8}$	$.11772 \times 10^{-11}$	$-.16874 \times 10^{-10}$
.3062*	$.14747 \times 10^{-9}$	$-.92666 \times 10^{-10}$	$.65583 \times 10^{-11}$	$-.17135 \times 10^{-10}$
.3445	$.21092 \times 10^{-9}$	$-.29071 \times 10^{-8}$	$.79284 \times 10^{-11}$	$-.90499 \times 10^{-11}$
.3827**	$.15464 \times 10^{-9}$	$-.56742 \times 10^{-8}$	$.40590 \times 10^{-11}$	$.46323 \times 10^{-11}$
.4210	$.28715 \times 10^{-9}$	$-.57931 \times 10^{-8}$	$-.33197 \times 10^{-11}$	$.16421 \times 10^{-10}$
.4593*	$-.60022 \times 10^{-10}$	$-.10194 \times 10^{-9}$	$-.93006 \times 10^{-11}$	$.16936 \times 10^{-10}$
.4976	$-.24656 \times 10^{-10}$	$.13015 \times 10^{-7}$	$-.77270 \times 10^{-11}$	$.16523 \times 10^{-11}$
.5358**	$.97411 \times 10^{-10}$	$.29814 \times 10^{-7}$	$.43709 \times 10^{-11}$	$-.20503 \times 10^{-10}$
.5741	$.12218 \times 10^{-9}$	$.35865 \times 10^{-7}$	$.18895 \times 10^{-10}$	$-.25353 \times 10^{-10}$
.6124*	$.78773 \times 10^{-11}$	$.48479 \times 10^{-10}$	$.12913 \times 10^{-11}$	$.22595 \times 10^{-11}$

* w, $\frac{\partial w}{\partial n}$, u_n , and u_t forced

** u_n and u_t forced

c. Ratios of Maximum Residuals to Maximum Values of Physical Parameter within the Shell

	w	$\frac{\partial w}{\partial n}$	u_n	u_t
Maximum residual along the boundary	$.28715 \times 10^{-9}$	$.35865 \times 10^{-7}$	$.18895 \times 10^{-10}$	$.25353 \times 10^{-10}$
Maximum value of the parameter within the shell	$.12242 \times 10^{-5}$	$.54894 \times 10^{-5}$	$.34236 \times 10^{-7}$	$.34236 \times 10^{-7}$
Percentage of maximum residual to maximum value	0.0235%	0.6534%	0.0552%	0.0741%

Contrails

Table 30. Clamped Spherical Shell with Square Planform Obtained by Least Squares Using Additional Points
 $(R/t = 50, R = 1.932, a = 1/\sqrt{2}, b = a \cos \pi/4)$

a. Values of the Physical Parameters along $\theta=0$

x/b	0.0	0.2	0.4	0.6	0.8	1.0
w	$.18461 \times 10^{-5}$	$.17430 \times 10^{-5}$	$.14300 \times 10^{-5}$	$.92187 \times 10^{-6}$	$.33124 \times 10^{-6}$	$-.16227 \times 10^{-6}$
$\frac{\partial w}{\partial n}$.0	$-.20721 \times 10^{-5}$	$-.41761 \times 10^{-5}$	$-.58220 \times 10^{-5}$	$-.54480 \times 10^{-5}$	$.19552 \times 10^{-6}$
M_n		$.42449 \times 10^{-2}$	$.39139 \times 10^{-2}$	$.20110 \times 10^{-2}$	$-.34778 \times 10^{-2}$	$-.14874 \times 10^{-1}$
u_n	.0	$-.38169 \times 10^{-7}$	$-.65872 \times 10^{-7}$	$-.72092 \times 10^{-7}$	$-.48401 \times 10^{-7}$	$.39207 \times 10^{-10}$
N_n		.90605	.86122	.79738	.72773	.65799

b. Residuals along the Boundary

y	w	$\frac{\partial w}{\partial n}$	u_n	u_t
.0*	$-.16228 \times 10^{-9}$	$.19559 \times 10^{-8}$	$.39211 \times 10^{-10}$.0
.0313	$-.95490 \times 10^{-10}$	$.17443 \times 10^{-8}$	$.27729 \times 10^{-10}$	$.86254 \times 10^{-10}$
.0625	$.64857 \times 10^{-10}$	$.94184 \times 10^{-9}$	$-.18009 \times 10^{-11}$	$.14135 \times 10^{-9}$
.0937	$.22050 \times 10^{-9}$	$-.75182 \times 10^{-9}$	$-.36791 \times 10^{-10}$	$.14387 \times 10^{-9}$
.1250*	$.27097 \times 10^{-9}$	$-.32930 \times 10^{-8}$	$-.62060 \times 10^{-10}$	$.89599 \times 10^{-10}$
.1563	$.17465 \times 10^{-9}$	$-.58558 \times 10^{-8}$	$-.66520 \times 10^{-10}$	$-.55946 \times 10^{-11}$
.1875	$-.17907 \times 10^{-10}$	$-.68179 \times 10^{-8}$	$-.48112 \times 10^{-10}$	$-.10847 \times 10^{-9}$
.2187	$-.18281 \times 10^{-9}$	$-.44126 \times 10^{-8}$	$-.15138 \times 10^{-10}$	$-.17724 \times 10^{-9}$
.2500*	$-.19430 \times 10^{-9}$	$-.20338 \times 10^{-8}$	$.17386 \times 10^{-10}$	$-.17557 \times 10^{-9}$
.2812	$-.18024 \times 10^{-10}$	$.10789 \times 10^{-7}$	$.35220 \times 10^{-10}$	$-.89314 \times 10^{-10}$
.3125**	$.22863 \times 10^{-9}$	$.17185 \times 10^{-7}$	$.32526 \times 10^{-10}$	$.58132 \times 10^{-10}$
.3437	$.31014 \times 10^{-9}$	$.14863 \times 10^{-7}$	$.15216 \times 10^{-10}$	$.19884 \times 10^{-9}$
.375*	$.28053 \times 10^{-10}$	$-.64081 \times 10^{-8}$	$-.46847 \times 10^{-11}$	$.23177 \times 10^{-9}$
.4063	$-.55032 \times 10^{-9}$	$-.26600 \times 10^{-7}$	$-.22078 \times 10^{-10}$	$.66488 \times 10^{-10}$
.4375**	$-.95947 \times 10^{-9}$	$-.48811 \times 10^{-7}$	$-.46306 \times 10^{-10}$	$-.28363 \times 10^{-9}$
.4687	$-.61435 \times 10^{-9}$	$-.44149 \times 10^{-7}$	$-.69544 \times 10^{-10}$	$-.54177 \times 10^{-9}$
.5000*	$.60863 \times 10^{-10}$	$.33217 \times 10^{-8}$	$.68304 \times 10^{-10}$	$.68287 \times 10^{-10}$

* w, $\frac{\partial w}{\partial n}$, u_n , and u_t forced
 ** u_n and u_t forced

c. Ratios of Maximum Residuals to Maximum Values of Physical Parameter within the Shell

	w	$\frac{\partial w}{\partial n}$	u_n	u_t
Maximum residual along the boundary	$.95947 \times 10^{-9}$	$.48811 \times 10^{-7}$	$.69544 \times 10^{-10}$	$.54177 \times 10^{-9}$
Maximum value of the parameter within the shell	$.18461 \times 10^{-5}$	$.58220 \times 10^{-5}$	$.72092 \times 10^{-7}$	$.72092 \times 10^{-7}$
Percentage of maximum residual to maximum value	0.0520%	0.8384%	0.0964%	0.7515%

Contrails

Table 31. Clamped Spherical Shell with Pentagonal Planform Obtained by Least Squares Using Additional Points
($R/t = 90$, $R = 1.932$, $a = 1/\sqrt{2}$, $b = a \cos \pi/5$)

a. Values of the Physical Parameters along $\theta=0$

x/b	0.0	0.2	0.4	0.6	0.8	1.0
w	$.19529 \times 10^{-5}$	$.18523 \times 10^{-5}$	$.15434 \times 10^{-5}$	$.10236 \times 10^{-5}$	$.38281 \times 10^{-6}$	$-.98797 \times 10^{-10}$
$\frac{\partial w}{\partial n}$.0	$-.17707 \times 10^{-5}$	$-.36448 \times 10^{-5}$	$-.53389 \times 10^{-5}$	$-.53548 \times 10^{-5}$	$.18942 \times 10^{-8}$
M_n		$.32355 \times 10^{-2}$	$.32715 \times 10^{-2}$	$.21759 \times 10^{-2}$	$-.23968 \times 10^{-2}$	$-.13734 \times 10^{-1}$
u_n	.0	$-.44986 \times 10^{-7}$	$-.78150 \times 10^{-7}$	$-.86728 \times 10^{-7}$	$-.59360 \times 10^{-7}$	$.28338 \times 10^{-10}$
N_n		.97978	.93523	.86749	.79095	.71263

b. Residuals along the Boundary

y	w	$\frac{\partial w}{\partial n}$	u_n	u_t
.0*	$-.98799 \times 10^{-10}$	$.18948 \times 10^{-8}$	$.28343 \times 10^{-10}$.0
.0259	$-.74664 \times 10^{-10}$	$.11925 \times 10^{-8}$	$.22903 \times 10^{-10}$	$.19179 \times 10^{-9}$
.0519	$-.88236 \times 10^{-11}$	$-.53640 \times 10^{-9}$	$.80006 \times 10^{-11}$	$.30683 \times 10^{-9}$
.0779	$.79732 \times 10^{-10}$	$-.23424 \times 10^{-8}$	$-.12610 \times 10^{-10}$	$.29539 \times 10^{-9}$
.1039*	$.16195 \times 10^{-9}$	$.31695 \times 10^{-8}$	$-.34318 \times 10^{-10}$	$.15399 \times 10^{-9}$
.1299	$.20410 \times 10^{-9}$	$-.24292 \times 10^{-8}$	$-.52821 \times 10^{-10}$	$-.69497 \times 10^{-10}$
.1558	$.17698 \times 10^{-9}$	$-.41681 \times 10^{-9}$	$-.64004 \times 10^{-10}$	$-.28812 \times 10^{-9}$
.1818	$.68675 \times 10^{-10}$	$.16662 \times 10^{-8}$	$-.62902 \times 10^{-10}$	$-.40466 \times 10^{-9}$
.2078*	$-.10243 \times 10^{-9}$	$.22309 \times 10^{-8}$	$-.43080 \times 10^{-10}$	$-.35083 \times 10^{-9}$
.2338	$-.28054 \times 10^{-9}$	$.30481 \times 10^{-8}$	$.44453 \times 10^{-12}$	$-.12544 \times 10^{-9}$
.2597**	$-.38006 \times 10^{-9}$	$-.33103 \times 10^{-8}$	$.63135 \times 10^{-10}$	$.18396 \times 10^{-9}$
.2857	$-.31604 \times 10^{-9}$	$-.53497 \times 10^{-8}$	$.11915 \times 10^{-9}$	$.41328 \times 10^{-9}$
.3117*	$-.58245 \times 10^{-10}$	$-.73593 \times 10^{-9}$	$.11474 \times 10^{-9}$	$.38134 \times 10^{-9}$
.3377	$.30802 \times 10^{-9}$	$.14476 \times 10^{-7}$	$-.14522 \times 10^{-10}$	$-.15623 \times 10^{-12}$
.3637**	$.56385 \times 10^{-9}$	$.37148 \times 10^{-7}$	$-.27204 \times 10^{-9}$	$-.58205 \times 10^{-9}$
.3896	$.47896 \times 10^{-9}$	$.47968 \times 10^{-7}$	$-.43906 \times 10^{-9}$	$-.84361 \times 10^{-9}$
.4156*	$.23522 \times 10^{-9}$	$.40048 \times 10^{-9}$	$.20829 \times 10^{-9}$	$.15133 \times 10^{-9}$

* w, $\frac{\partial w}{\partial n}$, u_n and u_t forced

** u_n and u_t forced

c. Ratios of Maximum Residuals to Maximum Values of Physical Parameter within the Shell

	w	$\frac{\partial w}{\partial n}$	u_n	u_t
Maximum residual along the boundary	$.56385 \times 10^{-9}$	$.47968 \times 10^{-7}$	$.43905 \times 10^{-9}$	$.84361 \times 10^{-9}$
Maximum value of the parameter within the shell	$.19529 \times 10^{-5}$	$.53548 \times 10^{-5}$	$.86728 \times 10^{-7}$	$.86728 \times 10^{-7}$
Percentage of maximum residual to maximum value	0.0289%	0.8975%	0.5062%	0.9727%

Contrails

Table 32. Clamped Spherical Shell with Hexagonal Planform Obtained by Least Squares Using Additional Points

($R/t = 50$, $R = 1.932$, $a = 1/\sqrt{2}$, $b = a \cos \pi/6$)

a. Values of the Physical Parameters along $\theta=0$

x/b	0.0	0.2	0.4	0.6	0.8	1.0
w	$.19734 \times 10^{-5}$	$.18775 \times 10^{-5}$	$.15785 \times 10^{-5}$	$.10631 \times 10^{-5}$	$.40692 \times 10^{-6}$	$.26676 \times 10^{-6}$
$\frac{\partial w}{\partial n}$.0	$-.15828 \times 10^{-5}$	$-.33290 \times 10^{-5}$	$-.50141 \times 10^{-5}$	$-.52263 \times 10^{-5}$	$.71067 \times 10^{-6}$
M_n		$.27499 \times 10^{-2}$	$.29473 \times 10^{-2}$	$.22032 \times 10^{-2}$	$-.18417 \times 10^{-2}$	$-.13005 \times 10^{-1}$
u_n	.0	$-.47809 \times 10^{-7}$	$-.83449 \times 10^{-7}$	$-.93359 \times 10^{-7}$	$-.64641 \times 10^{-7}$	$-.35129 \times 10^{-11}$
N_n		1.00412	.96082	.89184	.81164	.72899

b. Residuals along the Boundary

y	w	$\frac{\partial w}{\partial n}$	u_n	u_t
.0*	$.26677 \times 10^{-9}$	$.71130 \times 10^{-9}$	$-.35120 \times 10^{-11}$.0
.0221	$.13002 \times 10^{-9}$	$-.60100 \times 10^{-9}$	$.50466 \times 10^{-11}$	$.22766 \times 10^{-9}$
.0442	$-.19179 \times 10^{-9}$	$-.32265 \times 10^{-9}$	$.24013 \times 10^{-10}$	$.35772 \times 10^{-9}$
.0663	$-.48521 \times 10^{-9}$	$.41706 \times 10^{-9}$	$.36737 \times 10^{-10}$	$.33007 \times 10^{-9}$
.0884*	$-.54015 \times 10^{-9}$	$.10609 \times 10^{-9}$	$.25779 \times 10^{-10}$	$.14714 \times 10^{-9}$
.1105	$-.28503 \times 10^{-9}$	$.55906 \times 10^{-9}$	$-.15722 \times 10^{-10}$	$-.12272 \times 10^{-9}$
.1326	$.14978 \times 10^{-9}$	$.11689 \times 10^{-7}$	$-.75740 \times 10^{-10}$	$-.36692 \times 10^{-9}$
.1547	$.48870 \times 10^{-9}$	$.11361 \times 10^{-7}$	$-.12315 \times 10^{-9}$	$-.47109 \times 10^{-9}$
.1768*	$.47386 \times 10^{-9}$	$.84189 \times 10^{-9}$	$-.11919 \times 10^{-9}$	$-.37008 \times 10^{-9}$
.1989	$.54125 \times 10^{-10}$	$-.17363 \times 10^{-7}$	$-.39891 \times 10^{-10}$	$-.88925 \times 10^{-10}$
.2209**	$-.52043 \times 10^{-9}$	$-.32849 \times 10^{-7}$	$.97603 \times 10^{-10}$	$.24680 \times 10^{-9}$
.2431	$-.79748 \times 10^{-9}$	$-.30652 \times 10^{-7}$	$.21867 \times 10^{-9}$	$.44717 \times 10^{-9}$
.2652*	$-.42353 \times 10^{-9}$	$-.14721 \times 10^{-9}$	$.20534 \times 10^{-9}$	$.34406 \times 10^{-9}$
.2873	$.49413 \times 10^{-9}$	$.53309 \times 10^{-7}$	$-.38590 \times 10^{-10}$	$-.89862 \times 10^{-10}$
.3093**	$.12605 \times 10^{-9}$	$.10070 \times 10^{-9}$	$-.45745 \times 10^{-9}$	$-.63116 \times 10^{-9}$
.3315	$.10759 \times 10^{-9}$	$.95139 \times 10^{-7}$	$-.65625 \times 10^{-9}$	$-.77002 \times 10^{-9}$
.4135*	$.41357 \times 10^{-9}$	$.14820 \times 10^{-9}$	$.30378 \times 10^{-9}$	$.17538 \times 10^{-9}$

* w, $\partial w/\partial n$, u_n and u_t forced

** u_n and u_t forced

c. Ratios of Maximum Residuals to Maximum Values of Physical Parameter within the Shell

	w	$\frac{\partial w}{\partial n}$	u_n	u_t
Maximum residual along the boundary	$.12605 \times 10^{-5}$	$.10070 \times 10^{-9}$	$.65625 \times 10^{-9}$	$.77002 \times 10^{-9}$
Maximum value of the parameter within the shell	$.19734 \times 10^{-5}$	$.52263 \times 10^{-5}$	$.93359 \times 10^{-7}$	$.93359 \times 10^{-7}$
Percentage of maximum residual to maximum value	0.0639%	1.9268%	0.7029%	0.8248%

Contrails

Table 33. Spherical Shell Supported Along the Boundary Shear Diaphragm Triangular Planform
 Obtained by Least Squares Using Additional Points
 ($R/t = 50$, $R = 1.932$, $a = 1/\sqrt{2}$, $b = a \cos \pi/3$)

a. Values of the Physical Parameters along $\theta=0$

x/b	0.0	0.2	0.4	0.6	0.8	1.0
w	$.19311 \times 10^{-5}$	$.18095 \times 10^{-5}$	$.13900 \times 10^{-5}$	$.58654 \times 10^{-6}$	$-.66706 \times 10^{-6}$	$-.23707 \times 10^{-5}$
$\frac{\partial w}{\partial n}$.0	$-.36261 \times 10^{-5}$	$-.84488 \times 10^{-5}$	$-.14443 \times 10^{-4}$	$-.21023 \times 10^{-4}$	$-.26940 \times 10^{-4}$
M_n		$.10855 \times 10^{-1}$	$.13152 \times 10^{-1}$	$.15257 \times 10^{-1}$	$.16178 \times 10^{-1}$	$.16117 \times 10^{-1}$
u_n	.0	$-.22440 \times 10^{-7}$	$-.45125 \times 10^{-7}$	$-.53058 \times 10^{-7}$	$-.27722 \times 10^{-7}$	$.46518 \times 10^{-7}$
N_n		1.07080	.89992	.71544	.49518	.12142

b. Residuals along the Boundary

y	w	M_n	u_t	N_n
.0*	$-.23707 \times 10^{-5}$	$.16117 \times 10^{-1}$.0	.12142
.0383	$-.24371 \times 10^{-5}$	$.16499 \times 10^{-1}$	$.34060 \times 10^{-7}$.16601
.0765	$-.25963 \times 10^{-5}$	$.17399 \times 10^{-1}$	$.65334 \times 10^{-7}$.29615
.1148	$-.27445 \times 10^{-5}$	$.18176 \times 10^{-1}$	$.90883 \times 10^{-7}$.49835
.1531*	$-.27537 \times 10^{-5}$	$.18072 \times 10^{-1}$	$.10786 \times 10^{-6}$.74318
.1913	$-.25250 \times 10^{-5}$	$.16567 \times 10^{-1}$	$.11429 \times 10^{-6}$.98112
.2296	$-.20366 \times 10^{-5}$	$.13696 \times 10^{-1}$	$.11030 \times 10^{-6}$	1.14646
.2679	$-.13684 \times 10^{-5}$	$.10182 \times 10^{-1}$	$.99226 \times 10^{-7}$	1.17395
.3062*	$-.68977 \times 10^{-6}$	$.72780 \times 10^{-2}$	$.87858 \times 10^{-7}$	1.02727
.3444	$-.20853 \times 10^{-6}$	$.62793 \times 10^{-2}$	$.85325 \times 10^{-7}$.73152
.3827**	$-.91494 \times 10^{-7}$	$.77742 \times 10^{-2}$	$.10024 \times 10^{-6}$.39327
.4210	$-.38390 \times 10^{-6}$	$.10885 \times 10^{-1}$	$.13683 \times 10^{-6}$.18709
.4593*	$-.96558 \times 10^{-6}$	$.12944 \times 10^{-1}$	$.19164 \times 10^{-6}$.28938
.4975	$-.15830 \times 10^{-5}$	$.10324 \times 10^{-1}$	$.25318 \times 10^{-6}$.75657
.5358	$-.19803 \times 10^{-5}$	$.13796 \times 10^{-2}$	$.30655 \times 10^{-6}$	1.38218
.5741	$-.21057 \times 10^{-5}$	$.72008 \times 10^{-2}$	$.34319 \times 10^{-6}$	1.63356
.6124*	$-.22911 \times 10^{-5}$	$.10907 \times 10^{-1}$	$.21349 \times 10^{-6}$.87385

* w, M_n , u_t and N_n forced

** u_t and N_n forced

c. Ratios of Maximum Residuals to Maximum Values
 of Physical Parameter within the Shell

	w	M_n	u_t	N_n
Maximum residual along the boundary	$.27535 \times 10^{-5}$	$.18176 \times 10^{-1}$	$.34319 \times 10^{-6}$	1.63356
Maximum value of the parameter within the shell	$.19311 \times 10^{-5}$	$.16178 \times 10^{-1}$	$.53058 \times 10^{-7}$	1.07080
Percentage of maximum residual to maximum value	142.59%	112.35%	646.82%	152.56%

Contrails

Table 34. Spherical Shell Supported Along the Boundary by Shear Diaphragm Square Planform
 Obtained by Least Squares Using Additional Points
 ($R/t = 50$, $R = 1.932$, $a = 1/\sqrt{2}$, $b = a \cos \pi/4$)

a. Values of the Physical Parameters along $\theta=0$

x/b	0.0	0.2	0.4	0.6	0.8	1.0
w	$.38476 \times 10^{-5}$	$.37359 \times 10^{-5}$	$.33653 \times 10^{-5}$	$.26475 \times 10^{-5}$	$.15049 \times 10^{-5}$	$-.59144 \times 10^{-10}$
$\frac{\partial w}{\partial n}$.0	$-.22962 \times 10^{-5}$	$-.52734 \times 10^{-5}$	$-.92327 \times 10^{-5}$	$-.13551 \times 10^{-4}$	$-.15905 \times 10^{-4}$
M_n		$.50225 \times 10^{-2}$	$.63841 \times 10^{-2}$	$.75717 \times 10^{-2}$	$.65608 \times 10^{-2}$	$-.86492 \times 10^{-8}$
u_n	.0	$-.12896 \times 10^{-6}$	$-.25392 \times 10^{-6}$	$-.36583 \times 10^{-6}$	$-.44797 \times 10^{-6}$	$-.47917 \times 10^{-6}$
N_n		1.10110	.94414	.69283	.36720	$.26986 \times 10^{-4}$

b. Residuals along the Boundary

y	w	M_n	u_t	N_n
.0*	$-.59252 \times 10^{-10}$	$-.94684 \times 10^{-8}$.0	$.26964 \times 10^{-4}$
.0313	$-.58078 \times 10^{-10}$	$.28493 \times 10^{-6}$	$-.70508 \times 10^{-11}$	$.65640 \times 10^{-5}$
.0625	$-.43732 \times 10^{-10}$	$.85259 \times 10^{-6}$	$-.10882 \times 10^{-10}$	$-.39756 \times 10^{-4}$
.0938	$.59797 \times 10^{-11}$	$.95973 \times 10^{-6}$	$-.98449 \times 10^{-11}$	$.76383 \times 10^{-4}$
.1250*	$.10010 \times 10^{-9}$	$-.32122 \times 10^{-6}$	$-.45807 \times 10^{-11}$	$-.69655 \times 10^{-4}$
.1563	$.20156 \times 10^{-9}$	$-.19326 \times 10^{-5}$	$.22702 \times 10^{-11}$	$-.11489 \times 10^{-4}$
.1875	$.26828 \times 10^{-9}$	$-.37256 \times 10^{-5}$	$.75533 \times 10^{-11}$	$.69954 \times 10^{-4}$
.2188	$.19114 \times 10^{-9}$	$-.35868 \times 10^{-5}$	$.91984 \times 10^{-11}$	$.12239 \times 10^{-3}$
.2500*	$.59430 \times 10^{-10}$	$-.21589 \times 10^{-7}$	$.72536 \times 10^{-11}$	$.10204 \times 10^{-3}$
.2813	$-.41856 \times 10^{-9}$	$.67146 \times 10^{-5}$	$.36661 \times 10^{-11}$	$.10371 \times 10^{-4}$
.3125**	$-.69181 \times 10^{-9}$	$.13363 \times 10^{-4}$	$.59917 \times 10^{-12}$	$-.90845 \times 10^{-4}$
.3438	$-.60883 \times 10^{-9}$	$.13560 \times 10^{-4}$	$-.13673 \times 10^{-11}$	$-.10986 \times 10^{-3}$
.3750*	$-.20203 \times 10^{-10}$	$-.11490 \times 10^{-7}$	$-.36486 \times 10^{-11}$	$-.57295 \times 10^{-5}$
.4063	$.10802 \times 10^{-9}$	$-.30322 \times 10^{-4}$	$-.74512 \times 10^{-11}$	$.12313 \times 10^{-3}$
.4375**	$.19790 \times 10^{-9}$	$-.67508 \times 10^{-4}$	$-.96332 \times 10^{-11}$	$.47788 \times 10^{-4}$
.4687	$.17805 \times 10^{-9}$	$-.78681 \times 10^{-4}$	$-.26639 \times 10^{-11}$	$-.30251 \times 10^{-3}$
.5000*	$.29647 \times 10^{-10}$	$-.90853 \times 10^{-7}$	$.82745 \times 10^{-11}$	$-.31985 \times 10^{-4}$

* w, M_n , u_t and N_n forced

** u_t and N_n forced

c. Ratios of Maximum Residuals to Maximum Values of Physical Parameter within the Shell

	w	M_n	u_t	N_n
Maximum residual along the boundary	$.19790 \times 10^{-9}$	$.78681 \times 10^{-4}$	$.10882 \times 10^{-10}$	$.30251 \times 10^{-3}$
Maximum value of the parameter within the shell	$.38476 \times 10^{-5}$	$.75717 \times 10^{-2}$	$.47917 \times 10^{-6}$	1.01100
Percentage of maximum residual to maximum value	0.051%	1.039%	0.002%	0.027%

Contrails

Table 35. Spherical Shell Supported Along the Boundary by Shear Diaphragm Pentagonal Planform
 Obtained by Least Squares Using Additional Points
 ($R/t = 50$, $R = 1.932$, $a = 1/\sqrt{2}$, $b = a \cos \pi/5$)

a. Values of the Physical Parameters along $\theta=0$

x/b	0.0	0.2	0.4	0.6	0.8	1.0
w	$.38342 \times 10^{-5}$	$.37424 \times 10^{-5}$	$.34223 \times 10^{-5}$	$.27511 \times 10^{-5}$	$.15977 \times 10^{-5}$	$.42396 \times 10^{-7}$
$\frac{\partial w}{\partial n}$.0	$-.16704 \times 10^{-5}$	$-.41134 \times 10^{-5}$	$-.78381 \times 10^{-5}$	$-.12283 \times 10^{-4}$	$-.13909 \times 10^{-4}$
M_n		$.33567 \times 10^{-2}$	$.49530 \times 10^{-2}$	$.67019 \times 10^{-2}$	$.62094 \times 10^{-2}$	$-.46376 \times 10^{-4}$
u_n	.0	$-.14463 \times 10^{-6}$	$-.28100 \times 10^{-6}$	$-.39970 \times 10^{-6}$	$-.48441 \times 10^{-6}$	$-.51525 \times 10^{-6}$
N_n		1.15017	1.05389	.84052	.50386	$.91213 \times 10^{-2}$

b. Residuals along the Boundary

y	w	M_n	u_t	N_n
.0*	$.42396 \times 10^{-7}$	$-.46377 \times 10^{-4}$.0	$.91212 \times 10^{-2}$
.0259	$.25631 \times 10^{-7}$	$-.86286 \times 10^{-5}$	$.40365 \times 10^{-8}$	$.13495 \times 10^{-1}$
.0519	$-.16807 \times 10^{-7}$	$.58515 \times 10^{-4}$	$.69221 \times 10^{-8}$	$.24733 \times 10^{-1}$
.0779	$-.64771 \times 10^{-7}$	$.50610 \times 10^{-4}$	$.77930 \times 10^{-8}$	$.37811 \times 10^{-1}$
.1039*	$-.94733 \times 10^{-7}$	$-.11195 \times 10^{-3}$	$.63120 \times 10^{-8}$	$.46347 \times 10^{-1}$
.1299	$-.90587 \times 10^{-7}$	$-.39913 \times 10^{-3}$	$.28119 \times 10^{-8}$	$.45212 \times 10^{-1}$
.1559	$-.51764 \times 10^{-7}$	$-.64154 \times 10^{-3}$	$-.17078 \times 10^{-8}$	$.33272 \times 10^{-1}$
.1818	$.51032 \times 10^{-8}$	$-.59467 \times 10^{-3}$	$-.57661 \times 10^{-8}$	$.15143 \times 10^{-1}$
.2078*	$.52443 \times 10^{-7}$	$-.92730 \times 10^{-4}$	$-.77651 \times 10^{-8}$	$.62393 \times 10^{-3}$
.2338	$.64051 \times 10^{-7}$	$.76790 \times 10^{-3}$	$-.64780 \times 10^{-8}$	$.79016 \times 10^{-3}$
.2598**	$.28499 \times 10^{-7}$	$.15239 \times 10^{-2}$	$-.15453 \times 10^{-8}$	$.20964 \times 10^{-1}$
.2857	$-.42847 \times 10^{-7}$	$.14417 \times 10^{-2}$	$.61676 \times 10^{-8}$	$.53009 \times 10^{-1}$
.3117*	$-.11868 \times 10^{-6}$	$-.10705 \times 10^{-3}$	$.14467 \times 10^{-7}$	$.72239 \times 10^{-1}$
.3377	$-.16278 \times 10^{-6}$	$-.30349 \times 10^{-2}$	$.19991 \times 10^{-7}$	$.46885 \times 10^{-1}$
.3637**	$-.15592 \times 10^{-6}$	$-.59354 \times 10^{-2}$	$.18435 \times 10^{-7}$	$-.31646 \times 10^{-1}$
.3896	$-.11227 \times 10^{-6}$	$-.59770 \times 10^{-2}$	$.44740 \times 10^{-8}$	$-.93316 \times 10^{-1}$
.4156*	$-.73767 \times 10^{-7}$	$-.19854 \times 10^{-4}$	$-.29116 \times 10^{-7}$	$.84766 \times 10^{-1}$

* w, M_n , u_t and N_n forced

** u_t and N_n forced

c. Ratios of Maximum Residuals to Maximum Values
 of Physical Parameter within the Shell

	w	M_n	u_t	N_n
Maximum residual along the boundary	$.16278 \times 10^{-6}$	$.59770 \times 10^{-2}$	$.29116 \times 10^{-7}$	$.93316 \times 10^{-1}$
Maximum value of the parameter within the shell	$.38342 \times 10^{-5}$	$.67019 \times 10^{-2}$	$.51525 \times 10^{-6}$	1.15017
Percentage of maximum residual to maximum value	4.24%	89.18%	5.65%	8.11%

Contrails

Table 36. Spherical Shell Supported Along the Boundary by Shear Diaphragm Hexagonal Planform
 Obtained by Least Squares Using Additional Points
 ($R/t = 50$, $R = 1.932$, $a = 1/\sqrt{2}$, $b = a \cos \pi/6$)

a. Values of the Physical Parameters along $\theta=0$

x/b	0.0	0.2	0.4	0.6	0.8	1.0
w	$.36351 \times 10^{-5}$	$.35534 \times 10^{-5}$	$.32582 \times 10^{-5}$	$.26193 \times 10^{-5}$	$.15064 \times 10^{-5}$	$.78332 \times 10^{-7}$
$\frac{dw}{dn}$.0	$-.14044 \times 10^{-5}$	$-.36030 \times 10^{-5}$	$-.70338 \times 10^{-5}$	$-.11066 \times 10^{-4}$	$-.10546 \times 10^{-4}$
M_n		$.27234 \times 10^{-2}$	$.42915 \times 10^{-2}$	$.59531 \times 10^{-2}$	$.53785 \times 10^{-2}$	$-.16292 \times 10^{-3}$
u_n	.0	$-.14311 \times 10^{-6}$	$-.27579 \times 10^{-6}$	$-.38466 \times 10^{-6}$	$-.45266 \times 10^{-6}$	$-.46804 \times 10^{-6}$
N_n		1.14571	1.08850	.93754	.64240	$.66907 \times 10^{-1}$

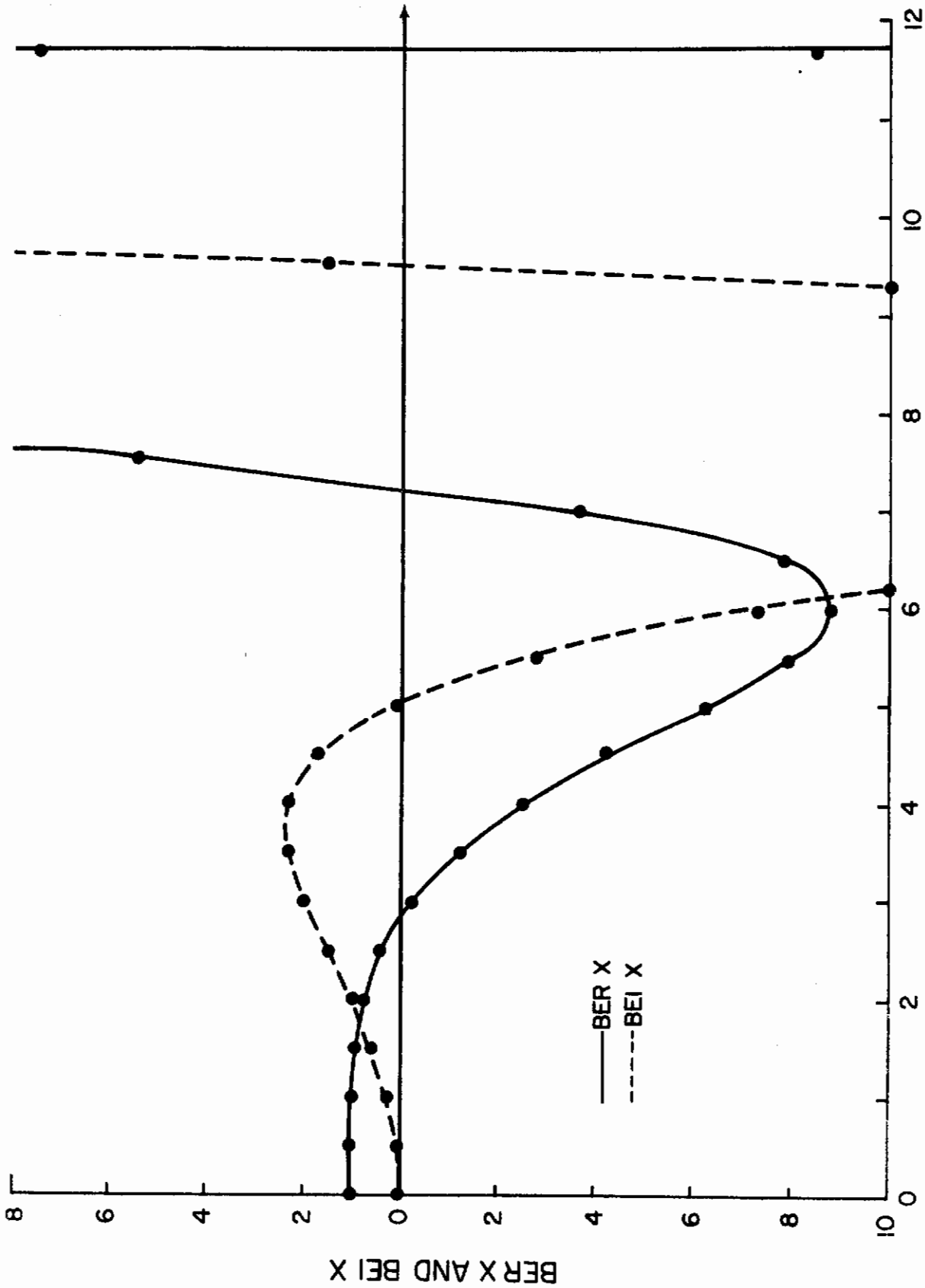
b. Residuals along the Boundary

y	w	M_n	u_t	N_n
.0*	$.78332 \times 10^{-7}$	$-.16292 \times 10^{-3}$.0	$.66907 \times 10^{-1}$
.0221	$.40620 \times 10^{-7}$	$-.60166 \times 10^{-4}$	$.78521 \times 10^{-6}$	$.76022 \times 10^{-1}$
.0442	$-.54124 \times 10^{-7}$	$.10733 \times 10^{-3}$	$.13324 \times 10^{-7}$.10073
.0663	$-.15921 \times 10^{-6}$	$.27329 \times 10^{-4}$	$.14679 \times 10^{-7}$.13372
.0884*	$-.22150 \times 10^{-6}$	$-.51887 \times 10^{-3}$	$.11351 \times 10^{-7}$.16376
.1105	$-.20722 \times 10^{-6}$	$-.14019 \times 10^{-2}$	$.42339 \times 10^{-6}$.17903
.1326	$-.12093 \times 10^{-6}$	$-.20846 \times 10^{-2}$	$-.43817 \times 10^{-6}$.17150
.1547	$-.25120 \times 10^{-6}$	$-.18627 \times 10^{-2}$	$-.11304 \times 10^{-7}$.14199
.1768*	$.81467 \times 10^{-7}$	$-.34720 \times 10^{-3}$	$-.13341 \times 10^{-7}$.10279
.1989	$.77217 \times 10^{-7}$	$.20445 \times 10^{-2}$	$-.84403 \times 10^{-6}$	$.74609 \times 10^{-1}$
.2210**	$-.30707 \times 10^{-7}$	$.39381 \times 10^{-2}$	$.32612 \times 10^{-6}$	$.75920 \times 10^{-1}$
.2431	$-.20431 \times 10^{-6}$	$.34902 \times 10^{-2}$	$.18851 \times 10^{-7}$.10794
.2652*	$-.36466 \times 10^{-6}$	$-.44316 \times 10^{-3}$	$.32843 \times 10^{-7}$.14357
.2873	$-.43032 \times 10^{-6}$	$-.68773 \times 10^{-2}$	$.38205 \times 10^{-7}$.13492
.3093**	$-.36620 \times 10^{-6}$	$-.11972 \times 10^{-1}$	$.27819 \times 10^{-7}$	$.54291 \times 10^{-1}$
.3315	$-.21485 \times 10^{-6}$	$-.10388 \times 10^{-1}$	$-.44294 \times 10^{-6}$	$-.25515 \times 10^{-1}$
.3535*	$-.81047 \times 10^{-7}$	$-.86505 \times 10^{-4}$	$-.63919 \times 10^{-7}$.17343

* w, M_n , u_t and N_n forced
 ** u_t and N_n forced

c. Ratios of Maximum Residuals to Maximum Values
 of Physical Parameter within the Shell

	w	M_n	u_t	N_n
Maximum residual along the boundary	$.43032 \times 10^{-6}$	$.11972 \times 10^{-1}$	$.63919 \times 10^{-7}$.17903
Maximum value of the parameter within the shell	$.36351 \times 10^{-5}$	$.59531 \times 10^{-2}$	$.46804 \times 10^{-6}$	1.14571
Percentage of maximum residual to maximum value	11.84%	201.11%	13.66%	15.63%



VALUES OF THE ARGUMENT

Figure 16. Bessel-Kelvin functions

Table 37. Zeros of Bessel-Kelvin Functions of Order Zero

Zeros	ber X	bei X	ber' X	bei' X
1st zero	2.84892	5.02622	6.03871	3.77320
2nd zero	7.23883	9.45541	10.51364	8.28099
3rd zero	11.67396	13.89349	14.96844	12.74215
4th zero	16.11356	18.33398	19.41758	17.19343
5th zero	20.55463	22.77544	23.86430	21.64114

Table 38. Comparison of Solutions by Three Methods.
Clamped Square Planform.

Parameter	Point Matching Technique	Least Square Sense Technique	
		Case I	Case II
$\left(\frac{\text{Res. } w}{w}\right)_{\text{max.}}$	0.352%	0.006%	0.052%
$\left(\frac{\text{Res. } \frac{\partial w}{\partial n}}{\frac{\partial w}{\partial n}}\right)_{\text{max.}}$	26.685%	2.730%	0.838%
$\left(\frac{\text{Res. } u_n}{u_n}\right)_{\text{max.}}$	155.476%	17.840%	0.096%
$\left(\frac{\text{Res. } u_t}{u_t}\right)_{\text{max.}}$	31.195%	4.416%	0.752%
w at r = 0	0.1816×10^{-5}	0.18420×10^{-5}	0.18461×10^{-5}
$\left(\frac{\partial w}{\partial n}\right)_{\text{max at } \theta = 0}$	-0.57230×10^{-5}	-0.58103×10^{-5}	-0.58220×10^{-5}
$(u_n)_{\text{max. at } \theta = 0}$	-0.70107×10^{-7}	-0.71864×10^{-7}	-0.72092×10^{-7}
$M_n \text{ at } \begin{cases} r = a \cos \frac{\pi}{4} \\ \theta = 0 \end{cases}$	-0.14682×10^{-1}	-0.14782×10^{-1}	-0.14874×10^{-1}
$N_n \text{ at } \begin{cases} r = a \cos \frac{\pi}{4} \\ \theta = 0 \end{cases}$	0.63088	0.66067	0.65799

Contrails

This behavior was typical also in the cases of triangular, pentagonal, and hexagonal planforms. As the residuals on the boundary were reduced to a maximum of less than 1%, the values of the physical parameters within the shell changed only slightly.

The accuracy of these approximate types of solution are usually judged by two criteria: (a) the residuals encountered along the boundary and (b) the rate of convergence of solutions as the number of boundary points used is increased.

Using the boundary point least squares method (Case II), the maximum deviation from zero deflection along the boundary occurs in the case of the hexagon and is only 0.064% of the center deflection. The maximum deviations from zero normal slope, zero normal displacement, and zero tangential displacement along the boundary occurred in the case of the hexagonal planform and were 1.927%, 0.703%, and 0.825% of the maximum values, respectively.

Table 39 summarizes the values of the physical parameters at some significant points. As the number of sides of the planform increased the values of maximum radial displacement and radial in-plane forces evaluated at $\theta = 0$ and $r = 2a \cos \pi/n$ increased continuously and were maximum for the spherical shell with circular planform. The normal moments at $\theta = 0$, $r = 0.2a \cos \pi/n$ and at $\theta = 0$, $r = a \cos \pi/n$ decreased continuously as the number of sides increased and were minimal for the shell having circular planform. The center deflection and normal in-plane force at $(\theta = 0, r = a \cos \pi/n)$ were maximal for the hexagonal planform.

Ill-conditioning of the coefficient matrix does not only depend on the shape of the boundary but also on the boundary conditions required to be satisfied. This is exemplified by the problem of the spherical shallow shell supported along the boundary by shear diaphragm. In that case, the maximum deviation from exact boundary conditions between points matched could not be reduced for the pentagonal and hexagonal planforms, either by increasing the number of discrete points used on the boundary, or by the use of the least squares technique. When the least squares technique was used, the coefficient matrix became ill-conditioned.

In the preceding chapter the point matching solution was compared to the exact solution for a spherical shallow shell with square planform supported along the boundary by shear diaphragms. If we accept as an approximate solution any solution which gives maximum deviation from exact boundary conditions between the points matched less than or equal to that of the shell with square planform, then on the basis of this comparison the only acceptable problem is the case of a shell with triangular planform. Table 40 summarizes the results for shells supported along the boundary by shear diaphragms with triangular, square, and circular planforms. This shows that all the physical parameters increase as the number of sides of the planform is increased.

Table 39. Values of Physical Parameters for Clamped Spherical Shells
($R/t = 50$, $R = 1.932$, $a = 1/\sqrt{2}$)

Parameters	No. of Sides				
	3	4	5	6	∞
w at $r = 0$	0.122×10^{-5}	0.185×10^{-5}	0.195×10^{-5}	0.197×10^{-5}	0.195×10^{-5}
$\left(\frac{\partial w}{\partial n}\right)_{\max.}$	-0.549×10^{-5}	-0.582×10^{-5}	-0.535×10^{-5}	-0.523×10^{-5}	-0.472×10^{-5}
$(u_n)_{\max.}$	-0.342×10^{-7}	-0.721×10^{-7}	-0.867×10^{-7}	-0.934×10^{-7}	-1.038×10^{-7}
M_n at $\begin{cases} \theta = 0, \\ r = 0.2a \cos \pi/n \end{cases}$	0.604×10^{-2}	0.425×10^{-2}	0.324×10^{-2}	0.275×10^{-2}	0.185×10^{-2}
N_n at $\begin{cases} \theta = 0 \\ r = 0.2a \cos \pi/n \end{cases}$	0.582	0.906	0.980	1.004	1.031
M_n at $\begin{cases} \theta = 0 \\ r = a \cos \pi/n \end{cases}$	-0.162×10^{-1}	-0.149×10^{-1}	-0.137×10^{-1}	-0.130×10^{-1}	-0.100×10^{-1}
N_n at $\begin{cases} \theta = 0 \\ r = a \cos \pi/n \end{cases}$	0.424	0.658	0.713	0.729	0.703

Contrails

Table 40. Values of the Physical Parameters for a Spherical Shell Supported Along the Boundary by Shear Diaphragms; Triangular, Square and Circular Planforms ($R/t = 50$, $R = 1.932$, $a = 1/\sqrt{2}$)

Parameter	Number of Sides		
	3	4	∞
w at $r = 0$	0.304×10^{-5}	0.385×10^{-5}	1.387×10^{-5}
$\frac{\partial w}{\partial n}$ at $\begin{cases} \theta = 0 \\ r = a \cos \pi/n \end{cases}$	-0.155×10^{-4}	-0.159×10^{-5}	-0.518×10^{-5}
u_n at $\begin{cases} \theta = 0 \\ r = a \cos \pi/n \end{cases}$	-0.287×10^{-6}	-0.479×10^{-6}	-3.082×10^{-6}
$(M_n)_{\max.}$	0.980×10^{-2}	0.757×10^{-2}	2.479×10^{-2}
N_n at $\begin{cases} \theta = 0 \\ r = 0.2a \cos \pi/n \end{cases}$	0.766	1.101	1.621

Table 41 gives results from the solution of the problem of uniformly loaded plates having clamped regular polygonal shape (Ref. 24) and having the same planform dimensions as those of the shell referred to in Table 39.

Table 41. Uniformly Loaded Clamped Plates of Regular Polygonal Shape ($t = 0.03864$, $b = a \cos \pi/n$, $a = 1/\sqrt{2}$, $E = 30 \times 10^6$ lbs/in²)

No. of Sides	$\frac{w}{q_0}$ at $r = 0$	$\frac{M}{q_0}$ at $r = 0$	$\frac{M}{q_0}$ at $\begin{cases} r = b \\ \theta = 0 \end{cases}$
3	0.2380×10^{-5}	1.2265×10^{-2}	-2.9650×10^{-2}
4	0.7981×10^{-5}	2.2905×10^{-2}	-5.1325×10^{-2}
5	1.2574×10^{-5}	2.8902×10^{-2}	-6.1718×10^{-2}
6	1.5740×10^{-5}	3.2400×10^{-2}	-6.6750×10^{-2}
∞	2.4638×10^{-5}	4.0625×10^{-2}	-6.2500×10^{-2}

Contrails

The center deflection and moment of a clamped plate increases continuously as the number of sides of the regular polygon is increased, and the center deflection of a circular plate is 10.3 times that of a circular shell. But in the case of shells, the deflection at the center of the circular shell is only .165 that of a clamped shell with triangular planform; the moments decrease continuously as the number of sides is increased.

It is also interesting, in comparing a plate and a shell having the same planform dimensions and thicknesses (from Tables 39 and 41) that the ratio of the center deflection of the polygonal plate to that of the polygonal shell increases as the number of sides increases. This can be seen in Table 42.

Table 42. Ratio of the Center Deflection of a Polygonal Plate to That of a Polygonal Shell Having the Same Uniform Normal Loading and Dimensions (Clamped Boundaries)

	Number of Sides				
	3	4	5	6	∞
$w_{\text{plate}}/w_{\text{shell}}$	1.95	4.31	6.45	8.00	12.65

Contracts

V. SHALLOW SPHERICAL SHELLS HAVING ELLIPTICAL PLANFORMS

In this chapter, the results of further experience with the method are summarized; the noncircular curvilinear boundary is introduced by means of using an ellipse. The method of point matching is straightforwardly applied as in the previous chapter. Numerical results for the important physical quantities of transverse deflection, slope, bending moment, tangential displacement, and membrane force are reported, along with an evaluation of the accuracy of the method by means of examining the values of residuals along the boundary.

Consider the shallow shell with a spherical radius "R" loaded by uniform pressure of intensity "q₀" normal to the surface, having an elliptical planform. One quadrant of the ellipse having a semi-major axis of "a" and a semi-minor axis "b" is shown in Fig. 17. Certain relations among the polar coordinates "r" and "θ," the angle φ by which the outer normal n leads the radial direction, and the ψ between the n- and x-directions are:

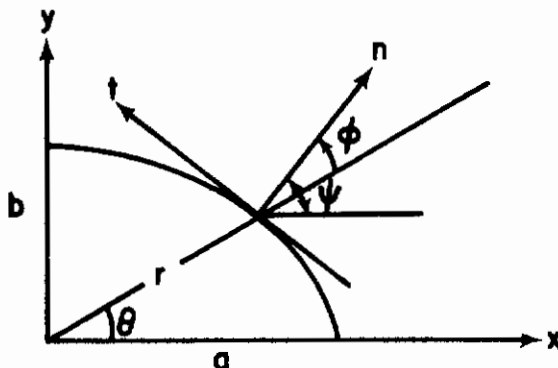


Figure 17. Typical Quadrant of an Ellipse

$$r = \frac{ab}{(b^2 \cos^2 \theta + a^2 \sin^2 \theta)^{1/2}}$$

$$\psi = \arctan \left(\frac{a^2}{b^2} \tan \theta \right) \tag{5-1}$$

$$\phi = \psi - \theta$$

Contrails

The problem was solved for different (a/b) ratios with five points matched on the boundary in the first quadrant. The following values were assigned for the constants

$$E = 30 \times 10^6$$

$$R = 5.8$$

$$q_0 = 1$$

$$b = 1$$

$$\nu = 0.3$$

A. EDGES CLAMPED

Case 1 - a/b = 1.5

Table 43 gives the values of the physical parameters along the radii $\theta = 0, \pi/4$ and $\pi/2$, while Table 44 gives the values of the residuals along the boundary at discrete points. The value of the maximum residual in each case was compared to the maximum value of the physical parameter under consideration within the shell. The ratios are tabulated in Table 45.

Case 2 - a/b = 1 (circular boundary)

Values of the physical parameters within the shell are given in Table 46 for comparison with Case 1.

B. EDGE SUPPORTED BY A SHEAR DIAPHRAGM

Case 1 - a/b = 1.5

Results are summarized in Tables 47, 48, and 49.

Case 2 - a/b = 1 (circular boundary)

Values within the shell of the physical parameters are given in Table 50 for comparison with a/b = 1.5.

C. COMPARISON BETWEEN CLAMPED AND SHEAR DIAPHRAGM SUPPORTED EDGES

One can directly compare values of center deflection, maximum slope, bending moment, tangential displacement, and membrane force for shells of the same size as aspect ratio (but different boundary conditions) by looking at Table 51.

Table 43 - Values of the Physical Parameters. Clamped Spherical Shell with Elliptical Planform [R/t = 50, R = 5.8", (a/b) = 1.5]

a. Along $\theta = 0$

x/a	0.0	0.2	0.4	0.6	0.8	1.0
w	0.34445x10 ⁻⁵	0.32048x10 ⁻⁵	0.25219x10 ⁻⁵	0.15271x10 ⁻⁵	0.50902x10 ⁻⁶	-0.17409x10 ⁻¹⁰
$\frac{\partial w}{\partial n}$	0.0	-0.15793x10 ⁻⁵	-0.29039x10 ⁻⁵	-0.35728x10 ⁻⁵	-0.29230x10 ⁻⁵	0.59217x10 ⁻¹⁰
M _n	*	0.38106x10 ⁻¹	0.30530x10 ⁻¹	0.14153x10 ⁻¹	-0.15737x10 ⁻¹	-0.63324x10 ⁻¹
v _n	0.0	-0.59626x10 ⁻⁷	-0.99350x10 ⁻⁷	-0.10310x10 ⁻⁶	-0.64923x10 ⁻⁷	0.45707x10 ⁻¹¹
N _n	*	0.17640x10 ¹	0.16049x10 ¹	0.13643x10 ¹	0.10854x10 ¹	0.83565

b. Along $\theta = \pi/4$

x/1.18b	0.0	0.2	0.4	0.6	0.8	1.0
w	0.34445x10 ⁻⁵	0.31897x10 ⁻⁵	0.24764x10 ⁻⁵	0.14694x10 ⁻⁵	0.47810x10 ⁻⁶	-0.10634x10 ⁻¹⁰
$\frac{\partial w}{\partial n}$	0.0	-0.23105x10 ⁻⁵	-0.41327x10 ⁻⁵	-0.48848x10 ⁻⁵	-0.38191x10 ⁻⁵	-0.15951x10 ⁻¹⁰
M _n	*	0.54957x10 ⁻¹	0.38586x10 ⁻¹	0.83205x10 ⁻²	-0.39491x10 ⁻¹	-0.10827
v _n	0.0	-0.54586x10 ⁻⁷	-0.90365x10 ⁻⁷	-0.93078x10 ⁻⁷	-0.58549x10 ⁻⁷	0.42251x10 ⁻¹¹
N _n	*	0.16151x10 ¹	0.15218x10 ¹	0.13790x10 ¹	0.12086x10 ¹	0.10460x10 ¹

* not evaluated

Contracts

c. Along $\theta = \pi/2$

x/b	0.0	0.2	0.4	0.6	0.8	1.0
W	0.34445×10^{-5}	0.31830×10^{-5}	0.24560×10^{-5}	0.14431×10^{-5}	0.46361×10^{-6}	-0.20822×10^{-10}
$\frac{\partial w}{\partial n}$	0.0	-0.25678×10^{-5}	-0.45538×10^{-5}	-0.53112×10^{-5}	-0.40834×10^{-5}	-0.18059×10^{-10}
M_n	*	0.57688×10^{-1}	0.37929×10^{-1}	0.26679×10^{-2}	-0.50829×10^{-1}	-0.12479
u_n	0.0	-0.54129×10^{-7}	-0.89449×10^{-7}	-0.91994×10^{-7}	-0.57982×10^{-7}	0.12631×10^{-12}
N_n	*	0.15888×10^1	0.15179×10^1	0.14094×10^1	0.12793×10^1	0.11529×10^1

* not evaluated

96

Contrails

Table 44 - Residuals Along the Boundary. Clamped Spherical Shell with Elliptical Planform (R/t = 50, R = 5.8", a/b = 1.5)

θ	w	$\frac{\partial w}{\partial n}$	u_n	u_t
0.0 *	-0.17506×10^{-10}	0.59197×10^{-10}	0.45581×10^{-11}	0.0
0.1963	-0.25243×10^{-10}	0.25170×10^{-9}	0.51508×10^{-9}	0.12177×10^{-8}
0.3927*	-0.18606×10^{-10}	0.10415×10^{-10}	0.37943×10^{-11}	-0.28121×10^{-12}
0.5890	-0.21458×10^{-11}	-0.78289×10^{-10}	-0.24588×10^{-9}	-0.19580×10^{-9}
0.7854*	-0.10652×10^{-10}	-0.15465×10^{-10}	0.42423×10^{-11}	-0.19282×10^{-12}
0.9817	0.17006×10^{-11}	0.56046×10^{-10}	0.51917×10^{-10}	0.24856×10^{-10}
1.1781*	0.80242×10^{-11}	-0.13695×10^{-10}	-0.13630×10^{-11}	-0.62178×10^{-13}
1.3744	-0.87688×10^{-11}	0.30465×10^{-10}	-0.88742×10^{-11}	-0.64128×10^{-11}
1.5708*	-0.20809×10^{-10}	-0.17255×10^{-10}	0.12837×10^{-12}	-0.20560×10^{-13}

*Points matched on the boundary

Table 45 - Ratio of Maximum Residuals to Maximum Values of Physical Parameters within the Shell. Clamped Spherical Shell with Elliptical Planform (R/t = 50, R = 5.8", a/b = 1.5)

	w	$\frac{\partial w}{\partial n}$	u_n	u_t
Maximum Residual along the Boundary	0.25243×10^{-10}	0.25170×10^{-9}	0.51508×10^{-9}	0.12177×10^{-8}
Maximum Value of the Physical Parameter within the Shell	0.34445×10^{-5}	0.53112×10^{-5}	0.99350×10^{-7}	0.99350×10^{-7}
Percentage of Maximum Residual to Maximum Value	0.0007%	0.0047%	0.5185%	1.2257%

Table 46 - Values of the Physical Parameters. Clamped Spherical Shell with Elliptical Planform [R/t = 50, R = 5.8", a/b = 1.0]

x/a	0.0	0.2	0.4	0.6	0.8	1.0
w	0.24625×10^{-5}	0.22750×10^{-5}	0.17544×10^{-5}	0.10299×10^{-5}	0.33054×10^{-6}	-0.15518×10^{-10}
$\frac{\partial w}{\partial n}$	0.0	-0.18401×10^{-5}	-0.32595×10^{-5}	-0.37955×10^{-5}	-0.29130×10^{-5}	0.10015×10^{-10}
M_n	*	0.48331×10^{-1}	0.33214×10^{-1}	0.64801×10^{-2}	-0.33702×10^{-1}	-0.88893×10^{-1}
u_n	0.0	-0.34414×10^{-7}	-0.56767×10^{-7}	-0.58173×10^{-7}	-0.36417×10^{-7}	0.82264×10^{-12}
N_n	*	0.11744×10^1	0.10937×10^1	0.97335	0.83566	0.71380

* not evaluated

Table 47 - Values of the Physical Parameters. Spherical Shell Supported at the Boundary by a Shear Diaphragm Elliptical Planform ($R/t = 50$, $R = 5.8"$, $a/b = 1.5$)

a. Along $\theta = 0$

x/a	0	0.2	0.4	0.6	0.8	1.0
w	0.14301×10^{-4}	0.13753×10^{-4}	0.12053×10^{-4}	0.90910×10^{-5}	0.49002×10^{-5}	-0.69636×10^{-10}
$\frac{\partial w}{\partial n}$	0.0	-0.36879×10^{-5}	-0.77194×10^{-5}	-0.12027×10^{-4}	-0.15651×10^{-4}	-0.16219×10^{-4}
M_n	*	0.96925×10^{-1}	1.03152×10^{-1}	1.02454×10^{-1}	0.76683×10^{-1}	0.40407×10^{-8}
u_n	0.0	-0.43321×10^{-6}	-0.82208×10^{-6}	-0.11155×10^{-5}	-0.12562×10^{-5}	0.12041×10^{-5}
N_n	*	0.37968×10^1	0.33252×10^1	0.25401×10^1	0.14495×10^1	0.20564×10^{-5}

* not evaluated

b. Along $\theta = \pi/4$

$x/1.18b$	0.0	0.2	0.4	0.6	0.8	1.0
w	0.14301×10^{-4}	0.13681×10^{-4}	0.11824×10^{-4}	0.87684×10^{-5}	0.46811×10^{-5}	-0.52101×10^{-10}
$\frac{\partial w}{\partial n}$	0.0	-0.57813×10^{-5}	-0.11456×10^{-4}	-0.16663×10^{-4}	-0.20540×10^{-4}	-0.21523×10^{-4}
M_n	*	0.14453	0.13889	0.12131	0.80003 $\times 10^{-1}$	0.18735 $\times 10^{-7}$
u_n	0.0	-0.44809×10^{-6}	-0.84876×10^{-6}	-0.11560×10^{-5}	-0.13290×10^{-5}	-0.13431×10^{-5}
N_n	*	0.19144×10^1	0.16858×10^1	0.12940×10^1	0.73175	0.83447 $\times 10^{-5}$

c. Along $\theta = \pi/2$

x/b	0.0	0.2	0.4	0.6	0.8	1.0
w	0.14301×10^{-4}	0.13649×10^{-4}	0.11723×10^{-4}	0.86256×10^{-5}	0.45809×10^{-5}	-0.72418×10^{-10}
$\frac{\partial w}{\partial n}$	0.0	-0.64972×10^{-5}	-0.12685×10^{-4}	-0.18105×10^{-4}	-0.22008×10^{-4}	-0.23234×10^{-4}
M _n	*	0.15286	0.14228	0.11905	0.75107×10^{-1}	-0.11862×10^{-6}
u _n	0.0	-0.46146×10^{-6}	-0.87645×10^{-6}	-0.12010×10^{-5}	-0.13972×10^{-5}	-0.14395×10^{-5}
N _n	*	0.15319×10^1	0.13261×10^1	0.99079	0.54077	-0.29802×10^{-7}

* not evaluated

Contrails

Table 48 - Residuals Along the Boundary. Spherical Shell Supported at the Boundary by a Shear Diaphragm Elliptical Planform (R/t = 50, R = 5.8", a/b = 1.5)

θ	w	M_n	u_t	N_n
0.0 *	-0.69988×10^{-10}	-0.44522×10^{-8}	0.0	0.18775×10^{-5}
0.1963	0.14272×10^{-8}	-0.62325×10^{-3}	0.24561×10^{-7}	0.18924
0.3927*	-0.65821×10^{-10}	0.14097×10^{-8}	-0.20358×10^{-11}	0.45598×10^{-5}
0.5890	-0.54836×10^{-9}	0.23181×10^{-3}	-0.45437×10^{-8}	-0.75865×10^{-1}
0.7854*	-0.52458×10^{-10}	-0.25381×10^{-7}	-0.26152×10^{-11}	0.83447×10^{-5}
0.9817	-0.23167×10^{-10}	-0.40467×10^{-4}	0.89259×10^{-9}	0.13588×10^{-1}
1.1781*	-0.10473×10^{-10}	-0.13261×10^{-7}	-0.11986×10^{-11}	-0.18179×10^{-5}
1.3744	-0.89136×10^{-10}	0.5858×10^{-5}	-0.14337×10^{-9}	-0.22936×10^{-2}
1.5788*	-0.72858×10^{-10}	-0.12990×10^{-8}	-0.41801×10^{-13}	-0.11921×10^{-6}

*Points matched on the boundary

Table 49 - Ratio of Maximum Residuals to Maximum Values of Physical Parameters within the Shell. Spherical Shell Supported at the Boundary by a Shear Diaphragm (R/t = 50, R = 5.8", a/b = 1.5)

	w	M _n	ut	M _n
Maximum Residual along the Boundary	0.14272x10 ⁻⁸	0.62325x10 ⁻³	0.24561x10 ⁻⁷	0.18924
Maximum Value of the Physical Parameter within the Shell	0.14301x10 ⁻⁴	0.15286	0.14395x10 ⁻⁵	0.37968x10 ⁻¹
Percentage of Maximum Residual to Maximum Value	0.0099%	0.4077%	1.7062%	4.9842%

Table 50 - Values of the Physical Parameters Spherical Shell Supported at the Boundary by a Shear Diaphragm. Elliptical Planform (R/t = 50, R = 5.8", a/b = 1.0)

x/a	0.0	0.2	0.4	0.6	0.8	1.0
w	0.11415x10 ⁻⁴	0.10885x10 ⁻⁴	0.93223x10 ⁻⁵	0.68242x10 ⁻⁵	0.35941x10 ⁻⁵	-0.33651x10 ⁻¹⁰
$\frac{\partial w}{\partial n}$	0.0	-0.52808x10 ⁻⁵	-0.10269x10 ⁻⁴	-0.14547x10 ⁻⁴	-0.17453x10 ⁻⁴	-0.17989x10 ⁻⁴
M _n	*	0.14524	0.13422	0.11112	0.69222x10 ⁻¹	-0.27536x10 ⁻⁶
u _n	0.0	-0.31445x10 ⁻⁶	-0.59359x10 ⁻⁶	-0.80443x10 ⁻⁶	-0.91947x10 ⁻⁶	-0.92192x10 ⁻⁶
N _n	*	0.17408x10 ⁻¹	0.15046x10 ⁻¹	0.11211x10 ⁻¹	0.60878	0.66459x10 ⁻⁵

* not evaluated

Contrails

Table 51 - Value of the Physical Parameters. Spherical Shallow Shell
with Elliptical Planform ($R/t = 50$, $R = 5.8''$, $b = 1''$)

Parameter	Clamped		Shear Diaphragm	
	$a/b = 1.5$	$a/b = 1.0$	$a/b = 1.5$	$a/b = 1.0$
w at $r = 0$	0.345×10^{-5}	0.246×10^{-5}	1.430×10^{-5}	1.142×10^{-5}
$\left(\frac{\partial w}{\partial n}\right)_{\max.}$	-0.531×10^{-5}	-0.380×10^{-5}	-2.323×10^{-5}	-1.799×10^{-5}
$(M_n)_{\max.}$	-0.125	-0.089	0.153	0.145
$(u_n)_{\max.}$	-0.103×10^{-8}	-0.058×10^{-8}	-1.440×10^{-8}	-0.922×10^{-8}
$(N_n)_{\max.}$	1.764	1.174	3.797	1.741

Contrails

VI. GENERAL EQUATIONS FOR SHALLOW SHELLS HAVING ARBITRARY CURVATURE

This chapter is a summary of theoretical investigations into thin shell theory with the aim of obtaining in a reasonably rigorous way a set of equations applicable to shallow shells having arbitrary curvature, material orthotropy, and subjected to thermal gradients.

In the first part the assumptions and approximations to be used later are discussed. The second part reviews the deep shell equations of Mushtari, Donnell, and Vlasov. These equations serve as a basis for the shallow-shell theory presented in the last part. In this last part the steps required to obtain the shallow-shell equations from the general equations are rigorously presented. The coupled, fourth-order governing differential equations of equilibrium and compatibility are derived, as well as the other useful relationships for bending moments, transverse shearing force, and membrane forces. These equations include the effects of rectangular material orthotropy and temperature variations in all directions.

A. ASSUMPTIONS AND APPROXIMATIONS

In this work Love's [25] first approximation that z/R may be neglected in comparison with unity for thin shells will be used, rather than the approach adopted by Vlasov [19] characterized by expanding $(1 + z/R)^{-1}$ in a power series, with the accuracy depending upon the number of terms retained. Thus, if one retains the least number of terms possible, then the two approaches will be identical. Further, the theory of thin shells employs Kirchhoff's assumptions originally made for plates: The straight lines which are normal to the middle surface before deformation remain so after deformation and retain their length. The errors introduced by Kirchhoff's hypothesis into the theory of thin shells are of the order of t/R in comparison to unity [26].

Further simplifications of the theory of shells is possible but the range of applicability will be consequently restricted to special cases. Of these are the membrane theory, and the Mushtari-Donnell simplifications. The latter two formulations may be characterized as being an intermediate case as compared to the membrane and bending theory, since Mushtari (see Ref. [26], p. 89) and Donnell [27] in their work neglected the displacements u and v in the formula for the change of curvature and twist in the cases where the stresses due to the moments are of a magnitude less than or equal to the stresses due to the membrane forces. In the next section of the report the general equations employing these assumptions will be presented.

In the derivations of the equations for thermoelastic shallow shells in Part C the assumption of Nazarov [28] and Mikhlin (see Ref. [26],

p. 95) that at every point of the middle surface the quantities $(\partial z)/(\partial x)^2$ and $(\partial x)/(\partial y)^2$ can be neglected in comparison to unity will be adopted, rather than Vlasov's [19] assumption that for shallow shells the Gaussian curvature is zero, reducing the Gauss equation to two terms.

B. MUSHTARI-DONNELL-VLASOV APPROACH

The main assumptions made by this approach are that one can disregard the tangential displacements u and v in the formula for the change of curvatures κ_α and κ_β and twist τ , resulting in

$$\kappa_\alpha = - \frac{1}{A} \frac{\partial}{\partial \alpha} \left(\frac{1}{A} \frac{\partial w}{\partial \alpha} \right) - \frac{1}{AB^2} \frac{\partial w}{\partial \beta} \quad (6-1a)$$

$$\kappa_\beta = - \frac{1}{B} \frac{\partial}{\partial \beta} \left(\frac{1}{B} \frac{\partial w}{\partial \beta} \right) - \frac{1}{A^2 B} \frac{\partial w}{\partial \alpha} \quad (6-1b)$$

$$\tau = - \frac{1}{AB} \left(\frac{\partial^2 w}{\partial \alpha \partial \beta} - \frac{1}{A} \frac{\partial A}{\partial \beta} \frac{\partial w}{\partial \alpha} - \frac{1}{B} \frac{\partial B}{\partial \alpha} \frac{\partial w}{\partial \beta} \right) \quad (6-1c)$$

where α and β are the orthogonal principal coordinates of the middle surface of the shell, and A and B are the corresponding coefficients of the metric tensor of the coordinates.

However, it should be mentioned that neglecting the displacements u and v in the formula for changes of curvature and twist will induce errors which, justifiably, are insignificant for the cases where the stresses due to moments are small in comparison with the stresses due to the membrane forces. Substituting the simplified expressions Eq. (6-1) into the expressions for the potential energy of the shell, and using the principle of minimum potential energy, one obtains the equilibrium equations for an element of the middle surface in terms of the displacements (Ref. 26, p. 89). Writing these equations in terms of the forces and moments one obtains

$$\frac{1}{AB} \left[\frac{\partial}{\partial \alpha} (BN_{\alpha\alpha}) + \frac{\partial}{\partial \beta} (AN_{\beta\alpha}) + \frac{\partial A}{\partial \beta} N_{\alpha\beta} - \frac{\partial B}{\partial \alpha} N_{\beta\beta} \right] + q_\alpha = 0 \quad (6-2a)$$

$$\frac{1}{AB} \left[\frac{\partial}{\partial \alpha} (BN_{\alpha\beta}) + \frac{\partial}{\partial \beta} (AN_{\beta\beta}) + \frac{\partial B}{\partial \alpha} N_{\beta\alpha} - \frac{\partial A}{\partial \beta} N_{\alpha\alpha} \right] + q_\beta = 0 \quad (6-2b)$$

Contrails

$$\frac{1}{AB} \left[\frac{\partial}{\partial \alpha} (BQ_\alpha) + \frac{\partial}{\partial \beta} (AQ_\beta) \right] - \frac{N_{\alpha\alpha}}{R_\alpha} - \frac{N_{\beta\beta}}{R_\beta} + q_n = 0 \quad (6-2c)$$

$$\frac{1}{AB} \left[\frac{\partial}{\partial \alpha} (BM_{\alpha\alpha}) + \frac{\partial}{\partial \beta} (AM_{\beta\alpha}) + \frac{\partial A}{\partial \beta} M_{\alpha\beta} - \frac{\partial B}{\partial \alpha} M_{\beta\beta} \right] - Q_\alpha = 0 \quad (6-2d)$$

$$\frac{1}{AB} \left[\frac{\partial}{\partial \alpha} (BM_{\alpha\beta}) + \frac{\partial}{\partial \beta} (AM_{\beta\beta}) + \frac{\partial B}{\partial \alpha} M_{\beta\alpha} - \frac{\partial A}{\partial \beta} M_{\alpha\alpha} \right] - Q_\beta = 0 \quad (6-2e)$$

$$N_{\alpha\beta} - N_{\beta\alpha} + \frac{M_{\alpha\beta}}{R_\alpha} - \frac{M_{\beta\alpha}}{R_\beta} = 0 \quad (6-2f)$$

Comparing these equations with the equations of equilibrium of general, thin-shell theory we find that the quantities Q_α/R_α and Q_β/R_β involving the transverse shearing forces are missing from Eqs. (6-2a) and (6-2b), respectively. Goldenveizer [21] deduced the compatibility conditions of strain in the deformed middle surface directly from the conditions of Gauss and Codazzi. They are

$$\left\{ \begin{aligned} & B \frac{\partial \kappa_\beta}{\partial \alpha} + \frac{\partial B}{\partial \alpha} (\kappa_\beta - \kappa_\alpha) - A \frac{\partial \tau}{\partial \beta} - 2 \frac{\partial A}{\partial \beta} \tau + \frac{1}{R_\beta} \frac{\partial A}{\partial \beta} \gamma_{\alpha\beta} \\ & + \frac{1}{R_\alpha} \left[A \frac{\partial \gamma_{\alpha\beta}}{\partial \beta} + \frac{\partial A}{\partial \beta} \gamma_{\alpha\beta} - B \frac{\partial \epsilon_\beta}{\partial \alpha} - \frac{\partial B}{\partial \alpha} (\epsilon_\beta - \epsilon_\alpha) \right] \end{aligned} \right\} = 0 \quad (6-3a)$$

$$\left\{ \begin{aligned} & A \frac{\partial \kappa_\alpha}{\partial \beta} + \frac{\partial A}{\partial \beta} (\kappa_\alpha - \kappa_\beta) - B \frac{\partial \tau}{\partial \alpha} - 2 \frac{\partial B}{\partial \alpha} \tau + \frac{1}{R_\alpha} \frac{\partial B}{\partial \alpha} \gamma_{\alpha\beta} \\ & + \frac{1}{R_\beta} \left[B \frac{\partial \gamma_{\alpha\beta}}{\partial \alpha} + \frac{\partial B}{\partial \alpha} \gamma_{\alpha\beta} - A \frac{\partial \epsilon_\alpha}{\partial \beta} - \frac{\partial A}{\partial \beta} (\epsilon_\alpha - \epsilon_\beta) \right] \end{aligned} \right\} = 0 \quad (6-3b)$$

$$\begin{aligned} & \frac{\kappa_z}{R_\beta} + \frac{\kappa_\beta}{R_\alpha} + \frac{1}{AB} \left\{ \frac{\partial}{\partial \alpha} \frac{1}{A} \left[B \frac{\partial \epsilon_\beta}{\partial \alpha} + \frac{\partial B}{\partial \alpha} (\epsilon_\beta - \epsilon_\alpha) - \frac{A}{2} \frac{\partial \gamma_{\alpha\beta}}{\partial \beta} - \frac{\partial A}{\partial \beta} \gamma_{\alpha\beta} \right] \right. \\ & \left. + \frac{\partial}{\partial \beta} \frac{1}{B} \left[A \frac{\partial \epsilon_\alpha}{\partial \beta} + \frac{\partial A}{\partial \beta} (\epsilon_\alpha - \epsilon_\beta) - \frac{B}{2} \frac{\partial \gamma_{\alpha\beta}}{\partial \alpha} - \frac{\partial B}{\partial \alpha} \gamma_{\alpha\beta} \right] \right\} = 0 \end{aligned} \quad (6-3c)$$

Applying the same approximations to the conditions of Codazzi [i.e., Eqs. (6-3a) and (6-3b)] they will reduce to

$$\frac{\partial B \kappa_\beta}{\partial \alpha} - \kappa_z \frac{\partial B}{\partial \alpha} - \frac{\partial A \tau}{\partial \beta} - \tau \frac{\partial A}{\partial \beta} = \frac{1}{R_\alpha} \left(\frac{\partial B \epsilon_\beta}{\partial \alpha} - \epsilon_\alpha \frac{\partial B}{\partial \alpha} \right) = \frac{B}{R_\alpha R_\beta} \frac{\partial w}{\partial \alpha} \quad (6-4a)$$

and

$$\frac{\partial A \kappa_\alpha}{\partial \beta} - \kappa_\beta \frac{\partial A}{\partial \beta} - \frac{\partial B \tau}{\partial \alpha} - \tau \frac{\partial B}{\partial \alpha} = \frac{1}{R_\beta} \left(\frac{\partial A \epsilon_\alpha}{\partial \beta} - \epsilon_\beta \frac{\partial A}{\partial \beta} \right) = \frac{A}{R_\alpha R_\beta} \frac{\partial w}{\partial \beta} \quad (6-4b)$$

Upon substitution into Eqs. (6-2d) and (6-2e) one arrives at the following expressions for Q_α and Q_β :

$$Q_\alpha = -D \frac{1}{A} \left[\frac{\partial}{\partial \alpha} (\nabla^2 w) + \frac{(1-\nu)}{R_\alpha R_\beta} \frac{\partial w}{\partial \alpha} \right] \quad (6-5a)$$

$$Q_\beta = -D \frac{1}{B} \left[\frac{\partial}{\partial \beta} (\nabla^2 w) + \frac{(1-\nu)}{R_\alpha R_\beta} \frac{\partial w}{\partial \beta} \right] \quad (6-5b)$$

where

$$D = \frac{Et^3}{12(1-\nu^2)}$$

and ∇^2 is the Laplacian differential operator.

Contrails

The quantities

$$\frac{1}{R_\alpha R_\beta} \frac{\partial w}{\partial \alpha} \text{ and } \frac{1}{R_\alpha R_\beta} \frac{\partial w}{\partial \beta}$$

are neglected in comparison with

$$\frac{\partial}{\partial \alpha} \nabla_w^2 \text{ and } \frac{\partial}{\partial \beta} \nabla_w^2 .$$

For shells with zero Gaussian curvature the justification is obvious; however, as an approximation, it can be used for other cases. The right hand sides of Eqs. (6-5) will contain first-, second-, and third-order derivatives. If the transverse displacements involve functions which vary rapidly with the shell coordinates, terms involving first-order derivatives can be neglected in comparison with those containing second- and third-order derivatives. Hence, employing this assumption and substituting into Eq. (6-2c), we obtain

$$D\nabla_w^4 + \frac{N_{\alpha\alpha}}{R_\alpha} + \frac{N_{\beta\beta}}{R_\beta} = q_n . \quad (6-6)$$

Vlasov transformed the equation further by introducing an auxiliary stress function $\phi(\alpha, \beta)$ defined by

$$N_{\alpha\alpha} = \frac{1}{B} \frac{\partial}{\partial \beta} \left(\frac{1}{B} \frac{\partial \phi}{\partial \beta} \right) + \frac{1}{A^2 B} \frac{\partial \beta}{\partial \alpha} \frac{\partial \phi}{\partial \alpha} \quad (6-7a)$$

$$N_{\beta\beta} = \frac{1}{A} \frac{\partial}{\partial \alpha} \left(\frac{1}{A} \frac{\partial \phi}{\partial \alpha} \right) + \frac{1}{AB^2} \frac{\partial A}{\partial \beta} \frac{\partial \phi}{\partial \beta} \quad (6-7b)$$

$$N_{\beta\alpha} = N_{\alpha\beta} = - \frac{1}{AB} \left(\frac{\partial^2 \phi}{\partial \alpha \partial \beta} - \frac{1}{A} \frac{\partial A}{\partial \beta} \frac{\partial \phi}{\partial \alpha} - \frac{1}{B} \frac{\partial B}{\partial \alpha} \frac{\partial \phi}{\partial \beta} \right) . \quad (6-7c)$$

Upon substitution in Eqs. (6-2a) and (6-2b), we see that these equations for the case $q_\alpha = q_\beta = 0$ will be satisfied identically if the condition that

Contrails

$$\frac{1}{R_a R_\beta} \frac{1}{B} \frac{\partial \Phi}{\partial \beta} = \frac{1}{R_a R_\beta} \frac{1}{A} \frac{\partial \Phi}{\partial \alpha} = 0 \quad (6-8)$$

relative to the other terms in the equations. This is justifiable if $\Phi(\alpha, \beta)$ is a rapidly varying function, as argued before. Introducing the Gauss condition for the deformed middle surface, Eq. (6-3c), the expression for the change in curvature and twist as given in Eqs. (6-1), and for ϵ_a , ϵ_β , and $\gamma_{a\beta}$ the isotropic stress-strain relations

$$\epsilon_a = \frac{1}{Et} (N_{aa} - \nu N_{\beta\beta}) \quad (6-9a)$$

$$\epsilon_\beta = \frac{1}{Et} (-\nu N_{aa} + N_{\beta\beta}) \quad (6-9b)$$

$$\gamma_{a\beta} = \frac{2(1 + \nu)}{Et} N_{a\beta} \quad (6-9c)$$

we obtain the compatibility equation

$$\nabla^4 \Phi + \frac{1 + \nu}{AB} \left[\frac{\partial}{\partial \alpha} \left(\frac{1}{R_a R_\beta} \frac{B}{A} \frac{\partial \Phi}{\partial \alpha} \right) + \frac{\partial}{\partial \beta} \left(\frac{1}{R_a R_\beta} \frac{A}{B} \frac{\partial \Phi}{\partial \beta} \right) \right] = Et \left(\frac{\kappa_a}{R_\beta} + \frac{\kappa_\beta}{R_a} \right) \quad (6-10)$$

The second part of the left side of Eq. (6-10) can be neglected in accordance with our assumptions, and then reduces to

$$\nabla^4 \Phi = \frac{\kappa_a}{R_\beta} + \frac{\kappa_\beta}{R_a} \quad (6-11)$$

As an example, consider the class of cylindrical shells as shown in Fig. 18.

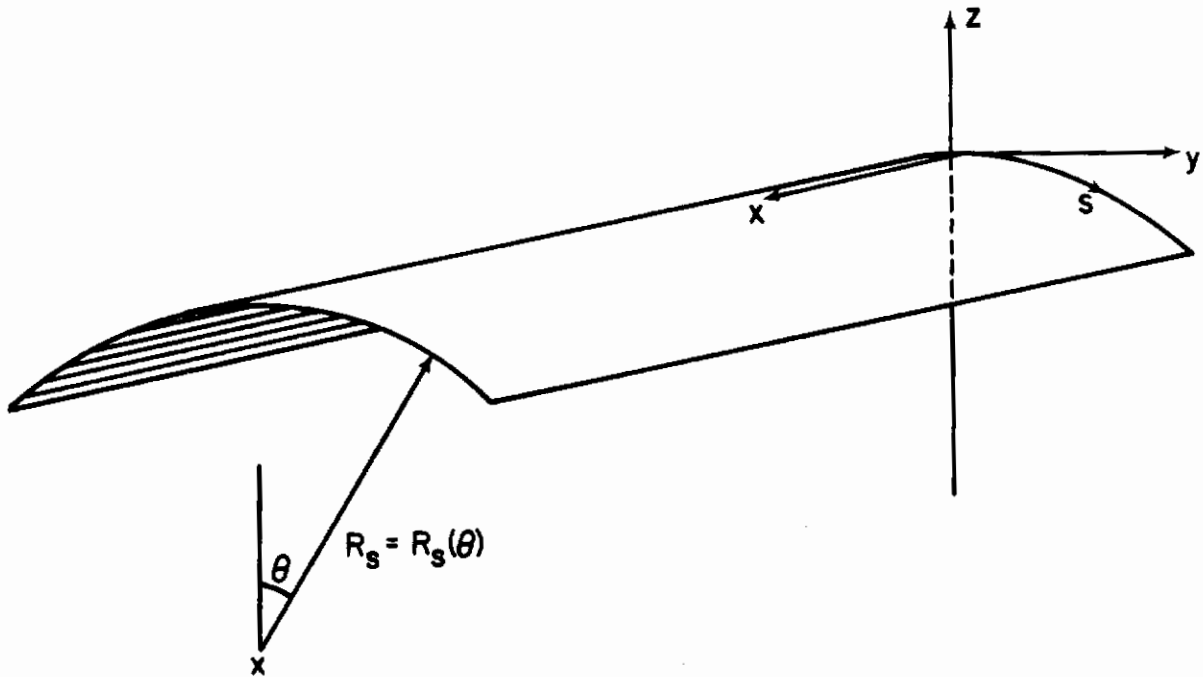


Figure 18. Cylindrical shell

In this example the α -curves are the generators lying in the x-direction while the β -curves are in the s-direction; therefore

$$A = B = 1$$

$$R_\alpha = R_x = \infty$$

$$R_\beta = R_s(s)$$

Substituting into Eqs. (6-1) we get the following expressions for the change of curvature and twist:

$$\kappa_x = - \frac{\partial^2 w}{\partial x^2}$$

$$\kappa_s = - \frac{\partial^2 w}{\partial s^2} \tag{6-12}$$

$$\tau = - \frac{\partial^2 w}{\partial x \partial s}$$

and, from Eqs. (6-5),

$$\begin{aligned} N_{xx} &= \frac{\partial^2 \phi}{\partial s^2} \\ N_{ss} &= \frac{\partial^2 \phi}{\partial x^2} \\ N_{xs} &= - \frac{\partial^2 \phi}{\partial x \partial s} \end{aligned} \quad (6-13)$$

Consequently, the governing differential equations will be

$$D \left[\frac{\partial^4 w}{\partial x^4} + 2 \frac{\partial^4 w}{\partial x^2 \partial s^2} + \frac{\partial^4 w}{\partial s^4} \right] + \frac{1}{R} \frac{\partial^2 \phi}{\partial x^2} = q_n \quad (6-14)$$

and

$$\frac{\partial^4 \phi}{\partial x^4} + 2 \frac{\partial^4 \phi}{\partial x^2 \partial s^2} + \frac{\partial^4 \phi}{\partial s^4} - \frac{Et}{R} \frac{\partial^2 w}{\partial x^2} = 0 \quad (6-15)$$

In general, for cylindrical shells, $s = R\theta$, where $R = R(\theta)$; e.g.,

$$R = \text{constant} \quad (\text{circular cylindrical shell})$$

and

$$R = \frac{ab}{(a^2 \sin^2 \theta + b^2 \cos^2 \theta)^{1/2}} \quad (\text{elliptical cylindrical shell}).$$

C. ORTHOTROPIC SHALLOW SHELLS SUBJECTED TO PRESSURE AND THERMAL LOADING

Flügge [29] analyzed cylindrical plywood and ribbed shells and Ambartsyanyan [30] developed the governing differential equations for anisotropic shallow shells using Vlasov's assumption. In the present derivation we will use the basic Mushtari [26] and Donnell [27] assumption; i.e., disregarding the tangential displacements in the equations

Contrails

for change in curvature and twist. Let

$$z = z(x,y) \quad (6-16)$$

be the equation of the middle surface in the Cartesian system of coordinates O-xyz (Fig. 19). This function becomes especially simple for shells, the middle surfaces of which are sections of elliptic or hyperbolic paraboloids, or of circular cylinders, in which case one will have the quadric surface

$$z = a_0 - a_1x - a_2y - a_3x^2 - a_4xy - a_5y^2 \quad (6-17)$$

where the a_i 's are constants.

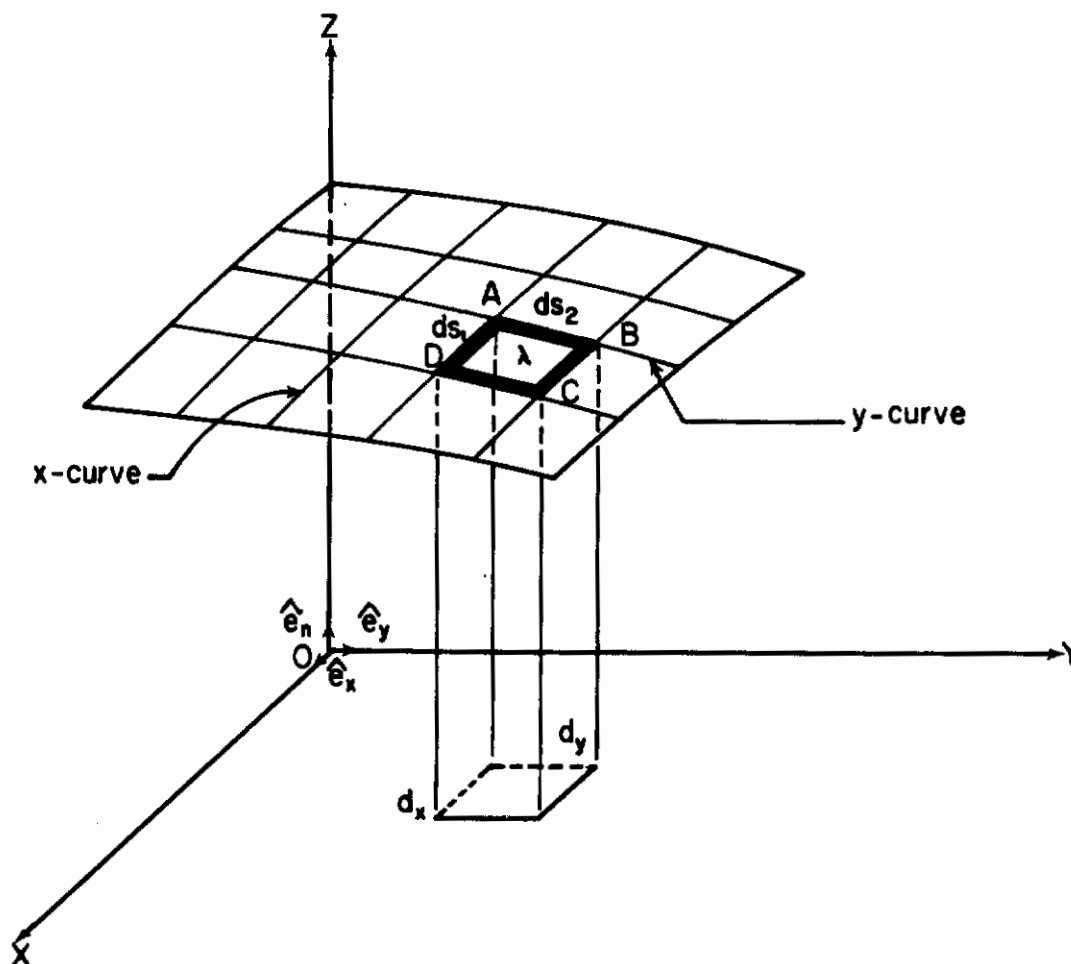


Figure 19. Shell element and its rectangular projection

Contraails

The points of the middle surface are determined by the Cartesian coordinates x, y of their projections, and the parameters x and y will serve as curvilinear coordinates on the middle surface. The x -curves of the curvilinear system of coordinates are plane curves generated by the intersection of the middle surface with planes parallel to the plane xoz while the y -curves are generated by the intersection of the middle surface with planes parallel to plane $yo z$. The square of the length of an element of the middle surface in curvilinear coordinates is

$$ds^2 = g_{ij} d\alpha_i d\alpha_j \quad , \quad (6-18)$$

where the g_{ij} are the coefficients of the metric tensor. For Cartesian coordinates g_{ij} takes the value of the Kronecker delta δ_{ij} , and Eq. (6-18) will be

$$ds^2 = dx^2 + dy^2 + dz^2 \quad (6-19)$$

From Eq. (6-16) we can write

$$dz = \frac{\partial z}{\partial x} dx + \frac{\partial z}{\partial y} dy \quad (6-20)$$

Substituting into Eq. (6-19)

$$ds^2 = \left[1 + \left(\frac{\partial z}{\partial x} \right)^2 \right] dx^2 + 2 \frac{\partial z}{\partial x} \frac{\partial z}{\partial y} dx dy + \left[1 + \left(\frac{\partial z}{\partial y} \right)^2 \right] dy^2 \quad (6-21)$$

From Eq. (6-21) we conclude that the system of curvilinear coordinates consisting of the x -curves and y -curves in general is not an orthogonal system of curvilinear coordinates for the middle surface, and the angle λ between the x -curves and y -curves (Fig. 19) is given by

$$\cos \lambda = \frac{\frac{\partial z}{\partial x} \frac{\partial z}{\partial y}}{\left\{ \left[1 + \left(\frac{\partial z}{\partial x} \right)^2 \right] \left[1 + \left(\frac{\partial z}{\partial y} \right)^2 \right] \right\}^{1/2}} \quad (6-22)$$

Contrails

Equation (6-21) is usually referred to as the first quadratic form and consequently the first fundamental quantities are

$$A^2 = 1 + \left(\frac{\partial z}{\partial x}\right)^2$$

$$AB \cos \lambda = \frac{\partial z}{\partial y} \frac{\partial z}{\partial x}$$

$$B^2 = 1 + \left(\frac{\partial z}{\partial y}\right)^2$$

Consider as a first example the case of a circular cylindrical shell (see Fig. 18). In this case z is a function of y only;

$$(z + R)^2 + y^2 = R^2 \quad (R \text{ is constant})$$

$$z = (R^2 - y^2)^{1/2} - R$$

$$\frac{\partial z}{\partial y} = -y(R^2 - y^2)^{-1/2} = -\tan \theta$$

$$\frac{\partial z}{\partial x} = 0$$

As a second case, take the spherical shell shown in Fig. 20.

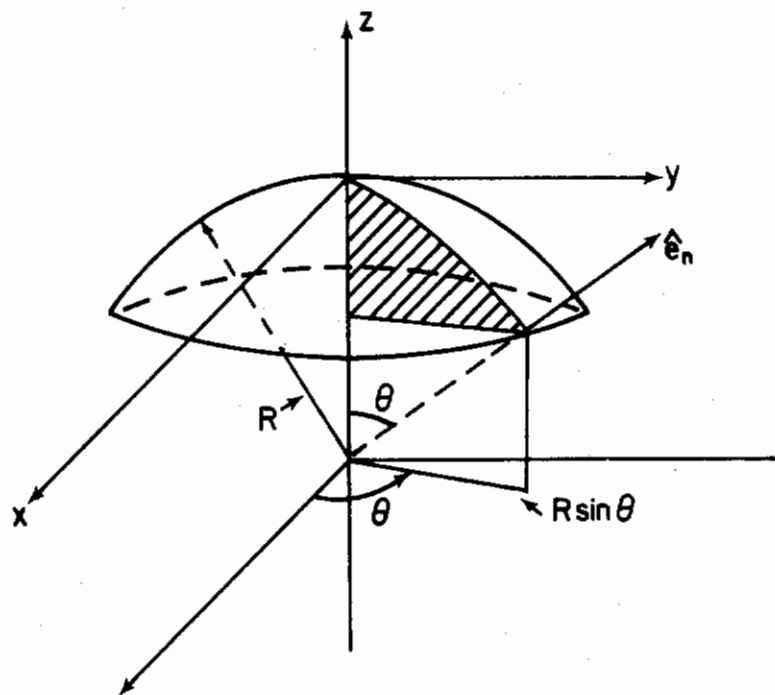


Figure 20. Spherical shell

$$(z + R)^2 + x^2 + y^2 = R^2$$

$$z = (R^2 - x^2 - y^2)^{1/2} - R$$

$$\frac{\partial z}{\partial x} = x(R^2 - x^2 - y^2)^{-1/2} = \cos \theta \tan \phi$$

$$\frac{\partial z}{\partial y} = y(R^2 - x^2 - y^2)^{-1/2} = \sin \theta \tan \phi$$

It is worth noting that in the case of cylindrical shells the x-curves and the y-curves form an orthogonal curvilinear system, while for the spherical shell they do not.

The theory of shallow shells is appropriately based on the assumption that one should neglect the squares and the product of $\frac{\partial z}{\partial y}$ and $\frac{\partial z}{\partial x}$ in comparison to unity [28]; thus

Contrails

$$\left(\frac{\partial z}{\partial x}\right)^2 \ll 1$$

$$\frac{\partial z}{\partial x} \frac{\partial z}{\partial y} \ll 1 \quad (6-23)$$

$$\left(\frac{\partial z}{\partial y}\right)^2 \ll 1$$

Based on this assumption the arc lengths and included angles of the curvilinear curves will be

$$ds_x = \left[1 + \left(\frac{\partial z}{\partial x}\right)^2\right] dx \cong dx$$

$$ds_y = \left[1 + \left(\frac{\partial z}{\partial y}\right)^2\right] dy \cong dy \quad (6-24)$$

$$\cos \lambda = \frac{\frac{\partial z}{\partial x} \frac{\partial z}{\partial y}}{\left\{ \left[1 + \left(\frac{\partial z}{\partial x}\right)^2\right] \left[1 + \left(\frac{\partial z}{\partial y}\right)^2\right] \right\}^{1/2}} \cong 0$$

Hence, the incremental lengths of the arcs of the x-curves and the y-curves can be identified with increments of the Cartesian coordinates, and the x and y curves are orthogonal. Therefore, the well-known equations of the theory of thin shells in an orthogonal curvilinear system of coordinates are applicable in this case. The curvatures $1/R_x$ and $1/R_y$ of the x-curves and y-curves, respectively, and the torsion $1/R_{xy}$ of the surface will reduce to

$$\begin{aligned} \frac{1}{R_x} &= - \frac{\partial^2 z}{\partial x^2} \\ \frac{1}{R_y} &= - \frac{\partial^2 z}{\partial y^2} \\ \frac{1}{R_{xy}} &= - \frac{\partial^2 z}{\partial x \partial y} \end{aligned} \quad (6-25)$$

Contrails

The simplified Mushtari-Donnell equations for the change of curvature are

$$\begin{aligned}\kappa_x &= -\frac{\partial^2 w}{\partial x^2} \\ \kappa_y &= -\frac{\partial^2 w}{\partial y^2} \\ \tau &= -\frac{\partial^2 w}{\partial x \partial y}\end{aligned}\tag{6-26}$$

The equations of equilibrium are obtainable from Eqs. (6-2) making use of the fact that $N_{xy} = N_{yx}$ and $M_{xy} = M_{yx}$. This gives

$$\frac{\partial N_x}{\partial x} + \frac{\partial N_{xy}}{\partial y} + q_x = 0\tag{6-27a}$$

$$\frac{\partial N_y}{\partial y} + \frac{\partial N_{xy}}{\partial x} + q_y = 0\tag{6-27b}$$

$$\frac{\partial Q_x}{\partial x} + \frac{\partial Q_y}{\partial y} - \frac{N_x}{R_x} - 2\frac{N_{xy}}{R_{xy}} - \frac{N_y}{R_y} + q_n = 0\tag{6-27c}$$

$$\frac{\partial M_x}{\partial x} + \frac{\partial M_{xy}}{\partial y} - Q_x = 0\tag{6-27d}$$

$$\frac{\partial M_y}{\partial y} + \frac{\partial M_{xy}}{\partial x} - Q_y = 0\tag{6-27e}$$

where the generalized forces are defined on Figure 21.

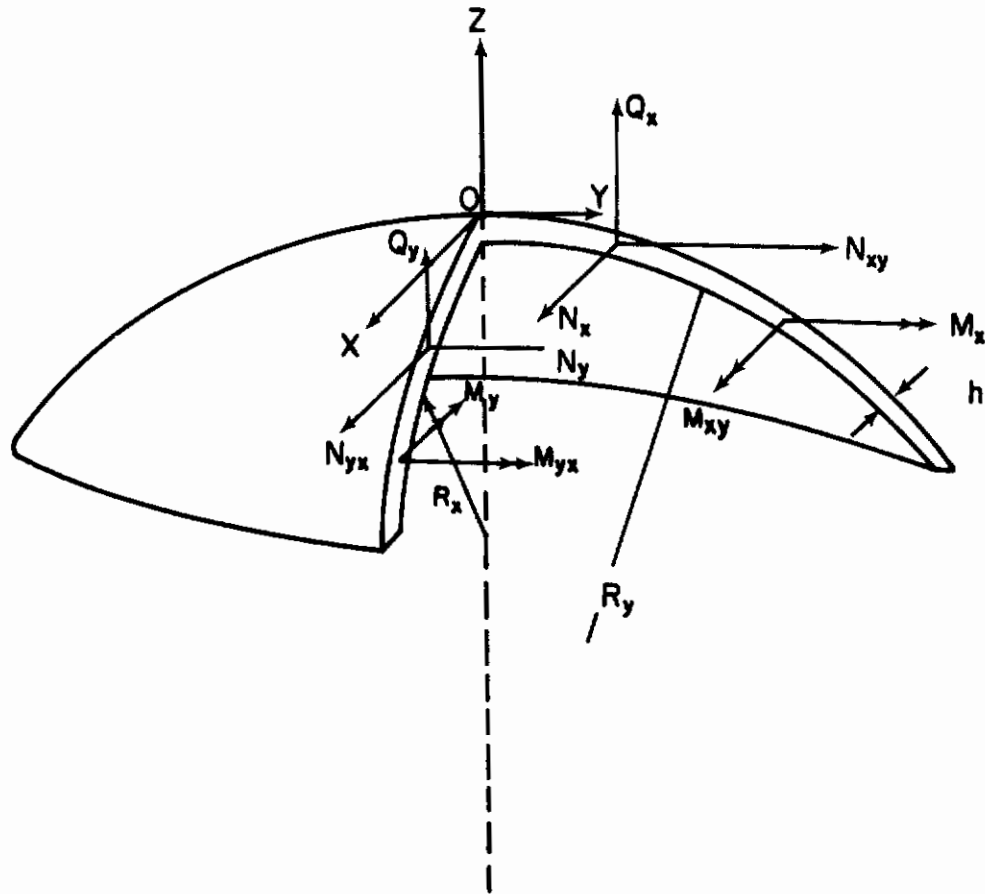


Figure 21. Sign convention for a shallow spherical shell

The direct strains (stretching) in the x and y directions, and the shear strains are

$$\epsilon_x = \frac{\partial u}{\partial x} + \frac{w}{R_x}$$

$$\epsilon_y = \frac{\partial v}{\partial y} + \frac{w}{R_y} \tag{6-28}$$

$$\gamma_{xy} = \frac{\partial u}{\partial y} + \frac{\partial v}{\partial x} + 2 \frac{w}{R_{xy}}$$

where the term $2 \frac{w}{R_{xy}}$ accounts for the nonorthogonality of the system of curves.

Contrails

The conditions of Codazzi of the deformed middle surface [Eqs. (6-3a) and (6-3b)] become (as discussed previously, the terms involving the tangential components of the displacement may be neglected)

$$\frac{\partial \kappa_y}{\partial x} - \frac{\partial \tau}{\partial y} + \frac{1}{R_x} \left(\frac{\partial \gamma_{xy}^*}{\partial y} - \frac{\partial \epsilon_y^*}{\partial x} \right) = 0 \quad (6-29a)$$

and

$$\frac{\partial \kappa_x}{\partial y} - \frac{\partial \tau}{\partial x} + \frac{1}{R_y} \left(\frac{\partial \gamma_{xy}^*}{\partial x} - \frac{\partial \epsilon_x^*}{\partial y} \right) = 0 \quad (6-29b)$$

where ϵ_x^* , ϵ_y^* , γ^* are defined by

$$\epsilon_x^* = - \frac{\partial^2 z}{\partial x^2} w = \frac{w}{R_x}$$

$$\epsilon_y^* = - \frac{\partial^2 z}{\partial y^2} w = \frac{w}{R_y}$$

$$\gamma_{xy}^* = - 2 \frac{\partial^2 z}{\partial x \partial y} w = 2 \frac{w}{R_{xy}}$$

while the Gauss equation of the deformed middle surface Eq. (6-3c) be

$$\frac{\kappa_x}{R_y} - 2 \frac{\tau}{R_{xy}} + \frac{\kappa_y}{R_x} + \frac{\partial}{\partial x} \left[\frac{\partial \epsilon_y}{\partial x} - \frac{1}{2} \frac{\partial \gamma_{xy}}{\partial y} \right] + \frac{\partial}{\partial y} \left[\frac{\partial \epsilon_x}{\partial y} - \frac{1}{2} \frac{\partial \gamma_{xy}}{\partial x} \right] = 0 \quad (6-30)$$

The total strain (stretching and bending) at any point along the thickness of the shell will be

Contrails

$$\bar{\epsilon}_x = \epsilon_x + z \kappa_x$$

$$\bar{\epsilon}_y = \epsilon_y + z \kappa_y \quad (6-31)$$

$$\bar{\gamma}_{xy} = \gamma_{xy} + 2z\tau$$

The stress-strain relations for an orthotropic material subjected to a temperature gradient $T = T(x,y,z)$ are

$$\bar{\epsilon}_x = \frac{\bar{\sigma}_x}{E_x} - \frac{\nu_x}{E_x} \bar{\sigma}_y + \alpha_x T$$

$$\bar{\epsilon}_y = -\frac{\nu_y}{E_y} \bar{\sigma}_x + \frac{1}{E_y} \bar{\sigma}_y + \alpha_y T \quad (6-32)$$

$$\bar{\gamma}_{xy} = \frac{\bar{\sigma}_{xy}}{G}$$

with the condition that

$$\frac{\nu_x}{E_x} = \frac{\nu_y}{E_y}$$

because of the symmetry of the stress-strain equations. Thus, for an orthotropic material we have four independent elastic constants and two independent coefficients of thermal expansion. Inverting Eq. (6-32) gives

$$\bar{\sigma}_x = \frac{E_x}{1 - \nu_x \nu_y} \left[\bar{\epsilon}_x + \nu_y \bar{\epsilon}_y - (\alpha_x + \nu_y \alpha_y) T \right] \quad (6-33a)$$

$$\bar{\sigma}_y = \frac{E_y}{1 - \nu_x \nu_y} \left[\nu_x \bar{\epsilon}_x + \bar{\epsilon}_y - (\alpha_y + \nu_x \alpha_x) T \right] \quad (6-33b)$$

$$\bar{\sigma}_{xy} = G \gamma_{xy} \quad (6-33c)$$

Contrails

Assuming that we can represent $T(x,y,z)$ as

$$T = \sum_{n=0}^N T_n(x,y) z^n \quad (6-34)$$

it can be represented as two series, one containing the even powers of z (symmetric) while the other contains the odd powers of z (antisymmetric); i.e.,

$$T = \sum_{n=0,2}^N T_n(x,y) z^n + \sum_{n=1,3}^N T_n^*(x,y) z^n \quad (6-35)$$

The resultant force and moments resulting from integration along the depth are

$$N_x = \frac{E_x}{(1 - \nu_x \nu_y)} \left[t(\epsilon_x + \nu_y \epsilon_y) - 2(\alpha_x + \nu_y \alpha_y) \sum_{n=0,2}^N \frac{(t/2)^{n+1}}{(n+1)} T_n(x,y) \right] \quad (6-36a)$$

$$N_y = \frac{E_y}{(1 - \nu_x \nu_y)} \left[t(\nu_x \epsilon_x + \epsilon_y) - 2(\alpha_y + \nu_x \alpha_x) \sum_{n=0,2}^N \frac{(t/2)^{n+1}}{(n+1)} T_n(x,y) \right] \quad (6-36b)$$

$$N_{xy} = t G \gamma_{xy} \quad (6-36c)$$

$$M_x = \frac{E_x}{(1 - \nu_x \nu_y)} \left[\frac{t^3}{12}(\kappa_x + \nu_y \kappa_y) - 2(\alpha_x + \nu_y \alpha_y) \sum_{n=1,3}^N \frac{(t/2)^{n+2}}{(n+2)} T_n^*(x,y) \right] \quad (6-36d)$$

Contrails

$$M_y = \frac{E_y}{(1 - \nu \nu)} \left[\frac{t^3}{12} (\nu_x \kappa_x + \kappa_y) - 2 (\alpha_y + \nu_x \alpha_x) \sum_{n=1,3}^N \frac{(t/2)^{n+2}}{(n+2)} T_n^*(x,y) \right] \quad (6-36e)$$

and

$$M_{xy} = \frac{2t^3 G}{12} \tau \quad (6-36f)$$

Inverting Eqs. (6-36) we find

$$\epsilon_x = \frac{1}{t} \left[\frac{1}{E_x} (N_x - \nu_x N_y) + 2\alpha_x \sum_{n=0,2}^N \frac{(t/2)^{n+1}}{(n+1)} T_n(x,y) \right] \quad (6-37a)$$

$$\epsilon_y = \frac{1}{t} \left[\frac{1}{E_y} (-\nu_y N_x + N_y) + 2\alpha_y \sum_{n=0,2}^N \frac{(t/2)^{n+1}}{(n+1)} T_n(x,y) \right] \quad (6-37b)$$

and

$$\gamma_{xy} = \frac{N_{xy}}{tG} \quad (6-37c)$$

Assuming the existence of a stress function $\phi = \phi(x,y)$ and a potential function $\Omega = \Omega(x,y)$,

$$N_x = \frac{\partial^2 \phi}{\partial y^2} + \Omega$$

$$N_y = \frac{\partial^2 \phi}{\partial x^2} + \Omega \quad (6-38)$$

$$N_{xy} = - \frac{\partial^2 \phi}{\partial x \partial y}$$

From Eqs. (6-27a) and (6-27b) it can be seen that it is necessary to define Ω by

Contrails

and

$$\frac{\partial \Omega}{\partial x} = - q_x \quad (6-39)$$

$$\frac{\partial \Omega}{\partial y} = - q_y$$

The values of the transverse shear Q_x and Q_y are obtained upon substitution into Eqs. (6-27d) and (6-27e);

$$Q_x = \left[- \frac{t^3 E_x}{12(1 - \nu_x \nu_y)} \frac{\partial^3 w}{\partial x^3} - \left(\frac{t^3 \nu_y E_x}{12(1 - \nu_x \nu_y)} + \frac{2t^3 G}{12} \right) \frac{\partial^3 w}{\partial x \partial y^2} - 2 \frac{E_x (\alpha_x + \nu_y \alpha_y)}{(1 - \nu_x \nu_y)} \sum_{n=1,3}^N \frac{(t/2)^{n+2}}{(n+2)} \frac{\partial T_n^*(x,y)}{\partial x} \right] \quad (6-40a)$$

and

$$Q_y = \left[- \left(\frac{t^3 E_y \nu_x}{12(1 - \nu_x \nu_y)} + \frac{2t^3 G}{12} \right) \frac{\partial^3 w}{\partial y \partial x^2} - \frac{t^3 E_y}{12(1 - \nu_x \nu_y)} \frac{\partial^3 w}{\partial x^3} - \frac{2E_y (\alpha_y + \nu_x \alpha_x)}{1 - \nu_x \nu_y} \sum_{n=1,3,\dots}^N \frac{(t/2)^{n+2}}{(n+2)} \frac{\partial T_n^*(x,y)}{\partial y} \right] \quad (6-40b)$$

And from Eq. (6-27c) we get

Contrails

$$\begin{aligned}
 D_x \frac{\partial^4 w}{\partial x^4} + 2D_{xy} \frac{\partial^4 w}{\partial x^2 \partial y^2} + D_y \frac{\partial^4 w}{\partial y^4} + \frac{1}{R_x} \frac{\partial^2 \phi}{\partial y^2} - \frac{2}{R_{xy}} \frac{\partial^2 \phi}{\partial x \partial y} \\
 + \frac{1}{R_y} \frac{\partial^2 \phi}{\partial x^2} = q - \Omega \left(\frac{1}{R_x} + \frac{1}{R_y} \right) - \frac{2}{(1 - \nu_x \nu_y)} \sum_{n=1,3,\dots}^N \frac{(t/2)^{n+2}}{n+2} \\
 \left[E_x (\alpha_x + \nu_y \alpha_y) \frac{\partial^2 T_n^*(x,y)}{\partial x^2} + E_y (\alpha_y + \nu_x \alpha_x) \frac{\partial^2 T_n^*(x,y)}{\partial y^2} \right]
 \end{aligned}
 \tag{6-41}$$

where

$$D_x = \frac{t^3 E_x}{12(1 - \nu_x \nu_y)}$$

$$D_{xy} = \frac{t^3}{12} \left(\frac{\nu_y E_x}{(1 - \nu_x \nu_y)} + 2G \right) = \frac{t^3}{12} \left(\frac{\nu_x E_y}{(1 - \nu_x \nu_y)} + 2G \right)$$

$$D_y = \frac{t^3 E_y}{12(1 - \nu_x \nu_y)}$$

substituting into Eq. (6-30) we get the second governing differential equation,

$$\begin{aligned}
 \frac{1}{t} \left[\frac{1}{E_y} \frac{\partial^4 \phi}{\partial x^4} + \left(-\frac{\nu_y}{E_y} - \frac{\nu_x}{E_x} + \frac{1}{G} \right) \frac{\partial^4 \phi}{\partial x^2 \partial y^2} + \frac{1}{E_x} \frac{\partial^4 \phi}{\partial y^4} \right] \\
 - \frac{1}{R_y} \frac{\partial^2 w}{\partial x^2} + \frac{2}{R_{xy}} \frac{\partial^2 w}{\partial x \partial y} - \frac{1}{R_x} \frac{\partial^2 w}{\partial y^2} = -\frac{1}{t} \left[\left(\frac{1 - \nu_y}{E_y} \right) \frac{\partial^2 \Omega}{\partial x^2} \right. \\
 \left. + \frac{1 - \nu_x}{E_x} \frac{\partial^2 \Omega}{\partial y^2} \right] - \frac{2}{t} \sum_{n=0,2}^N \frac{(n/2)^{n+1}}{(n+1)} \left(\alpha_x \frac{\partial^2 T_n(x,y)}{\partial x^2} + \alpha_y \frac{\partial^2 T_n(x,y)}{\partial y^2} \right)
 \end{aligned}
 \tag{6-42}$$

The general forms given by Eqs. (6-41) and (6-42) can be specialized for isothermal, isotropic shells as follows.

1. Thermoelastic Isotropic Shallow Shells

The governing differential equations for this case are

$$D\nabla^4 w + \frac{1}{R_x} \frac{\partial^2 \phi}{\partial y^2} - \frac{2}{R_{xy}} \frac{\partial^2 \phi}{\partial x \partial y} + \frac{1}{R_y} \frac{\partial^2 \phi}{\partial x^2} = q_n - \left(\frac{1}{R_x} + \frac{1}{R_y} \right) \Omega$$

$$- \frac{2E\alpha}{1-\nu} \sum_{n=1,3}^N \frac{(t/2)^{n+2}}{(n+2)} \nabla^2 T_n^*(x,y)$$

and

$$\frac{1}{Et} \nabla^4 \phi - \frac{1}{R_y} \frac{\partial^2 w}{\partial x^2} + \frac{2}{R_{xy}} \frac{\partial^2 w}{\partial x \partial y} - \frac{1}{R_x} \frac{\partial^2 w}{\partial y^2} = - \frac{1-\nu}{Et} \Delta^2 \Omega$$

$$- \frac{2\alpha}{h} \sum_{n=0,2}^N \frac{(t/2)^{n+1}}{(n+1)} \nabla^2 T_n(x,y)$$

2. Elastic Isotropic Shallow Shell

$$D\nabla^4 w + \frac{1}{R_x} \frac{\partial^2 \phi}{\partial y^2} - \frac{2}{R_{xy}} \frac{\partial^2 \phi}{\partial x \partial y} + \frac{1}{R_y} \frac{\partial^2 \phi}{\partial x^2} = q_n - \left(\frac{1}{R_x} + \frac{1}{R_y} \right) \Omega$$

and

$$\frac{1}{Et} \nabla^4 \phi - \frac{1}{R_y} \frac{\partial^2 w}{\partial x^2} + \frac{2}{R_{xy}} \frac{\partial^2 w}{\partial x \partial y} - \frac{1}{R_x} \frac{\partial^2 w}{\partial y^2} = - \frac{(1-\nu)}{Et} \nabla^2 \Omega$$

These equations duplicate the well-known forms given previously in Ref. 16.

VII - SOLUTIONS OF THE ORTHOTROPIC THERMOELASTIC SHELL EQUATIONS FOR CIRCULAR CYLINDRICAL CURVATURE

The general differential equations for orthotropic shallow shells with thermal gradient, Eqs. (6-41) and (6-42), can be written as

$$L_1 \left(\frac{\partial}{\partial x}, \frac{\partial}{\partial y} \right) w + L_3 \left(\frac{\partial}{\partial x}, \frac{\partial}{\partial y} \right) \phi = \left[q_n - \Omega \left(\frac{1}{R_x} + \frac{1}{R_y} \right) - \sum_{n=1,3}^N \frac{(t/2)^{n+2}}{(n+2)} \left(P_x \frac{\partial^2 T_n(x,y)}{\partial x^2} + P_y \frac{\partial^2 T_n(x,y)}{\partial y^2} \right) \right] \quad (7-1)$$

$$L_2 \left(\frac{\partial}{\partial x}, \frac{\partial}{\partial y} \right) \phi - L_3 \left(\frac{\partial}{\partial x}, \frac{\partial}{\partial y} \right) w = - \left\{ \left[(1-\nu_y) F_x \frac{\partial^2 \Omega}{\partial x^2} + (1-\nu_x) F_y \frac{\partial^2 \Omega}{\partial y^2} \right] + \frac{2}{t} \sum_{n=0,2}^N \frac{(t/2)^{n+1}}{(n+1)} \left(\alpha_x \frac{\partial^2 T_n(x,y)}{\partial x^2} + \alpha_y \frac{\partial^2 T_n(x,y)}{\partial y^2} \right) \right\} \quad (7-2)$$

where

$$L_1 = D_x \frac{\partial^4}{\partial x^4} + 2D_{xy} \frac{\partial^4}{\partial x^2 \partial y^2} + D_y \frac{\partial^4}{\partial y^4}$$

$$L_2 = F_x \frac{\partial^4}{\partial x^4} + 2F_{xy} \frac{\partial^4}{\partial x^2 \partial y^2} + F_y \frac{\partial^4}{\partial y^4}$$

$$L_3 = \frac{1}{R_y} \frac{\partial^2}{\partial x^2} - \frac{2}{R_{xy}} \frac{\partial^2}{\partial x \partial y} + \frac{1}{R_x} \frac{\partial^2}{\partial y^2}$$

$$D_x = \frac{t^3 E_x}{12(1-\nu_x \nu_y)}$$

$$D_{xy} = \frac{t^3}{12} \left[\frac{\nu_y E_x}{(1-\nu_x \nu_y)} + 2G \right] = \frac{t^3}{12} \left[\frac{\nu_x E_y}{(1-\nu_x \nu_y)} + 2G \right]$$

$$D_y = \frac{t^3 E_y}{12(1-\nu_x \nu_y)}$$

Contrails

$$F_x = \frac{1}{tE_y}$$

$$F_{xy} = \frac{1}{2t} \left(-\frac{\nu_x}{E_x} - \frac{\nu_y}{E_y} + \frac{1}{G} \right)$$

$$F_y = \frac{1}{tE_x}$$

$$P_x = \frac{2E_x(\alpha_x + \nu_y \alpha_y)}{1 - \nu_x \nu_y}$$

$$P_y = \frac{2E_y(\alpha_y + \nu_x \alpha_x)}{1 - \nu_x \nu_y}$$

In the case of a circular cylindrical shell (Fig. 18) we have

$$\frac{1}{R_x} = \frac{1}{R_{xy}} = 0$$

$$\frac{1}{R_y} = \frac{1}{R}$$

and Eq. (7-1) reduces to

$$\begin{aligned} L_1 \left(\frac{\partial}{\partial x}, \frac{\partial}{\partial y} \right) w + L_3 \left(\frac{\partial}{\partial x}, \frac{\partial}{\partial y} \right) \phi = & \left[q_n - \frac{\Omega}{R} \right. \\ & \left. - \sum_{n=1,3}^N \frac{(t/2)^{n+2}}{(n+2)} \left(P_x \frac{\partial^2 T_n(x,y)}{\partial x^2} + P_y \frac{\partial^2 T_n(x,y)}{\partial y^2} \right) \right] \end{aligned} \quad (7-3)$$

while Eq. (7-2) remains unchanged. In this case the operator $L_3 \left(\frac{\partial}{\partial x}, \frac{\partial}{\partial y} \right)$ will take the form $L_3 = \frac{1}{R} \frac{\partial^2}{\partial x^2}$

Contrails

The solution of Eqs. (7-1) and (7-2) can be written as

$$\left. \begin{aligned} w &= w_p + w_c \\ \phi &= \phi_p + \phi_c \end{aligned} \right\} \quad (7-4)$$

while w_p and ϕ_p are the particular solutions while w_c and ϕ_c are the complementary solutions. One form of particular solution will be given later in Part D of this chapter.

Complementary solutions to the homogeneous equations

$$L_1\left(\frac{\partial}{\partial x}, \frac{\partial}{\partial y}\right)w + L_3\left(\frac{\partial}{\partial x}, \frac{\partial}{\partial y}\right)\phi = 0 \quad (7-5)$$

$$-L_3\left(\frac{\partial}{\partial x}, \frac{\partial}{\partial y}\right)w + L_2\left(\frac{\partial}{\partial x}, \frac{\partial}{\partial y}\right)\phi = 0 \quad (7-6)$$

can be obtained either by:

- (1) Uncoupling Eqs. (7-5) and (7-6), or by
- (2) Using the auxiliary function technique which will be discussed in detail in the following sections.

A. THE AUXILIARY FUNCTION METHOD

This technique was used extensively by V. Z. Vlasov [19], S. A. Ambartsumyan [20] and A. L. Goldenveizer [21] for solving problems in linear shell theory and requires the introduction of auxiliary functions. Thus the problem which was originally described by a system of simultaneous differential equations (i.e., Eqs. (7-5) and (7-6) can be described by a single differential equation of a higher order in the auxiliary functions. Choosing

$$w = L_2\left(\frac{\partial}{\partial x}, \frac{\partial}{\partial y}\right)\psi(x, y) \quad (7-7)$$

$$\phi = L_3\left(\frac{\partial}{\partial x}, \frac{\partial}{\partial y}\right)\psi(x, y) \quad (7-8)$$

Eq. (7-6) will be identically satisfied, while from Eq. (7-5) we obtain

$$\left[L_1 \left(\frac{\partial}{\partial x}, \frac{\partial}{\partial y} \right) L_2 \left(\frac{\partial}{\partial x}, \frac{\partial}{\partial y} \right) + L_3 \left(\frac{\partial}{\partial x}, \frac{\partial}{\partial y} \right) L_3 \left(\frac{\partial}{\partial x}, \frac{\partial}{\partial y} \right) \right] \psi(x, y) = 0 \quad (7-9)$$

where $\psi(x, y)$ is the auxiliary function. Eq. (7-9), which appears in explicit form as

$$P_1 \frac{\partial^8 \psi}{\partial x^8} + P_2 \frac{\partial^8 \psi}{\partial x^6 \partial y^2} + P_3 \frac{\partial^8 \psi}{\partial x^4 \partial y^4} + P_4 \frac{\partial^8 \psi}{\partial x^2 \partial y^6} + P_5 \frac{\partial^8 \psi}{\partial y^8} + P_6 \frac{\partial^4 \psi}{\partial x^4} = 0 \quad (7-10)$$

where

$$P_1 = D_x F_x$$

$$P_2 = 2(D_x F_{xy} + D_{xy} F_x)$$

$$P_3 = D_x F_y + 4D_{xy} F_{xy} + D_y F_x$$

$$P_4 = 2(D_{xy} F_y + D_y F_{xy})$$

$$P_5 = D_y F_y$$

$$P_6 = \frac{1}{R^2}$$

can be considered the replacement equation for the homogeneous system, Eqs. (7-5) and (7-6).

By virtue of Eqs. (7-7) and (7-8), the slopes, membrane forces, bending and twisting moments, transverse shears and displacements can be obtained in terms of the auxiliary function (Goldenveizer in his work refers to the auxiliary function as the potential function).

$$\frac{\partial w_\epsilon}{\partial x} = \left(F_x \frac{\partial^5}{\partial x^5} + 2F_{xy} \frac{\partial^5}{\partial x^3 \partial y^2} + F_y \frac{\partial^5}{\partial x \partial y^4} \right) \psi(x, y) \quad (7-11)$$

$$\frac{\partial w_\epsilon}{\partial y} = \left(F_x \frac{\partial^5}{\partial x^4 \partial y} + 2F_{xy} \frac{\partial^5}{\partial x^2 \partial y^3} + F_y \frac{\partial^5}{\partial y^5} \right) \psi(x, y) \quad (7-12)$$

Contrails

$$N_{x_c} = \frac{1}{R} \frac{\partial^4 \psi(x, y)}{\partial x^2 \partial y^2} \quad (7-13)$$

$$N_{y_c} = \frac{\partial^4 \psi(x, y)}{\partial x^4} \quad (7-14)$$

$$N_{xy_c} = \frac{1}{R} \frac{\partial^4 \psi(x, y)}{\partial x^3 \partial y} \quad (7-15)$$

$$\begin{aligned} M_{x_c} = -D_x \left[F_x \frac{\partial^6 \psi(x, y)}{\partial x^6} + (2F_{xy} + \nu_y F_x) \frac{\partial^6 \psi(x, y)}{\partial x^4 \partial y^2} \right. \\ \left. + (F_y + 2\nu_y F_{xy}) \frac{\partial^6 \psi(x, y)}{\partial x^2 \partial y^4} + \nu_y F_y \frac{\partial^6 \psi(x, y)}{\partial y^6} \right] \end{aligned} \quad (7-16)$$

$$\begin{aligned} M_{y_c} = -D_y \left[\nu_x F_x \frac{\partial^6 \psi(x, y)}{\partial x^6} + (F_x + 2\nu_x F_{xy}) \frac{\partial^6 \psi(x, y)}{\partial x^4 \partial y^2} \right. \\ \left. + (2F_{xy} + \nu_x F_y) \frac{\partial^6 \psi(x, y)}{\partial x^2 \partial y^4} + F_y \frac{\partial^6 \psi(x, y)}{\partial y^6} \right] \end{aligned} \quad (7-17)$$

$$M_{xy_c} = -\frac{2t^3 G}{12} \left[F_x \frac{\partial^6 \psi(x, y)}{\partial x^5 \partial y} + 2F_{xy} \frac{\partial^6 \psi(x, y)}{\partial x^3 \partial y^3} + F_y \frac{\partial^6 \psi(x, y)}{\partial x \partial y^5} \right] \quad (7-18)$$

$$\begin{aligned} Q_{x_c} = - \left[D_x F_x \frac{\partial^7 \psi(x, y)}{\partial x^7} + (2D_x F_{xy} + D_{xy} F_x) \frac{\partial^7 \psi(x, y)}{\partial x^5 \partial y^2} \right. \\ \left. + (D_x F_y + 2D_{xy} F_{xy}) \frac{\partial^7 \psi(x, y)}{\partial x^3 \partial y^4} + D_{xy} F_y \frac{\partial^7 \psi(x, y)}{\partial x \partial y^6} \right] \end{aligned} \quad (7-19)$$

Contrails

Now let us suppose the existence of three arbitrary, sufficiently smooth functions u , v , and w derived from the equations of equilibrium, Eqs. (6-27a) and (6-27b), in terms of the displacements:

$$\left(\frac{tE_x}{1-\nu_x\nu_y} \frac{\partial^2}{\partial x^2} + tG \frac{\partial^2}{\partial y^2} \right) u + \left(\frac{tE_x\nu_y}{1-\nu_x\nu_y} + tG \right) \frac{\partial^2 v}{\partial x \partial y} = - \frac{t\nu_y E_x}{R(1-\nu_x\nu_y)} \frac{\partial w}{\partial x} \quad (7-27)$$

$$\left(\frac{t\nu_x E_y}{1-\nu_x\nu_y} + tG \right) \frac{\partial^2 u}{\partial x \partial y} + \left(tG \frac{\partial^2}{\partial x^2} + \frac{tE_y}{1-\nu_x\nu_y} \frac{\partial^2}{\partial y^2} \right) v = - \frac{tE_y}{R(1-\nu_x\nu_y)} \frac{\partial w}{\partial y} \quad (7-28)$$

or equivalently in operator form as

$$L_5 \begin{pmatrix} u_c \\ v_c \end{pmatrix} = \begin{pmatrix} - \frac{t\nu_y E_x}{R(1-\nu_x\nu_y)} \frac{\partial w}{\partial x} \\ - \frac{tE_y}{R(1-\nu_x\nu_y)} \frac{\partial w}{\partial y} \end{pmatrix} \quad (7-29)$$

Supposing that the region is simply-connected, then from Eqs. (7-29) we can write.

$$\begin{pmatrix} u_c \\ v_c \end{pmatrix} = L_5^{-1} \left(\frac{\partial}{\partial x}, \frac{\partial}{\partial y} \right) \begin{pmatrix} - \frac{t\nu_y E_x}{R(1-\nu_x\nu_y)} \frac{\partial w}{\partial x} \\ - \frac{tE_y}{R(1-\nu_x\nu_y)} \frac{\partial w}{\partial y} \end{pmatrix} + \begin{pmatrix} u_0 \\ v_0 \end{pmatrix} \quad (7-30)$$

and from Eq. (7-7)

$$\psi(x, y) = L_2^{-1} \left(\frac{\partial}{\partial x}, \frac{\partial}{\partial y} \right) w + \psi_0(x, y) \quad (7-31)$$

where $L_2^{-1} \left(\frac{\partial}{\partial x}, \frac{\partial}{\partial y} \right)$ and $L_5^{-1} \left(\frac{\partial}{\partial x}, \frac{\partial}{\partial y} \right)$ are the inverse operators of $L_2 \left(\frac{\partial}{\partial x}, \frac{\partial}{\partial y} \right)$, and $L_5 \left(\frac{\partial}{\partial x}, \frac{\partial}{\partial y} \right)$, respectively.

Contrails

With the value of the auxiliary function $\psi(x, y)$ given by Eq. (7-31), the expressions for u and v can be obtained from Eq. (7-26)

$$\begin{Bmatrix} u_c \\ v_c \end{Bmatrix} = L_4 \left(\frac{\partial}{\partial x}, \frac{\partial}{\partial y} \right) L_2^{-1} \left(\frac{\partial}{\partial x}, \frac{\partial}{\partial y} \right) w + L_4 \left(\frac{\partial}{\partial x}, \frac{\partial}{\partial y} \right) \psi_0(x, y) \quad (7-32)$$

For the uniqueness of the displacements then the expressions of u_c and v_c given by Eqs. (7-30) and (7-32) should be equivalent; i.e.,

$$\begin{aligned} & L_4 \left(\frac{\partial}{\partial x}, \frac{\partial}{\partial y} \right) L_2^{-1} \left(\frac{\partial}{\partial x}, \frac{\partial}{\partial y} \right) w + L_4 \left(\frac{\partial}{\partial x}, \frac{\partial}{\partial y} \right) \psi_0(x, y) \\ &= L_5^{-1} \left(\frac{\partial}{\partial x}, \frac{\partial}{\partial y} \right) \left\{ \begin{array}{l} -\frac{t\nu_y E_x}{R(1-\nu_x\nu_y)} \frac{\partial w}{\partial x} \\ -\frac{tE_y}{R(1-\nu_x\nu_y)} \frac{\partial w}{\partial y} \end{array} \right\} + \begin{Bmatrix} u_0 \\ v_0 \end{Bmatrix} \end{aligned} \quad (7-33)$$

In order that $\begin{Bmatrix} u_0 \\ v_0 \end{Bmatrix}$ is the homogeneous solution of Eq. (7-7); i.e.,

$$L_4 \left(\frac{\partial}{\partial x}, \frac{\partial}{\partial y} \right) \psi_0(x, y) = \begin{Bmatrix} u_0 \\ v_0 \end{Bmatrix} \quad (7-34)$$

implies that

$$L_4 \left(\frac{\partial}{\partial x}, \frac{\partial}{\partial y} \right) L_2^{-1} \left(\frac{\partial}{\partial x}, \frac{\partial}{\partial y} \right) w = L_5^{-1} \left(\frac{\partial}{\partial x}, \frac{\partial}{\partial y} \right) \left\{ \begin{array}{l} -\frac{t\nu_y E_x}{R(1-\nu_x\nu_y)} \frac{\partial w}{\partial x} \\ -\frac{tE_y}{R(1-\nu_x\nu_y)} \frac{\partial w}{\partial y} \end{array} \right\} \quad (7-35)$$

But

$$w \equiv L_2 \left(\frac{\partial}{\partial x}, \frac{\partial}{\partial y} \right) L_2^{-1} \left(\frac{\partial}{\partial x}, \frac{\partial}{\partial y} \right) w \quad (7-36)$$

Let $L_5 \left(\frac{\partial}{\partial x}, \frac{\partial}{\partial y} \right)$ operate on Eq. (7-31), remembering that

Contrails

$$L_5 \left(\frac{\partial}{\partial x}, \frac{\partial}{\partial y} \right) L_5^{-1} \left(\frac{\partial}{\partial x}, \frac{\partial}{\partial y} \right) = I \quad (7-37)$$

(the identify operator), we get

$$L_5 \left(\frac{\partial}{\partial x}, \frac{\partial}{\partial y} \right) L_4 \left(\frac{\partial}{\partial x}, \frac{\partial}{\partial y} \right) L_2^{-1} \left(\frac{\partial}{\partial x}, \frac{\partial}{\partial y} \right) = \left\{ \begin{array}{l} - \frac{t v_y E_x}{R(1-v_x v_y)} \frac{\partial}{\partial x} \left[L_2^{-1} \left(\frac{\partial}{\partial x}, \frac{\partial}{\partial y} \right) w \right] \\ - \frac{t E_y}{R(1-v_x v_y)} \frac{\partial}{\partial y} \left[L_2^{-1} \left(\frac{\partial}{\partial x}, \frac{\partial}{\partial y} \right) w \right] \end{array} \right\} \quad (7-38)$$

If we have a set of equations in partial derivatives

$$\sum_{i=1}^n a_{ij} \left(\frac{\partial}{\partial x_q} \right) u_j = 0 \quad \left\{ \begin{array}{l} i = 1, 2, \dots, n \\ 1 \leq q \leq k \end{array} \right. \quad (7-39)$$

where u_j are the unknown functions and $a_{ij} \frac{\partial}{\partial x_q}$ the linear differential operators of finite order and with constant coefficients, this set of equations in partial derivatives can be replaced by a set of algebraic equations

$$\sum_{i=1}^n a_{ij} \lambda_q V_j = 0 \quad \left\{ \begin{array}{l} i = 1, 2, \dots, n \\ 1 \leq q \leq k \end{array} \right. \quad (7-40)$$

where the partial differentiation with respect to x_q was replaced by some parameter λ_q

Suppose that the first $(n-1)$ equations of (7-40) enable us to express V_1, V_2, \dots, V_{n-1} in terms of V_n

$$V_i = \frac{D_i(\lambda_1, \lambda_2, \dots, \lambda_k)}{Q(\lambda_1, \lambda_2, \dots, \lambda_k)} v_n \quad (i=1, 2, \dots, n-1) \quad (7-41)$$

where D_i and Q can be taken as polynomials in $\lambda_1, \lambda_2, \dots, \lambda_k$.

Contrails

Introducing the function Π such that

$$u_i = D_i \left(\frac{\partial}{\partial x_1}, \frac{\partial}{\partial x_2}, \dots, \frac{\partial}{\partial x_k} \right) \Pi \quad (7-42)$$

(i=1,2,...,n-1)

$$u_n = Q \left(\frac{\partial}{\partial x_1}, \frac{\partial}{\partial x_2}, \dots, \frac{\partial}{\partial x_k} \right) \Pi \quad (7-43)$$

and substituting into Eq. (7-39) we get

$$\left\{ \sum_{j=1}^{n-1} a_{nj} \left(\frac{\partial}{\partial x_q} \right) D_j \left(\frac{\partial}{\partial x_q} \right) + a_{nn} \left(\frac{\partial}{\partial x_q} \right) Q \left(\frac{\partial}{\partial x_q} \right) \right\} \Pi = K \left(\frac{\partial}{\partial x_q} \right) \Pi = 0 \quad (7-44)$$

where $K(\lambda_q)$ is the determinant of the set of Eqs. (7-40). Hence any function Π satisfying (7-44) provides by means of Eqs. (7-42) and (7-43) a solution to the set of Eqs. (7-39).

Denoting the operator of differentiation with respect to α by ρ and the operator of differentiation with respect of y by λ then the

operators $L_2 \left(\frac{\partial}{\partial x}, \frac{\partial}{\partial y} \right)$, $L_4 \left(\frac{\partial}{\partial x}, \frac{\partial}{\partial y} \right)$, $L_5 \left(\frac{\partial}{\partial x}, \frac{\partial}{\partial y} \right)$ will be

$$L_2(\rho, \lambda) = F_x \rho^4 + 2F_{xy} \rho^2 \lambda^2 + F_y \lambda^4 \quad (7-45)$$

$$L_4(\rho, \lambda) = \left\{ \begin{array}{l} \frac{F_y}{R} \rho \lambda^2 - \frac{F_y V_x}{R} \rho^3 \\ \frac{1}{R} \left(\frac{v_x}{tE_x} - \frac{1}{tG} \right) \rho^2 \lambda - \frac{F_y}{R} \lambda^3 \end{array} \right\} \quad (7-46)$$

$$L_5(\rho, \lambda) = \left\{ \begin{array}{ll} \left(\frac{tE_x}{1-v_x v_y} \rho^2 + tG \lambda^2 \right) & \left(\frac{tE_x v_y}{1-v_x v_y} + tG \right) \lambda \rho \\ \left(\frac{t v_x E_y}{1-v_x v_y} + tG \right) \rho \lambda & \left(tG \rho^2 + \frac{tE_y}{1-v_x v_y} \lambda^2 \right) \end{array} \right\} \quad (7-47)$$

From which we see that Eq. (7-38) is identically satisfied upon substituting for $L_4 \left(\frac{\partial}{\partial x}, \frac{\partial}{\partial y} \right)$ and $L_5 \left(\frac{\partial}{\partial x}, \frac{\partial}{\partial y} \right)$ the expressions for $L_4(\rho, \lambda)$ and

Contrails

$L_5(\rho, \lambda)$ given by Eqs. (7-46) and (7-47). Further the auxiliary function $\psi_0(x, y)$ should satisfy the differential equation

$$L_2 \left(\frac{\partial}{\partial x}, \frac{\partial}{\partial y} \right) \psi_0(x, y) = 0 \quad (7-48)$$

$$F_x \frac{\partial^4 \psi_0(x, y)}{\partial x^4} + 2F_{xy} \frac{\partial^4 \psi_0(x, y)}{\partial x^2 \partial y^2} + F_y \frac{\partial^4 \psi_0(x, y)}{\partial y^4} = 0 \quad (7-49)$$

Eq. (7-49) is a generalization of the well known biharmonic equation. According to Lekhnitskii [31] the fourth order differential operator can be decomposed into four linear operators of the first order. The characteristic equation of Eq. (7-49) is:

$$F_y s^4 + 2F_{xy} s^2 + F_x = 0 \quad (7-50)$$

Denote the roots of Eq. (7-50) by $s_1, s_2, s_3,$ and s_4 . The general solution of Eq. (7-49) depends on the roots $s_1, s_2, s_3,$ and s_4 . Hence Eq. (7-48) can be represented in the form

$$D_4 D_3 D_2 D_1 \psi_0(x, y) = 0 \quad (7-51)$$

where

$$D_i = \frac{\partial}{\partial x} - s_i \frac{\partial}{\partial y}, \quad i = 1, 2, 3, 4 \quad (7-52)$$

By means of Eq. (7-51) the integration of a single equation of fourth order is reduced to the integration of four equations of first order. Assuming that the roots s_k are distinct we denote

$$D_1 \psi_0(x, y) = \psi_1(x, y) \quad (7-53)$$

$$D_2 \psi_1(x, y) = \psi_2(x, y) \quad (7-54)$$

$$D_3 \psi_2(x, y) = \psi_3(x, y) \quad (7-55)$$

From Eq. (7-55) we conclude that the function $\psi_3(x, y)$ should satisfy

$$D_4 \psi_3(x, y) = 0 \quad (7-56)$$

Contrails

The general integral of Eq. (7-56) is an arbitrary function of the argument $(x+s_k y)$ and is denoted by

$$\psi_3(x, y) = f_4'''(x+s_4 y) \quad (7-57)$$

The function $\psi_2(x, y)$ should satisfy the nonhomogeneous equation of the first order

$$D_3 \psi_2(x, y) = f_4'''(x+s_4 y) \quad (7-58)$$

Integrating Eq. (7-58) we obtain

$$\psi_2(x, y) = f_3''(x+s_3 y) + \frac{f_4''(x+s_4 y)}{(s_4 - s_3)} \quad (7-59)$$

Proceeding in the same way we obtain $\psi_1(x, y)$ and finally $\psi_0(x, y)$, and after changing the notation of the arbitrary functions we obtain the general expression for $\psi_0(x, y)$:

$$\psi_0(x, y) = f_1(x+s_1 y) + f_2(x+s_2 y) + f_3(x+s_3 y) + f_4(x+s_4 y) = \sum_{k=1}^4 F_k(x+s_k y) \quad (7-60)$$

According to Savin [32] it is impossible for Eq. (7-50) to have real roots, as will be seen later. Let us assume that

$$\begin{aligned} s_1 &= \zeta_1 + i\eta_1 \\ s_2 &= \zeta_2 + i\eta_2 \\ s_3 &= \zeta_1 - i\eta_1 \\ s_4 &= \zeta_2 - i\eta_2 \end{aligned} \quad (7-61)$$

arranged such that

$$\begin{aligned} \eta_1 &> 0 \\ \eta_2 &> 0 \\ \eta_1 &\neq \eta_2 \end{aligned} \quad (7-62)$$

Contraails

Since the function $\psi_0(x,y)$ is a real function of x and y , then we can denote

$$\begin{aligned}Z_1 &= x + s_1y = x + \zeta_1y + i\eta_1y \\Z_2 &= x + s_2y = x + \zeta_2y + i\eta_2y\end{aligned}\tag{7-63}$$

Hence, Eq. (7-60) can be rewritten in the form

$$\psi_0(x,y) = f_1(Z_1) + f_2(Z_2) + \overline{f_1(Z_1)} + \overline{f_2(Z_2)}\tag{7-64}$$

where $f_1(Z_1)$ and $f_2(Z_2)$ are analytic functions. $\overline{f_1(Z_1)}$ and $\overline{f_2(Z_2)}$ are the complex conjugates of the functions $f_1(Z_1)$ and $f_2(Z_2)$, respectively. Introduce

$$\frac{df_1}{dZ_1} = q(Z_1)\tag{7-65}$$

$$\frac{df_2}{dZ_2} = \chi(Z_2)$$

then

$$\overline{\frac{df_1}{dZ_1}} = \overline{q(Z_1)}\tag{7-66}$$

$$\overline{\frac{df_2}{dZ_2}} = \overline{\chi(Z_2)}$$

From Eq. (7-64) and by using the expressions given by Eqs. (7-65) and (7-66) one can obtain the general equations for the displacement components $u(x,y)$ and $v(x,y)$

$$u(x,y) = 2\text{Re}[p_1q(Z_1) + p_2\chi(Z_2)]\tag{7-67}$$

$$v(x,y) = 2\text{Re}[q_1q(Z_1) + q_2\chi(Z_2)]\tag{7-68}$$

where

$$\left. \begin{aligned} p_1 &= F_y s_1^2 - \frac{v_x}{E_x} \\ p_2 &= F_y s_2^2 - \frac{v_x}{E_x} \end{aligned} \right\} \quad (7-69)$$

$$\left. \begin{aligned} q_1 &= \frac{-\frac{v_x}{E_x} s_1^2 + F_x}{s_1} \\ q_2 &= \frac{-\frac{v_x}{E_x} s_2^2 + F_y}{s_2} \end{aligned} \right\} \quad (7-70)$$

The general form of Eqs. (7-67) through (7-70) for the case of anisotropic elastic bodies were given by Lekhnitski [31] and Savin [32]

Let

$$\psi_0(x,y) = R_1(Z_1) + R_2(Z_2) + \overline{R_1(Z_1)} + \overline{R_2(Z_2)} \quad (7-71)$$

but

$$u = \frac{F_y}{R} \left[\frac{\partial^3 \psi_0(x,y)}{\partial x \partial y^2} - v_x \frac{\partial^3 \psi_0(x,y)}{\partial x^3} \right] \quad (7-72)$$

$$v = \frac{1}{R} \left[\left(\frac{v_x}{tE_x} - \frac{1}{tG} \right) \frac{\partial^3 \psi_0(x,y)}{\partial x^2 \partial y} - F_y \frac{\partial^3 \psi_0(x,y)}{\partial y^3} \right] \quad (7-73)$$

Substituting for $\psi_0(x,y)$ into Eqs. (7-72) we get

$$u = \frac{2F_y}{R} \left\{ \operatorname{Re}[(s_1^2 - v_x) R_1'''(Z_1) + (s_2 - v_x) R_2'''(Z_2)] \right\} \quad (7-74)$$

In order that Eqs. (7-76) and (7-74) be compatible then we require that

$$F_y \frac{s_1^2}{R} \neq 0 \tag{7-75}$$

$$F \frac{s_2^2}{R} \neq 0$$

but s_1^2 and s_2^2 are

$$s_1^2 = - \frac{F_{xy} + \sqrt{F_{xy}^2 - F_x F_y}}{F_y} \tag{7-76}$$

$$s_2^2 = - \frac{F_{xy} - \sqrt{F_{xy}^2 - F_x F_y}}{F_y}$$

Excluding the case $R = \infty$ (in which case the cylindrical shell degenerates into a rectangular plate) we find that the requirements given by Eqs. (7-75) are always satisfied. Hence the auxiliary function technique is admissible for all ranges of elastic constants. The authors would like to caution the reader that in the case of cylindrical shells, this technique rendered no difficulties, but in cases of other types of shells it might. It was pointed out by Mishonov [33] that certain difficulties may be incurred in the case of spherical shells.

C. A SPECIAL CASE

For the case where

$$G = \frac{(E_x E_y)^{1/2}}{2[1 + (\nu_x \nu_y)^{1/2}]} \tag{7-77}$$

then

$$F_{xy} - F_x F_y = 0 \tag{7-78}$$

and the characteristic equation, Eq. (7-50) will have double roots. Consequently, Eq. (7-76) reduces to

$$s_1^2 = s_2^2 = - \frac{F_{xy}}{F_y} \tag{7-79}$$

For this case it can be verified that

$$\psi_0(x,y) = \bar{Z}f_1(Z) + \overline{Zf_1(Z)} + f_2(Z) + \overline{f_2(Z)} \tag{7-80}$$

Contrails

After investigating the governing differential equations for this special case, it was concluded that a simple solution exists. This solution will be introduced in the following section and we feel that this form of the solution is more attractive since it resembles the Levy type solution discussed later in this chapter.

In this case D_{xy} and F_{xy} will be given by

$$\left. \begin{aligned} D_{xy} &= \frac{t^3(E_x E_y)^{1/2}}{12(1-\nu_x \nu_y)} \\ F_{xy} &= \frac{1}{t(E_x E_y)^{1/2}} \end{aligned} \right\} \quad (7-81)$$

and D_x , D_{xy} , and D_y will be related to F_x , F_{xy} , and F_y , respectively, by the following reactions:

$$\frac{D_x}{F_x} = \frac{D_{xy}}{F_{xy}} = \frac{D_y}{F_y} = \frac{t^4 E_x E_y}{12(1-\nu_x \nu_y)} = l^2 \quad (7-82)$$

In this case it is advantageous to write the governing homogeneous differential equations of shallow circular cylindrical shells, Eqs. (7-5) and (7-6) in the following form:

$$D_x \frac{\partial^4 w}{\partial x^4} + 2D_{xy} \frac{\partial^4 w}{\partial x^2 \partial y^2} + D_y \frac{\partial^4 w}{\partial y^4} + \frac{1}{R} \frac{\partial^2 \Phi}{\partial x^2} = 0 \quad (7-83)$$

$$F_x \frac{\partial^4 \Phi}{\partial x^4} + 2F_{xy} \frac{\partial^4 \Phi}{\partial x^2 \partial y^2} + F_y \frac{\partial^4 \Phi}{\partial y^4} - \frac{1}{R} \frac{\partial^2 w}{\partial x^2} = 0 \quad (7-84)$$

Multiplying Eq. (7-84) by l^2 we get

$$D_x \frac{\partial^4 \Phi}{\partial x^4} + 2D_{xy} \frac{\partial^4 \Phi}{\partial x^2 \partial y^2} + D_y \frac{\partial^4 \Phi}{\partial y^4} - \frac{l^2}{R} \frac{\partial^2 w}{\partial x^2} = 0 \quad (7-85)$$

Introducing the parameter λ as a multiplier to Eq. (7-85) and adding this to Eq. (7-83) yields

$$D_x \frac{\partial^4 (w + \lambda \Phi)}{\partial x^4} + 2D_{xy} \frac{\partial^4 (w + \lambda \Phi)}{\partial x^2 \partial y^2} + D_y \frac{\partial^4 (w + \lambda \Phi)}{\partial y^4} - \frac{\lambda l^2}{R} \frac{\partial^2}{\partial x^2} \left(w - \frac{1}{\lambda l^2} \Phi \right) = 0 \quad (7-86)$$

Contrails

Setting

$$\lambda^2 = \frac{1}{(iL)^2} = - \frac{12(1-\nu_x\nu_y)}{t^4 E_x E_y} \quad (7-87)$$

Eq. (7-86) reduces to

$$\left(D_x \frac{\partial^4}{\partial x^4} + 2D_{xy} \frac{\partial^4}{\partial x^2 \partial y^2} + D_y \frac{\partial^4}{\partial y^4} + \frac{iL}{R} \frac{\partial^2}{\partial x^2} \right) (w + \lambda\phi) = 0 \quad (7-88)$$

Solutions of Eq. (7-88) satisfying the boundary conditions of shear diaphragms at $x = 0, a$ (see Fig. 18) are obtained in Cartesian coordinates by assuming

$$w + \lambda\phi = Y_m(y) \sin \alpha x \quad (7-89)$$

where

$$\alpha = \frac{n\pi}{a}$$

substituting (7-89) into (7-84) gives

$$D_y Y_m''''(y) - 2\alpha^2 D_{xy} Y_m''(y) + \left(\alpha^4 D_x - \frac{iL\alpha^2}{R} \right) Y_m(y) = 0 \quad (7-90)$$

Let

$$Y_m(y) = C_j e^{\delta_j y} \quad (7-91)$$

Substituting Eq. (7-91) into Eq. (7-90) we obtain the characteristic equation

$$D_y \delta_j^4 - 2\alpha^2 D_{xy} \delta_j^2 + \alpha^2 \left(\alpha^2 D_x - \frac{iL}{R} \right) = 0 \quad (7-92)$$

Solutions of Eq. (7-92) are

$$\delta_j^2 = \frac{\alpha^2 D_{xy} \pm \left[\alpha^4 D_{xy}^2 - \alpha^2 D_y \left(\alpha^2 D_x - \frac{iL}{R} \right) \right]^{1/2}}{D_y} \quad (7-93)$$

But

$$D_{xy}^2 = D_x D_y \quad (7-94)$$

and Eq. (7-93) takes the form

$$\delta_j^2 = \alpha^2 \frac{D_{xy}}{D_y} \mp \left(\frac{i\alpha^2 L}{D_y R} \right)^{1/2} \quad (7-95)$$

Contrails

Remembering that

$$(\beta_1)^{1/2} = \mp \frac{\beta}{2}^{1/2} (1+i) \quad (7-96)$$

Substituting Eq. (7-96) into Eq. (7-95) we get

$$\delta_1^2 = \alpha^2 \frac{D_{xy}}{D_y} + \left(\frac{\alpha^2 l}{2D_y R} \right)^{1/2} + i \left(\frac{\alpha^2 l}{2D_y R} \right)^{1/2} \quad (7-97)$$

$$\delta_2^2 = \alpha^2 \frac{D_{xy}}{D_y} - \left(\frac{\alpha^2 l}{2D_y R} \right)^{1/2} - i \left(\frac{\alpha^2 l}{2D_y R} \right)^{1/2}$$

It can be verified that the square root of a number composed of a real part and an imaginary part can be written as

$$\left. \begin{aligned} (g+ih)^{1/2} &= \pm \sqrt{\frac{1}{2}} \left\{ [(g^2+h^2)^{1/2} + g]^{1/2} + i [(g^2+h^2)^{1/2} - g]^{1/2} \right\} \\ (g-ih)^{1/2} &= \pm \sqrt{\frac{1}{2}} \left\{ [(g^2+h^2)^{1/2} + g]^{1/2} - i [(g^2+h^2)^{1/2} - g]^{1/2} \right\} \end{aligned} \right\} \quad (7-98)$$

For convenience Eq. (7-97) can be rewritten as follows

$$\begin{aligned} \delta_1^2 &= a + ic \\ \delta_2^2 &= b - ic \end{aligned} \quad (7-99)$$

where

$$a = \alpha^2 \frac{D_{xy}}{D_y} + \left(\frac{\alpha^2 l}{2D_y R} \right)^{1/2}$$

$$b = \alpha^2 \frac{D_{xy}}{D_y} - \left(\frac{\alpha^2 l}{2D_y R} \right)^{1/2}$$

$$c = \left(\frac{\alpha^2 l}{2D_y R} \right)^{1/2}$$

Contrails

Comparing Eqs. (7-98) with (7-99) yields

$$\left. \begin{aligned}
 \delta_1 &= \sqrt{\frac{I}{2}} \left\{ [(a^2+c^2)^{\frac{1}{2}} + a]^{\frac{1}{2}} + i[(a^2+c^2)^{\frac{1}{2}} - a]^{\frac{1}{2}} \right\} \\
 \delta_2 &= -\sqrt{\frac{I}{2}} \left\{ [(a^2+c^2)^{\frac{1}{2}} + a]^{\frac{1}{2}} + i[(a^2+c^2)^{\frac{1}{2}} - a]^{\frac{1}{2}} \right\} \\
 \delta_3 &= \sqrt{\frac{I}{2}} \left\{ [(b^2+c^2)^{\frac{1}{2}} + b]^{\frac{1}{2}} - i[(b^2+c^2)^{\frac{1}{2}} - b]^{\frac{1}{2}} \right\} \\
 \delta_4 &= -\sqrt{\frac{I}{2}} \left\{ [(b^2+c^2)^{\frac{1}{2}} + b]^{\frac{1}{2}} - i[(b^2+c^2)^{\frac{1}{2}} - b]^{\frac{1}{2}} \right\}
 \end{aligned} \right\} \quad (7-100)$$

Let

$$\begin{aligned}
 \gamma_1 &= \sqrt{\frac{I}{2}} [(a^2+c^2)^{\frac{1}{2}} + a]^{\frac{1}{2}} \\
 \gamma_2 &= \sqrt{\frac{I}{2}} [(b^2+c^2)^{\frac{1}{2}} + b]^{\frac{1}{2}} \\
 \rho_1 &= \sqrt{\frac{I}{2}} [(a^2+c^2)^{\frac{1}{2}} - a]^{\frac{1}{2}} \\
 \rho_2 &= \sqrt{\frac{I}{2}} [(b^2+c^2)^{\frac{1}{2}} - b]^{\frac{1}{2}}
 \end{aligned} \quad (7-101)$$

Substituting Eqs. (7-101) into Eq. (7-100) gives the roots of the characteristic equation; then the roots are substituted into Eq. (7-91) yielding expression for $Y_m(y)$. After substituting $Y_m(y)$ into Eq. (7-89), one obtains the solution

$$\begin{aligned}
 (w+\gamma\varphi) &= (C_1 e^{(\gamma_1+i\rho_1)y} + C_2 e^{-(\gamma_1+i\rho_1)y} \\
 &\quad + C_3 e^{(\gamma_2-i\rho_2)y} + C_4 e^{-(\gamma_2-i\rho_2)y}) \sin \alpha x
 \end{aligned} \quad (7-102)$$

where

$$C_j = A_j + iB_j \quad j = (1,2,3,4)$$

Contrails

Further manipulation of Eq. (7-102) yields

$$\begin{aligned} w + \frac{1}{iL} \phi = & \{ [(A_1 \cosh \gamma_{1Y} + A_2 \sinh \gamma_{1Y}) \cos \rho_{1Y} \\ & + (A_3 \cosh \gamma_{1Y} + A_4 \sinh \gamma_{1Y}) \sin \rho_{1Y} \\ & + (A_5 \cosh \gamma_{2Y} + A_6 \sinh \gamma_{2Y}) \cos \rho_{2Y} \\ & + (A_7 \cosh \gamma_{2Y} + A_8 \sinh \gamma_{2Y}) \sin \rho_{2Y}] \sin \alpha x \\ & + i[A_1 \sinh \gamma_{1Y} + A_2 \cosh \gamma_{1Y}) \sin \rho_{1Y} \\ & - (A_3 \sinh \gamma_{1Y} + A_4 \cosh \gamma_{1Y}) \cos \rho_{1Y} \\ & - (A_5 \sinh \gamma_{2Y} + A_6 \cosh \gamma_{2Y}) \sin \rho_{2Y} \\ & + (A_7 \sinh \gamma_{2Y} + A_8 \cosh \gamma_{2Y}) \cos \rho_{2Y}] \sin \alpha x \} \end{aligned} \quad (7-103)$$

Eq. (7-103) yields the following expressions for "w" and "φ":

$$\begin{aligned} w = & [\cos \rho_{1Y} (A_{n1} \cosh \gamma_{1Y} + A_{n2} \sinh \gamma_{1Y}) \\ & + \sin \rho_{1Y} (A_{n3} \cosh \gamma_{1Y} + A_{n4} \sinh \gamma_{1Y}) \\ & + \cos \rho_{2Y} (A_{n5} \cosh \gamma_{2Y} + A_{n6} \sinh \gamma_{2Y}) \\ & + \sin \rho_{2Y} (A_{n7} \cosh \gamma_{2Y} + A_{n8} \sinh \gamma_{2Y})] \sin \alpha_n x \end{aligned} \quad (7-104)$$

$$\begin{aligned} \phi = & \left(\frac{t^4 E_x E_y}{12(1-\nu_x \nu_y)} \right)^{1/2} [- \sin \rho_{1Y} (A_{n1} \sinh \gamma_{1Y} + A_{n2} \cosh \gamma_{1Y}) \\ & + \cos \rho_{1Y} (A_{n3} \sinh \gamma_{1Y} + A_{n4} \cosh \gamma_{1Y}) \\ & + \sin \rho_{2Y} (A_{n5} \sinh \gamma_{2Y} + A_{n6} \cosh \gamma_{2Y}) \\ & - \cos \rho_{2Y} (A_{n7} \sinh \gamma_{2Y} + A_{n8} \cosh \gamma_{2Y})] \sin \alpha_n x \end{aligned} \quad (7-105)$$

D. A NAVIER-TYPE OF SOLUTION

A Navier-type solution is a special form which assumes that all edges are supported by "shear diaphragms"; i.e. the boundary conditions given by Eq. (2-21) apply. Consider a shallow, cylindrical shell whose planform dimensions are $a \times b$, having a cylindrical radius R . The boundary conditions are satisfied exactly by choosing

$$\left. \begin{aligned} w &= \sum_m \sum_n A_{m,n} \sin \alpha x \sin \beta y \\ \phi &= \sum_m \sum_n B_{m,n} \sin \alpha x \sin \beta y \end{aligned} \right\} \quad (7-106)$$

provided that the loading functions are also represented by compatible double sine series; i.e.,

$$\left. \begin{aligned} q &= \sum_m \sum_n a_{m,n} \sin \alpha x \sin \beta y \\ \Omega &= \sum_m \sum_n b_{m,n} \sin \alpha x \sin \beta y \\ T(x,y) &= \sum_{k=0,1}^N \sum_m \sum_n c_{k,m,n} \sin \alpha x \sin \beta y \end{aligned} \right\} \quad (7-107)$$

where

$$\left. \begin{aligned} \alpha &= \frac{m\pi}{a} & (m = 1, 2, \dots) \\ \beta &= \frac{n\pi}{b} & (n = 1, 2, \dots) \end{aligned} \right\} \quad (7-108)$$

Substituting Eqs. (7-106) and (7-107) into Eqs. (7-1) and (7-2) gives

$$\sum_n \sum_m \left[(\alpha^4 D_x + 2\alpha^2 \beta^2 D_{xy} + \beta^4 D_y) A_{mn} - \frac{\alpha^2}{R} B_{mn} \right] \sin \alpha x \sin \beta y$$

(7-109)

$$= \sum_n \sum_m \left[a_{mn} - \frac{b_{mn}}{R} + \sum_{k=1,3}^N \frac{(t/2)^{k+2}}{(k+2)} (\alpha^2 P_x + \beta^2 P_y) C_{kmn} \right] \sin \alpha x \sin \beta y$$

$$\sum_n \sum_m \left[(\alpha^4 F_x + 2\alpha^2 \beta^2 F_{xy} + \beta^4 F_y) B_{mn} + \frac{\alpha^2}{R} A_{mn} \right] \sin \alpha x \sin \beta y$$

$$= \sum_n \sum_m \left\{ \alpha^2 (1 - \nu_y) F_x + \beta^2 (1 - \nu_x) F_y \right\} b_{mn} + \frac{2}{t} \sum_{k=0,2}^N (\alpha^2 \alpha_x + \beta^2 \alpha_y) C_{kmn} \sin \alpha x \sin \beta y$$

(7-110)

which have a solution

$$A_{mn} = \frac{e_{22}\gamma_1 - e_{12}\gamma_2}{e_{11}e_{22} - e_{12}e_{21}} \quad (7-111)$$

$$B_{mn} = \frac{e_{11}\gamma_2 - e_{21}\gamma_1}{e_{11}e_{22} - e_{12}e_{21}} \quad (7-112)$$

where

$$e_{11} = \alpha^4 D_x + 2\alpha^2\beta^2 D_{xy} + \beta^4 D_y$$

$$e_{12} = -\frac{\alpha^2}{R}$$

$$e_{21} = \frac{\alpha^2}{R}$$

$$e_{22} = \alpha^4 F_x + 2\alpha^2\beta^2 F_{xy} + \beta^4 F_y$$

$$\gamma_1 = a_{mn} - \frac{b_{mn}}{R} + \sum_{k=1,3}^N \frac{(t/2)^{k+2}}{(k+2)} (\alpha^2 P_x + \beta^2 P_y) C_{kmn}$$

$$\gamma_2 = [\alpha^2(1-\nu_y)F_x + \beta^2(1-\nu_x)F_y] b_{mn} + \frac{2}{t} \sum_{k=0,2} (\alpha^2 \alpha_x + \beta^2 \alpha_y) C_{kmn}$$

Solution functions for slopes, membrane forces, bending and twisting moments, transverse shears, and displacements are

$$\frac{\partial w}{\partial x} = \sum_m \sum_n \alpha A_{mn} \cos \alpha x \sin \beta y \quad (7-113)$$

$$\frac{\partial w}{\partial y} = \sum_m \sum_n \beta A_{mn} \sin \alpha x \cos \beta y \quad (7-114)$$

$$N_x = \sum_m \sum_n (b_{mn} - \beta^2 B_{mn}) \sin \alpha x \sin \beta y \quad (7-115)$$

$$N_y = \sum_m \sum_n (b_{mn} - \alpha^2 B_{mn}) \sin \alpha x \sin \beta y \quad (7-116)$$

$$N_{xy} = -\sum_m \sum_n \alpha \beta \cos \alpha x \cos \beta y \quad (7-117)$$

$$M_x = D_x \left\{ \sum_m \sum_n \left[(\alpha^2 + \nu_y \beta^2) A_{mn} - \frac{24(\alpha_x + \nu_y \alpha_x)}{t^3} \sum_{k=1,3}^N \frac{(t/2)^{k+2}}{(k+2)} C_{kmn} \right] \sin \alpha x \sin \beta y \right\} \quad (7-118)$$

$$M_y = D_y \left\{ \sum_m \sum_n \left[(\nu_x \alpha^2 + \beta^2) A_{mn} - \frac{24(\alpha_y + \nu_x \alpha_x)}{t^3} \sum_{k=1,3}^N \frac{(t/2)^{k+2}}{(k+2)} C_{kmn} \right] \sin \alpha x \sin \beta y \right\} \quad (7-119)$$

$$M_{xy} = \frac{2t^3 G}{12} \left[\sum_m \sum_n \alpha \beta A_{mn} \cos \alpha x \cos \beta y \right] \quad (7-120)$$

$$Q_x = D_x \left\{ \sum_m \sum_n \left[(\alpha^3 + \nu_y \alpha \beta^2 + \frac{2t^3 G}{12 D_x} \alpha \beta^2) A_{mn} - \frac{24(\alpha_x + \nu_y \alpha_x)}{t^3} \sum_{k=1,3}^N \frac{(t/2)^{k+2}}{(k+2)} \alpha C_{kmn} \right] \cos \alpha x \sin \beta y \right\} \quad (7-121)$$

$$Q_y = D_y \left\{ \sum_m \sum_n \left[(\nu_x \alpha^2 \beta + \frac{2t^3 G}{12 D_y} \alpha^2 \beta + \beta^3) A_{mn} - \frac{24(\alpha_y + \nu_x \alpha_x)}{t^3} \sum_{k=1,3}^N \frac{(t/2)^{k+2}}{(k+2)} \beta C_{kmn} \right] \sin \alpha x \cos \beta y \right\} \quad (7-122)$$

$$u = \frac{1}{t} \left\{ \sum_m \sum_n \frac{1}{\alpha E_x} \left[(1 - \nu_x) b_{mn} - (\beta^2 - \nu_x \alpha^2) B_{mn} + 2E_x \alpha_x \sum_{k=0,2}^N \frac{(t/2)^{k+1}}{(k+1)} C_{kmn} \right] \cos \alpha x \sin \beta y \right\} \quad (7-123)$$

$$v = \frac{1}{t} \left(\sum_m \sum_n \left\{ \frac{A_{mn}}{\beta R} - \frac{1}{\beta E_y} \left[(1 - \nu_y) b_{mn} - (\alpha^2 - \nu_y \beta^2) B_{mn} + 2E_y \alpha_y \sum_{k=0,2}^N \frac{(t/2)^{k+1}}{(k+1)} C_{kmn} \right] \right\} \sin \alpha x \cos \beta y \right) \quad (7-124)$$

Contrails

It should be noted that the Navier type solution given above is a particular solution for the governing differential equations (7-1) and (7-2) and, as such, can be used in Eqs. (7-4) for this purpose.

E. A VOIGT-LEVY TYPE OF SOLUTION

This special method of solution is well known in the literature of vibrating (Ref. 34) and statically loaded (Ref. 35) plates. We shall here discuss the fundamental assumptions of the method and the method of determining the roots of the resulting characteristic equation.

Consider the case when only one of parallel edges has the shear diaphragm support conditions defined by Eqs. (2-21). If the curved edges $x = 0, a$, (see Fig. 18) are supported by shear diaphragms, then we can express an auxiliary function $\psi(x,y)$ in the form

$$\psi(x,y) = \sum_{m=1}^{\infty} F_m(y) \sin \alpha x \quad (7-125)$$

where

$$\alpha = \frac{n\pi}{a}, \quad n = 1, 2, \dots$$

substituting the expression for $\psi(x,y)$ given by Eq. (7-125) into Eq. (7-10) we obtain the following ordinary differential equation

$$\begin{aligned} P_5 \frac{\partial^8 F_m(y)}{\partial y^8} - \alpha^2 P_4 \frac{\partial^6 F_m(y)}{\partial y^6} + \alpha^4 P_3 \frac{\partial^4 F_m(y)}{\partial y^4} \\ - \alpha^6 P_2 \frac{\partial^2 F_m(y)}{\partial y^2} + \alpha^2 (\alpha^4 P_1 + P_6) F_m(y) = 0 \end{aligned} \quad (7-126)$$

We seek a solution of Eq. (7-126) in the form

$$F_m(y) = A e^{\tau y} \quad (7-127)$$

substituting Eq. (7-127) into Eq. (7-126), τ can be determined from the characteristic equation

$$P_5 \tau^8 - \alpha^2 P_4 \tau^6 + \alpha^4 P_3 \tau^4 - \alpha^6 P_2 \tau^2 + \alpha^2 (\alpha^4 P_1 + P_6) = 0 \quad (7-128)$$

Contrails

Some of the roots of Eq. (7-128) are zero for the case of $\alpha = 0$ which have no significance. A procedure for obtaining the roots of Eq. (7-128) is given in Ref. [36], where it was shown that the roots can be written as follows

$$\left. \begin{aligned} \tau_1 = -\tau_3 &= \zeta_1 + i\eta_1 \\ \tau_2 = -\tau_4 &= \zeta_1 - i\eta_1 \\ \tau_5 = -\tau_7 &= \zeta_2 + i\eta_2 \\ \tau_6 = -\tau_8 &= \zeta_2 - i\eta_2 \end{aligned} \right\} \quad (7-129)$$

Goldenveizer, [21] in his analysis of open cylindrical shells, studied the properties of the roots of a similar characteristic equation. No effort is made here to reproduce a corresponding analysis, however the reader is referred to Ref. [21], pp. 249-259 and 296-300 for relevant information.

Contrails

REFERENCES

1. Slater, J. C., "Electron Energy Bands in Metals," *Physical Review*, Vol. 45, 1934, pp. 794-801.
2. Barta, J., "On the Numerical Solution of a Two Dimensional Elasticity Problem," *Zeitschrift für Angewandte Mathematik und Mechanik*, Vol. 7, No. 3, 1937, pp. 184-185.
3. Conway, H. D., "The Approximate Analysis of Certain Boundary Value Problems," *Journal of Applied Mechanics*, Vol. 27, 1960, pp. 275-277.
4. Conway, H. D. and Leissa, A. W., "A Method for Investigating Buckling of Plates and Certain Other Eigenvalue Problems," *Journal of Applied Mechanics*, Vol. 27, 1960, pp. 557-558.
5. Niedenfuhr, F. W. and Leissa, A. W., "The Torsion of Prismatic Bars of Regular Polygonal Cross Section," *Journal of the Aero/Space Sciences*, Vol. 29, 1961, pp. 424-426.
6. Leissa, A. W. and Niedenfuhr, F. W., "A Study of the Cantilevered Square Plate Subjected to a Uniform Loading," *Journal of the Aero/Space Sciences*, Vol. 29, 1962, pp. 162-169.
7. Leissa, A. W., "A Method for Analyzing the Vibrations of Plates," *Journal of the Aero/Space Sciences*, Vol. 30, 1962, p. 475.
8. Leissa, A. W. and Clausen, W. E., "Application of Point Matching to Problems in Micromechanics," Fundamental Aspects of Fiber Reinforced Plastic Composites, edited by Schwartz and Schwartz, John Wiley and Sons, 1968, pp. 29-44.
9. Niedenfuhr, F. W., Leissa, A. W., and Lo, C. C. "A Study of the Point Matching Method as Applied to Thermally and Transversely Loaded Plates and Other Boundary Value Problems," *Technical Report No. AFFDL-TR-64-159*, October, 1964.
10. Lo, C. C., Niedenfuhr, F. W., and Leissa, A. W., "Further Studies in the Application of the Point Matching Technique to Plate Bending and Other Harmonic and Biharmonic Boundary Value Problems," *Technical Report, Contract No. AF 33(657)-8772*, June, 1965.
11. Leissa, A. W., "Investigation of the Utilization of the Point Matching Technique for the Solution of Various Boundary Value Problems," *Final Technical Report, Contract AF33(615)-2504*, October, 1966.
12. Conway, H. D. and Leissa, A. W., "Application of the Point Matching Method to Shallow Spherical Shell Theory," *Journal of Applied Mechanics*, Vol. 29, 1962, pp. 745-747.

Contrails

13. Clausen, W. E. and Leissa, A. W., "Stress Coupling Between Holes in Shallow Spherical Shells," Proceedings, Symposium of the International Association for Shell Structures, Leningrad, 1966.
14. Reissner, E., "Stress and Displacements of Shallow Spherical Shells," Journal of Mathematics and Physics, Part I, Vol. 25, 1946, pp. 80-85, Part II, Vol. 26, 1947, pp. 279-300.
15. Reissner, E., "On the Determination of Stresses and Displacements for Unsymmetrical Deformations of Shallow Spherical Shells," Journal of Mathematics and Physics, Vol. 38, 1959, pp. 16-35.
16. Neidenfuhr, F. W., Leissa, A. W., and Gaitens, M. J., "A Method of Analysis for Shallow Shells of Revolution Supported Elastically on Concentric Rings," Developments in Theoretical and Applied Mechanics, Vol. II, Pergamon Press, 1965.
17. Leissa, A. W. and Brann, J. H., "On the Torsion of Bars Having Symmetry Axes," International Journal of Mechanical Sciences, 1964, pp. 45-50.
18. Leissa, A. W., Hulbert, L. E., Hopper, A. T., and Clausen, W. E., "A Comparison of Approximate Methods for the Solution of Plate Bending Problems," Proceedings of the AIAA/ASME Ninth Structures, Structural Dynamics and Materials Conference, Palm Springs, Calif., April 1-3, 1968.
19. Vlasov, V. Z., General Theory of Shells and It's Application in Engineering, NASA Technical Translation, F-99, (1964).
20. Ambartsumyan, S. A., Theory of Anisotropic Shells, NASA Technical Translation, F-118, (1964).
21. Goldenveizer, A. L., Theory of Elastic Thin Shells, Pergamon Press, New York, (1961).
22. Leissa, A. W., "Utilization of the Point Matching Technique for Structural Shell Analysis," Quarterly Report No. 4, Contract No. F33615-67-C-1177, The Ohio State University Research Foundation, January 16, 1968. (Defense Documentation Number AD 684 173)
23. McLachlan, N. W., Bessel Functions for Engineers, Oxford University Press, Amen House, London, England, (1961).
24. Leissa, A. W., Lo, C. C., and Neidenfuhr, F. W., "Uniformly Loaded Plates of Regular Polygonal Shape," American Institute of Aeronautics and Astronautics Journal, Vol. 3, No. 3, pp. 566-567, March, 1965.
25. Love, A. E. H., A Treatise on the Mathematical Theory of Elasticity, Dover Publications, Inc. New York, (1944).

Contrails

26. Novozhilov, N. V., Thin Shell Theory, P. Noordhoff Lts, Groningen, The Netherlands, (1964).
27. Donnell, L. H., Stability of Thin Walled Tubes under Torsion, NACA Rep. 479, (1934).
28. Nazarov, A. A., On the Theory of Thin Shallow Shells, NACA Technical Memorandum 1426, (1956).
29. Flügge, W., Stresses in Shells, Springer-Verlag OHG, Berlin, (1962).
30. Ambartsumyan, S. A., On the Theory of Anisotropic Shallow Shells, NASA Technical Memorandum 1424, (1956).
31. Lekhnitskii, S. G., Theory of Elasticity of an Anisotropic Elastic Body, Holden-Day, Inc., San Francisco, (1963).
32. Savin, G. N., Stress Concentration Around Holes, Pergamon Press, New York, (1961).
33. Mishonov, M., On the Theory of Shallow Shells, P.M.M.: Journal of Applied Mathematics and Mechanics 22, 5, 972-979, (1958), Pergamon Press, Long Island City, N.Y.
34. Voigt, W., "Bemerkungen zu dem Problem der transversalen Schwingungen rechteckiger Platten." der Wissenschaftler, Gottingen, No. 6, 1893, pp. 225-230.
35. Levy, M., Compt. Rend., Vol. 129, 1899, pp. 535-539.
36. ASCE - Manuals of Engineering Practice - No. 31, Design of Cylindrical Concrete Shell Roofs, American Society of Civil Engineers, New York, (1952).

Contrails

APPENDIX A

EXPLICIT EQUATIONS FOR SLOPES, BENDING MOMENTS,
SHEARING FORCES, MEMBRANE FORCES AND TANGENTIAL
DISPLACEMENTS FOR ISOTROPIC SHALLOW SPHERICAL SHELLS

Contrails

Contrails

$$\begin{aligned}
 \frac{\partial W}{\partial n} = \frac{1}{\lambda} \left\{ & (C_{03} \text{ber}'x + C_{04} \text{bei}'x + C_{05} \text{ker}'x \right. \\
 & \left. + C_{06} \text{kei}'x) \cos \phi \right. \\
 & + \sum_{n=1}^{\infty} n C_{n1} x^{n-1} \cos(n\theta + \phi) - n C_{n2} x^{-(n+1)} \cos(n\theta - \phi) \\
 & - C_{n3} \left[\frac{1}{\sqrt{2}} (\text{ber}_{n-1} x + \text{bei}_{n-1} x) \cos n\theta \cos \phi + \frac{n \text{ber}_n x}{x} \cos(n\theta - \phi) \right] \\
 & + C_{n4} \left[\frac{1}{\sqrt{2}} (\text{ber}_{n-1} x - \text{bei}_{n-1} x) \cos n\theta \cos \phi - \frac{n \text{bei}_n x}{x} \cos(n\theta - \phi) \right] \\
 & - C_{n5} \left[\frac{1}{\sqrt{2}} (\text{ker}_{n-1} x + \text{kei}_{n-1} x) \cos n\theta \cos \phi + \frac{n \text{ker}_n x}{x} \cos(n\theta - \phi) \right] \\
 & + C_{n6} \left[\frac{1}{\sqrt{2}} (\text{ker}_{n-1} x - \text{kei}_{n-1} x) \cos n\theta \cos \phi - \frac{n \text{kei}_n x}{x} \cos(n\theta - \phi) \right] \\
 & + n \bar{C}_{n1} x^{n-1} \sin(n\theta + \phi) - n \bar{C}_{n2} x^{-(n+1)} \sin(n\theta - \phi) \\
 & - \bar{C}_{n3} \left[\frac{1}{\sqrt{2}} (\text{ber}_{n-1} x + \text{bei}_{n-1} x) \sin n\theta \cos \phi + \frac{n \text{ber}_n x}{x} \sin(n\theta - \phi) \right] \\
 & + \bar{C}_{n4} \left[\frac{1}{\sqrt{2}} (\text{ber}_{n-1} x - \text{bei}_{n-1} x) \sin n\theta \cos \phi - \frac{n \text{bei}_n x}{x} \sin(n\theta - \phi) \right] \\
 & - \bar{C}_{n5} \left[\frac{1}{\sqrt{2}} (\text{ker}_{n-1} x + \text{kei}_{n-1} x) \sin n\theta \cos \phi + \frac{n \text{ker}_n x}{x} \sin(n\theta - \phi) \right] \\
 & \left. + \bar{C}_{n6} \left[\frac{1}{\sqrt{2}} (\text{ker}_{n-1} x - \text{kei}_{n-1} x) \sin n\theta \cos \phi - \frac{n \text{kei}_n x}{x} \sin(n\theta - \phi) \right] \right\}
 \end{aligned}$$

Contrails

M_n (p.1 of 4)

$$\begin{aligned}
 M_n = & -\frac{D}{k^2} \left\{ C_{03} \left(-\left(\frac{1+\nu}{2}\right) \text{ber} i x - \left(\frac{1-\nu}{2}\right) \left(\text{bei} x + \frac{2 \text{ber}' x}{x} \right) \cos 2\phi \right) \right. \\
 & + C_{04} \left(\left(\frac{1+\nu}{2}\right) \text{ber} x + \left(\frac{1-\nu}{2}\right) \left(\text{ber} x - \frac{2 \text{bei}' x}{x} \right) \cos 2\phi \right) \\
 & + C_{05} \left(-\left(\frac{1+\nu}{2}\right) \text{ker} i x - \left(\frac{1-\nu}{2}\right) \left(\text{kei} x + \frac{2 \text{ker}' x}{x} \right) \cos 2\phi \right) \\
 & + C_{06} \left(\left(\frac{1+\nu}{2}\right) \text{ker} x + \left(\frac{1-\nu}{2}\right) \left(\text{ker} x - \frac{2 \text{kei}' x}{x} \right) \cos 2\phi \right) \\
 & + C_{13} \left(-\left(\frac{1+\nu}{2\sqrt{2}}\right) (\text{ber}' x + \text{bei}' x) \cos \theta \right. \\
 & \quad - \left(\frac{1-\nu}{2\sqrt{2}}\right) (\text{ber}' x + \text{bei}' x) \cos \theta \cos 2\phi \\
 & \quad + \left(\frac{1-\nu}{\sqrt{2}}\right) \left(\left(\frac{\text{ber} x + \text{bei} x}{x}\right) + 2 \left(\frac{\text{ber}' x - \text{bei}' x}{x^2}\right) \right) \cos(\theta - 2\phi) \Big) \\
 & + C_{14} \left(\left(\frac{1+\nu}{2\sqrt{2}}\right) (\text{ber}' x - \text{bei}' x) \cos \theta \right. \\
 & \quad + \left(\frac{1-\nu}{2\sqrt{2}}\right) (\text{ber}' x - \text{bei}' x) \cos \theta \cos 2\phi \\
 & \quad - \left(\frac{1-\nu}{\sqrt{2}}\right) \left(\left(\frac{\text{ber} x - \text{bei} x}{x}\right) - 2 \left(\frac{\text{ber}' x + \text{bei}' x}{x^2}\right) \right) \cos(\theta - 2\phi) \Big) \\
 & + C_{15} \left(-\left(\frac{1+\nu}{2\sqrt{2}}\right) (\text{ker}' x + \text{kei}' x) \cos \theta \right. \\
 & \quad - \left(\frac{1-\nu}{2\sqrt{2}}\right) (\text{ker}' x + \text{kei}' x) \cos \theta \cos 2\phi \\
 & \quad + \left(\frac{1-\nu}{\sqrt{2}}\right) \left(\left(\frac{\text{ker} x + \text{kei} x}{x}\right) + 2 \left(\frac{\text{ker}' x - \text{kei}' x}{x^2}\right) \right) \cos(\theta - 2\phi) \Big) \\
 & + C_{16} \left(\left(\frac{1+\nu}{2\sqrt{2}}\right) (\text{ker}' x - \text{kei}' x) \cos \theta \right. \\
 & \quad + \left(\frac{1-\nu}{2\sqrt{2}}\right) (\text{ker}' x - \text{kei}' x) \cos \theta \cos 2\phi \\
 & \quad - \left(\frac{1-\nu}{\sqrt{2}}\right) \left(\left(\frac{\text{ker} x - \text{kei} x}{x}\right) - 2 \left(\frac{\text{ker}' x + \text{kei}' x}{x^2}\right) \right) \cos(\theta - 2\phi) \Big)
 \end{aligned}$$

Contrails

M_n (p.2 of 4)

$$\begin{aligned}
 & + \bar{C}_{13} \left(-\left(\frac{1+\nu}{2\sqrt{2}}\right) (\text{ber}'x + \text{bei}'x) \sin \theta \right. \\
 & \quad \left. - \left(\frac{1-\nu}{2\sqrt{2}}\right) (\text{ber}'x + \text{bei}'x) \sin \theta \cos 2\phi \right. \\
 & \quad \left. + \left(\frac{1-\nu}{\sqrt{2}}\right) \left(\left(\frac{\text{bei}x + \text{ber}x}{x}\right) + 2\left(\frac{\text{ber}'x - \text{bei}'x}{x^2}\right) \right) \sin(\theta - 2\phi) \right) \\
 & + \bar{C}_{14} \left(\left(\frac{1+\nu}{2\sqrt{2}}\right) (\text{ber}'x - \text{bei}'x) \sin \theta \right. \\
 & \quad \left. + \left(\frac{1-\nu}{2\sqrt{2}}\right) (\text{ber}'x - \text{bei}'x) \sin \theta \cos 2\phi \right. \\
 & \quad \left. - \left(\frac{1-\nu}{\sqrt{2}}\right) \left(\left(\frac{\text{ber}x - \text{bei}x}{x}\right) - 2\left(\frac{\text{ber}'x + \text{bei}'x}{x^2}\right) \right) \sin(\theta - 2\phi) \right) \\
 & + \bar{C}_{15} \left(-\left(\frac{1+\nu}{2\sqrt{2}}\right) (\text{ker}'x + \text{kei}'x) \sin \theta \right. \\
 & \quad \left. - \left(\frac{1-\nu}{2\sqrt{2}}\right) (\text{ker}'x + \text{kei}'x) \sin \theta \cos 2\phi \right. \\
 & \quad \left. + \left(\frac{1-\nu}{\sqrt{2}}\right) \left(\left(\frac{\text{ker}x + \text{kei}x}{x}\right) + 2\left(\frac{\text{ker}'x - \text{kei}'x}{x^2}\right) \right) \sin(\theta - 2\phi) \right) \\
 & + \bar{C}_{16} \left(\left(\frac{1+\nu}{2\sqrt{2}}\right) (\text{ker}'x - \text{kei}'x) \sin \theta \right. \\
 & \quad \left. + \left(\frac{1-\nu}{2\sqrt{2}}\right) (\text{ker}'x - \text{kei}'x) \sin \theta \cos 2\phi \right. \\
 & \quad \left. - \left(\frac{1-\nu}{\sqrt{2}}\right) \left(\left(\frac{\text{ker}x - \text{kei}x}{x}\right) - 2\left(\frac{\text{ker}'x + \text{kei}'x}{x^2}\right) \right) \sin(\theta - 2\phi) \right) \\
 & + \sum_{n=2}^{\infty} \left[C_{n1} \left((1-\nu)(n)(n-1)x^{n-2} \cos(n\theta + 2\phi) \right) \right. \\
 & \quad \left. + C_{n2} \left((1-\nu)(n)(n+1)x^{-(n+2)} \cos(n\theta - 2\phi) \right) \right. \\
 & \quad \left. + C_{n3} \left(\left(\frac{1+\nu}{2}\right) (\text{bei}_{n-2}x + \frac{\sqrt{2}(n-1)}{x} (\text{ber}_{n-1}x + \text{bei}_{n-1}x)) \cos n\theta \right. \right. \\
 & \quad \left. \left. + \left(\frac{1-\nu}{2}\right) \text{bei}_{n-2}x \cos n\theta \cos 2\phi \right. \right. \\
 & \quad \left. \left. + (1-\nu) \left(\frac{n}{\sqrt{2}x} (\text{ber}_{n-1}x + \text{bei}_{n-1}x) + \frac{n(n+1)}{x^2} \text{ber}_n x \right) \cos(n\theta - 2\phi) \right) \right]
 \end{aligned}$$

Contrails

M_n (p.3 of 4)

$$\begin{aligned}
 & + C_{n4} \left(\left(\frac{1+\nu}{2} \right) \left(-ber_{n-2} x + \frac{\sqrt{2}(n-1)}{x} (bei_{n-1} x - ber_{n-1} x) \right) \cos n\theta \right. \\
 & \quad + \left(\frac{1-\nu}{2} \right) (-ber_{n-2} x) \cos n\theta \cos 2\phi \\
 & \quad \left. + (1-\nu) \left(\frac{n}{\sqrt{2}x} (bei_{n-1} x - ber_{n-1} x) + \frac{n(n+1)}{x^2} bei_n x \right) \cos(n\theta - 2\phi) \right) \\
 & + C_{n5} \left(\left(\frac{1+\nu}{2} \right) \left(keri_{n-2} x + \frac{\sqrt{2}(n-1)}{x} (ker_{n-1} x + kei_{n-1} x) \right) \cos n\theta \right. \\
 & \quad + \left(\frac{1-\nu}{2} \right) keri_{n-2} x \cos n\theta \cos 2\phi \\
 & \quad \left. + (1-\nu) \left(\frac{n}{\sqrt{2}x} (ker_{n-1} x + kei_{n-1} x) + \frac{n(n+1)}{x^2} ker_n x \right) \cos(n\theta - 2\phi) \right) \\
 & + C_{n6} \left(\left(\frac{1+\nu}{2} \right) \left(-ker_{n-2} x + \frac{\sqrt{2}(n-1)}{x} (kei_{n-1} x - ker_{n-1} x) \right) \cos n\theta \right. \\
 & \quad + \left(\frac{1-\nu}{2} \right) (-ker_{n-2} x) \cos n\theta \cos 2\phi \\
 & \quad \left. + (1-\nu) \left(\frac{n}{\sqrt{2}x} (kei_{n-1} x - ker_{n-1} x) + \frac{n(n+1)}{x^2} kei_n x \right) \cos(n\theta - 2\phi) \right) \\
 & + \sum_{n=2}^{\infty} \bar{C}_{n1} \left((1-\nu)(n)(n-1)x^{n-2} \sin(n\theta + 2\phi) \right) \\
 & \quad + \bar{C}_{n2} \left((1-\nu)(n)(n+1)x^{-(n+2)} \sin(n\theta - 2\phi) \right) \\
 & + \bar{C}_{n3} \left(\left(\frac{1+\nu}{2} \right) \left(bei_{n-2} x + \frac{\sqrt{2}(n-1)}{x} (ber_{n-1} x + bei_{n-1} x) \right) \sin n\theta \right. \\
 & \quad + \left(\frac{1-\nu}{2} \right) (bei_{n-2} x) \sin n\theta \cos 2\phi \\
 & \quad \left. + (1-\nu) \left(\frac{n}{\sqrt{2}x} (ber_{n-1} x + bei_{n-1} x) + \frac{n(n+1)}{x^2} ber_n x \right) \sin(n\theta - 2\phi) \right) \\
 & + \bar{C}_{n4} \left(\left(\frac{1+\nu}{2} \right) \left(-ber_{n-2} x + \frac{\sqrt{2}(n-1)}{x} (bei_{n-1} x - ber_{n-1} x) \right) \sin n\theta \right. \\
 & \quad + \left(\frac{1-\nu}{2} \right) (-ber_{n-2} x) \sin n\theta \cos 2\phi \\
 & \quad \left. + (1-\nu) \left(\frac{n}{\sqrt{2}x} (bei_{n-1} x - ber_{n-1} x) + \frac{n(n+1)}{x^2} bei_n x \right) \sin(n\theta - 2\phi) \right)
 \end{aligned}$$

Contrails

M_n (p.4 of 4)

$$\begin{aligned}
 & + \bar{C}_{n5} \left(\left(\frac{1+\nu}{2} \right) \chi \operatorname{Re} i_{n-2} x + \frac{\sqrt{2}(n-1)}{x} (\operatorname{Re} r_{n-1} x + \operatorname{Re} i_{n-1} x) \right) \sin n\theta \\
 & \quad + \left(\frac{1-\nu}{2} \right) \chi \operatorname{Re} i_{n-2} x \sin n\theta \cos 2\phi \\
 & \quad + (1-\nu) \left(\frac{n}{\sqrt{2}x} (\operatorname{Re} r_{n-1} x + \operatorname{Re} i_{n-1} x) + \frac{n(n+1)}{x^2} \operatorname{Re} r_n x \right) \sin(n\theta - 2\phi) \\
 & + \bar{C}_{n6} \left(\left(\frac{1+\nu}{2} \right) \chi (-\operatorname{Re} r_{n-2} x + \frac{\sqrt{2}(n-1)}{x} (\operatorname{Re} i_{n-1} x - \operatorname{Re} r_{n-1} x)) \right) \sin n\theta \\
 & \quad + \left(\frac{1-\nu}{2} \right) \chi (-\operatorname{Re} r_{n-2} x) \sin n\theta \cos 2\phi \\
 & \quad + (1-\nu) \left(\frac{n}{\sqrt{2}x} (\operatorname{Re} i_{n-1} x - \operatorname{Re} r_{n-1} x) + \frac{n(n+1)}{x^2} \operatorname{Re} i_n x \right) \sin(n\theta - 2\phi) \Big\}
 \end{aligned}$$

For M_t Replace ϕ by $(\phi + \frac{\pi}{2})$

Contrails

M_{nt} (p.1 of 3)

$$\begin{aligned}
 M_{nt} = & \frac{-D(1-\bar{\nu})}{l^2} \left\{ C_{03} \left(\left(\frac{ber'x}{2} + \frac{ber'x}{x} \right) \sin 2\phi \right) \right. \\
 & - C_{04} \left(\left(\frac{berx}{2} - \frac{bei'x}{x} \right) \sin 2\phi \right) + C_{05} \left(\left(\frac{ker'x}{2} + \frac{ker'x}{x} \right) \sin 2\phi \right) \\
 & - C_{06} \left(\left(\frac{kerx}{2} - \frac{kei'x}{x} \right) \sin 2\phi \right) + C_{12} \left(\frac{2}{x^3} \sin(\theta - 2\phi) \right) \\
 & + C_{13} \left(\frac{1}{2\sqrt{2}} (ber'x + bei'x) \cos \theta \sin 2\phi \right. \\
 & \quad \left. + \frac{1}{\sqrt{2}} \left(\left(\frac{berx + bei'x}{x} \right) + 2 \left(\frac{ber'x - bei'x}{x^2} \right) \right) \sin(\theta - 2\phi) \right) \\
 & + C_{14} \left(-\frac{1}{2\sqrt{2}} (ber'x - bei'x) \cos \theta \sin 2\phi \right. \\
 & \quad \left. - \frac{1}{\sqrt{2}} \left(\left(\frac{berx - bei'x}{x} \right) - 2 \left(\frac{ber'x + bei'x}{x^2} \right) \right) \sin(\theta - 2\phi) \right) \\
 & + C_{15} \left(\frac{1}{2\sqrt{2}} (ker'x + kei'x) \cos \theta \sin 2\phi \right. \\
 & \quad \left. + \frac{1}{\sqrt{2}} \left(\left(\frac{kerx + kei'x}{x} \right) + 2 \left(\frac{ker'x - kei'x}{x^2} \right) \right) \sin(\theta - 2\phi) \right) \\
 & + C_{16} \left(-\frac{1}{2\sqrt{2}} (ker'x - kei'x) \cos \theta \sin 2\phi \right. \\
 & \quad \left. - \frac{1}{\sqrt{2}} \left(\left(\frac{kerx - kei'x}{x} \right) - 2 \left(\frac{ker'x + kei'x}{x^2} \right) \right) \sin(\theta - 2\phi) \right) \\
 & - \bar{C}_{12} \left(\frac{2}{x^3} \cos(\theta - 2\phi) \right) \\
 & + \bar{C}_{13} \left(\frac{1}{2\sqrt{2}} (ber'x + bei'x) \sin \theta \sin 2\phi \right. \\
 & \quad \left. - \frac{1}{\sqrt{2}} \left(\left(\frac{berx + bei'x}{x} \right) + 2 \left(\frac{ber'x - bei'x}{x^2} \right) \right) \cos(\theta - 2\phi) \right) \\
 & + \bar{C}_{14} \left(-\frac{1}{2\sqrt{2}} (ber'x - bei'x) \sin \theta \sin 2\phi \right. \\
 & \quad \left. + \frac{1}{\sqrt{2}} \left(\left(\frac{berx - bei'x}{x} \right) - 2 \left(\frac{ber'x + bei'x}{x^2} \right) \right) \cos(\theta - 2\phi) \right)
 \end{aligned}$$

Contrails

M_{nt} (p.2 of 3)

$$\begin{aligned}
 & + \bar{C}_{15} \left(\frac{1}{2\sqrt{2}} (ker'x + kei'x) \sin\theta \sin 2\phi \right. \\
 & \quad \left. - \frac{1}{\sqrt{2}} \left(\left(\frac{kerx + keix}{x} \right) + 2 \left(\frac{ker'x - kei'x}{x^2} \right) \right) \cos(\theta - 2\phi) \right) \\
 & + \bar{C}_{16} \left(-\frac{1}{2\sqrt{2}} (ker'x - kei'x) \sin\theta \sin 2\phi \right. \\
 & \quad \left. + \frac{1}{\sqrt{2}} \left(\left(\frac{kerx - keix}{x} \right) - 2 \left(\frac{ker'x + kei'x}{x^2} \right) \right) \cos(\theta - 2\phi) \right) \\
 & + \sum_{n=2}^{\infty} \left[-C_{n1} (n(n-1)x^{n-2} \sin(n\theta + 2\phi)) \right. \\
 & \quad \left. + C_{n2} (n(n+1)x^{-(n+2)} \sin(n\theta - 2\phi)) \right. \\
 & \quad + C_{n3} \left(-\frac{1}{2} bei_{n-2} x \cos n\theta \sin 2\phi \right. \\
 & \quad \left. + \left(\frac{n}{\sqrt{2}} x (ber_{n-1} x + bei_{n-1} x) + \frac{n(n+1)}{x^2} ber_n x \right) \sin(n\theta - 2\phi) \right) \\
 & \quad + C_{n4} \left(\frac{1}{2} ber_{n-2} x \cos n\theta \sin 2\phi \right. \\
 & \quad \left. + \left(\frac{n}{\sqrt{2}} x (bei_{n-1} x - ber_{n-1} x) + \frac{n(n+1)}{x^2} bei_n x \right) \sin(n\theta - 2\phi) \right) \\
 & \quad + C_{n5} \left(-\frac{1}{2} kei_{n-2} x \cos n\theta \sin 2\phi \right. \\
 & \quad \left. + \left(\frac{n}{\sqrt{2}} x (ker_{n-1} x + kei_{n-1} x) + \frac{n(n+1)}{x^2} ker_n x \right) \sin(n\theta - 2\phi) \right) \\
 & \quad \left. + C_{n6} \left(\frac{1}{2} ker_{n-2} x \cos n\theta \sin 2\phi \right. \right. \\
 & \quad \left. \left. + \left(\frac{n}{\sqrt{2}} x (kei_{n-1} x - ker_{n-1} x) + \frac{n(n+1)}{x^2} kei_n x \right) \sin(n\theta - 2\phi) \right) \right] \\
 & + \sum_{n=2}^{\infty} \left[\bar{C}_{n1} (n(n-1)x^{n-2} \cos(n\theta + 2\phi)) \right. \\
 & \quad \left. - \bar{C}_{n2} (n(n+1)x^{-(n+2)} \cos(n\theta - 2\phi)) \right]
 \end{aligned}$$

Contrails

M_{nt} (p.3 of 3)

$$\begin{aligned} & + \bar{c}_{n3} \left(-\frac{1}{2} \text{bei}_{n-2} x \text{Sin} n\theta \text{Sin} 2\phi \right. \\ & \quad \left. - \left(\frac{n}{\sqrt{2}x} (\text{ber}_{n-1} x + \text{bei}_{n-1} x) + \frac{n(n+1)}{x^2} \text{ber}_n x \right) \text{Cos}(n\theta - 2\phi) \right) \\ & + \bar{c}_{n4} \left(\frac{1}{2} \text{ber}_{n-2} x \text{Sin} n\theta \text{Sin} 2\phi \right. \\ & \quad \left. - \left(\frac{n}{\sqrt{2}x} (\text{bei}_{n-1} x - \text{ber}_{n-1} x) + \frac{n(n+1)}{x^2} \text{bei}_n x \right) \text{Cos}(n\theta - 2\phi) \right) \\ & + \bar{c}_{n5} \left(-\frac{1}{2} \text{kei}_{n-2} x \text{Sin} n\theta \text{Sin} 2\phi \right. \\ & \quad \left. - \left(\frac{n}{\sqrt{2}x} (\text{ker}_{n-1} x + \text{kei}_{n-1} x) + \frac{n(n+1)}{x^2} \text{ker}_n x \right) \text{Cos}(n\theta - 2\phi) \right) \\ & + \bar{c}_{n6} \left(\frac{1}{2} \text{ker}_{n-2} x \text{Sin} n\theta \text{Sin} 2\phi \right. \\ & \quad \left. - \left(\frac{n}{\sqrt{2}x} (\text{kei}_{n-1} x - \text{ker}_{n-1} x) + \frac{n(n+1)}{x^2} \text{kei}_n x \right) \text{Cos}(n\theta - 2\phi) \right) \} \end{aligned}$$

Contrails

Q_n (p.1 of 3)

$$\begin{aligned}
 Q_n = & -\frac{D}{l^3} \left[-C_{03} \text{bei}'x \cos \phi + C_{04} \text{ber}'x \cos \phi \right. \\
 & - C_{05} \text{kei}'x \cos \phi + C_{06} \text{ker}'x \cos \phi \\
 & + C_{13} \left(\frac{1}{\sqrt{2}} (\text{beix} - \text{berx}) \cos \theta \cos \phi \right. \\
 & \quad \left. + \frac{1}{\sqrt{2}} \left(\frac{\text{ber}'x + \text{bei}'x}{x} \right) \cos(\theta - \phi) \right) \\
 & + C_{14} \left(-\frac{1}{\sqrt{2}} (\text{berx} + \text{beix}) \cos \theta \cos \phi \right. \\
 & \quad \left. - \frac{1}{\sqrt{2}} \left(\frac{\text{ber}'x - \text{bei}'x}{x} \right) \cos(\theta - \phi) \right) \\
 & + C_{15} \left(\frac{1}{\sqrt{2}} (\text{keix} - \text{kerx}) \cos \theta \cos \phi \right. \\
 & \quad \left. + \frac{1}{\sqrt{2}} \left(\frac{\text{ker}'x + \text{kei}'x}{x} \right) \cos(\theta - \phi) \right) \\
 & + C_{16} \left(-\frac{1}{\sqrt{2}} (\text{kerx} + \text{keix}) \cos \theta \cos \phi \right. \\
 & \quad \left. - \frac{1}{\sqrt{2}} \left(\frac{\text{ker}'x - \text{kei}'x}{x} \right) \cos(\theta - \phi) \right) \\
 & + \bar{C}_{13} \left(\frac{1}{\sqrt{2}} (\text{beix} - \text{berx}) \sin \theta \cos \phi \right. \\
 & \quad \left. + \frac{1}{\sqrt{2}} \left(\frac{\text{ber}'x + \text{bei}'x}{x} \right) \sin(\theta - \phi) \right) \\
 & + \bar{C}_{14} \left(-\frac{1}{\sqrt{2}} (\text{berx} + \text{beix}) \sin \theta \cos \phi \right. \\
 & \quad \left. - \frac{1}{\sqrt{2}} \left(\frac{\text{ber}'x - \text{bei}'x}{x} \right) \sin(\theta - \phi) \right) \\
 & + \bar{C}_{15} \left(\frac{1}{\sqrt{2}} (\text{keix} - \text{kerx}) \sin \theta \cos \phi \right. \\
 & \quad \left. + \frac{1}{\sqrt{2}} \left(\frac{\text{ker}'x + \text{kei}'x}{x} \right) \sin(\theta - \phi) \right) \\
 & + \bar{C}_{16} \left(-\frac{1}{\sqrt{2}} (\text{kerx} + \text{keix}) \sin \theta \cos \phi \right. \\
 & \quad \left. - \frac{1}{\sqrt{2}} \left(\frac{\text{ker}'x - \text{kei}'x}{x} \right) \sin(\theta - \phi) \right)
 \end{aligned}$$

Contrails

Q_n (p.2 of 3)

$$+ C_{23} \left(\text{bei}'x \cos 2\theta \cos \phi - 2 \left(\frac{\text{bei}x}{x} + \frac{2 \text{ber}'x}{x^2} \right) \cos(2\theta - \phi) \right)$$

$$+ C_{24} \left(-\text{ber}'x \cos 2\theta \cos \phi + 2 \left(\frac{\text{ber}x}{x} - \frac{2 \text{bei}'x}{x^2} \right) \cos(2\theta - \phi) \right)$$

$$+ C_{25} \left(\text{kei}'x \cos 2\theta \cos \phi - 2 \left(\frac{\text{kei}x}{x} + \frac{2 \text{ker}'x}{x^2} \right) \cos(2\theta - \phi) \right)$$

$$+ C_{26} \left(-\text{ker}'x \cos 2\theta \cos \phi + 2 \left(\frac{\text{ker}x}{x} - \frac{2 \text{kei}'x}{x^2} \right) \cos(2\theta - \phi) \right)$$

$$+ \bar{C}_{23} \left(\text{bei}'x \sin 2\theta \cos \phi - 2 \left(\frac{\text{bei}x}{x} + \frac{2 \text{ber}'x}{x^2} \right) \sin(2\theta - \phi) \right)$$

$$+ \bar{C}_{24} \left(-\text{ber}'x \sin 2\theta \cos \phi + 2 \left(\frac{\text{ber}x}{x} - \frac{2 \text{bei}'x}{x^2} \right) \sin(2\theta - \phi) \right)$$

$$+ \bar{C}_{25} \left(\text{kei}'x \sin 2\theta \cos \phi - 2 \left(\frac{\text{kei}x}{x} + \frac{2 \text{ker}'x}{x^2} \right) \sin(2\theta - \phi) \right)$$

$$+ \bar{C}_{26} \left(-\text{ker}'x \sin 2\theta \cos \phi + 2 \left(\frac{\text{ker}x}{x} - \frac{2 \text{kei}'x}{x^2} \right) \sin(2\theta - \phi) \right)$$

$$+ \sum_{n=3}^N \left\{ C_{n3} \left(\left\{ \frac{1}{\sqrt{2}} (\text{ber}_{n-3}x - \text{bei}_{n-3}x) - \frac{2(n-2)}{x} \text{bei}_{n-2}x \right\} \cos n\theta \cos \phi \right. \right.$$

$$\left. - \left(\frac{n \text{bei}_{n-2}x}{x} + \frac{\sqrt{2}(n)(n-1)}{x^2} (\text{ber}_{n-1}x + \text{bei}_{n-1}x) \right) \cos(n\theta - \phi) \right)$$

$$+ C_{n4} \left(\left\{ \frac{1}{\sqrt{2}} (\text{ber}_{n-3}x + \text{bei}_{n-3}x) + \frac{2(n-2)}{x} \text{ber}_{n-2}x \right\} \cos n\theta \cos \phi \right.$$

$$\left. + \left(\frac{n \text{ber}_{n-2}x}{x} - \frac{\sqrt{2}(n)(n-1)}{x^2} (\text{bei}_{n-1}x - \text{ber}_{n-1}x) \right) \cos(n\theta - \phi) \right)$$

$$+ C_{n5} \left(\left\{ \frac{1}{\sqrt{2}} (\text{ker}_{n-3}x - \text{kei}_{n-3}x) - \frac{2(n-2)}{x} \text{kei}_{n-2}x \right\} \cos n\theta \cos \phi \right.$$

$$\left. - \left(\frac{n \text{kei}_{n-2}x}{x} + \frac{\sqrt{2}(n)(n-1)}{x^2} (\text{ker}_{n-1}x + \text{kei}_{n-1}x) \right) \cos(n\theta - \phi) \right)$$

$$+ C_{n6} \left(\left\{ \frac{1}{\sqrt{2}} (\text{ker}_{n-3}x + \text{kei}_{n-3}x) + \frac{2(n-2)}{x} \text{ker}_{n-2}x \right\} \cos n\theta \cos \phi \right.$$

$$\left. + \left(\frac{n \text{ker}_{n-2}x}{x} - \frac{\sqrt{2}(n)(n-1)}{x^2} (\text{kei}_{n-1}x - \text{ker}_{n-1}x) \right) \cos(n\theta - \phi) \right)$$

Contrails

Q_n (p.3 of 3)

$$\begin{aligned}
 & + \bar{C}_{n3} \left(\left\{ \frac{1}{\sqrt{2}} (\text{ber}_{n-3} x - \text{bei}_{n-3} x) - \frac{2(n-2)}{x} \text{bei}_{n-2} x \right\} \text{Sin } n\theta \text{Cos } \phi \right. \\
 & \quad \left. - \left(\frac{n \text{bei}_{n-2} x}{x} + \frac{\sqrt{2}(n)(n-1)}{x^2} (\text{ber}_{n-1} x + \text{bei}_{n-1} x) \right) \text{Sin}(n\theta - \phi) \right) \\
 & + \bar{C}_{n4} \left(\left\{ \frac{1}{\sqrt{2}} (\text{ber}_{n-3} x + \text{bei}_{n-3} x) + \frac{2(n-2)}{x} \text{ber}_{n-2} x \right\} \text{Sin } n\theta \text{Cos } \phi \right. \\
 & \quad \left. + \left(\frac{n \text{ber}_{n-2} x}{x} - \frac{\sqrt{2}(n)(n-1)}{x^2} (\text{bei}_{n-1} x - \text{ber}_{n-1} x) \right) \text{Sin}(n\theta - \phi) \right) \\
 & + \bar{C}_{n5} \left(\left\{ \frac{1}{\sqrt{2}} (\text{ker}_{n-3} x - \text{kei}_{n-3} x) - \frac{2(n-2)}{x} \text{kei}_{n-2} x \right\} \text{Sin } n\theta \text{Cos } \phi \right. \\
 & \quad \left. - \left(\frac{n \text{kei}_{n-2} x}{x} + \frac{\sqrt{2}(n)(n-1)}{x^2} (\text{ker}_{n-1} x + \text{kei}_{n-1} x) \right) \text{Sin}(n\theta - \phi) \right) \\
 & + \bar{C}_{n6} \left(\left\{ \frac{1}{\sqrt{2}} (\text{ker}_{n-3} x + \text{kei}_{n-3} x) + \frac{2(n-2)}{x} \text{ker}_{n-2} x \right\} \text{Sin } n\theta \text{Cos } \phi \right. \\
 & \quad \left. + \left(\frac{n \text{ker}_{n-2} x}{x} - \frac{\sqrt{2}(n)(n-1)}{x^2} (\text{kei}_{n-1} x - \text{ker}_{n-1} x) \right) \text{Sin}(n\theta - \phi) \right) \left. \right\}]
 \end{aligned}$$

Contrails

V_n (p.1 of 15)

$$\begin{aligned}
 V_n = & -\frac{D}{L^3} \left[-C_{03} \left\{ \text{bei}'x \cos \phi + (1-\nu) \left[\left(\frac{\text{bei}'x}{2} - \frac{\text{bei}x}{x} - \frac{2\text{ber}'x}{x^2} \right) \sin 2\phi \sin \phi \right. \right. \right. \\
 & \left. \left. \left. - \left(\text{bei}x + \frac{2\text{ber}'x}{x} \right) \cos 2\phi \left(-L \sin \phi \frac{\partial \phi}{\partial r} + \frac{1}{x} \cos \phi \frac{\partial \phi}{\partial \theta} \right) \right] \right\} \\
 & + C_{04} \left\{ \text{ber}'x \cos \phi + (1-\nu) \left[\left(\frac{\text{ber}'x}{2} - \frac{\text{ber}x}{x} + \frac{2\text{kei}'x}{x^2} \right) \sin 2\phi \sin \phi \right. \right. \\
 & \left. \left. \left. - \left(\text{ber}x - \frac{2\text{kei}'x}{x} \right) \cos 2\phi \left(-L \sin \phi \frac{\partial \phi}{\partial r} + \frac{1}{x} \cos \phi \frac{\partial \phi}{\partial \theta} \right) \right] \right\} \\
 & - C_{05} \left\{ \text{kei}'x \cos \phi + (1-\nu) \left[\left(\frac{\text{kei}'x}{2} - \frac{\text{kei}x}{x} - \frac{2\text{ker}'x}{x^2} \right) \sin 2\phi \sin \phi \right. \right. \\
 & \left. \left. \left. - \left(\text{kei}x + \frac{2\text{ker}'x}{x} \right) \cos 2\phi \left(-L \sin \phi \frac{\partial \phi}{\partial r} + \frac{1}{x} \cos \phi \frac{\partial \phi}{\partial \theta} \right) \right] \right\} \\
 & + C_{06} \left\{ \text{ker}'x \cos \phi + (1-\nu) \left[\left(\frac{\text{ker}'x}{2} - \frac{\text{ker}x}{x} + \frac{2\text{kei}'x}{x^2} \right) \sin 2\phi \sin \phi \right. \right. \\
 & \left. \left. \left. - \left(\text{ker}x - \frac{2\text{kei}'x}{x} \right) \cos 2\phi \left(-L \sin \phi \frac{\partial \phi}{\partial r} + \frac{1}{x} \cos \phi \frac{\partial \phi}{\partial \theta} \right) \right] \right\} \\
 & + C_{12} (1-\nu) \left\{ \frac{4}{x^2} \cos(\theta-3\phi) - \frac{2}{x^2} \cos(\theta-\phi) \right. \\
 & \left. - \frac{4}{x^3} \cos(\theta-2\phi) \left(-L \sin \phi \frac{\partial \phi}{\partial r} + \frac{1}{x} \cos \phi \frac{\partial \phi}{\partial \theta} \right) \right\}
 \end{aligned}$$

Contrails

V_n (p.2 of 15)

$$\begin{aligned}
 & -C_{13} \left\{ \frac{1}{\sqrt{2}} \left[(\text{ber} x - \text{ber}' x) \cos \theta \cos \phi + \left(\frac{\text{ber}' x + \text{bei}' x}{x} \right) \cos(\theta - \phi) \right] \right. \\
 & \quad + (1-\nu) \left(\frac{1}{2\sqrt{2}} \left[(\text{ber} x - \text{ber}' x) \cos \theta \sin \phi \right. \right. \\
 & \qquad \qquad \qquad \left. \left. + \left(\frac{\text{ber}' x + \text{bei}' x}{x} \right) \sin(\theta - \phi) \right] \sin 2\phi \right. \\
 & \quad + \frac{1}{\sqrt{2}} \left[\left\{ \left(\frac{\text{ber}' x + \text{bei}' x}{x} \right) - 2 \left(\frac{\text{ber} x + \text{ber}' x}{x^2} \right) \right. \right. \\
 & \qquad \qquad \qquad \left. \left. - 4 \left(\frac{\text{ber}' x - \text{bei}' x}{x^3} \right) \right\} \sin(\theta - 2\phi) \sin \phi \right. \\
 & \quad \left. - \left\{ \left(\frac{\text{ber} x + \text{ber}' x}{x^2} \right) + 2 \left(\frac{\text{ber}' x - \text{bei}' x}{x^3} \right) \right\} \cos(\theta - 3\phi) \right] \\
 & \quad - \left[\frac{1}{\sqrt{2}} (\text{ber}' x + \text{bei}' x) \cos \theta \cos 2\phi - \sqrt{2} \left\{ \left(\frac{\text{ber} x + \text{ber}' x}{x} \right) \right. \right. \\
 & \qquad \qquad \left. \left. + 2 \left(\frac{\text{ber}' x - \text{bei}' x}{x^2} \right) \right\} \cos(\theta - 2\phi) \left(-L \sin \phi \frac{\partial \phi}{\partial r} + \frac{1}{x} \cos \phi \frac{\partial \phi}{\partial \theta} \right) \right] \left. \right\} \\
 & + C_{14} \left\{ -\frac{1}{\sqrt{2}} \left[(\text{ber} x + \text{ber}' x) \cos \theta \cos \phi - \left(\frac{\text{ber}' x - \text{bei}' x}{x} \right) \cos(\theta - \phi) \right] \right. \\
 & \quad + (1-\nu) \left(-\frac{1}{2\sqrt{2}} \left[(\text{ber} x + \text{ber}' x) \cos \theta \sin \phi \right. \right. \\
 & \qquad \qquad \qquad \left. \left. - \left(\frac{\text{ber}' x - \text{bei}' x}{x} \right) \sin(\theta - \phi) \right] \sin 2\phi \right. \\
 & \quad + \frac{1}{\sqrt{2}} \left[\left\{ \left(\frac{\text{ber}' x - \text{bei}' x}{x} \right) - 2 \left(\frac{\text{ber} x - \text{ber}' x}{x^2} \right) \right. \right. \\
 & \qquad \qquad \qquad \left. \left. + 4 \left(\frac{\text{ber}' x + \text{bei}' x}{x^3} \right) \right\} \sin(\theta - 2\phi) \sin \phi \right. \\
 & \quad \left. - \left\{ \left(\frac{\text{ber} x - \text{ber}' x}{x^2} \right) - 2 \left(\frac{\text{ber}' x + \text{bei}' x}{x^3} \right) \right\} \cos(\theta - 3\phi) \right] \\
 & \quad + \left[-\frac{1}{\sqrt{2}} (\text{ber}' x - \text{bei}' x) \cos \theta \cos 2\phi + \sqrt{2} \left\{ \left(\frac{\text{ber} x - \text{ber}' x}{x} \right) \right. \right. \\
 & \qquad \qquad \left. \left. - 2 \left(\frac{\text{ber}' x + \text{bei}' x}{x^2} \right) \right\} \cos(\theta - 2\phi) \left(-L \sin \phi \frac{\partial \phi}{\partial r} + \frac{1}{x} \cos \phi \frac{\partial \phi}{\partial \theta} \right) \right] \left. \right\}
 \end{aligned}$$

Contrails

V_n (p.3 of 15)

$$\begin{aligned}
 & - C_{15} \left\{ \frac{1}{\sqrt{2}} \left[(k_{er}x - k_{ei}x) \cos \theta \cos \phi + \left(\frac{k_{er}'x + k_{ei}'x}{x} \right) \cos(\theta - \phi) \right] \right. \\
 & \quad + (1-\nu) \left(\frac{1}{2\sqrt{2}} \left[(k_{er}x - k_{ei}x) \cos \theta \sin \phi \right. \right. \\
 & \quad \quad \left. \left. + \left(\frac{k_{er}'x + k_{ei}'x}{x} \right) \sin(\theta - \phi) \right] \sin 2\phi \right. \\
 & \quad \left. + \frac{1}{\sqrt{2}} \left[\left\{ \left(\frac{k_{er}'x + k_{ei}'x}{x} \right) - 2 \left(\frac{k_{er}x + k_{ei}x}{x^2} \right) \right. \right. \right. \\
 & \quad \quad \left. \left. - 4 \left(\frac{k_{er}'x - k_{ei}'x}{x^3} \right) \right\} \sin(\theta - 2\phi) \sin \phi \right. \right. \\
 & \quad \quad \left. - \left\{ \left(\frac{k_{er}x + k_{ei}x}{x^2} \right) + 2 \left(\frac{k_{er}'x - k_{ei}'x}{x^3} \right) \right\} \cos(\theta - 3\phi) \right] \\
 & \quad \left. - \left[\frac{1}{\sqrt{2}} (k_{er}'x + k_{ei}'x) \cos \theta \cos 2\phi - \sqrt{2} \left\{ \left(\frac{k_{er}x + k_{ei}x}{x} \right) \right. \right. \right. \\
 & \quad \quad \left. \left. + 2 \left(\frac{k_{er}'x - k_{ei}'x}{x^2} \right) \right\} \cos(\theta - 2\phi) \left(-L \sin \phi \frac{\partial \phi}{\partial r} + \frac{1}{x} \cos \phi \frac{\partial \phi}{\partial \theta} \right) \right] \right\} \\
 & + C_{16} \left\{ -\frac{1}{\sqrt{2}} \left[(k_{er}x + k_{ei}x) \cos \theta \cos \phi - \left(\frac{k_{er}'x - k_{ei}'x}{x} \right) \cos(\theta - \phi) \right] \right. \\
 & \quad + (1-\nu) \left(-\frac{1}{2\sqrt{2}} \left[(k_{er}x + k_{ei}x) \cos \theta \sin \phi \right. \right. \\
 & \quad \quad \left. \left. - \left(\frac{k_{er}'x - k_{ei}'x}{x} \right) \sin(\theta - \phi) \right] \sin 2\phi \right. \\
 & \quad \left. + \frac{1}{\sqrt{2}} \left[\left\{ \left(\frac{k_{er}x - k_{ei}x}{x} \right) - 2 \left(\frac{k_{er}x - k_{ei}x}{x^2} \right) \right. \right. \right. \\
 & \quad \quad \left. \left. + 4 \left(\frac{k_{er}'x + k_{ei}'x}{x^3} \right) \right\} \sin(\theta - 2\phi) \sin \phi \right. \right. \\
 & \quad \quad \left. - \left\{ \left(\frac{k_{er}x - k_{ei}x}{x^2} \right) - 2 \left(\frac{k_{er}'x + k_{ei}'x}{x^3} \right) \right\} \cos(\theta - 3\phi) \right] \\
 & \quad \left. + \left[-\frac{1}{\sqrt{2}} (k_{er}'x - k_{ei}'x) \cos \theta \cos 2\phi + \sqrt{2} \left\{ \left(\frac{k_{er}x - k_{ei}x}{x} \right) \right. \right. \right. \\
 & \quad \quad \left. \left. - 2 \left(\frac{k_{er}'x + k_{ei}'x}{x^2} \right) \right\} \cos(\theta - 2\phi) \left(-L \sin \phi \frac{\partial \phi}{\partial r} + \frac{1}{x} \cos \phi \frac{\partial \phi}{\partial \theta} \right) \right] \right\}
 \end{aligned}$$

Contrails

v_n (p. 4 of 15)

$$\begin{aligned} & -4 C_{21} (1-\nu) \left\{ \left(-L \sin \phi \frac{\partial \phi}{\partial r} + \frac{1}{x} \cos \phi \frac{\partial \phi}{\partial \theta} \right) + \frac{1}{x} \cos \phi \right\} \cos (2\theta + 2\phi) \\ & + 12 C_{22} (1-\nu) \left\{ \frac{\cos (2\theta - 3\phi)}{x^5} + \frac{\sin (2\theta - 2\phi) \sin \phi}{x^5} \right. \\ & \quad \left. - \frac{1}{x^2} \left(-L \sin \phi \frac{\partial \phi}{\partial r} + \frac{1}{x} \cos \phi \frac{\partial \phi}{\partial \theta} \right) \right\} \end{aligned}$$

Contrails

V_n (p.5 of 15)

$$\begin{aligned}
 &+ C_{23} \left\{ \text{bei}'x \cos 2\theta \cos \phi - 2 \left(\frac{\text{bei}x}{x} + \frac{2\text{ber}'x}{x^2} \right) \cos(2\theta - \phi) \right. \\
 &\quad + (1-\nu) \left(\frac{1}{2} \text{bei}'x \cos 2\theta \sin 2\phi \sin \phi \right. \\
 &\quad \quad + 4 \left(\frac{\text{ber}'x}{x^2} - \frac{3\text{ber}x}{x^3} + \frac{6\text{bei}'x}{x^4} \right) \cos(2\theta - 3\phi) \\
 &\quad \quad + 2 \left(\frac{\text{bei}x}{x} + \frac{3\text{ber}'x}{x^2} - \frac{6\text{ber}x}{x^3} + \frac{12\text{bei}'x}{x^4} \right) \sin(2\theta - 2\phi) \sin \phi \\
 &\quad \quad + \frac{\text{bei}x}{x} \sin 2\theta \sin 2\phi \cos \phi \\
 &\quad \quad \left. - \left[\text{bei}x \cos 2\theta \cos 2\phi + 4 \left(\frac{\text{ber}'x}{x} - \frac{3\text{ber}x}{x^2} \right. \right. \right. \\
 &\quad \quad \quad \left. \left. + \frac{6\text{bei}'x}{x^3} \right) \cos(2\theta - 2\phi) \right] \left[-L \sin \phi \frac{\partial \phi}{\partial r} + \frac{1}{x} \cos \phi \frac{\partial \phi}{\partial \theta} \right] \left. \right\} \\
 &- C_{24} \left\{ -\text{ber}'x \cos 2\theta \cos \phi + 2 \left(\frac{\text{ber}x}{x} - \frac{2\text{bei}'x}{x^2} \right) \cos(2\theta - \phi) \right. \\
 &\quad + (1-\nu) \left(\frac{1}{2} \text{ber}'x \cos 2\theta \sin 2\phi \sin \phi \right. \\
 &\quad \quad - 4 \left(\frac{\text{bei}'x}{x^2} - \frac{3\text{bei}x}{x^3} - \frac{6\text{ber}'x}{x^4} \right) \cos(2\theta - 3\phi) \\
 &\quad \quad + 2 \left(\frac{\text{ber}x}{x} - \frac{3\text{bei}'x}{x^2} + \frac{6\text{bei}x}{x^3} + \frac{12\text{ber}'x}{x^4} \right) \sin(2\theta - 2\phi) \sin \phi \\
 &\quad \quad + \frac{\text{ber}x}{x} \sin 2\theta \sin 2\phi \cos \phi \\
 &\quad \quad \left. - \left[\text{ber}x \cos 2\theta \cos 2\phi - 4 \left(\frac{\text{bei}'x}{x} - \frac{3\text{bei}x}{x^2} \right. \right. \right. \\
 &\quad \quad \quad \left. \left. - \frac{6\text{ber}'x}{x^3} \right) \cos(2\theta - 2\phi) \right] \left[-L \sin \phi \frac{\partial \phi}{\partial r} + \frac{1}{x} \cos \phi \frac{\partial \phi}{\partial \theta} \right] \left. \right\}
 \end{aligned}$$

Contrails

V_n (p.6 of 15)

$$\begin{aligned}
 & + C_{25} \left\{ \text{kei}'x \cos 2\theta \cos \phi - 2 \left(\frac{\text{kei}'x}{x} + \frac{2 \text{ker}'x}{x^2} \right) \cos(2\theta - \phi) \right. \\
 & \quad + (1-\nu) \left(\frac{1}{2} \text{kei}'x \cos 2\theta \sin 2\phi \sin \phi \right. \\
 & \quad \quad + 4 \left(\frac{\text{ker}'x}{x^2} - \frac{3 \text{ker}x}{x^3} + \frac{6 \text{kei}'x}{x^4} \right) \cos(2\theta - 3\phi) \\
 & \quad \quad + 2 \left(\frac{\text{kei}x}{x} + \frac{3 \text{ker}'x}{x^2} - \frac{6 \text{ker}x}{x^3} + \frac{12 \text{kei}'x}{x^4} \right) \sin(2\theta - 2\phi) \sin \phi \\
 & \quad \quad + \frac{\text{kei}x}{x} \sin 2\theta \sin 2\phi \cos \phi \\
 & \quad \quad \left. - \left[\text{kei}x \cos 2\theta \cos 2\phi + 4 \left(\frac{\text{ker}'x}{x} - \frac{3 \text{ker}x}{x^2} \right. \right. \right. \\
 & \quad \quad \quad \left. \left. \left. + \frac{6 \text{kei}'x}{x^3} \right) \cos(2\theta - 2\phi) \right] \left[-L \sin \phi \frac{\partial \phi}{\partial r} + \frac{1}{x} \cos \phi \frac{\partial \phi}{\partial \theta} \right] \right\} \\
 & - C_{26} \left\{ - \text{ker}'x \cos 2\theta \cos \phi + 2 \left(\frac{\text{ker}x}{x} - \frac{2 \text{kei}'x}{x^2} \right) \cos(2\theta - \phi) \right. \\
 & \quad + (1-\nu) \left(\frac{1}{2} \text{ker}'x \cos 2\theta \sin 2\phi \sin \phi \right. \\
 & \quad \quad - 4 \left(\frac{\text{kei}'x}{x^2} - \frac{3 \text{kei}x}{x^3} - \frac{6 \text{ker}'x}{x^4} \right) \cos(2\theta - 3\phi) \\
 & \quad \quad + 2 \left(\frac{\text{ker}x}{x} - \frac{3 \text{kei}'x}{x^2} + \frac{6 \text{kei}x}{x^3} + \frac{12 \text{ker}'x}{x^4} \right) \sin(2\theta - 2\phi) \sin \phi \\
 & \quad \quad + \frac{\text{ker}x}{x} \sin 2\theta \sin 2\phi \cos \phi \\
 & \quad \quad \left. - \left[\text{ker}x \cos 2\theta \cos 2\phi - 4 \left(\frac{\text{kei}'x}{x} - \frac{3 \text{kei}x}{x^2} \right. \right. \right. \\
 & \quad \quad \quad \left. \left. \left. - \frac{6 \text{ker}'x}{x^3} \right) \cos(2\theta - 2\phi) \right] \left[-L \sin \phi \frac{\partial \phi}{\partial r} + \frac{1}{x} \cos \phi \frac{\partial \phi}{\partial \theta} \right] \right\} \\
 & + 2 \bar{C}_{12} (1-\nu) \left\{ \frac{2 \sin(\theta - 3\phi)}{x^4} - \frac{\sin(\theta - \phi)}{x^2} - \frac{2 \sin(\theta - 2\phi)}{x^3} \left[-L \sin \phi \frac{\partial \phi}{\partial r} \right. \right. \\
 & \quad \quad \quad \left. \left. + \frac{1}{x} \cos \phi \frac{\partial \phi}{\partial \theta} \right] \right\}
 \end{aligned}$$

Contrails

V_n (p.7 of 15)

$$\begin{aligned}
 & + \bar{C}_{13} \left\{ \frac{1}{\sqrt{2}} \left[(berx - berx) \sin \theta \cos \phi + \left(\frac{ber'x + bei'x}{x} \right) \sin(\theta - \phi) \right] \right. \\
 & \quad + (1-\nu) \left[\frac{1}{2\sqrt{2}} \left[(berx - berx) \sin \theta \sin \phi + \left(\frac{ber'x + bei'x}{x} \right) \cos(\theta - \phi) \right] \sin 2\phi \right. \\
 & \quad \quad + \frac{1}{\sqrt{2}} \left\{ \left[\left(\frac{ber'x + bei'x}{x} \right) - 2 \left(\frac{berx + bei'x}{x^2} \right) \right. \right. \\
 & \quad \quad \quad \left. \left. - 4 \left(\frac{ber'x - bei'x}{x^3} \right) \right] \cos(\theta - 2\phi) \sin \phi \right. \right. \\
 & \quad \quad \quad \left. \left. + \left[\left(\frac{berx + bei'x}{x^2} \right) + 2 \left(\frac{ber'x - bei'x}{x^3} \right) \right] \sin(\theta - 3\phi) \right\} \right. \\
 & \quad \quad \left. + \left\{ \frac{1}{\sqrt{2}} (ber'x + bei'x) \sin \theta \cos 2\phi - \sqrt{2} \left[\left(\frac{berx + bei'x}{x} \right) \right. \right. \right. \\
 & \quad \quad \quad \left. \left. + 2 \left(\frac{ber'x - bei'x}{x^2} \right) \right] \sin(\theta - 2\phi) \right\} \left\{ -L \sin \phi \frac{\partial \phi}{\partial r} + \frac{1}{x} \cos \phi \frac{\partial \phi}{\partial \theta} \right\} \right\} \\
 & + \bar{C}_{14} \left\{ -\frac{1}{\sqrt{2}} \left[(berx + bei'x) \sin \theta \cos \phi + \left(\frac{ber'x - bei'x}{x} \right) \sin(\theta - \phi) \right] \right. \\
 & \quad + (1-\nu) \left[\frac{1}{2\sqrt{2}} \left[-(berx + bei'x) \sin \theta \sin \phi - \left(\frac{ber'x - bei'x}{x} \right) \cos(\theta - \phi) \right] \sin 2\phi \right. \\
 & \quad \quad - \frac{1}{\sqrt{2}} \left\{ \left[\left(\frac{ber'x - bei'x}{x} \right) - 2 \left(\frac{berx - bei'x}{x^2} \right) \right. \right. \\
 & \quad \quad \quad \left. \left. + 4 \left(\frac{ber'x + bei'x}{x^3} \right) \right] \cos(\theta - 2\phi) \sin \phi \right. \right. \\
 & \quad \quad \quad \left. \left. + \left[\left(\frac{berx - bei'x}{x^2} \right) - 2 \left(\frac{ber'x + bei'x}{x^3} \right) \right] \sin(\theta - 3\phi) \right\} \right. \\
 & \quad \quad \left. + \left\{ -\frac{1}{\sqrt{2}} (ber'x - bei'x) \sin \theta \cos 2\phi + \sqrt{2} \left[\left(\frac{berx - bei'x}{x} \right) \right. \right. \right. \\
 & \quad \quad \quad \left. \left. - 2 \left(\frac{ber'x + bei'x}{x^2} \right) \right] \sin(\theta - 2\phi) \right\} \left\{ -L \sin \phi \frac{\partial \phi}{\partial r} + \frac{1}{x} \cos \phi \frac{\partial \phi}{\partial \theta} \right\} \right\}
 \end{aligned}$$

Contrails

V_n (p.8 of 15)

$$\begin{aligned}
 & + \bar{c}_{15} \left\{ \frac{1}{\sqrt{2}} \left[(k_{er}x - k_{er}x) \sin \theta \cos \phi + \left(\frac{k_{er}'x + k_{ei}'x}{x} \right) \sin(\theta - \phi) \right] \right. \\
 & \quad + (1-\nu) \left\{ \frac{1}{2\sqrt{2}} \left[(k_{er}x - k_{er}x) \sin \theta \sin \phi + \left(\frac{k_{er}'x + k_{ei}'x}{x} \right) \cos(\theta - \phi) \right] \sin 2\phi \right. \\
 & \quad \quad + \frac{1}{\sqrt{2}} \left\{ \left[\left(\frac{k_{er}'x + k_{ei}'x}{x} \right) - 2 \left(\frac{k_{er}x + k_{ei}x}{x^2} \right) \right. \right. \\
 & \quad \quad \quad \left. \left. - 4 \left(\frac{k_{er}'x - k_{ei}'x}{x^3} \right) \right] \cos(\theta - 2\phi) \sin \phi \right. \right. \\
 & \quad \quad \quad \left. \left. + \left[\left(\frac{k_{er}x + k_{ei}x}{x^2} \right) + 2 \left(\frac{k_{er}'x - k_{ei}'x}{x^3} \right) \right] \sin(\theta - 3\phi) \right\} \right. \\
 & \quad \quad \left. + \left\{ \frac{1}{\sqrt{2}} (k_{er}'x + k_{ei}'x) \sin \theta \cos 2\phi - \sqrt{2} \left[\left(\frac{k_{er}x + k_{ei}x}{x} \right) \right. \right. \right. \\
 & \quad \quad \quad \left. \left. + 2 \left(\frac{k_{er}'x - k_{ei}'x}{x^2} \right) \right] \sin(\theta - 2\phi) \right\} \left\{ -L \sin \phi \frac{\partial \phi}{\partial r} + \frac{1}{x} \cos \phi \frac{\partial \phi}{\partial \theta} \right\} \right\} \\
 & + \bar{c}_{16} \left\{ -\frac{1}{\sqrt{2}} \left[(k_{er}x + k_{ei}x) \sin \theta \cos \phi + \left(\frac{k_{er}'x - k_{ei}'x}{x} \right) \sin(\theta - \phi) \right] \right. \\
 & \quad + (1-\nu) \left\{ \frac{1}{2\sqrt{2}} \left[-(k_{er}x + k_{ei}x) \sin \theta \sin \phi - \left(\frac{k_{er}'x - k_{ei}'x}{x} \right) \cos(\theta - \phi) \right] \sin 2\phi \right. \\
 & \quad \quad - \frac{1}{\sqrt{2}} \left\{ \left[\left(\frac{k_{er}'x - k_{ei}'x}{x} \right) - 2 \left(\frac{k_{er}x - k_{ei}x}{x^2} \right) \right. \right. \\
 & \quad \quad \quad \left. \left. + 4 \left(\frac{k_{er}'x + k_{ei}'x}{x^3} \right) \right] \cos(\theta - 2\phi) \sin \phi \right. \right. \\
 & \quad \quad \quad \left. \left. + \left[\left(\frac{k_{er}x - k_{ei}x}{x^2} \right) - 2 \left(\frac{k_{er}'x + k_{ei}'x}{x^3} \right) \right] \sin(\theta - 3\phi) \right\} \right. \\
 & \quad \quad \left. + \left\{ -\frac{1}{\sqrt{2}} (k_{er}'x - k_{ei}'x) \sin \theta \cos 2\phi + \sqrt{2} \left[\left(\frac{k_{er}x - k_{ei}x}{x} \right) \right. \right. \right. \\
 & \quad \quad \quad \left. \left. - 2 \left(\frac{k_{er}'x + k_{ei}'x}{x^2} \right) \right] \sin(\theta - 2\phi) \right\} \left\{ -L \sin \phi \frac{\partial \phi}{\partial r} + \frac{1}{x} \cos \phi \frac{\partial \phi}{\partial \theta} \right\} \right\} \\
 & - 4 \bar{c}_{21} (1-\nu) \left\{ \left(-L \sin \phi \frac{\partial \phi}{\partial r} + \frac{1}{x} \cos \phi \frac{\partial \phi}{\partial \theta} \right) + \frac{1}{x} \cos \phi \right\} \sin(2\theta + 2\phi) \\
 & + 12 \bar{c}_{22} (1-\nu) \left\{ \frac{\sin(2\theta - 3\phi)}{x^5} - \frac{\cos(2\theta - 2\phi) \sin \phi}{x^5} \right. \\
 & \quad \quad \left. - \frac{\sin(2\theta - 2\phi)}{x^4} \left(-L \sin \phi \frac{\partial \phi}{\partial r} + \frac{1}{x} \cos \phi \frac{\partial \phi}{\partial \theta} \right) \right\}
 \end{aligned}$$

Contrails

V_n (p.9 of 15)

$$\begin{aligned}
 & + \bar{C}_{23} \left\{ \text{ber}'x \sin 2\theta \cos \phi - 2 \left(\frac{\text{bei}x}{x} + \frac{2\text{ber}'x}{x^2} \right) \sin(2\theta - \phi) \right. \\
 & \quad + (1-\nu) \left(\frac{1}{2} \text{ber}'x \sin 2\theta \sin 2\phi \sin \phi \right. \\
 & \quad \quad - 4 \left[\frac{\text{ber}'x}{x^2} - \frac{3\text{ber}x}{x^3} + \frac{6\text{bei}'x}{x^4} \right] \sin(2\theta - 3\phi) \\
 & \quad \quad - 2 \left[\frac{\text{bei}x}{x} - \frac{6\text{ber}x}{x^3} + \frac{12\text{bei}'x}{x^4} + \frac{3\text{ber}'x}{x^2} \right] \cos(2\theta - 2\phi) \sin \phi \\
 & \quad \quad - \frac{\text{bei}x}{x} \cos 2\theta \sin 2\phi \cos \phi \\
 & \quad \quad \left. - \left[\text{ber}x \sin 2\theta \cos 2\phi + 4 \left(\frac{\text{ber}'x}{x} - \frac{3\text{ber}x}{x^2} \right. \right. \right. \\
 & \quad \quad \quad \left. \left. \left. + \frac{6\text{bei}'x}{x^3} \right) \sin(2\theta - 2\phi) \right] \left[-L \sin \phi \frac{\partial \phi}{\partial r} + \frac{1}{x} \cos \phi \frac{\partial \phi}{\partial \theta} \right] \right\}
 \end{aligned}$$

$$\begin{aligned}
 & - \bar{C}_{24} \left\{ -\text{ber}'x \sin 2\theta \cos \phi + 2 \left(\frac{\text{ber}x}{x} - \frac{2\text{bei}'x}{x^2} \right) \sin(2\theta - \phi) \right. \\
 & \quad + (1-\nu) \left(\frac{1}{2} \text{ber}'x \sin 2\theta \sin 2\phi \sin \phi \right. \\
 & \quad \quad + 4 \left(\frac{\text{bei}'x}{x^2} - \frac{3\text{bei}x}{x^3} + \frac{6\text{ber}'x}{x^4} \right) \sin(2\theta - 3\phi) \\
 & \quad \quad - 2 \left(\frac{\text{ber}x}{x} - \frac{3\text{bei}'x}{x^2} + \frac{6\text{bei}x}{x^3} + \frac{12\text{ber}'x}{x^4} \right) \cos(2\theta - 2\phi) \sin \phi \\
 & \quad \quad - \frac{\text{ber}x}{x} \cos 2\theta \sin 2\phi \cos \phi \\
 & \quad \quad \left. - \left[\text{ber}x \sin 2\theta \cos 2\phi - 4 \left(\frac{\text{bei}'x}{x} - \frac{3\text{bei}x}{x^2} \right. \right. \right. \\
 & \quad \quad \quad \left. \left. \left. - \frac{6\text{ber}'x}{x^3} \right) \sin(2\theta - 2\phi) \right] \left[-L \sin \phi \frac{\partial \phi}{\partial r} + \frac{1}{x} \cos \phi \frac{\partial \phi}{\partial \theta} \right] \right\}
 \end{aligned}$$

Contrails

V_n (p.10 of 15)

$$\begin{aligned}
 & + \bar{C}_{25} \left\{ kei'x \sin 2\theta \cos \phi - 2 \left(\frac{ker'x}{x} + \frac{2ker'x}{x^2} \right) \sin(2\theta - \phi) \right. \\
 & \quad + (1-\nu) \left(\frac{1}{2} kei'x \sin 2\theta \sin 2\phi \sin \phi \right. \\
 & \quad - 4 \left[\frac{ker'x}{x^2} - \frac{3kerx}{x^3} + \frac{6kei'x}{x^4} \right] \sin(2\theta - 3\phi) \\
 & \quad - 2 \left[\frac{keix}{x} + \frac{3ker'x}{x^2} - \frac{6kerx}{x^3} + \frac{12kei'x}{x^4} \right] \cos(2\theta - 2\phi) \sin \phi \\
 & \quad - \frac{kerx}{x} \cos 2\theta \sin 2\phi \cos \phi \\
 & \quad \left. - \left[kerx \sin 2\theta \cos 2\phi + 4 \left(\frac{ker'x}{x} - \frac{3kerx}{x^2} \right. \right. \right. \\
 & \quad \left. \left. \left. + \frac{6kei'x}{x^3} \right) \sin(2\theta - 2\phi) \right] \left[-L \sin \phi \frac{\partial \phi}{\partial r} + \frac{1}{x} \cos \phi \frac{\partial \phi}{\partial \theta} \right] \right\}
 \end{aligned}$$

$$\begin{aligned}
 & - \bar{C}_{26} \left\{ -ker'x \sin 2\theta \cos \phi + 2 \left(\frac{kerx}{x} - \frac{2kei'x}{x^2} \right) \sin(2\theta - \phi) \right. \\
 & \quad + (1-\nu) \left(\frac{1}{2} ker'x \sin 2\theta \sin 2\phi \sin \phi \right. \\
 & \quad + 4 \left(\frac{kei'x}{x^2} - \frac{3keix}{x^3} + \frac{6ker'x}{x^4} \right) \sin(2\theta - 3\phi) \\
 & \quad - 2 \left(\frac{kerx}{x} - \frac{3kei'x}{x^2} + \frac{6kerx}{x^3} + \frac{12ker'x}{x^4} \right) \cos(2\theta - 2\phi) \sin \phi \\
 & \quad - \frac{kerx}{x} \cos 2\theta \sin 2\phi \cos \phi \\
 & \quad \left. - \left[kerx \sin 2\theta \cos 2\phi - 4 \left(\frac{kei'x}{x} - \frac{3keix}{x^2} - \frac{6ker'x}{x^3} \right. \right. \right. \\
 & \quad \left. \left. \left. \sin(2\theta - 2\phi) \right] \left[-L \sin \phi \frac{\partial \phi}{\partial r} + \frac{1}{x} \cos \phi \frac{\partial \phi}{\partial \theta} \right] \right\}
 \end{aligned}$$

Contrails

V_n (p.11 of 15)

$$\begin{aligned}
 & + \sum_{n=3}^{\infty} -C_{n1} (1-\nu) \left\{ 2n(n-1)x^{n-3} \sin(n\theta+2\phi) \sin\phi \right. \\
 & \quad + n^2(n-1)x^{n-3} \cos(n\theta+3\phi) \\
 & \quad \left. + 2n(n-1)x^{n-2} \cos(n\theta+2\phi) \left[-L \sin\phi \frac{\partial\phi}{\partial r} + \frac{1}{x} \cos\phi \frac{\partial\phi}{\partial\theta} \right] \right\} \\
 & + C_{n2} (1-\nu) \left\{ 2n(n+1)x^{-(n+3)} \sin(n\theta-2\phi) \sin\phi \right. \\
 & \quad + n^2(n+1)x^{-(n+3)} \cos(n\theta-3\phi) \\
 & \quad \left. - 2n(n+1)x^{-(n+2)} \cos(n\theta-2\phi) \left[-L \sin\phi \frac{\partial\phi}{\partial r} + \frac{1}{x} \cos\phi \frac{\partial\phi}{\partial\theta} \right] \right\} \\
 & - \bar{C}_{n1} \left\{ -2n(n-1)x^{n-3} \cos(n\theta+2\phi) \sin\phi \right. \\
 & \quad + n^2(n-1)x^{n-3} \sin(n\theta+3\phi) \\
 & \quad \left. + 2n(n-1)x^{n-2} \sin(n\theta+2\phi) \left[-L \sin\phi \frac{\partial\phi}{\partial r} + \frac{1}{x} \cos\phi \frac{\partial\phi}{\partial\theta} \right] \right\} (1-\nu) \\
 & + \bar{C}_{n2} \left\{ -2n(n+1)x^{-(n+3)} \cos(n\theta-2\phi) \sin\phi \right. \\
 & \quad + n^2(n+1)x^{-(n+3)} \sin(n\theta-3\phi) \\
 & \quad \left. - 2n(n+1)x^{-(n+2)} \sin(n\theta-2\phi) \left[-L \sin\phi \frac{\partial\phi}{\partial r} + \frac{1}{x} \cos\phi \frac{\partial\phi}{\partial\theta} \right] \right\} (1-\nu)
 \end{aligned}$$

Contrails

V_n (p.12 of 15)

$$\begin{aligned}
 &+ C_{n3} \left\{ \left[\frac{1}{\sqrt{2}} (\text{ber}_{n-3} x - \text{bei}_{n-3} x) - \frac{2(n-2)\text{ber}_{n-2} x}{x} \right] \text{Cos } n\theta \text{ Cos } \phi \right. \\
 &\quad - \left[\frac{n}{x} \text{bei}_{n-2} x + \frac{\sqrt{2}n(n-1)}{x^2} (\text{ber}_{n-1} x + \text{bei}_{n-1} x) \right] \text{Cos}(n\theta - \phi) \\
 &\quad + (1-\nu) \left\{ \left[\frac{1}{2\sqrt{2}} (\text{ber}_{n-3} x - \text{bei}_{n-3} x) + \frac{\text{ber}_{n-2} x}{x} \right] \text{Cos } n\theta \text{ Sin } \phi \text{ Sin } 2\phi \right. \\
 &\quad \quad + \frac{n}{2x} \text{bei}_{n-2} x \text{ Sin}(n\theta - \phi) \text{ Sin } 2\phi \\
 &\quad \quad + \left[\frac{n}{x} \text{bei}_{n-2} x + \frac{n(n+1)}{\sqrt{2}x^2} (\text{ber}_{n-1} x + \text{bei}_{n-1} x) \right. \\
 &\quad \quad \quad \left. + \frac{2n(n+1)}{x^3} \text{ber}_n x \right] \text{Sin}(n\theta - 2\phi) \text{ Sin } \phi \\
 &\quad \quad + \left[\frac{n^2}{\sqrt{2}x^2} (\text{ber}_{n-1} x + \text{bei}_{n-1} x) + \frac{n^2(n+1)}{x^3} \text{ber}_n x \right] \text{Cos}(n\theta - 3\phi) \\
 &\quad \quad + \left[-\text{bei}_{n-2} x \text{ Cos } n\theta \text{ Cos } 2\phi - \left\{ \frac{\sqrt{2}n}{x} (\text{ber}_{n-1} x + \text{bei}_{n-1} x) \right. \right. \\
 &\quad \quad \quad \left. \left. + \frac{2n(n+1)}{x^2} \text{ber}_n x \right\} \text{Cos}(n\theta - 2\phi) \right] \left[-L \text{Sin } \phi \frac{\partial \phi}{\partial r} + \frac{1}{x} \text{Cos } \phi \frac{\partial \phi}{\partial \theta} \right] \left. \right\} \\
 &+ C_{n4} \left\{ \left[\frac{1}{\sqrt{2}} (\text{ber}_{n-3} x + \text{bei}_{n-3} x) + \frac{2(n-2)}{x} \text{ber}_{n-2} x \right] \text{Cos } n\theta \text{ Cos } \phi \right. \\
 &\quad + \left[\frac{n}{x} \text{ber}_{n-2} x - \frac{\sqrt{2}}{x} n(n-1) (\text{bei}_{n-1} x - \text{ber}_{n-1} x) \right] \text{Cos}(n\theta - \phi) \\
 &\quad + (1-\nu) \left\{ \left[\frac{1}{2\sqrt{2}} (\text{ber}_{n-3} x + \text{bei}_{n-3} x) - \frac{\text{ber}_{n-2} x}{x} \right] \text{Cos } n\theta \text{ Sin } 2\phi \text{ Sin } \phi \right. \\
 &\quad \quad - \frac{n}{2x} \text{ber}_{n-2} x \text{ Sin}(n\theta - \phi) \text{ Sin } 2\phi \\
 &\quad \quad + \left[-\frac{n}{x} \text{ber}_{n-2} x + \frac{n(n+1)}{\sqrt{2}x^2} (\text{bei}_{n-1} x - \text{ber}_{n-1} x) \right. \\
 &\quad \quad \quad \left. + \frac{2n(n+1)}{x^3} \text{bei}_n x \right] \text{Sin}(n\theta - 2\phi) \text{ Sin } \phi \\
 &\quad \quad + \left[\frac{n^2}{\sqrt{2}x^2} (\text{bei}_{n-1} x - \text{ber}_{n-1} x) + \frac{n^2(n+1)}{x^3} \text{bei}_n x \right] \text{Cos}(n\theta - 3\phi) \\
 &\quad \quad + \left[\text{ber}_{n-2} x \text{ Cos } n\theta \text{ Cos } 2\phi - \left\{ \frac{\sqrt{2}n}{x} (\text{bei}_{n-1} x - \text{ber}_{n-1} x) \right. \right. \\
 &\quad \quad \quad \left. \left. + \frac{2n(n+1)}{x^2} \text{bei}_n x \right\} \text{Cos}(n\theta - 2\phi) \right] \left[-L \text{Sin } \phi \frac{\partial \phi}{\partial r} + \frac{1}{x} \text{Cos } \phi \frac{\partial \phi}{\partial \theta} \right] \left. \right\}
 \end{aligned}$$

Contrails

V_n (p.13 of 15)

$$\begin{aligned}
 & + C_{n5} \left\{ \left[\frac{1}{\sqrt{2}} (\ker_{n-3} x - \ker_{n-3} x) - \frac{2(n-2)}{x} \ker_{n-2} x \right] \cos n\theta \cos \phi \right. \\
 & \quad - \left[\frac{n}{x} \ker_{n-2} x + \frac{\sqrt{2}n(n-1)}{x^2} (\ker_{n-1} x + \ker_{n-1} x) \right] \cos(n\theta - \phi) \\
 & \quad + (1-\gamma) \left(\left[\frac{1}{2\sqrt{2}} (\ker_{n-3} x - \ker_{n-3} x) + \frac{\ker_{n-2} x}{x} \right] \cos n\theta \sin \phi \sin 2\phi \right. \\
 & \quad \quad + \frac{n}{2x} \ker_{n-2} x \sin(n\theta - \phi) \sin 2\phi \\
 & \quad \quad + \left[\frac{n}{x} \ker_{n-2} x + \frac{n(n+1)}{\sqrt{2}x^2} (\ker_{n-1} x + \ker_{n-1} x) \right. \\
 & \quad \quad \quad \left. + \frac{2n(n+1)}{x^3} \ker_n x \right] \sin(n\theta - 2\phi) \sin \phi \\
 & \quad \quad + \left[\frac{n^2}{\sqrt{2}x^2} (\ker_{n-1} x + \ker_{n-1} x) + \frac{n^2(n+1)}{x^3} \ker_n x \right] \cos(n\theta - 3\phi) \\
 & \quad \quad + \left[-\ker_{n-2} x \cos n\theta \cos 2\phi - \left\{ \frac{\sqrt{2}n}{x} (\ker_{n-1} x + \ker_{n-1} x) \right. \right. \\
 & \quad \quad \quad \left. \left. + \frac{2n(n+1)}{x^2} \ker_n x \right\} \cos(n\theta - 2\phi) \right] \left[-L \sin \phi \frac{\partial \phi}{\partial r} + \frac{1}{x} \cos \phi \frac{\partial \phi}{\partial \theta} \right] \left. \right\} \\
 & + C_{n6} \left\{ \left[\frac{1}{\sqrt{2}} (\ker_{n-3} x + \ker_{n-3} x) + \frac{2(n-2)}{x} \ker_{n-2} x \right] \cos n\theta \cos \phi \right. \\
 & \quad + \left[\frac{n}{x} \ker_{n-2} x - \frac{\sqrt{2}n(n-1)}{x} (\ker_{n-1} x - \ker_{n-1} x) \right] \cos(n\theta - \phi) \\
 & \quad + (1-\gamma) \left(\left[\frac{1}{2\sqrt{2}} (\ker_{n-3} x + \ker_{n-3} x) - \frac{\ker_{n-2} x}{x} \right] \cos n\theta \sin 2\phi \sin \phi \right. \\
 & \quad \quad - \frac{n}{2x} \ker_{n-2} x \sin(n\theta - \phi) \sin 2\phi \\
 & \quad \quad + \left[-\frac{n}{x} \ker_{n-2} x + \frac{n(n+1)}{\sqrt{2}x^2} (\ker_{n-1} x - \ker_{n-1} x) \right. \\
 & \quad \quad \quad \left. + \frac{2n(n+1)}{x^3} \ker_n x \right] \sin(n\theta - 2\phi) \sin \phi \\
 & \quad \quad + \left[\frac{n^2}{\sqrt{2}x^2} (\ker_{n-1} x - \ker_{n-1} x) + \frac{n^2(n+1)}{x^3} \ker_n x \right] \cos(n\theta - 3\phi) \\
 & \quad \quad + \left[\ker_{n-2} x \cos n\theta \cos 2\phi - \left\{ \frac{\sqrt{2}n}{x} (\ker_{n-1} x - \ker_{n-1} x) \right. \right. \\
 & \quad \quad \quad \left. \left. + \frac{2n(n+1)}{x^2} \ker_n x \right\} \cos(n\theta - 2\phi) \right] \left[-L \sin \phi \frac{\partial \phi}{\partial r} + \frac{1}{x} \cos \phi \frac{\partial \phi}{\partial \theta} \right] \left. \right\}
 \end{aligned}$$

Contrails

V_n (p.14 of 15)

$$\begin{aligned}
 & + \bar{C}_{n3} \left\{ \left[\frac{1}{\sqrt{2}} (\text{ber}_{n-3} x - \text{bei}_{n-3} x) - \frac{2(n-2)}{x} \text{bei}_{n-2} x \right] \text{Sin } n\theta \text{Cos } \phi \right. \\
 & \quad - \left[\frac{n}{x} \text{bei}_{n-2} x + \frac{\sqrt{2}n(n-1)}{x^2} (\text{ber}_{n-1} x + \text{bei}_{n-1} x) \right] \text{Sin}(n\theta - \phi) \\
 & \quad + (1-\nu) \left(\left[\frac{1}{2\sqrt{2}} (\text{ber}_{n-3} x - \text{bei}_{n-3} x) - \frac{\text{bei}_{n-2} x}{x} \right] \text{Sin } n\theta \text{Sin } 2\phi \text{Sin } \phi \right. \\
 & \quad \quad - \frac{n}{2x} \text{bei}_{n-2} x \text{Cos}(n\theta - \phi) \text{Sin } 2\phi \\
 & \quad \quad - \left[\frac{n}{x} \text{bei}_{n-2} x + \frac{n(n+1)}{\sqrt{2}x^2} (\text{ber}_{n-1} x + \text{bei}_{n-1} x) \right. \\
 & \quad \quad \quad \left. + \frac{2n(n+1)}{x^3} \text{ber}_n x \right] \text{Cos}(n\theta - 2\phi) \text{Sin } \phi \\
 & \quad \quad + \left[\frac{n^2}{\sqrt{2}x^2} (\text{ber}_{n-1} x + \text{bei}_{n-1} x) + \frac{n^2(n+1)}{x^3} \text{ber}_n x \right] \text{Sin}(n\theta - 3\phi) \\
 & \quad \quad \left. + \left[-\text{bei}_{n-2} x \text{Sin } n\theta \text{Cos } 2\phi - \left\{ \frac{\sqrt{2}n}{x} (\text{ber}_{n-1} x + \text{bei}_{n-1} x) \right. \right. \right. \\
 & \quad \quad \quad \left. \left. + \frac{2n(n+1)}{x^2} \text{ber}_n x \right\} \text{Sin}(n\theta - 2\phi) \right] \left[-L \text{Sin } \phi \frac{\partial \phi}{\partial r} + \frac{1}{x} \text{Cos } \phi \frac{\partial \phi}{\partial \theta} \right] \left. \right\} \\
 & + \bar{C}_{n4} \left\{ \left[\frac{1}{\sqrt{2}} (\text{ber}_{n-3} x + \text{bei}_{n-3} x) + \frac{2(n-2)}{x} \text{ber}_{n-2} x \right] \text{Sin } n\theta \text{Cos } \phi \right. \\
 & \quad + \left[\frac{n}{x} \text{ber}_{n-2} x - \frac{\sqrt{2}n(n-1)}{x^2} (\text{bei}_{n-1} x - \text{ber}_{n-1} x) \right] \text{Sin}(n\theta - \phi) \\
 & \quad + (1-\nu) \left(\left[\frac{1}{2\sqrt{2}} (\text{ber}_{n-3} x + \text{bei}_{n-3} x) + \frac{\text{ber}_{n-2} x}{x} \right] \text{Sin } n\theta \text{Sin } 2\phi \text{Sin } \phi \right. \\
 & \quad \quad + \frac{n}{2x} \text{ber}_{n-2} x \text{Cos}(n\theta - \phi) \text{Sin } 2\phi \\
 & \quad \quad + \left[\frac{n}{x} \text{ber}_{n-2} x - \frac{n(n+1)}{x^2} (\text{bei}_{n-1} x - \text{ber}_{n-1} x) \right. \\
 & \quad \quad \quad \left. - \frac{2n(n+1)}{x^3} \text{bei}_n x \right] \text{Cos}(n\theta - 2\phi) \text{Sin } \phi \\
 & \quad \quad + \left[\frac{n^2}{\sqrt{2}x^2} (\text{bei}_{n-1} x - \text{ber}_{n-1} x) + \frac{n^2(n+1)}{x^3} \text{bei}_n x \right] \text{Sin}(n\theta - 3\phi) \\
 & \quad \quad \left. + \left[\text{ber}_{n-2} x \text{Sin } n\theta \text{Cos } 2\phi - \left\{ \frac{\sqrt{2}n}{x} (\text{bei}_{n-1} x - \text{ber}_{n-1} x) \right. \right. \right. \\
 & \quad \quad \quad \left. \left. + \frac{2n(n+1)}{x^2} \text{bei}_n x \right\} \text{Sin}(n\theta - 2\phi) \right] \left[-L \text{Sin } \phi \frac{\partial \phi}{\partial r} + \frac{1}{x} \text{Cos } \phi \frac{\partial \phi}{\partial \theta} \right] \left. \right\}
 \end{aligned}$$

Contrails

V_n (p.15 of 15)

$$\begin{aligned}
 & + \bar{c}_{n5} \left\{ \left[\frac{1}{\sqrt{2}} (\ker_{n-3} x - \ker_{n-3} x) - \frac{2(n-2)}{x} \ker_{n-2} x \right] \sin n\theta \cos \phi \right. \\
 & \quad - \left[\frac{n}{x} \ker_{n-2} x + \frac{\sqrt{2} n(n-1)}{x^2} (\ker_{n-1} x + \ker_{n-1} x) \right] \sin(n\theta - \phi) \\
 & \quad + (1-\nu) \left\{ \left[\frac{1}{2\sqrt{2}} (\ker_{n-3} x - \ker_{n-3} x) - \frac{\ker_{n-2} x}{x} \right] \sin n\theta \sin 2\phi \sin \phi \right. \\
 & \quad \quad - \frac{n}{2x} \ker_{n-2} x \cos(n\theta - \phi) \sin 2\phi \\
 & \quad \quad - \left[\frac{n}{x} \ker_{n-2} x + \frac{n(n+1)}{\sqrt{2} x^2} (\ker_{n-1} x + \ker_{n-1} x) \right. \\
 & \quad \quad \quad \left. + \frac{2n(n+1)}{x^3} \ker_n x \right] \cos(n\theta - 2\phi) \sin \phi \\
 & \quad \quad + \left[\frac{n^2}{\sqrt{2} x^2} (\ker_{n-1} x + \ker_{n-1} x) + \frac{n^2(n+1)}{x^3} \ker_n x \right] \sin(n\theta - 3\phi) \\
 & \quad \quad \left. + \left[-\ker_{n-2} x \sin n\theta \cos 2\phi - \left\{ \frac{\sqrt{2} n}{x} (\ker_{n-1} x + \ker_{n-1} x) \right. \right. \right. \\
 & \quad \quad \quad \left. \left. + \frac{2n(n+1)}{x^2} \ker_n x \right\} \sin(n\theta - 2\phi) \right] \left[-L \sin \phi \frac{\partial \phi}{\partial r} + \frac{1}{x} \cos \phi \frac{\partial \phi}{\partial \theta} \right] \left. \right\} \\
 & + \bar{c}_{n6} \left\{ \left[\frac{1}{\sqrt{2}} (\ker_{n-3} x + \ker_{n-3} x) + \frac{2(n-2)}{x} \ker_{n-2} x \right] \sin n\theta \cos \phi \right. \\
 & \quad + \left[\frac{n}{x} \ker_{n-2} x - \frac{\sqrt{2} n(n-1)}{x^2} (\ker_{n-1} x - \ker_{n-1} x) \right] \sin(n\theta - \phi) \\
 & \quad + (1-\nu) \left\{ \left[\frac{1}{2\sqrt{2}} (\ker_{n-3} x + \ker_{n-3} x) + \frac{\ker_{n-2} x}{x} \right] \sin n\theta \sin 2\phi \sin \phi \right. \\
 & \quad \quad + \frac{n}{2x} \ker_{n-2} x \cos(n\theta - \phi) \sin 2\phi \\
 & \quad \quad + \left[\frac{n}{x} \ker_{n-2} x - \frac{n(n+1)}{x^2} (\ker_{n-1} x - \ker_{n-1} x) \right. \\
 & \quad \quad \quad \left. - \frac{2n(n+1)}{x^3} \ker_n x \right] \cos(n\theta - 2\phi) \sin \phi \\
 & \quad \quad + \left[\frac{n^2}{\sqrt{2} x^2} (\ker_{n-1} x - \ker_{n-1} x) + \frac{n^2(n+1)}{x^3} \ker_n x \right] \sin(n\theta - 3\phi) \\
 & \quad \quad \left. + \left[\ker_{n-2} x \sin n\theta \cos 2\phi - \left\{ \frac{\sqrt{2} n}{x} (\ker_{n-1} x - \ker_{n-1} x) \right. \right. \right. \\
 & \quad \quad \quad \left. \left. + \frac{2n(n+1)}{x^2} \ker_n x \right\} \sin(n\theta - 2\phi) \right] \left[-L \sin \phi \frac{\partial \phi}{\partial r} + \frac{1}{x} \cos \phi \frac{\partial \phi}{\partial \theta} \right] \left. \right\}
 \end{aligned}$$

Contrails

N_{nn} (p.1 of 3)

$$\begin{aligned}
 N_{nn} = \frac{1}{|\lambda|\lambda^2} \left\{ \right. & C_{03} \left(\text{ber } x \sin^2 \phi + \frac{\text{bei}'x}{x} \cos 2\phi \right) \\
 & + C_{04} \left(\text{bei } x \sin^2 \phi - \frac{\text{ber}'x}{x} \cos 2\phi \right) \\
 & + C_{05} \left(\text{ker } x \sin^2 \phi + \frac{\text{kei}'x}{x} \cos 2\phi \right) \\
 & + C_{06} \left(\text{kei } x \sin^2 \phi - \frac{\text{ker}'x}{x} \cos 2\phi \right) \\
 & + C_{08} \left(\frac{\cos 2\phi}{x^2} \right) \\
 & + \frac{C_{10}}{\sqrt{2}} \left((\text{ber}'x - \text{bei}'x) \cos \theta \sin^2 \phi \right. \\
 & \quad \left. + \left(\left(\frac{\text{ber } x - \text{bei } x}{x} \right) - 2 \left(\frac{\text{ber}'x + \text{bei}'x}{x^2} \right) \right) \cos(\theta - 2\phi) \right) \\
 & + \frac{C_{14}}{\sqrt{2}} \left((\text{ber}'x + \text{bei}'x) \cos \theta \sin^2 \phi \right. \\
 & \quad \left. + \left(\left(\frac{\text{ber } x + \text{bei } x}{x} \right) + 2 \left(\frac{\text{ber}'x - \text{bei}'x}{x^2} \right) \right) \cos(\theta - 2\phi) \right) \\
 & + \frac{C_{15}}{\sqrt{2}} \left((\text{ker}'x - \text{kei}'x) \cos \theta \sin^2 \phi \right. \\
 & \quad \left. + \left(\left(\frac{\text{ker } x - \text{kei } x}{x} \right) - 2 \left(\frac{\text{ker}'x + \text{kei}'x}{x^2} \right) \right) \cos(\theta - 2\phi) \right) \\
 & + \frac{C_{16}}{\sqrt{2}} \left((\text{ker}'x + \text{kei}'x) \cos \theta \sin^2 \phi \right. \\
 & \quad \left. + \left(\left(\frac{\text{ker } x + \text{kei } x}{x} \right) + 2 \left(\frac{\text{ker}'x - \text{kei}'x}{x^2} \right) \right) \cos(\theta - 2\phi) \right) \\
 & + \frac{C_{13}}{\sqrt{2}} \left((\text{ber}'x - \text{bei}'x) \sin \theta \sin^2 \phi \right. \\
 & \quad \left. + \left(\left(\frac{\text{ber } x - \text{bei } x}{x} \right) - 2 \left(\frac{\text{ber}'x + \text{bei}'x}{x^2} \right) \right) \sin(\theta - 2\phi) \right) \\
 & + \frac{C_{14}}{\sqrt{2}} \left((\text{ber}'x + \text{bei}'x) \sin \theta \sin^2 \phi \right. \\
 & \quad \left. + \left(\left(\frac{\text{ber } x + \text{bei } x}{x} \right) + 2 \left(\frac{\text{ber}'x - \text{bei}'x}{x^2} \right) \right) \sin(\theta - 2\phi) \right)
 \end{aligned}$$

Contrails

N_{nn} (p.2 of 3)

$$\begin{aligned}
 & + \frac{\bar{C}_{15}}{\sqrt{2}} \left((\ker'x - \operatorname{kei}'x) \sin \theta \sin^2 \phi \right. \\
 & \quad \left. + \left(\frac{\ker x - \operatorname{kei} x}{x} - 2 \left(\frac{\ker'x + \operatorname{kei}'x}{x^2} \right) \right) \sin(\theta - 2\phi) \right) \\
 & + \frac{\bar{C}_{16}}{\sqrt{2}} \left((\ker'x + \operatorname{kei}'x) \sin \theta \sin^2 \phi \right. \\
 & \quad \left. + \left(\frac{\ker x + \operatorname{kei} x}{x} + 2 \left(\frac{\ker'x - \operatorname{kei}'x}{x^2} \right) \right) \sin(\theta - 2\phi) \right) \\
 & + C_{17} \left(\frac{\cos(\theta + 2\phi)}{x} \right) \\
 & - \bar{C}_{17} \left(\frac{\sin(\theta + 2\phi)}{x} \right) \\
 & + \sum_{n=2}^{\infty} C_{n3} \left(- \left(\operatorname{ber}_{n-2} x \sin^2 \phi + \frac{n-1}{\sqrt{2}x} (\operatorname{ber}_{n-1} x - \operatorname{bei}_{n-1} x) \right) \cos n\theta \right. \\
 & \quad \left. + \left(\frac{n}{\sqrt{2}x} (\operatorname{ber}_{n-1} x - \operatorname{bei}_{n-1} x) - \frac{n(n+1)}{x^2} \operatorname{bei}_n x \right) \cos(n\theta - 2\phi) \right) \\
 & + C_{n4} \left(- \left(\operatorname{bei}_{n-2} x \sin^2 \phi + \frac{n-1}{\sqrt{2}x} (\operatorname{ber}_{n-1} x + \operatorname{bei}_{n-1} x) \right) \cos n\theta \right. \\
 & \quad \left. + \left(\frac{n}{\sqrt{2}x} (\operatorname{ber}_{n-1} x + \operatorname{bei}_{n-1} x) + \frac{n(n+1)}{x^2} \operatorname{ber}_n x \right) \cos(n\theta - 2\phi) \right) \\
 & + C_{n5} \left(- \left(\ker_{n-2} x \sin^2 \phi + \frac{n-1}{\sqrt{2}x} (\ker_{n-1} x - \operatorname{kei}_{n-1} x) \right) \cos n\theta \right. \\
 & \quad \left. + \left(\frac{n}{\sqrt{2}x} (\ker_{n-1} x - \operatorname{kei}_{n-1} x) - \frac{n(n+1)}{x^2} \operatorname{kei}_n x \right) \cos(n\theta - 2\phi) \right) \\
 & + C_{n6} \left(- \left(\operatorname{kei}_{n-2} x \sin^2 \phi + \frac{n-1}{\sqrt{2}x} (\ker_{n-1} x + \operatorname{kei}_{n-1} x) \right) \cos n\theta \right. \\
 & \quad \left. + \left(\frac{n}{\sqrt{2}x} (\ker_{n-1} x + \operatorname{kei}_{n-1} x) + \frac{n(n+1)}{x^2} \ker_n x \right) \cos(n\theta - 2\phi) \right) \\
 & - C_{n7} \left(n(n-1) x^{n-2} \cos(n\theta + 2\phi) \right) \\
 & - C_{n8} \left(n(n+1) x^{-(n+2)} \cos(n\theta - 2\phi) \right)
 \end{aligned}$$

Contrails

N_{nn} (p.3 of 3)

$$\begin{aligned}
 & + \bar{C}_{n3} \left(-(\text{ber}_{n-2} x \sin^2 \phi + \frac{n-1}{\sqrt{2}x} (\text{ber}_{n-1} x - \text{bei}_{n-1} x)) \sin n\theta \right. \\
 & \quad \left. + \left(\frac{n}{\sqrt{2}x} (\text{ber}_{n-1} x - \text{bei}_{n-1} x) - \frac{n(n+1)}{x^2} \text{bei}_n x \right) \sin(n\theta - 2\phi) \right) \\
 & + \bar{C}_{n4} \left(-(\text{bei}_{n-2} x \sin^2 \phi + \frac{n-1}{\sqrt{2}x} (\text{ber}_{n-1} x + \text{bei}_{n-1} x)) \sin n\theta \right. \\
 & \quad \left. + \left(\frac{n}{\sqrt{2}x} (\text{ber}_{n-1} x + \text{bei}_{n-1} x) + \frac{n(n+1)}{x^2} \text{ber}_n x \right) \sin(n\theta - 2\phi) \right) \\
 & + \bar{C}_{n5} \left(-(\text{ker}_{n-2} x \sin^2 \phi + \frac{n-1}{\sqrt{2}x} (\text{ker}_{n-1} x - \text{kei}_{n-1} x)) \sin n\theta \right. \\
 & \quad \left. + \left(\frac{n}{\sqrt{2}x} (\text{ker}_{n-1} x - \text{kei}_{n-1} x) - \frac{n(n+1)}{x^2} \text{kei}_n x \right) \sin(n\theta - 2\phi) \right) \\
 & + \bar{C}_{n6} \left(-(\text{kei}_{n-2} x \sin^2 \phi + \frac{n-1}{\sqrt{2}x} (\text{ker}_{n-1} x + \text{kei}_{n-1} x)) \sin n\theta \right. \\
 & \quad \left. + \left(\frac{n}{\sqrt{2}x} (\text{ker}_{n-1} x + \text{kei}_{n-1} x) + \frac{n(n+1)}{x^2} \text{ker}_n x \right) \sin(n\theta - 2\phi) \right) \\
 & - \bar{C}_{n7} \left(n(n-1)x^{n-2} \sin(n\theta + 2\phi) \right) \\
 & - \bar{C}_{n8} \left(n(n+1)x^{-(n+2)} \sin(n\theta - 2\phi) \right) \}
 \end{aligned}$$

Contrails

N_{nt} (p.1 of 3)

$$\begin{aligned}
 N_{nt} = \frac{1}{|\lambda| l^2} \left\{ \right. & C_{03} \left(\left(\frac{\text{ber}x}{2} - \frac{\text{bei}'x}{x} \right) \sin 2\phi \right) \\
 & + C_{04} \left(\left(\frac{\text{bei}x}{2} + \frac{\text{ber}'x}{x} \right) \sin 2\phi \right) \\
 & + C_{05} \left(\left(\frac{\text{ker}x}{2} - \frac{\text{kei}'x}{x} \right) \sin 2\phi \right) \\
 & + C_{06} \left(\left(\frac{\text{kei}x}{2} + \frac{\text{ker}'x}{x} \right) \sin 2\phi \right) \\
 & - C_{08} \left(\frac{1}{x^2} \sin 2\phi \right) \\
 & + \frac{C_{13}}{\sqrt{2}} \left(\frac{1}{2} (\text{ber}'x - \text{bei}'x) \cos \theta \sin 2\phi \right. \\
 & \quad \left. + \left(\left(\frac{\text{ber}x - \text{beix}}{x} \right) - 2 \left(\frac{\text{ber}'x + \text{bei}'x}{x^2} \right) \right) \sin(\theta - 2\phi) \right) \\
 & + \frac{C_{14}}{\sqrt{2}} \left(\frac{1}{2} (\text{ber}'x + \text{bei}'x) \cos \theta \sin 2\phi \right. \\
 & \quad \left. + \left(\left(\frac{\text{ber}x + \text{beix}}{x} \right) + 2 \left(\frac{\text{ber}'x - \text{bei}'x}{x^2} \right) \right) \sin(\theta - 2\phi) \right) \\
 & + \frac{C_{15}}{\sqrt{2}} \left(\frac{1}{2} (\text{ker}'x - \text{kei}'x) \cos \theta \sin 2\phi \right. \\
 & \quad \left. + \left(\left(\frac{\text{ker}x - \text{keix}}{x} \right) - 2 \left(\frac{\text{ker}'x + \text{kei}'x}{x^2} \right) \right) \sin(\theta - 2\phi) \right) \\
 & + \frac{C_{16}}{\sqrt{2}} \left(\frac{1}{2} (\text{ker}'x + \text{kei}'x) \cos \theta \sin 2\phi \right. \\
 & \quad \left. + \left(\left(\frac{\text{ker}x + \text{keix}}{x} \right) + 2 \left(\frac{\text{ker}'x - \text{kei}'x}{x^2} \right) \right) \sin(\theta - 2\phi) \right) \\
 & - C_{19} \left(\frac{\sin(\theta + 2\phi)}{x} \right)
 \end{aligned}$$

Contrails

N_{nt} (p.2 of 3)

$$\begin{aligned}
 & + \frac{\bar{C}_{13}}{\sqrt{2}} \left(\frac{1}{2} (\text{ber}'x - \text{bei}'x) \sin \theta \sin 2\phi \right. \\
 & \quad \left. - \left(\left(\frac{\text{ber}x - \text{beix}}{x} \right) - 2 \left(\frac{\text{ber}'x + \text{bei}'x}{x^2} \right) \right) \cos(\theta - 2\phi) \right) \\
 & + \frac{\bar{C}_{14}}{\sqrt{2}} \left(\frac{1}{2} (\text{ber}'x + \text{bei}'x) \sin \theta \sin 2\phi \right. \\
 & \quad \left. - \left(\left(\frac{\text{ber}x + \text{beix}}{x} \right) + 2 \left(\frac{\text{ber}'x - \text{bei}'x}{x^2} \right) \right) \cos(\theta - 2\phi) \right) \\
 & + \frac{\bar{C}_{15}}{\sqrt{2}} \left(\frac{1}{2} (\text{ker}'x - \text{kei}'x) \sin \theta \sin 2\phi \right. \\
 & \quad \left. - \left(\left(\frac{\text{ker}x - \text{keix}}{x} \right) - 2 \left(\frac{\text{ker}'x + \text{kei}'x}{x^2} \right) \right) \cos(\theta - 2\phi) \right) \\
 & + \frac{\bar{C}_{16}}{\sqrt{2}} \left(\frac{1}{2} (\text{ker}'x + \text{kei}'x) \sin \theta \sin 2\phi \right. \\
 & \quad \left. - \left(\left(\frac{\text{ker}x + \text{keix}}{x} \right) + 2 \left(\frac{\text{ker}'x - \text{kei}'x}{x^2} \right) \right) \cos(\theta - 2\phi) \right) \\
 & - \bar{C}_{19} \left(\frac{\cos(\theta + 2\phi)}{x} \right) \\
 & + \sum_{n=2}^{\infty} C_{n3} \left(- \frac{\text{ber}_{n-2}x}{2} \cos n\theta \sin 2\phi \right. \\
 & \quad \left. + \left(\frac{n}{\sqrt{2}x} (\text{ber}_{n-1}x - \text{bei}_{n-1}x) - \frac{n(n+1)}{x^2} \text{bei}_n x \right) \sin(n\theta - 2\phi) \right) \\
 & + C_{n4} \left(- \frac{\text{bei}_{n-2}x}{2} \cos n\theta \sin 2\phi \right. \\
 & \quad \left. + \left(\frac{n}{\sqrt{2}x} (\text{ber}_{n-1}x + \text{bei}_{n-1}x) + \frac{n(n+1)}{x^2} \text{ber}_n x \right) \sin(n\theta - 2\phi) \right) \\
 & + C_{n5} \left(- \frac{\text{ker}_{n-2}x}{2} \cos n\theta \sin 2\phi \right. \\
 & \quad \left. + \left(\frac{n}{\sqrt{2}x} (\text{ker}_{n-1}x - \text{kei}_{n-1}x) - \frac{n(n+1)}{x^2} \text{kei}_n x \right) \sin(n\theta - 2\phi) \right) \\
 & + C_{n6} \left(- \frac{\text{kei}_{n-2}x}{2} \cos n\theta \sin 2\phi \right. \\
 & \quad \left. + \left(\frac{n}{\sqrt{2}x} (\text{ker}_{n-1}x + \text{kei}_{n-1}x) + \frac{n(n+1)}{x^2} \text{ker}_n x \right) \sin(n\theta - 2\phi) \right)
 \end{aligned}$$

Contrails

N_{nt} (p.3 of 3)

$$\begin{aligned}
 &+ C_{n7} (n(n-1)x^{n-2} \sin(n\theta + 2\phi)) \\
 &- C_{n8} (n(n+1)x^{-(n+2)} \sin(n\theta - 2\phi)) \\
 &- \bar{C}_{n3} \left(\frac{\text{ber}_{n-2} x}{2} \sin n\theta \sin 2\phi \right. \\
 &\quad \left. + \left(\frac{n}{\sqrt{2}} x (\text{ber}_{n-1} x - \text{bei}_{n-1} x) - \frac{n(n+1)}{x^2} \text{bei}_n x \right) \cos(n\theta - 2\phi) \right) \\
 &- \bar{C}_{n4} \left(\frac{\text{bei}_{n-2} x}{2} \sin n\theta \sin 2\phi \right. \\
 &\quad \left. + \left(\frac{n}{\sqrt{2}} x (\text{ber}_{n-1} x + \text{bei}_{n-1} x) + \frac{n(n+1)}{x^2} \text{ber}_n x \right) \cos(n\theta - 2\phi) \right) \\
 &- \bar{C}_{n5} \left(\frac{\text{ker}_{n-2} x}{2} \sin n\theta \sin 2\phi \right. \\
 &\quad \left. + \left(\frac{n}{\sqrt{2}} x (\text{ker}_{n-1} x - \text{kei}_{n-1} x) - \frac{n(n+1)}{x^2} \text{kei}_n x \right) \cos(n\theta - 2\phi) \right) \\
 &- \bar{C}_{n6} \left(\frac{\text{kei}_{n-2} x}{2} \sin n\theta \sin 2\phi \right. \\
 &\quad \left. + \left(\frac{n}{\sqrt{2}} x (\text{ker}_{n-1} x + \text{kei}_{n-1} x) + \frac{n(n+1)}{x^2} \text{ker}_n x \right) \cos(n\theta - 2\phi) \right) \\
 &- \bar{C}_{n7} (n(n-1)x^{n-2} \cos(n\theta + 2\phi)) \\
 &+ \bar{C}_{n8} (n(n+1)x^{-(n+2)} \cos(n\theta - 2\phi)) \}
 \end{aligned}$$

Contrails

N_k (p.1 of 4)

$$\text{let } \alpha = -D/|\lambda|(1-\nu)$$

$$\begin{aligned}
 N_k = \frac{1}{|\lambda|l^2} & \left\{ C_{03} \left(\left(\left(\frac{\text{ber}x}{2} - \frac{\text{bei}'x}{x} \right) + \alpha \left(\frac{\text{beix}}{2} + \frac{\text{ber}'x}{x} \right) \right) \sin 2\phi \right) \right. \\
 & + C_{04} \left(\left(\left(\frac{\text{beix}}{2} + \frac{\text{ber}'x}{x} \right) - \alpha \left(\frac{\text{ber}x}{2} - \frac{\text{bei}'x}{x} \right) \right) \sin 2\phi \right) \\
 & + C_{05} \left(\left(\left(\frac{\text{ker}x}{2} - \frac{\text{kei}'x}{x} \right) + \alpha \left(\frac{\text{keix}}{2} + \frac{\text{ker}'x}{x} \right) \right) \sin 2\phi \right) \\
 & + C_{06} \left(\left(\left(\frac{\text{keix}}{2} + \frac{\text{ker}'x}{x} \right) - \alpha \left(\frac{\text{ker}x}{2} - \frac{\text{kei}'x}{x} \right) \right) \sin 2\phi \right) \\
 & - C_{08} \left(\frac{1}{x^2} \sin 2\phi \right) \\
 & + C_{12} \left(\frac{2\alpha}{x^3} \sin(\theta - 2\phi) \right) \\
 & + \frac{C_{13}}{\sqrt{2}} \left(\frac{1}{2} \left((\text{ber}'x - \text{bei}'x) + \alpha(\text{ber}'x + \text{bei}'x) \right) \cos \theta \sin 2\phi \right. \\
 & \quad + \left(\left(\left(\frac{\text{ber}x - \text{beix}}{x} \right) - 2 \left(\frac{\text{ber}'x + \text{bei}'x}{x^2} \right) \right) + \alpha \left(\left(\frac{\text{ber}x + \text{beix}}{x} \right) \right. \right. \\
 & \quad \left. \left. + 2 \left(\frac{\text{ber}'x - \text{bei}'x}{x^2} \right) \right) \right) \sin(\theta - 2\phi) \right) \\
 & + \frac{C_{14}}{\sqrt{2}} \left(\frac{1}{2} \left((\text{ber}'x + \text{bei}'x) - \alpha(\text{ber}'x - \text{bei}'x) \right) \cos \theta \sin 2\phi \right. \\
 & \quad + \left(\left(\left(\frac{\text{ber}x + \text{beix}}{x} \right) + 2 \left(\frac{\text{ber}'x - \text{bei}'x}{x^2} \right) \right) - \alpha \left(\left(\frac{\text{ber}x - \text{beix}}{x} \right) \right. \right. \\
 & \quad \left. \left. - 2 \left(\frac{\text{ber}'x + \text{bei}'x}{x^2} \right) \right) \right) \sin(\theta - 2\phi) \right) \\
 & + \frac{C_{15}}{\sqrt{2}} \left(\frac{1}{2} \left((\text{ker}'x - \text{kei}'x) + \alpha(\text{ker}'x + \text{kei}'x) \right) \cos \theta \sin 2\phi \right. \\
 & \quad + \left(\left(\left(\frac{\text{ker}x - \text{keix}}{x} \right) - 2 \left(\frac{\text{ker}'x + \text{kei}'x}{x^2} \right) \right) + \alpha \left(\left(\frac{\text{ker}x + \text{keix}}{x} \right) \right. \right. \\
 & \quad \left. \left. + 2 \left(\frac{\text{ker}'x - \text{kei}'x}{x^2} \right) \right) \right) \sin(\theta - 2\phi) \right)
 \end{aligned}$$

Contrails

N_k (p.2 of 4)

$$\begin{aligned}
 & + \frac{C_{15}}{\sqrt{2}} \left(\frac{1}{2} ((k_{er}'x + k_{ei}'x) - \alpha(k_{er}'x - k_{ei}'x)) \cos \theta \sin 2\phi \right. \\
 & \quad + \left(\left(\left(\frac{k_{er}x + k_{ei}x}{x} \right) + 2 \left(\frac{k_{er}'x - k_{ei}'x}{x^2} \right) \right) - \alpha \left(\left(\frac{k_{er}x - k_{ei}x}{x} \right) \right. \right. \\
 & \quad \quad \left. \left. - 2 \left(\frac{k_{er}'x + k_{ei}'x}{x^2} \right) \right) \right) \sin(\theta - 2\phi) \\
 & - C_{19} \left(\frac{\sin(\theta + 2\phi)}{x} \right) \\
 & + \frac{\bar{C}_{12}}{\sqrt{2}} \left(\frac{1}{2} ((ber'x - bei'x) + \alpha(ber'x + bei'x)) \sin \theta \sin 2\phi \right. \\
 & \quad - \left(\left(\left(\frac{berx - bei'x}{x} \right) - 2 \left(\frac{ber'x + bei'x}{x^2} \right) \right) + \alpha \left(\left(\frac{berx + bei'x}{x} \right) \right. \right. \\
 & \quad \quad \left. \left. + 2 \left(\frac{ber'x - bei'x}{x^2} \right) \right) \right) \cos(\theta - 2\phi) \\
 & + \frac{\bar{C}_{14}}{\sqrt{2}} \left(\frac{1}{2} ((ber'x + bei'x) - \alpha(ber'x - bei'x)) \sin \theta \sin 2\phi \right. \\
 & \quad - \left(\left(\left(\frac{berx + bei'x}{x} \right) + 2 \left(\frac{ber'x - bei'x}{x^2} \right) \right) - \alpha \left(\left(\frac{berx - bei'x}{x} \right) \right. \right. \\
 & \quad \quad \left. \left. - 2 \left(\frac{ber'x + bei'x}{x^2} \right) \right) \right) \cos(\theta - 2\phi) \\
 & + \frac{\bar{C}_{15}}{\sqrt{2}} \left(\frac{1}{2} ((ker'x - kei'x) + \alpha(ker'x + kei'x)) \sin \theta \sin 2\phi \right. \\
 & \quad - \left(\left(\left(\frac{kerx - kei'x}{x} \right) - 2 \left(\frac{ker'x + kei'x}{x^2} \right) \right) + \alpha \left(\left(\frac{kerx + kei'x}{x} \right) \right. \right. \\
 & \quad \quad \left. \left. + 2 \left(\frac{ker'x - kei'x}{x^2} \right) \right) \right) \cos(\theta - 2\phi) \\
 & + \frac{\bar{C}_{16}}{\sqrt{2}} \left(\frac{1}{2} ((ker'x + kei'x) - \alpha(ker'x - kei'x)) \sin \theta \sin 2\phi \right. \\
 & \quad - \left(\left(\left(\frac{kerx + kei'x}{x} \right) + 2 \left(\frac{ker'x - kei'x}{x^2} \right) \right) - \alpha \left(\left(\frac{kerx - kei'x}{x} \right) \right. \right. \\
 & \quad \quad \left. \left. - 2 \left(\frac{ker'x + kei'x}{x^2} \right) \right) \right) \cos(\theta - 2\phi)
 \end{aligned}$$

Contrails

N_k (p.3 of 4)

$$\begin{aligned}
 & -\bar{C}_{19} \left(\frac{\cos(\theta+2\phi)}{x} \right) \\
 & + \sum_{n=2}^{\infty} \left[-C_{n1} (\alpha n(n-1) x^{n-2} \sin(n\theta+2\phi)) \right. \\
 & \quad \left. + C_{n2} (\alpha n(n+1) x^{-(n+2)} \sin(n\theta-2\phi)) \right. \\
 & \quad + C_{n3} \left(-\frac{1}{2} (\text{ber}_{n-2} x + \alpha \text{bei}_{n-2} x) \cos n\theta \sin 2\phi \right. \\
 & \quad \left. + \left(\left(\frac{n}{\sqrt{2}} x (\text{ber}_{n-1} x - \text{bei}_{n-1} x) - \frac{n(n+1)}{x^2} \text{bei}_n x \right) \right. \right. \\
 & \quad \left. \left. + \alpha \left(\frac{n}{\sqrt{2}} x (\text{ber}_{n-1} x + \text{bei}_{n-1} x) + \frac{n(n+1)}{x^2} \text{ber}_n x \right) \right) \sin(n\theta-2\phi) \right) \\
 & \quad + C_{n4} \left(-\frac{1}{2} (\text{bei}_{n-2} x - \alpha \text{ber}_{n-2} x) \cos n\theta \sin 2\phi \right. \\
 & \quad \left. + \left(\left(\frac{n}{\sqrt{2}} x (\text{ber}_{n-1} x + \text{bei}_{n-1} x) + \frac{n(n+1)}{x^2} \text{ber}_n x \right) \right. \right. \\
 & \quad \left. \left. + \alpha \left(\frac{n}{\sqrt{2}} x (\text{bei}_{n-1} x - \text{ber}_{n-1} x) + \frac{n(n+1)}{x^2} \text{bei}_n x \right) \right) \sin(n\theta-2\phi) \right) \\
 & \quad + C_{n5} \left(-\frac{1}{2} (\text{ker}_{n-2} x + \alpha \text{kei}_{n-2} x) \cos n\theta \sin 2\phi \right. \\
 & \quad \left. + \left(\left(\frac{n}{\sqrt{2}} x (\text{ker}_{n-1} x - \text{kei}_{n-1} x) - \frac{n(n+1)}{x^2} \text{kei}_n x \right) \right. \right. \\
 & \quad \left. \left. + \alpha \left(\frac{n}{\sqrt{2}} x (\text{ker}_{n-1} x + \text{kei}_{n-1} x) + \frac{n(n+1)}{x^2} \text{ker}_n x \right) \right) \sin(n\theta-2\phi) \right) \\
 & \quad + C_{n6} \left(-\frac{1}{2} (\text{kei}_{n-2} x - \alpha \text{ker}_{n-2} x) \cos n\theta \sin 2\phi \right. \\
 & \quad \left. + \left(\left(\frac{n}{\sqrt{2}} x (\text{ker}_{n-1} x + \text{kei}_{n-1} x) + \frac{n(n+1)}{x^2} \text{ker}_n x \right) \right. \right. \\
 & \quad \left. \left. + \alpha \left(\frac{n}{\sqrt{2}} x (\text{kei}_{n-1} x - \text{ker}_{n-1} x) + \frac{n(n+1)}{x^2} \text{kei}_n x \right) \right) \sin(n\theta-2\phi) \right) \\
 & \quad + C_{n7} (n(n-1) x^{n-2} \sin(n\theta+2\phi)) \\
 & \quad - C_{n8} (n(n+1) x^{-(n+2)} \sin(n\theta-2\phi))
 \end{aligned}$$

Contrails

N_k (p.4 of 4)

$$\begin{aligned}
 & + \bar{C}_{n1} (\alpha n(n-1) x^{n-2} \cos(n\theta + 2\phi)) \\
 & - \bar{C}_{n2} (\alpha n(n+1) x^{-(n+2)} \cos(n\theta - 2\phi)) \\
 & - \bar{C}_{n3} \left(\frac{1}{2} (\text{ber}_{n-2} x + \alpha \text{bei}_{n-2} x) \sin n\theta \sin 2\phi \right. \\
 & \quad + \left(\left(\frac{n}{\sqrt{2}x} (\text{ber}_{n-1} x - \text{bei}_{n-1} x) - \frac{n(n+1)}{x^2} \text{bei}_n x \right) \right. \\
 & \quad \left. \left. + \alpha \left(\frac{n}{\sqrt{2}x} (\text{ber}_{n-1} x + \text{bei}_{n-1} x) + \frac{n(n+1)}{x^2} \text{ber}_n x \right) \right) \cos(n\theta - 2\phi) \right) \\
 & - \bar{C}_{n4} \left(\frac{1}{2} (\text{bei}_{n-2} x - \alpha \text{ber}_{n-2} x) \sin n\theta \sin 2\phi \right. \\
 & \quad + \left(\left(\frac{n}{\sqrt{2}x} (\text{ber}_{n-1} x + \text{bei}_{n-1} x) + \frac{n(n+1)}{x^2} \text{ber}_n x \right) \right. \\
 & \quad \left. \left. + \alpha \left(\frac{n}{\sqrt{2}x} (\text{bei}_{n-1} x - \text{ber}_{n-1} x) + \frac{n(n+1)}{x^2} \text{bei}_n x \right) \right) \cos(n\theta - 2\phi) \right) \\
 & - \bar{C}_{n5} \left(\frac{1}{2} (\text{ker}_{n-2} x + \alpha \text{kei}_{n-2} x) \sin n\theta \sin 2\phi \right. \\
 & \quad + \left(\left(\frac{n}{\sqrt{2}x} (\text{ker}_{n-1} x - \text{kei}_{n-1} x) - \frac{n(n+1)}{x^2} \text{kei}_n x \right) \right. \\
 & \quad \left. \left. + \alpha \left(\frac{n}{\sqrt{2}x} (\text{ker}_{n-1} x + \text{kei}_{n-1} x) + \frac{n(n+1)}{x^2} \text{ker}_n x \right) \right) \cos(n\theta - 2\phi) \right) \\
 & - \bar{C}_{n6} \left(\frac{1}{2} (\text{kei}_{n-2} x - \alpha \text{ker}_{n-2} x) \sin n\theta \sin 2\phi \right. \\
 & \quad + \left(\left(\frac{n}{\sqrt{2}x} (\text{ker}_{n-1} x + \text{kei}_{n-1} x) + \frac{n(n+1)}{x^2} \text{ker}_n x \right) \right. \\
 & \quad \left. \left. + \alpha \left(\frac{n}{\sqrt{2}x} (\text{kei}_{n-1} x - \text{ker}_{n-1} x) + \frac{n(n+1)}{x^2} \text{kei}_n x \right) \right) \cos(n\theta - 2\phi) \right) \\
 & - \bar{C}_{n7} (n(n-1) x^{n-2} \cos(n\theta + 2\phi)) \\
 & + \bar{C}_{n8} (n(n+1) x^{-(n+2)} \cos(n\theta - 2\phi)) \left. \right\}
 \end{aligned}$$

Contrails

u_r (p.1 of 3)

$$u_r = u \cos \phi + v \sin \phi$$

$$\begin{aligned}
 u_r = \frac{R}{R} \left\{ \left[-C_{01} x - C_{03}(1+\nu) \text{bei}'x + C_{04}(1+\nu) \text{ber}'x - C_{05}(1+\nu) \text{kei}'x \right. \right. \\
 \left. \left. + C_{06}(1+\nu) \text{ker}'x - C_{08}(1+\nu) \frac{1}{x} \right] \cos \phi \right. \\
 - C_{11} \frac{x^2}{2} \cos(\theta - \phi) \\
 + 2C_{19}(1+\nu) \ln x \cos(\theta + \phi) \\
 + C_{13} \frac{(1+\nu)}{\sqrt{2}} \left[-(\text{ber}x - \text{bei}x) \cos \theta \cos \phi + \left(\frac{\text{ber}'x + \text{bei}'x}{x} \right) \cos(\theta - \phi) \right] \\
 - C_{14} \frac{(1+\nu)}{\sqrt{2}} \left[(\text{ber}x + \text{bei}x) \cos \theta \cos \phi + \left(\frac{\text{ber}'x - \text{bei}'x}{x} \right) \cos(\theta - \phi) \right] \\
 + C_{15} \frac{(1+\nu)}{\sqrt{2}} \left[-(\text{ker}x - \text{kei}x) \cos \theta \cos \phi + \left(\frac{\text{ker}'x + \text{kei}'x}{x} \right) \cos(\theta - \phi) \right] \\
 - C_{16} \frac{(1+\nu)}{\sqrt{2}} \left[(\text{ker}x + \text{kei}x) \cos \theta \cos \phi + \left(\frac{\text{ker}'x - \text{kei}'x}{x} \right) \cos(\theta - \phi) \right] \\
 + C_{18}(1+\nu) \frac{1}{x^2} \cos(\theta - \phi) \\
 - \bar{C}_{11} \frac{x^2}{2} \sin(\theta - \phi) \\
 - 2\bar{C}_{19}(1+\nu) \ln x \sin(\theta + \phi) \\
 + \bar{C}_{13} \frac{(1+\nu)}{\sqrt{2}} \left[-(\text{ber}x - \text{bei}x) \sin \theta \cos \phi + \left(\frac{\text{ber}'x + \text{bei}'x}{x} \right) \sin(\theta - \phi) \right] \\
 - \bar{C}_{14} \frac{(1+\nu)}{\sqrt{2}} \left[(\text{ber}x + \text{bei}x) \sin \theta \cos \phi + \left(\frac{\text{ber}'x - \text{bei}'x}{x} \right) \sin(\theta - \phi) \right] \\
 + \bar{C}_{15} \frac{(1+\nu)}{\sqrt{2}} \left[-(\text{ker}x - \text{kei}x) \sin \theta \cos \phi + \left(\frac{\text{ker}'x + \text{kei}'x}{x} \right) \sin(\theta - \phi) \right] \\
 - \bar{C}_{16} \frac{(1+\nu)}{\sqrt{2}} \left[(\text{ker}x + \text{kei}x) \sin \theta \cos \phi + \left(\frac{\text{ker}'x - \text{kei}'x}{x} \right) \sin(\theta - \phi) \right] \\
 + \bar{C}_{18}(1+\nu) \frac{1}{x^2} \sin(\theta - \phi)
 \end{aligned}$$

Contrails

u_r (p.2 of 3)

$$\begin{aligned}
 & + \sum_{n=2}^{\infty} -C_{n1} \frac{x^{n+1}}{n+1} \cos(n\theta - \phi) \\
 & \quad + C_{n2} \frac{x^{-(n-1)}}{n-1} \cos(n\theta + \phi) \\
 & \quad + C_{n3} (1+\nu) \left[-\frac{1}{\sqrt{2}} (\text{ber}_{n-1} x - \text{bei}_{n-1} x) \cos n\theta \cos \phi \right. \\
 & \quad \quad \quad \left. + \frac{n}{x} \text{bei}_n x \cos(n\theta - \phi) \right] \\
 & \quad - C_{n4} (1+\nu) \left[\frac{1}{\sqrt{2}} (\text{ber}_{n-1} x + \text{bei}_{n-1} x) \cos n\theta \cos \phi \right. \\
 & \quad \quad \quad \left. + \frac{n}{x} \text{ber}_n x \cos(n\theta - \phi) \right] \\
 & \quad + C_{n5} (1+\nu) \left[-\frac{1}{\sqrt{2}} (\text{ker}_{n-1} x - \text{kei}_{n-1} x) \cos n\theta \cos \phi \right. \\
 & \quad \quad \quad \left. + \frac{n}{x} \text{kei}_n x \cos(n\theta - \phi) \right] \\
 & \quad - C_{n6} (1+\nu) \left[\frac{1}{\sqrt{2}} (\text{ker}_{n-1} x + \text{kei}_{n-1} x) \cos n\theta \cos \phi \right. \\
 & \quad \quad \quad \left. + \frac{n}{x} \text{ker}_n x \cos(n\theta - \phi) \right] \\
 & \quad - C_{n7} (1+\nu) n x^{n-1} \cos(n\theta + \phi) \\
 & \quad + C_{n8} (1+\nu) n x^{-(n+1)} \cos(n\theta - \phi) \\
 & \quad - \bar{C}_{n1} \frac{x^{n+1}}{n+1} \sin(n\theta - \phi) \\
 & \quad + \bar{C}_{n2} \frac{x^{-(n-1)}}{n-1} \sin(n\theta + \phi)
 \end{aligned}$$

Contrails

u_r (p.3 of 3)

$$\begin{aligned} & + \bar{c}_{n3} \left[-\frac{1}{\sqrt{2}} (\text{ber}_{n-1} x - \text{bei}_{n-1} x) \sin n\theta \cos \phi + \frac{n}{x} \text{bei}_n x \sin(n\theta - \phi) \right] (1+\nu) \\ & - \bar{c}_{n4} \left[\frac{1}{\sqrt{2}} (\text{ber}_{n-1} x + \text{bei}_{n-1} x) \sin n\theta \cos \phi + \frac{n}{x} \text{ber}_n x \sin(n\theta - \phi) \right] (1+\nu) \\ & + \bar{c}_{n5} \left[-\frac{1}{\sqrt{2}} (\text{ker}_{n-1} x - \text{kei}_{n-1} x) \sin n\theta \cos \phi + \frac{n}{x} \text{kei}_n x \sin(n\theta - \phi) \right] (1+\nu) \\ & - \bar{c}_{n6} \left[\frac{1}{\sqrt{2}} (\text{ker}_{n-1} x + \text{kei}_{n-1} x) \sin n\theta \cos \phi + \frac{n}{x} \text{ker}_n x \sin(n\theta - \phi) \right] (1+\nu) \\ & - \bar{c}_{n7} (1+\nu) n x^{n-1} \sin(n\theta + \phi) \\ & + \bar{c}_{n8} (1+\nu) n x^{(n+1)} \sin(n\theta - \phi) \} \end{aligned}$$

Contrails

APPENDIX B

USEFUL KELVIN-BESSEL FUNCTION IDENTITIES

Contrails

Contrails

$$\text{ber}_1 x = (\text{ber}'x - \text{bei}'x) / \sqrt{2}$$

$$\text{ber}_2 x = (2x^{-1} \text{bei}'x - \text{ber } x)$$

$$\text{ber}_3 x = \left[-8x^{-2} (\text{ber}'x + \text{bei}'x) + 4x^{-1} (\text{ber } x - \text{bei } x) - (\text{ber}'x - \text{bei}'x) \right] / \sqrt{2}$$

$$\text{ber}_4 x = \left[48x^{-3} \text{ber}'x + 24x^{-2} \text{bei } x - 8x^{-1} \text{bei}'x - \text{ber } x \right]$$

$$\text{ber}_5 x = \left[-384x^{-4} (\text{ber}'x - \text{bei}'x) - 192x^{-3} (\text{ber } x + \text{bei } x) + 72x^{-2} (\text{ber}'x + \text{bei}'x) - 12x^{-1} (\text{ber } x - \text{bei } x) + (\text{ber}'x - \text{bei}'x) \right] / \sqrt{2}$$

$$\text{ber}_6 x = \left[-3840x^{-5} \text{bei}'x + 1920x^{-4} \text{ber } x - 768x^{-3} \text{ber}'x - 144x^{-2} \text{bei } x + 18x^{-1} \text{bei}'x - \text{ber } x \right]$$

$$\text{ber}_7 x = \left[46080x^{-6} (\text{ber}'x + \text{bei}'x) - 23040x^{-5} (\text{ber } x - \text{bei } x) + 9600x^{-4} (\text{ber}'x - \text{bei}'x) + 1920x^{-3} (\text{ber } x + \text{bei } x) - 288x^{-2} (\text{ber}'x + \text{bei}'x) + 24x^{-1} (\text{ber } x - \text{bei } x) - (\text{ber}'x - \text{bei}'x) \right] / \sqrt{2}$$

$$\text{ber}_8 x = \left[-645120x^{-7} \text{ber}'x - 322560x^{-6} \text{bei } x + 138240x^{-5} \text{bei}'x - 28800x^{-4} \text{ber } x + 4800x^{-3} \text{ber}'x + 480x^{-2} \text{bei } x - 32x^{-1} \text{bei}'x + \text{ber } x \right]$$

$$\text{ber}'_1 x = \left[-x^{-1} (\text{ber}'x - \text{bei}'x) - (\text{ber } x + \text{bei } x) \right] / \sqrt{2}$$

$$\text{ber}'_2 x = \left[-4x^{-2} \text{bei}'x + 2x^{-1} \text{ber } x - \text{ber}'x \right]$$

Contrails

$$\text{ber}'_3 x = \left[\begin{aligned} &24x^{-3} (\text{ber}'x + \text{bei}'x) - 12x^{-2} (\text{ber } x - \text{bei } x) \\ &+ 5x^{-1} (\text{ber}'x - \text{bei}'x) + (\text{ber } x + \text{bei } x) \end{aligned} \right] / \sqrt{2}$$

$$\text{ber}'_4 x = \left[\begin{aligned} &-192x^{-4} \text{ber}'x - 96x^{-3} \text{bei } x + 40x^{-2} \text{bei}'x \\ &- 8x^{-1} \text{ber } x + \text{ber}'x \end{aligned} \right]$$

$$\text{ber}'_5 x = \left[\begin{aligned} &1920x^{-5} (\text{ber}'x - \text{bei}'x) - 960x^{-4} (\text{ber } x + \text{bei } x) \\ &- 408x^{-3} (\text{ber}'x + \text{bei}'x) + 84x^{-2} (\text{ber } x - \text{bei } x) \\ &- 13x^{-1} (\text{ber}'x - \text{bei}'x) - (\text{ber } x + \text{bei } x) \end{aligned} \right] / \sqrt{2}$$

$$\text{ber}'_6 x = \left[\begin{aligned} &23040x^{-6} \text{bei}'x - 11520x^{-5} \text{ber } x + 4992x^{-4} \text{ber}'x \\ &+ 1056x^{-3} \text{bei } x - 180x^{-2} \text{bei}'x + 18x^{-1} \text{ber } x \\ &- \text{ber}'x \end{aligned} \right]$$

The corresponding equations for $\text{bei}_n x$ and $\text{bei}'x$ can be obtained by replacing $\text{ber } x$ and $\text{ber}'x$ by $\text{bei } x$ and $\text{bei}'x$ and by replacing $\text{bei } x$ and $\text{bei}'x$ by $(-\text{ber } x)$ and $(-\text{ber}'x)$, respectively.

APPENDIX C

A BIBLIOGRAPHY ON SHALLOW SHELLS

Contrails

Contrails

The bibliography on shallow shells listed below was compiled from Applied Mechanics Reviews, wherein abstracts of each publication may be found. For this purpose, the entries are listed in order of year and serial number as found in Applied Mechanics Reviews. Papers dealing specifically with vibrations, dynamic response, or buckling are not included, the scope of the listing being limited to static deflection analysis. Further, it must be recognized that this listing is far from complete, primary omissions being theses, government research reports, less well-known foreign journals, and articles prior to 1948.

- 1948 - 953. Vekua, I. N., "On the theory of thin shallow elastic shells" (in Russian), Appl. Math. Mech. (Prikl. Mat. Mekh.), Jan.-Feb. 1948, vol. 12, pp. 69-74.
954. Ambartsumyan, S. A., "On the theory of anisotropic shallow shells" (in Russian), Appl. Math. Mech. (Prikl. Mat. Mekh.), Jan.-Feb. 1948, vol. 12, pp. 75-80.
- 1949 - 448. Reissner, Eric, "Stresses and small displacements of shallow spherical shells. II," J. Math. Phys., Jan. 1947, vol. 26, pp. 279-300.
- 1950 - 452. Ambartsumyan, S. A., On the calculation of shallow shells (in Russian), Prikl. Mat. Mekh. II, 527-532 (1947).
- 1955 - 2683. Reissner, E., Small rotationally symmetric deformations of shallow helicoidal shells, J. Appl. Mech. 22, I, 31-34, Mar. 1955.
- 1957 - 424. Johnson, M. W., and Reissner, E., On inextensional deformations of shallow elastic shells, J. Math. Phys. 34, 4, 335-346, Jan. 1956.
427. Vorovich, I. I., On certain direct methods in the nonlinear theory of shallow shells, Dokladi Akad. Nauk SSSR (N.S.) 105, 1, 42-45, 1955 (translated from Russian by M. D. Friedman, 572 California St., Newtonville 60, Mass.)
1062. Ambartsumyan, S. A., On the theory of anisotropic shallow shells, NACA TM 1424, 11 pp., Dec. 1956.
1378. Naghdi, P. M., Note on the equations of shallow elastic shells, Quart. Appl. Math. 14, 3, 331-333 (Notes), Oct. 1956.
1063. Ambartsumyan, S. A., On the calculation of shallow shells, NACA TM 1425, 11 pp., Dec. 1956.
1064. Nazarov, A. A., On the theory of thin shallow shells, NACA TM 1426, 7 pp., Dec. 1956.

Contrails

- 1957 - 1759. Simons, R. M., A power series for the nonlinear equations for axi-symmetrical bending of shallow spherical shells, J. Math. Phys. 35, 2, 164-176, July 1956.
- 1958 - 2071. Simons, R. M., A power series solution of the nonlinear equations for axi-symmetrical bending of shallow spherical shells, J. Math. Phys. 35, 2, 164-176, July 1956.
806. DeSilva, C. N., and Naghdi, P. M. Asymptotic solutions of a class of elastic shells of revolution with variable thickness, Quart. Appl. Math. 15, 2, 169-182, July 1957.
804. Oniashvili, O. D., Certain dynamic problems in the theory of shells (in Russian), Moscow, Academy of Science, 1957, 196 pp.
- 1959 - 5976. Reissner, E., Rotationally symmetric problems in the theory of thin elastic shells, Proc. Third U. S. Nat. Congr. Appl. Mech., June 1958; Amer. Soc. Mech. Engrs., 1958, 51-69.
4396. Reissner, E., Symmetric bending of shallow shells of revolution, J. Math. Mech. 7, 2, 121-140, Mar. 1958.
5472. Vlasov, V. Z., Theory of space vibration of thin-walled bars and shells as well as aerodynamic stability of suspension bridges (in English), 9th Congrès Intern. Mecan. Appl., Univ. Bruxelles, 1957; 7, 519-526.
5973. Grigoliuk, E. I., Stability of nonhomogeneous elastoplastic shells, Soviet Phys.-Doklady 3, 2, 438-441, Dec. 1958, (Translation of Dokladi Akad. Nauk SSSR (N. S.) 119, 4, 663-666, Mar.-Apr. 1958 by Amer. Inst. Phys., Inc., New York, N. Y.)
5461. Librescu, L., Some problems of the theory of a class of nonhomogeneous elastic thin shells (in Roumanian), Studii Si Cercetari Mecan. Appl. 10, 1, 187-202, 1959.
3304. Vorovich, I. I., On the Bubnov-Galerkin method in the nonlinear theory of shallow shells (in Russian), Dokladi Akad. Nauk SSSR (N. S.) 110, 5, 723-726, 1956.
2845. Ramaswamy, G. S., Research on a new doubly curved shell. Part I. The theory of a shell in the form of Prandtl membrane, Civ. Engng, Lond. 53, 626, 899-900 Aug. 1958.
2305. Oravas, G.-A., Transverse bending of thin shallow shells of translation (in English), Ost. Ing-Arch. 11, 4, 264-276, Dec. 1957.

Contrails

- 1959 - 684. Oravas, G.-A., Stress and strain in thin shallow spherical calotte shells (in English), Publ. Int. Assn. Bridge Struct. Engng. 17, 139-160, 1957.
5978. Bridgland, T. F., Jr., and Nash, W. A., Elastic deformations of shallow shell in the form of an elliptic paraboloid, Proc. Third U. S. Nat. Congr. Appl. Mech., June 1958; Amer. Soc. Mech. Engrs., 1958, 265-271.
- 1960 - 5085. Reissner, E., The edge effect in symmetric bending of shallow shells of revolution, Comm. Pure Appl. Math. 12, 2, 385-398, May 1959.
4497. Silkin, E. I., Analysis of shallow shells on an elastic contour (in Russian), Izu. Akad. Nauk SSSR, Otd. Tekh. Nauk no. 8, 101-106, Aug. 1958.
6249. Kornishin, M. S., and Mushtari, Kh. M., A certain algorithm of the solution of nonlinear problems of the theory of shallow shells, Appl. Math. Mech. (Prikl. Mat. Mekh.) 23, 1, 211-218, 1959. (Pergamon Press, 122 E. 55th St., New York 22, N. Y.)
3887. Oravas, G.-A., Analysis of thin elastic shallow segmental shells (in English), Publ. Int. Assn. Bridge Struct. Engng. 18, 201-214, 1958.
2759. Mishonov, M., On the theory of shallow shells Appl. Math. Mech. (Prikl. Mat. Mekh.) 22, 5, 972-979, 1958. (Pergamon Press, 122 E. 55th St., New York 22, N. Y.)
2752. Flugge, W., and Conrad, D. A., A note on the calculation of shallow shells, ASME Trans. 81E (J. Appl. Mech.), 4, 683-685 (Brief Notes), Dec. 1959.
2214. Oravas, G.-A., Transverse Flexure of shallow barrel shells, Trans. Engng. Inst. Canada 3, 1, 23-31, Apr. 1959.
636. Reissner, E., On the determination of stresses and displacements for unsymmetrical deformations of shallow spherical shells, J. Math. Phys. 38, 1, 16-35, Apr. 1959.
- 1961 - 4071. Krasiukov, V. P., The calculation of flat shells by the method of finite differences (in Ukrainian), Nauk Zap. Kievsk. In-ta 16, 16, 247-258, 1957; Ref. Zh. Mekh. no. 4, 1959, Rev. 4153.

Contrails

- 1961 - 4662. Apeland, K., Stress analysis of translational shells, Proc. Amer. Soc. Civ. Engrs. 87, Em 1 (J. Engng. Mech. Div.), 111-139, Feb. 1961.
2393. Pshenichnov, G. I., On the analysis of latticed shallow cylindrical shells (in Russian), Inzhener. Sbornik Akad. Nauk SSSR 26, 59-65, 1958.
1854. Pelka, Z., Computation of translational shells by means of the funicular polygon (in Polish), Rozprawy Inz. 7, 4, 465-480, 1959.
1297. Tsurkov, I. S., Elastic equilibrium of rectangular panel-type shallow shells undergoing finite deflections (in Russian), Inzhener. Sbornik Akad. Nauk SSSR 26, 49-53, 1958.
146. Csonka, P., Formulas for calculation of stresses in shell domes (in German), Bautechnik 37, 2, 59-62, Feb. 1960.
145. Tooth, A. S., Kenedi, R. M., and Hossack, J. D. W., The use of semi-graphical methods in the stress and deformation analysis of shell forms, Struct. Engr. 38, 4, 129-137, Apr. 1960.
5283. Soare, M., Application of the many-point method for the study of shells (in German), Rev. Mecan. Appl. 5, 3, 417-436, 1960.
6549. Kalmanok, A. S., The analysis of rectangular membrane plates by analogy with doubly-curved, flat shells (in Russian), Rasschet Prostranstv. Konstruktsii no. 4; Moscow, Gosstroizdat, 1958, 415-450; Ref. Zh. Mekh. no. 7, 1959, Rev. 7967.
4673. Mushtari, Kh. M., and Surkin, R. G., Medium bending of shallow spherical panels, square in shape, with nonlinear relations between stresses and strains (in Russian), Zh. Prikl. Mekh. Tekh. Fiz. 2, 162-165, 1960.
4070. Kassimor, D. M., The analysis of a particular, concrete problem of a prismatic shell (in Azerb.) Elmi Esserler Azerb. Univ. no. 11, 49-72, 1957; Ref. Zh. Mekh. no. 4, 1959, Rev. 4151.
5277. Dulacska, E., Thin-shell construction of elliptical ground plan (in Hungarian). Melyépitéstudományi Szemle 10, 6, 284-286, June 1960.
5278. Monakhenko, D. V., and Proskurayakov, V. B., Scaling the state of stress of thin shallow shells (in Russian), Izv. Akad. Nauk SSSR, Otd. Tekh. Nauk, Mekh. i Mash. no. 6, 161-163, Nov./Dec. 1960.

Contrails

- 1961 - 6569. Svirskii, I. V., Utilization of similarity considerations for the improvement of the convergence of a process of successive approximation in shell analysis, Appl. Math. Mech. (Prikl. Mat. Mekh.) 24, 1, 177-190, 1960.
(Pergamon Press, 122 E. 55th St., New York 22, N. Y.)
5281. Pshenichnov, G. I., Static analysis of lattice-type shallow cylindrical shells (in Russian), Inzhener. Sbornik Akad. Nauk SSSR 27, 171-178, 1960.
6567. Dawoud, R. H., Symmetrically loaded shallow shells of revolution, Mathematika 7, 13, 23-35, June 1960.
5953. Ross, C., The simplified design of concrete hyperbolic paraboloid roofs, Civ. Engng., Lond. 56, 654, 65-66, Jan. 1961.
153. Lawruk, B., A hinged thin shallow spherical shell rectangular in the horizontal projection (in English), Bull. Acad. Polonaise Sci. (IV) 7, 7/8, 413-418, 1959.
- 1962 - 3248. Mushtari, Kh. M., Basic theory of shallow shells with fillers (in Russian), Izv. Akad. Nauk SSSR, Otd Tekh. Nauk, Mekh. i Mash. no. 2, 24-29, Mar/Apr. 1961.
6993. Flugge, W., Statics and dynamics of shells [Statik und Dynamik der Schalen], 3rd edition, Berlin, Springer-Verlag, 1962, vii + 292 pp. DM 36.
6341. Duddeck, H., Bending theory of a shallow hyperbolic paraboloid shell defined by $z = c xy$ (in German), Ing.-Arch. 31, 1, 44-78, 1962.
5761. Berezovsky, A. A., Nonlinear integral equations of shallow shells of revolution (in Russian), Inzhener.-Zh. 4, 5, 44-53, May 1961.
6345. Klimov, B., Contribution to the general bending theory of shallow shells with variable thickness (in German), Acta Techn. Acad. Sci. Hungaricae, Budapest 34, 3/4, 403-420, 1961.
5173. Jenssen, O., Shallow hyperbolic paraboloidal shells, Acta Polytech. Scandinavica no. 310 (Civ. Engng. Bldg. Construct. Ser. 14), 18 pp., 1961.
5169. Tsuboi, Y., and Akino, K., Theories and applications of antisymmetrical bending state for spherical shell and cylindrical shell, Rep. Inst. Indust. Sci., Tokyo Univ. 11, 2, 105 pp., Sept. 1961.

Contrails

- 1962 - 1538. Reissner, E., Note on finite inextensional deformations of shallow elastic shells, J. Math. Phys. 40, 253-259, 1961.
3242. Librescu, L., On the Elasto-dynamic problem of nonhomogeneous thin shells (in Roumanian), Studii si Cercetari Mecan. Apl., Inst. Mecan Apl., Acad. Rep. Pop. Romine 12, 4, 861-876, 1961.
2598. Pshenichnov, G. I., Large deflections of latticed shallow-cylindrical shells (in Russian), Inzhener. Sbornik Akad. Nauk SSSR 31, 101-107, 1961.
726. Onat, E. T., Plastic analysis of shallow conical shells, Proc. Amer. Soc. Civ. Engrs. 86, EM 6 (J. Engng. Mech. Div.), 1-12, Dec. 1960.
2578. Popov, E. P., and Medwadowski, S. J., Membrane stresses in hyperbolic paraboloid shells circular in plan (in English), Publ. Int. Assn. Bridge Struct. Engng. 20, 283-297, 1960.
1997. Lawruk, B., Hinged, thin, shallow spherical shell with rectangular projection (in English), Arch. Mech. Stos. 11, 6, 767-782, 1959.
2590. Munro, J., The linear analysis of thin shallow shells, Proc. Instn. Civ. Engrs. 19, 291-306, July 1961.
1342. Lederer, F., Spherical shells above polygonal base (in German), Acta Technica, Prague 6, 1, 1-29, 1961.
130. Librescu, L., Elastic multilayer shells (in German), Rev. Mecan. Appl. 5, 5, 695-710, 1960.
127. Paria, G., Bending of a shallow spherical shell under uniform pressures with the boundary partly clamped and partly simply-supported, Bull. Calcutta Math. Soc. 52, 2, 79-86, June 1960.
6964. Mushtari, Kh. M., and Teregulov, I. G., Theory of shallow orthotropic shells of medium thickness (in Russian), Izv. Akad. Nauk SSSR, Otd. Tekh. Nauk, Mekh. i Mash. no. 6, 60-67, Nov./Dec. 1959.
1341. Krstic, M., Analysis of an elastic spherical shell whose base projection is an equilateral triangle (in German), Bautechnik 38, 4, 134-136, Apr. 1961.

Contrails

- 1963 - 5037. Feldman, M. P., Computing shallow shells, taking into account creep of the material (in Russian), Nauchn. Soobshch. Dnepropetr. Inzh. -Stroit, In-ta no. 56, 10 pps., 1960; Ref. Zh. Mekh. no. 8, 1961, Rev. 8 V 250.
6937. Soare, M., Theory of bending of anticlastic hyperbolic paraboloid (in Russian), Rev. Mecan. Appl. 7, 3, 595-616, 1962.
6935. Mushtari, Kh. M., Theory of three-layered shallow shells having a core with layers of varying thickness (in Russian), Izv. Akad. Nauk SSSR, Otd. Tekh. Nauk, Mekh. i Mashinostr. no. 4, 71-76, July/Aug. 1962.
6324. Conway, H. D., and Leissa, A. W., Application of the point-matching method to shallow-spherical-shell theory, Trans. ASME 84 F (J. Appl. Mech.) 4, 745-747 (Brief Notes), Dec. 1962.
5064. Vasil'kov, B. S., Analysis of shells with nonsymmetric contour [Raschet obolochek ne simmetricheskim konturom], Moscow, Gosstroizdat, 1962, 123 pp. 0.42 r. (Paper-bound)
3236. Rzhantsyn, A. R., Shallow shells and corrugated floors [Pologie obolochki i volnistye nastily], Moscow, Gosstroizdat, 1960, 128 pp. 0.43 r.
743. Munro, J., and Ahuja, B. M., An investigation of the strain distribution in reinforced concrete shallow thin shells of negative Gaussian curvature (in English), Proceedings of the Symposium on Shell Research, Delft, Aug. 30-Sept. 2, 1961; New York, John Wiley & Sons, Inc., 1962, 58-78.
- 1964 - 120. Lance, R. H., and Onat, E. T., Analysis of plastic shallow conical shells, Trans. ASME 30 E (J. Appl. Mech.), 2, 199-209, June 1963.
736. Gradowczyk, M. H., Some remarks on the theory of shallow spherical shells (in English), Ingen.-Arch. 32, 5, 297-303, 1963.
1360. Apte, V. P., and Phadke, B. S., Analysis of a shallow funicular shell by the method of finite differences, J. Instn. Engrs., India 43, 7 (Part CI4), 389-397, Mar. 1963.
1990. Szmodits, K., General equations of shell analysis (in English), Acta Tech., Acad. Sci. Hungaricae, Budapest 41, 3/4, 459-471, 1962.

Contrails

- 1964 - 2591. Gravina, P. B. J., On the analysis of shallow spherical shells (in Italian), G. Genio Civile 100, 8, 439-453, Aug. 1962.
3196. Apeland, K., Analysis of bending stresses in translational shells, including anisotropic and inhomogeneous properties, Acta Polytech. Scandinavica Ci 22, 161 pp., 1963.
3769. Hlavacek, I., Asymmetrical deflections of initially deformed spherical shell under external pressure (in Russian), Apl. Mat. Ceskoslov. Akad. Ved. 8, 6, 399-410, 1963.
4345. Petrov, V. V., Investigation of finite flexures of plates and shallow shells by the method of successive loading (in Russian), Teoriya Plastin i Obolochek, Kiev, Akad. Nauk USSR, 1962, 328-331; Ref. Zh. Mekh. no. 7, 1963, Rev. 7 V 42.
4353. Burmistrov, E. F., Flexure of a shallow constructively orthotropic shell, rectangular in projection, which has pliable edges (in Russian), Teoriya Plastin i Obolochek, Kiev, Akad. Nauk USSR, 1962, 431-434; Ref. Zh. Mekh. no. 7, 1963, Rev. 7 V 45.
5007. Jahanshahi, A., Force singularities of shallow cylindrical shells, Trans. ASME 30 E (J. Appl. Mech.) 3, 342-346, Sept. 1963.
5011. Nazarov, N. A., Calculation of shallow shells reinforced by stiffening ribs (in Russian), Inzh. Konstruktsii. Soprotivlenie Waterialov. Stroit. Mekhan., Leningrad, 1962, 110-117; Ref. Zh. Mekh. no. 7, 1963, Rev. 7 V 76.
5636. Wempner, G. A., Axisymmetric deflections of shallow conical shells, Proc. Amer. Soc. Civil Engrs. 90, EM 2 (J. Engng. Mech. Div.) (Part I), 181-193, Apr. 1964.
5637. Reissner, E., On asymptotic solutions for nonsymmetric deformations of shallow shells of revolution, Internat. J. Engng. Sci. 2, 1, 27-43, Apr. 1964.
7003. Slechta, J., The analysis of shallow shells using the method of finite differences (in German), Acta Tech., Prague 8, 5, 441-451, 1963.
7010. Raizer, U. D., Taking into account the bending moments in the calculation of a shallow conoidal shell and shallow shells of variable curvature (in Russian), Issled po Teor. Sooruzh, Part 12, Moscow, Gosstroizdat, 1963, 257-265; Ref. Zh. Mekh. no. 1, 1964, Rev. 1 V 72.

Contrails

- 1964 - 7020. Galimov, N. K., Theory of thin shallow shells with a filler for finite flexures (in Russian), Nelinein. Teor. Plas. i Obolochek, Kazan; Kazansk. Un-ta, 1962, 61-69; Ref. Zh. Mekh. no. 1, 1964, Rev. 1 V 46.
7030. Mason, J., An Analysis of shallow sectorial orthotropic (in English), Bygningsstat. Medd. 34, 3, 79-88, Dec. 1963.
- 1965 - 149. Mishonov, M., Boundary effect of shells according to nonlinear theory (in Bulgarian), Izv. In-ta Vodno Stop. i Str-vo Bk. 4, 111-128, 1963; Ref. Zh. Mekh. no. 5, 1964, Rev. 5 V 59.
783. Leyko, J., Approximate differential equations of shrink joined cylindrical shells, Arch. Budowy Maszyn 11, 1, 9-13, 1964.
1415. Aass, A., Jr., A contribution to the bending theory of elliptic paraboloid shells (in English), Publ. Internat. Assoc. Bridge Struct. Engng. 23, 1-26, 1963.
1418. Havelya, S. P., Question of the solution of problems of the theory of shallow shells by the method of plane approximations (in Ukrainian), Teor. i Prykl. Mat., L'vivsk. Un-ta, part 2, 1963, 65-67; Ref. Zh. Mekh. no. 7, 1964, Rev. 7 V 76.
1421. Grigolyuk, E. I., and Chulkov, P. P., General large-deflection theory of elastic sandwich shallow shells (in English), Arch. Mech. Stos. 16, 1, 123-133, 1964.
1981. Buivol, V. M., Question of the stressed state of shallow spherical shells with circular holes (in Ukrainian), Prikl. Mekh. 9, 2, 212-216, 1963; Ref. Zh. Mekh. no. 8, 1964, Rev. 8 V 120.
2023. Chang, W. Y., Chen, H. W., and Yang, H. S., Stress analysis of the shallow hyperbolic parabolic shell (in Chinese), Chinese J. Civil Engng. 10, 3, 1-14, 1964.
2024. Wan-Shie, T., Simplified analysis of the spherical shallow shell with polygonal base (in Chinese), Chinese J. Civil Engng. 10, 3, 15-18, 1964.
2027. Berezovskii, A. A., Nonlinear integral and differential equations of shallow shells and their application (in Russian), Teoriya Obolochek i Plastin, Erevan, Akad. Nauk ArmSSR, 1964, 226-233; Ref. Zh. Mekh. no. 8, 1964, Rev. 8 V 94.

Contrails

- 1965 - 2030. Grigolyuk, E. I., and Chulkov, P. P., General theory of elastic sandwich shells of large flexure (in Russian), Vopr. Dinamiki i Prochnosti, Part 10, Riga, Akad. Nauk LatvSSR, 1963, 95-108; Ref. Zh. Mekh. no. 8, 1964, Rev. 8 V 91.
3357. Klimow, B., On the calculation of shallow shells with double, varying curvature (in German), Acta. Tech., Acad. Sci. Hungaricae, Budapest 49, 1/2, 37-54, 1964.
3362. Havelya, S. P., and Kosarchin, V. M., Elastic equilibrium of a shallow spherical shell bounded by an ellipse and a rectangle (in Russian), Zb. Robit. Aspirantiv L'vivsk. In-ta Pryrodn. Nauk, L'viv 1963, 23-29; Ref. Zh. Mekh. no. 10, 1964, Rev. 10 V 71.
3369. Bykov, D. L., Investigation of medium and large flexures of shallow spherical segments with arbitrary axisymmetric loads (in Russian), Teor. Obolochek i Plastin, Erevan, Akad. Nauk ArmSSR, 1964, 293-300; Ref. Zh. Mekh. no. 10, 1964, Rev. 10 V 57.
4648. Famili, J., and Archer, R. R., Finite asymmetric deformation of shallow spherical shells, AIAA J. 3, 3, 506-510, Mar. 1965.
5322. Shevchenko, V. D., Effect of certain geometric parameters on the stressed-strained state of shallow shells (in Ukrainian), Prykl. Mekh., Akad. Nauk UkrRSR, Kiev 9, 4, 367-373, 1963.
6647. Reissner, E., and Wan, F. Y. M., Rotating shallow elastic shells of revolution, J. Soc. Industr. Appl. Math. 13, 1, 333-352, Mar. 1965.
6650. Fischer, L., An approximate analysis for shallow shells of translation, Concrete Construct. Engng. 59, 12, 425-436, Dec. 1964.
6651. Yokoo, Y., Nakamura, T., and Matsui, T., Limit analysis of shallow parabolic cylindrical shells (in English), Trans. Archit. Inst. Japan no. 106, 10-17, Dec. 1964.
6656. Buivol, V. N., Shallow spherical shell weakened by symmetrically disposed holes (in Ukrainian), Prykl. Mekh. Akad. Nauk UkrRSR, Kiev 9, 1, 52-58, 1963.
- 1966 - 123. Kornishin, M. S., Non-linear problems of the theory of plates and slanting shells and methods of their solution (in Russian), Moscow, Nauka, 1964, 192 pp. 81 k.

Contrails

- 1966 - 127. Shevlyakov, Yu. A., and Shevchenko, V. P., A shallow spherical shell under the action of concentrated forces and moments (in Russian), Prikl. Mekh., 1, 2, 74-77, 1965.
139. Mikeladze, M. Sh., Theory of shallow anisotropic plastic shells, Soviet Physics -- Doklady 10, 2, 166-168, Aug. 1965. (Translation of Dokladi Akad. Nauk, SSSR 160, 4, 789-791, Feb. 1965 by American Institute of Physics, New York, N. Y.)
775. Hotzler, H., The elastic stress and strain distribution in a shallow thin spherical shell with rectangular cross section (in German), Bautechnik 42, 1, 13-20, Jan. 1965.
1427. Mikeladze, M. Sh., Basic equations in the quasimembrane theory of orthotropic cylindrical plastic shells (in Russian), Prikl. Mekh. 1, 1, 62-69, 1965.
1441. Kayuk, Ya. F., and Alekseeva, M. K., Application of the small parameter method to the analysis of stress distribution of shallow shells (in Russian), Prikl. Mekh. 1, 7, 45-49, 1965.
2133. Shevlyakov, Yu. A., and Shevchenko, V. P., Solution of the problem of bending of shallow spherical shells (in Ukrainian), Prikl. Mekh., 10, 4, 382-391, 1964.
2143. Belonozov, S. M., and Ismailov, M. A., First boundary-value problem for the differential equation of elastic equilibrium a shallow cylindrical shell (in Russian), Differents. Uravneniyal, 2, 219-226, 1965; Ref. Zh., Mekh. no. 10, 1965, Rev. 10 V 100.
2827. Soare, M., On symmetric bending of a shallow paraboloidal shell of revolution over circular base (in German), Bauingenieur 40, 7, 260-265, July 1965.
2831. Ho, K.-C., and Fu, C., Simplified method of analysis for elliptical paraboloidal shallow shells under the action of concentrated loads (in English), Publ. Internat. Assoc. Bridge Struct. Engng. 24, 125-141, 1964.
3468. Dekhtyar, A. S., Limit equilibrium of shallow shells with a plane base (in Russian), Prikl. Mekh. 1, 8, 68-73, 1965.
3498. Prusakov. O. P., and Kholod, A. G., Certain form of nonlinear equations of shallow sandwich shells with rigid cores (in Ukrainian), Prikl. Mekh. 10, 6, 581-586, 1964.

Contrails

- 1966 - 4187. Mikeladze, M. Sh., Estimate of the carrying capacity of shallow shells of revolution and stretched-bent round plates (in Russian), Prikl. Mekh. 1, 2, 40-47, 1965.
4879. Lardner, T. J., and Simmonds, J. G., Lateral deformation of shallow shells of revolution, Internat. J. Solids and Struct. 1, 4, 377-384, Nov. 1965.
4886. Derkach, P. Kh., and Shevchenko, V. P., The limit load of a shallow spherical shell, Soviet Engng. J. 5, 1, 161-164 (Brief Communications), Jan./Feb. 1965. (Translation of Inzhener. Zh. 5, 1, 189-192, 1965 by Faraday Press, Inc., New York, N. Y.)
5500. DeRuntz, J. A., Jr., and Hodge, P. G., Jr., The significance of the concentrated load in the limit analysis of conical shells, Trans. ASME 33 E (J. Appl. Mech.) 1, 93-101, Mar. 1966.
5524. Tsurpal, I. A., and Shul'ga, N. A., Fundamental equations of the theory of thin shallow shells taking into account physical nonlinearities (in Russian), Prikl. Mekh. 1, 12, 15-21, 1965.
6200. Shevlyakov, Yu. A., and Shevchenko, V. P., Concentrated forces and bending moments on a shallow cylindrical shell (in Russian), Prikl. Mekh. 2, 1, 120-123, 1966.
6206. Shablii, O. N., Carrying capacity of shallow spherical shells clamped at the edge (in Russian), Prikl. Mekh. 1, 11, 7-11, 1965.
6925. Abd El Wahab, H. A., The shallow spherical shell with elliptic core under constant pressure (in German), Abh. Broonschweig. Wissen. Gesellsch. 16, 23-61, 1964.
7679. Jenssen, O., An example of how to obtain a nearly membrane state of stress in a shallow hyperbolic paraboloidal shell (in English), Acta Polytech. Scandinavica Ci 30, 18 pp., 1965.
7685. Reismann, H., Thurston, G. A., and Holston, A. A., The shallow spherical shell subjected to point load or hot spot (in English), ZAMM 45, 2/3, 95-103, May 1965.
- 1967 - 128. Rossettos, J. N., An asymptotic analysis for large deflections of pressurized shallow spherical membrane shells, AIAA J. 4, 6, 1121-1123 (Tech. Notes), June 1966.

Contrails

- 1967 - 133. Penning, F. A., Nonaxisymmetric behavior of shallow shells loaded at the apex, Journal of Applied Mechanics, Transactions of the ASME, Series E 33, 3, 699-700 (Brief Notes), Sept. 1966.
138. Schumann, W., On the elastic deflection of a very shallow sandwich shell into a plate (in German), Acta Mechanica 1, 4, 395-402 (Communications), 1965.
883. Forsberg, K., and Flugge, W., Point load on a shallow elliptic paraboloid, Journal of Applied Mechanics, Transactions of the ASME, Series E 33, 3, 575-585, Sept. 1966.
885. Bushnell, D., Influence coefficients for externally pressurized spherical shells, AIAA Journal 4, 8, 1472-1474 (Technical Notes), Aug. 1966.
1620. Akhund-zade, M. Yu., and Tagiev, I. G., Approximate method of solving the equations of equilibrium of shallow shells in the case of large flexures (in Russian), AzerbSSR, Elmler Akad. Kheberleri, Fiz. Tekhn. Verijazijjat Elmleri Ser., Izv. Akad. Nauk SzerbSSR, Ser. Fiz. Tekhn. i Matem. Nauk no. 3, 3-7 (1965); RZM no. 6 (1966), Rev 6 V 61.
1626. Hossack, J. D. W., Experimental investigation of the nonlinear behavior of shallow spherical shells, Nuclear Structural Engineering 1, 3, 285-294 (Mar. 1965).
2333. Petrov, V. V., Analysis of flexible plates and shallow shells by the variational method of V. Z. Vlasov (in Russian), Prikladnaya Mekhanika 2, 5, 55-57 (1966).
2347. Mikeladze, M. Sh., Shallow anisotropic plastic shells, Nuclear Structural Engineering 14, 4, 414-418 (Apr. 1965).
3192. Kachanov, L. M., executive editor, Issledovaniya po uprugosti; Sbornik 4 (Investigations on elasticity and plasticity, No. 4); Izd. Leningradskogo Universiteta (1965), 219 pp., 0.98 r. (Paperbound).
3201. Powell, G. H., Compact solution of doubly-curved shell equation, Journal of the Engineering Mechanics Division, Proceedings of the American Society of Civil Engineers 92, EM 5, 1-21 (Oct. 1966).
3207. Havelya, S. P., and Kosarchyn, V. M., Solution by digital computer of some problems in the theory of shells of revolution (in Ukrainian), Visnyk Lvivsk. Un-tu, Ser. Mekhan.-Matem. part 2, 92-95 (1965); RZM no. 8 (1966), Rev 8 V 65.

Contrails

- 1967 - 3215. Piechocki, W., Finite deflections of a locally loaded shallow spherical membrane (in Polish), Mechanika Teoretyczna i Stosowana 2, 2, 45-58 (1964).
4664. McElman, J. A., Eccentrically stiffened shallow shells of double curvature, National Aeronautics and Space Administration Technical Note D-3826, 34 pp. (Feb. 1967).
4665. Rossettos, J. N., Deformation of shallow spherical sandwich shells under local loading, National Aeronautics and Space Administration Technical Note D-3855, 45 pp. (Feb. 1967).
6380. Lardner, T. J., On the stress distribution in a shallow logarithmic shell of revolution, Journal of Mathematics and Physics 45, 1, 23-34 (Mar. 1966).

Security Classification

DOCUMENT CONTROL DATA - R & D

(Security classification of title, body of abstract and indexing annotation must be entered when the overall report is classified)

1. ORIGINATING ACTIVITY (Corporate author) The Ohio State University Research Foundation 1314 Kinnear Rd., Columbus, Ohio 43212		2a. REPORT SECURITY CLASSIFICATION Unclassified	
		2b. GROUP N/A	
3. REPORT TITLE ANALYSIS OF SHALLOW SHELLS BY THE METHOD OF POINT MATCHING			
4. DESCRIPTIVE NOTES (Type of report and inclusive dates) Final Report December 1, 1966 through March 31, 1969			
5. AUTHOR(S) (First name, middle initial, last name) Arthur W. Leissa Adel S. Kadi			
6. REPORT DATE August 1969	7a. TOTAL NO. OF PAGES 226	7b. NO. OF REFS 36	
8a. CONTRACT OR GRANT NO. F33615-67-C-1177	9a. ORIGINATOR'S REPORT NUMBER(S) AFFDL-TR-69-71		
b. PROJECT NO.	9b. OTHER REPORT NO(S) (Any other numbers that may be assigned this report) Report # 7		
c. BPS No. 7(61146703-62405334)			
d.			
10. DISTRIBUTION STATEMENT This document has been approved for public release and sale; its distribution is unlimited.			
11. SUPPLEMENTARY NOTES		12. SPONSORING MILITARY ACTIVITY Air Force Flight Dynamics Laboratory Wright-Patterson Air Force Base, Ohio 45433	
13. ABSTRACT This report summarizes a study aimed at extending the applicability of the method of point matching to problems of statically loaded shallow shells, and deriving a set of shell equations for arbitrary curvature including the effects of orthotropy and thermal loading. The accuracy of the method is investigated by solving a problem for which an exact solution exists -- the uniformly loaded, shallow spherical shell supported along a square boundary by means of shear diaphragms. Solutions to the governing system of differential equations are derived in polar coordinates in terms of Kelvin-Bessel functions and then expressed in a general form for boundaries having arbitrary normal and tangential directions. Further experiences with the method are demonstrated on problems of shallow spherical shells having regular polygonal and elliptical boundaries. For contrast, clamped and shear diaphragm edge conditions are studied. General solutions for circular cylindrical shallow shells, where the effects of rectangular orthotropy and thermal gradients are retained, are obtained by means of the auxiliary function approach.			

14. KEY WORDS	LINK A		LINK B		LINK C	
	ROLE	WT	ROLE	WT	ROLE	WT
Point matching						
Shallow shells						
Arbitrary curvature						
Circular cylindrical						
Spherical						
Arbitrary loading						
Arbitrary shape						
Regular polygonal boundaries						
Elliptical boundaries						
Clamped						
Shear diaphragm						
Orthotropy						
Thermal gradients						
Auxiliary function						
Navier type solution						
Levy type solution						
Kelvin-Bessel functions						
Boundary point least squares						
Least squares						